

Flow cell separation in fluctuating g-field

A thesis submitted for the degree of Doctor of Philosophy

by

Tian Han

Institute for Bioengineering, Brunel University London

April, 2015

Abstract

Field flow fractionation of particles in rotating coiled column has been investigated in recent year. In contrast to the classical mode of field flow fractionation in narrow channels, the use of rotating coiled columns offers the possibility of large sample loading. In this thesis, the potential for new cell separation methods based on the use of flow fractionation in fluctuating *g*-fields generated in rotating coil columns is examined. The effects of operational conditions (flow rate and rotational speed – Chapter 3 and Chapter 5); cell properties (cell flexibility – Chapter 4); and column shapes (different inner diameters and coil geometries – Chapter 6) on the flow behaviour of a model system of red blood cells (RBCs) from different species, which differ markedly in size, shape & density, flowing in a single phase of buffered saline have been characterised.

Operational Conditions: For a particular rotational speed, there was a minimum flow rate which caused all the cells to be retained in the column and a maximum flow rate at which all cells were eluted. Both the minimum and maximum flow rate were increased when a higher rotational speed was applied. Differences in the behaviour of sheep & hen RBCs have been used to develop a separation method using a continuously increasing flow gradient. This separation could be speeded up by using a step flow gradient. The effects of cell load and rotational direction on the behaviour of RBCs in the column was also studied in this thesis.

Cell Properties: The minimum flow rate was found to correlate with cell diameter/cell volume of the RBCs as expected for a sedimentation related process and was partially described by a theoretic equation developed for particles by Fedotov and colleagues (Fedotov et al. 2005). However cell dependent departures from this equation were found which appear to indicate that cell specific surface properties may also be involved for cells (Chapter 3). By contrast the maximum flow rate showed no correlation with cell diameter/cell volume. An effect of cell deformability on the flow separation behaviour of the cells has been demonstrated. Chemical fixation of sheep RBCs with glutaraldehyde rendered the normally deformable RBCs rigid and non-deformable and resulted in the fixed sheep RBCs eluting significantly earlier than unfixed sheep RBCs. This difference was great enough that a mixture of deformable (unfixed) and non-deformable (fixed) sheep RBCs could be separated. Fixed cells tended to show cell aggregation, which could be reduced by the addition of surfactant.

Column Geometry: An effect of column shapes on the flow separation behaviour of cells has been demonstrated showing that the optimisation of column design is an important feature of this mode of cell separation. For columns with the same cross sectional area, a “horizontal” rectangular column provided better separation than a circular column and a “vertical” rectangular column gave the least efficient separation. A possible explanation for this behaviour is suggested the thinner sedimentation layer and less secondary flow. Differences in the behaviour of various species of RBCs in the “horizontal” rectangular column have been used to study the efficiency of separation of a mixture of sheep and hen RBCs, and a mixture of rabbit and hen RBCs.

This work shows similarities and differences with other reports on cell/particle separations in rotating coiled columns in single phases and also in aqueous two phases systems (ATPS) and these are discussed.

Fedotov P.S., Kronrod V.A. & Kasatonova O.N. (2005). *Simulation of the motion of solid particles in the carries liquid flow in a rotating coiled column.* J. Anal. Chem., 60, 4, 310-316.

Acknowledgements

The thesis presented here is impossible to be achieved without countless supports. First, I would like to express my sincere gratitude to my supervisor, Professor Derek Fisher, for giving me this PhD study opportunity and also for his knowledge, patient guidance and invaluable encouragement. His instructions, ideas, attitudes to research and life not only guide my PhD study, presenting and writing skill, but also develop my mind to think critically. I would also like to thank my supervisor, Dr. Svetlana Ignatova, who allowed me to finish my experiments with tremendous freedom and supported me with her expertise and experience. I am very grateful for my supervisors for finding opportunities and supporting me to attend conferences.

I would also like to thank Dr. Remco van den Heuvel, my previous supervisor, for his special knowledge and technical supports in the early stage of this thesis. I cannot forget the advices from Professor Ian Sutherland who was able to view from an overall perspective of this research work; Dr. Quan Long and Dr. Carola König who provided important comments on research direction and precious discussion; Dr. Peter Hewitson who fixed instruments refused to cooperate; and Dr. Ian Garrard who prepared a mock viva for me.

I am grateful to Jenny Kume for her kindness, considerations and helpful administrative supports and advices; and Roger Paton for his help in ordering necessary materials for this work. I would like to thank all the people who supported this thesis for their knowledge and assistance.

I also wish to thank all students for their company, joyful time and treasured memories during the time we spend together. My thanks go to everyone in BIB for their kindness and hospitality.

Finally, special thanks to my parents who provided the funding, understanding and unconditional supports for me during the period of study. Without their encouragement, I have no chance to be able to complete this thesis.

Table of contents

Chapter 1. Introduction and Literature Review	1
1.1. Counter-current chromatography (CCC) design and centrifugal force fields (fluctuating g-field)	1
1.1.1. Countercurrent chromatography (CCC)	1
1.1.1.1. CCC setup	2
1.1.1.2. Hydrostatic CCC	2
1.1.1.3. Hydrodynamic CCC	3
1.1.2. Type of columns	6
1.1.2.1. Column orientations	6
1.1.2.2. Column geometry	7
1.1.3. Nonsynchronous CCC and Synchronous CCC design	8
1.1.3.1. Nonsynchronous CCC design	8
1.1.3.2. Synchronous CCC design	9
i. J type CCC design	10
ii. X-L type CCC design	12
1.1.4. Principle of hydrodynamic CCC	13
1.1.4.1. Air, liquid and bead in CCC	13
1.1.4.2. Distribution ratio	14
1.1.5. Orbital motion and G field of hydrodynamic CCC	14
1.1.5.1. β and Orbital motion	14
1.1.5.2. Direction and magnitude of g-field	15
1.1.5.3. G-level calculation for CCC	18
1.1.5.4. Liquid distribution and phase mixing	19
1.2. Introduction of red blood cell	22
i. Red blood cells for vertebrates	22
ii. Red blood cells for human	22
iii. Osmotic fragility	23
iv. Suspension stability	23
1.3. Behaviour of cell and particle in rotating coiled column	25
1.3.1. Introduction	25
1.3.2. Cell separation in non-synchronous Counter-Current Chromatography (NSCCC) by aqueous two-polymer phase system (ATPS)	28
1.3.2.1. ATPS for cell separation and design of CCC for ATPS	28
1.3.2.2. Bacterial cell separation by toroidal coil centrifuge	29

1.3.2.3. Erythrocyte separation by Nonsynchronous CCC -----	30
1.3.2.4. <i>S. typhimurium</i> separation by Nonsynchronous CCC -----	34
1.3.3. <i>Cell separation in non-synchronous Counter-Current Chromatography (NSCCC)</i> <i>by single phase</i> -----	36
1.3.3.1. Erythrocyte separation -----	37
1.3.3.2. Rat liver cell and mast cell separation -----	41
1.3.3.3. Blood cell components separation -----	43
1.3.4. <i>Particle separation by CCC</i> -----	46
1.3.4.1. Particle separation by 2 phases system -----	46
i. Lipoprotein separation by cross-axis CCC via ATPS -----	46
ii. Trace element separation by 2 phases system -----	47
1.3.4.2. Particle separation by single phase -----	47
1.3.5. <i>Related applications of similar mechanism on cells by Ito Y.</i> -----	53
1.3.6. <i>Conclusion</i> -----	58
1.4. Discussion and Conclusion -----	59
Aims and Objectives -----	61
Chapter 2. Experimental set up, methods and materials -----	63
2.1. Introduction -----	63
2.2. Countercurrent chromatography (CCC) experimental set up -----	63
2.2.1. <i>CCC centrifuge</i> -----	63
2.2.1.1. J type CCC -----	63
2.2.1.2. CCC column -----	63
2.2.1.3. CCCE Cantilever CCC -----	65
2.2.2. <i>Sample loop</i> -----	66
2.2.3. <i>UV detector and the signal recorder</i> -----	66
2.2.4. <i>Fraction collector</i> -----	67
2.3. Materials and Buffer preparation method -----	67
2.3.1. <i>Isotonic buffer</i> -----	67
2.3.1.1. Isotonic buffer preparation -----	67
2.3.1.2. Testing of isotonic buffer for RBC studies -----	67
2.3.2. <i>Cell fixation solution preparation</i> -----	69
2.3.3. <i>Surfactant (Tween® 20) added isotonic buffer preparation</i> -----	70
2.4. Blood sample preparation methods -----	70
2.4.1. <i>Blood sample wash method</i> -----	70
2.4.2. <i>Red blood cell fixation method</i> -----	71
2.4.2.1. Cell fixation method -----	71

2.4.2.2. Cell fixation result test -----	71
2.4.3. Sheep RBCs ghost cell preparation -----	73
2.5. Analytical methods -----	74
2.5.1. Fractionated sample analyse method -----	74
2.5.2. Peak area measure method -----	75
2.5.3. Cell size measurement method -----	75
2.5.4. Cell density measurement -----	79
2.5.5. Cell number counting method -----	80
2.6. Discussion and Conclusion -----	81
Chapter 3. Fundamental behaviour of red blood cells in fluctuating g-field -----	84
3.1. Summary -----	84
3.2. Experimental -----	84
3.2.1. Sheep RBCs behaviour in CCCE cantilever -----	84
3.2.2. Relationship between pumping direction and rotational direction -----	86
3.2.3. The effect of flow rate and rotational speed on the behaviour of sheep RBCs in Milli-CCC® -----	88
3.2.4. Behaviour of sheep RBCs in Milli-CCC®: Increasing flow rate decreases retention of cells in the column -----	89
3.2.5. Behaviour of sheep RBCs in Milli-CCC®: decreasing flow rate increases retention of cells -----	91
3.2.6. Behaviour of sheep RBCs in Milli-CCC®: Flow rate required to elute retained cells. Introduction of “step flow” -----	93
3.2.7. Behaviour of sheep RBCs in Milli-CCC®. Detailed analysis of retention of cells in coil on flow rate at two different rotational speeds. Reproducibility of recovery of cells -----	95
3.2.8. Behaviour of RBCs from sheep and 8 other animal species in Milli-CCC®. The concept of maximum flow rate and minimum flow rate and their determination at different initial rotational speeds -----	97
3.2.9. Behaviour of sheep RBCs in Milli-CCC®: Studies on the integrity of cells retained and then eluted from the column (PEAK B) -----	100
3.2.10. Comparison between behaviour of RBCs ghost cell and intact RBCs -----	102
3.3. Discussion -----	105
3.3.1. Pumping direction and Rotational direction -----	105
3.3.2. Minimum and Maximum operational conditions: influence of flow rate and rotational speed -----	105
3.3.2.1. Minimum and maximum operational conditions -----	105

3.3.2.2. Minimum and maximum flow rates for different species of RBC: influence of, cell diameter and cell density -----	106
3.3.2.3. Elution of ghost cells in minimum operational condition -----	107
3.3.3. <i>Theoretical analysis of Flow behaviour of cells in rotating coils</i> -----	108
3.3.3.1. Comparison of experimentally determined of min Flow data with theoretical equation developed by Fedotov et al -----	108
3.3.3.2. Source of deviation from “Fedotov Equation”: Impact of values of cell radius and density used to calculate V_f -----	110
3.3.3.3. Introduction of factor α into “Fedotov Equation” to correct theoretical values to experimental values of minimum flow -----	113
3.3.3.4. Possible explanations for cell specific properties that give rise to the cell specific differences between experimental Min flow and calculated V_f from “Fedotov Equation”: correlations with α -----	116
3.4. Conclusion -----	155
Chapter 4. Influence of cell membrane deformability on RBCs in fluctuating g-field --	
-----	119
4.1. Summary -----	119
4.2. Experimental -----	119
4.2.1. <i>Retention of fixed RBCs</i> -----	119
4.2.2. <i>Elution behaviour of fixed RBCs</i> -----	122
4.2.2.1. Fixed RBCs elution in step flow at relatively high g-field (1000 RPM) -----	
-----	122
4.2.2.2. Fixed RBCs elution in step flow at relatively low g-field (500 RPM) -----	
-----	126
4.3. Discussion -----	131
4.3.1. <i>Discussion of sedimentation and elution behaviours of unfixed and glutaraldehyde fixed RBCs</i> -----	131
4.3.1.1. Fixed cells are less retained than unfixed cells -----	131
4.3.1.2. Fixation affects the performance of sheep RBCs more than hen RBCs -	133
4.3.2. <i>Discussion of on the difficulty to remove cells formed by sedimentation of fixed hen RBCs in high g-field</i> -----	133
4.4. Conclusion -----	135
Chapter 5. Behaviour of RBCs elution and flow cell separation -----	136
5.1. Summary -----	136
5.2. Experimental -----	136
5.2.1. <i>Behaviour of RBCs elution</i> -----	136

5.2.1.1. RBCs elution in flow gradient -----	137
5.2.1.2. RBCs elution in step flow -----	140
5.2.1.3. Flow cell separation in improved step flow -----	144
5.2.2. <i>Loading test of flow cell separation</i> -----	149
5.2.3. <i>Separation of fixed and unfixed sheep RBCs in step flow</i> -----	150
5.2.4. <i>Fixed sheep and hen RBCs separation in step flow; problems of cell aggregation, reduced by Tween[®] 20</i> -----	153
5.3. Discussion -----	158
5.3.1. <i>Rotation with flow gradient</i> -----	158
5.3.2. <i>Rotation with step flow</i> -----	158
5.3.3. <i>Cell separation in improved step flow</i> -----	161
5.3.4. <i>Loading capacity test</i> -----	163
5.3.5. <i>Discussion of separation of unfixed and fixed sheep RBCs</i> -----	163
5.3.6. <i>Discussion of separation of fixed sheep RBCs and fixed hen RBCs</i> -----	164
5.4. Conclusion -----	166
Chapter 6. Behaviour of RBCs elution in different tube shape -----	167
6.1. Summary -----	167
6.2. Experimental -----	167
6.2.1. <i>Sedimentation behaviour of RBCs in different CCC columns</i> -----	168
6.2.1.1. <i>Sedimentation behaviour of RBCs in 1.6 mm ID circular column B</i> ----	168
6.2.1.2. <i>Influence of flow direction and coil rotation on the sedimentation behaviour of RBCs in circular column B and rectangular columns (C and D)</i> -----	169
6.2.2. <i>Elution behaviour of RBCs in 1.6 mm ID circular column</i> -----	171
6.2.3. <i>Elution behaviour of RBCs in rectangular columns (Columns C and D)</i> -----	174
6.2.3.1. <i>Elution behaviour of RBCs by pumping from head to tail in rectangular columns</i> -----	174
6.2.3.2. <i>Flow cell separation of sheep and hen RBCs in rectangular column</i> ----	177
6.2.3.3. <i>Elution behaviour of RBCs in species by flow gradient in rectangular column (column C)</i> -----	179
6.2.3.4. <i>Flow cell separation of rabbit and hen RBCs in rectangular column C</i> -	181
6.3. Discussion -----	184
6.3.1. <i>Minimum flow rate for sheep RBCs in column A and column B</i> -----	184
6.3.2. <i>The sediment behaviour of RBCs in rectangular column</i> -----	184
6.3.3. <i>Elution of mixed RBCs in rectangular columns C and D</i> -----	184
6.3.4. <i>Elution order and flow cell separation in column rectangular column C</i> -----	185
6.4. Conclusion -----	186

Chapter 7. General discussion and conclusion	187
7.1. Discussion of sedimentation behaviour of RBCs	187
7.1.1. Movement of RBCs in rotating coiled columns	187
7.1.2. Pumping direction and rotational direction	189
7.1.3. Discussion of minimum and maximum operational condition	189
7.2. Discussion of elution behaviour of RBCs	190
7.2.1. Comparison of cell separation by non-synchronous CCC and J-type CCC --	191
7.2.2. Comparison with nonsynchronous CCC separation of blood cell components ---	
.....	192
7.2.3. Comparison with particle separations by Fedotov et al.	193
7.2.4. Comparison with latex particles in BIB	194
7.2.5. Comparison with field flow fractionation and elutriation	195
7.3. Conclusion	197
Appendix	200
References	202

List of Figures

Figure 1.1.1. Schematic diagram of a typical CCC setup. From Garrard et al., 2008. -----	2
Figure 1.1.2. Schematic of structure and principle of centrifugal partition chromatography. From Berthod, 2002. -----	3
Figure 1.1.3. Countercurrent chromatography configurations having parallel axes. From Conway, 1990. -----	4
Figure 1.1.4. Rotary seal free flow through centrifuge systems for performing CCC. From Ito, 1991. -----	4
Figure 1.1.5. Design of J-type CCC. From Ito & Conway, 1996. -----	5
Figure 1.1.6. Schematic illustration of column and antitwisting feed tube motion in the planet gear drive. From Conway, 1990. -----	5
Figure 1.1.7. Solvent distribution in (multilayer) column of CCC. From Ito & Conway, 1996. -----	6
Figure 1.1.8. Columns applied in centrifugal Countercurrent chromatographs. From Conway, 1990. -----	7
Figure 1.1.9. Different tubing geometry for hydrodynamic CCC. From Degenhardt et al., 2001. -----	7
Figure 1.1.10. Cross sectional view of nonsynchronous CCC. From Kazufusa et al., 2007. - -----	8
Figure 1.1.11. Revolution mechanism of nonsynchronous CCC. From Kazufusa et al., 2007. -----	9
Figure 1.1.12. A series of synchronous seal free flow through CCC designs. From Yoichi & Ito, 1998. -----	10
Figure 1.1.13. Cross section of prototype Milli rotor. From Lee et al., 2003. -----	11
Figure 1.1.14. Orientation of the column holder in five different types of cross-axis CCC. From Yoichi & Ito, 1998. -----	12
Figure 1.1.15. Cross-section of XLL cross-axis CCC. From Shibusawa et al., 1992. -----	12

Figure 1.1.16. Characterization of the head and tail of helical and spiral columns. From Conway, 1990. -----	13
Figure 1.1.17. Distribution of equal volumes of heavy (shaded) and light phases of a two-phase system in a rotating helical column as a function of the rate of rotation. From Conway, 1990. -----	13
Figure 1.1.18. Distribution of heavy (shaded) and light phases of a two-phase systems in Countercurrent chromatographs at high rate of rotation. From Conway, 1990. -----	14
Figure 1.1.19. Orbits of an arbitrary point at various values of β on the planet gear column holder. From Conway, 1990. -----	15
Figure 1.1.20a. Scale drawing of the force vector in different orbital position of the column holder and its angle γ_r . Vectors for reversed motion from 120° to 240° are displaced for clarity. From Conway, 1990. -----	16
Figure 1.1.20b. Inclination, γ_r , of the force vector, F , to the radius, r , through the arbitrary point P , on the planet gear column holder. γ_r is shown for various β values during one orbit of the holder. From Conway, 1990. -----	16
Figure 1.1.21. Magnitude of g force (F) on an arbitrary point P on the planet gear column holder as a function of the revolution angle. From Conway, 1990. -----	16
Figure 1.1.22. Relative magnitude and direction of the force vectors at various positions on planet gear column holder. From Conway, 1990. -----	17
Figure 1.1.23. Schematic comparison of centrifugal force fields in planar and angle rotor centrifuges. From Ito, 1986. -----	17
Figure 1.1.24. Motion of nonsynchronous centrifuge rotor. From van den Heuvel & Konig, 2011. -----	18
Figure 1.1.25. Variation of the tangential velocity with angular position in the column for J-type centrifuge for a 110mm rotor radius and a rotational speed of 800 RPM. The dependence of this variation on beta values is shown for beta values from 0.125 to 0.625. From Wood, 2010. -----	19
Figure 1.1.26a. Magnitude and direction of the resultant force vectors for $\beta = 0.85$ in the planet gear chromatography and the visually observed mixing zoon in multilayer-coil columns (shaded area). From Conway, 1990. -----	20

Figure 1.1.26b. The uncoiled column moving in a tailward direction relative to the settling and mixing area. From Conway, 1990. -----	20
Figure 1.3.1. The distribution of two different strains of E.coli in a two-phases polymer system, where (○) In upper phase; (●) at interface; (□) in lower phase. From Sutherland et al., 1987. -----	29
Figure 1.3.2. A gradient separation of a mixture of two strains of E.coli cells, where (○) mixture of ATCC 8739 (I) and ATCC11303 (II); (▽) rerun of I; (△) rerun of II. From Ref Sutherland et al., 1987; Sutherland & Ito, 1978. -----	30
Figure 1.3.3. Cross-sectional view of the nonsynchronous flow through coil planet centrifuge. From Sutherland & Ito, 1980. -----	31
Figure 1.3.4. Partition of dog, sheep and human RBCs in ATPS (5% (w/w) Dextran 500 – 4% (w/w) PEF 6000) in varying compositions of isotonic phosphate buffered saline. From Sutherland & Ito, 1980. -----	31
Figure 1.3.5. Results of sheep/dog RBCs separation. From Sutherland & Ito, 1980. -----	32
Figure 1.3.6. Results of human/dog RBCs separation. From Sutherland & Ito, 1980. ----	33
Figure 1.3.7. Separation results of fresh sheep/dog RBCs as done by Sutherland & Ito (B) From Harris et al., 1984. -----	34
Figure 1.3.8. Separation of cells of S. typhimurium G30 containing long/short chain LPS. From Leive et al., 1984. -----	35
Figure 1.3.9. Separation of S. typhimurium strain on the polymer phase system with the nonsynchronous flow through coil planet centrifuge. From Ito et al., 1983. -----	36
Figure 1.3.10. Separation of human and sheep erythrocytes. From Ito et al., 1979. -----	37
Figure 1.3.11. Sketch of nonsynchronous flow through coil planet centrifuge. From Ito et al., 1980. -----	38
Figure 1.3.12. Separation of human and sheep erythrocytes. From Ito et al., 1980. -----	39
Figure 1.3.13. Separation of human and sheep erythrocytes by elutriation with the nonsynchronous flow through coil planet centrifuge. From Ito et al., 1983. -----	40

Figure 1.3.14. Elutriation of rat liver cells with the nonsynchronous flow through coil planet centrifuge. Damaged cells were eluted first as a sharp peak while most of the viable cells were retained in the coiled column. From Ito et al., 1983. -----	41
Figure 1.3.15. Separation of mast cells from other leukocytes. From Okada et al., 1996. --- -----	42
Figure 1.3.16. Elution of rat mast cells using nonsynchronous CPC with multilayer column. From Shinomiya et al., 2005. -----	43
Figure 1.3.17. Effects of revolution and rotation on the separation of sheep blood cell components using nonsynchronous CPC and eccentric column assembly. From Shinomiya et al., 2005. -----	44
Figure 1.3.18 Effect of increasing rotational speed on the separation of sheep blood components using nonsynchronous CPC. From Shinomiya et al., 2005. -----	45
Figure 1.3.19. Effect of increasing rotational speed on the separation of human blood cell components using the nonsynchronous CPC (Coil Planet Centrifuge). From Shinomiya et al., 2005. -----	45
Figure 1.3.20. X-L type Countercurrent chromatography separation of HDL and LDL from human serum with ATPS. From Shibusawa, 1997. -----	46
Figure 1.3.21. Group preconcentration and recovery of Zr(IV), Hf(IV), Nb(V), and Ta(V) in the 2 phases liquid system. From Spivakov et al., 2002. -----	47
Figure 1.3.22. Principle of particle separation with a rotating coiled tube in a single phase. From Ito et al., 1983. -----	48
Figure 1.3.23. Retention of a solid sample in PTFE columns with different β values. And the effect of column rotation speed and mobile phase flow rate. From Fedotov et al., 2003. -----	49
Figure 1.3.24. Separation of latex beads. From Fedotov et al., 2000. -----	50
Figure 1.3.25. Separation of humic substance and quartz particles. From Fedotov et al., 2000. -----	50
Figure 1.3.26. The fractionation of model silica gel samples. From Katasonova et al., 2003. -----	51

Figure 1.3.27. The fractionation of quartz sand. From Katasonova et al., 2003. -----	52
Figure 1.3.28. Fractionation of a mixture of standard sample of silica gel (“150nm”, “400nm”, “900nm”) in a conoidal rotating coil column eluted by deionized water. From Fedotov et al., 2010. -----	53
Figure 1.3.29. Design of the flow through centrifuge. From Ito et al., 1975. -----	54
Figure 1.3.30. Photograph of the separation centrifuge (left) and conventional batch density gradient separation and proposed continuous method for cell separation by density gradient centrifugation for continuous separation. From Ito & Shinomiya, 2001. -----	55
Figure 1.3.31. Stroboscopic observation of the separation column with coloured percoll layers. From Ito & Shinomiya, 2001. -----	55
Figure 1.3.32. The result of separation of human buffy coat by the continuous density gradient centrifugal method of Figure 1.3.30. From Ref Ito & Shinomiya, 2001. -----	56
Figure 1.3.33. Different leukocyte populations in each fraction obtained from buffy coat. From Shiono et al., 2005. -----	56
Figure 1.3.34. Separation of cultured human mast cells. From Shiono et al., 2005. -----	57
Figure 1.3.35. Progenitor frequencies in peripheral blood (A) and umbilical cord blood (B). From Shiono et al., 2007. -----	58
Figure 2.2.1.a. Column B -----	64
Figure 2.2.1.b. Column C -----	64
Figure 2.2.1.c. Column D -----	64
Figure 2.2.2. G-field comparison between 4 applied columns in this thesis derived by method of van den Heuvel & Konig (2011). -----	64
Figure 2.2.3. Illustration of CCCE cantilever centrifuge with coil rotating in horizontal plane. From van den Heuvel & Sutherland, 2007. -----	66
Figure 2.3.1. Comparison between sheep blood re-suspended by isotonic buffer and sheep blood re-suspended by H ₂ O -----	68
Figure 2.4.1. The result of sheep RBCs fixation results test -----	72

Figure 2.4.2.a. Light micrograph of unfixed sheep RBCs (top left); Figure 2.4.2.b. Light micrograph of glutaraldehyde fixed sheep RBCs (top right) (400X). -----	73
Figure 2.4.3.a. Light micrograph of unfixed hen RBCs (bottom left); Figure 2.4.3.b. Light micrograph of glutaraldehyde fixed hen RBCs (bottom right) (400X). -----	73
Figure 2.4.4. Light micrograph of prepared sheep RBCs ghost cell by biological microscope (400X). -----	74
Figure 2.5.1. The defined distance from light micrograph of stage micrometer (800X). -	76
Figure 2.5.2. The measurement of sheep RBCs size from light micrographs (800X) -----	76
Figure 2.5.3. The diameters of different RBCs in species measured by microscope. -----	77
Figure 2.5.4. Cell volumes of different RBCs in species (coulter counter). -----	77
Figure 2.5.5. The diameter of different species of RBCs as measured by coulter counter. --- -----	78
Figure 2.5.6. The comparison of cell diameters measured by microscope and coulter counter. -----	78
Figure 2.5.7. The comparison of cell volumes measured by coulter counter and are from literatures. -----	79
Figure 2.5.8. Relationship between refractive index and SIP density. From Percoll-methodology and applications, n.d.. -----	80
Figure 2.5.9. Illustration of haemocytometer applied in this thesis, where 1 mm ² is divided into 400 blue squares. -----	81
Figure 3.2.1. Behaviour of sheep RBCs in CCCE cantilever (clockwise direction). -----	85
Figure 3.2.2. Behaviour of sheep RBCs in CCCE cantilever (counter-clockwise direction). -----	86
Figure 3.2.3. Comparison of the 2 nd column volume elution components between 4 operation combinations of flow direction (head to tail and tail to head) and coil rotation (clockwise and counter-clockwise). -----	87
Figure 3.2.4. Relationship between initial flow rate and the behaviour of sheep RBCs at 500 RPM. -----	90

Figure 3.2.5. A405 analyses for relationship between initial flow rate and the behaviour of sheep RBCs at 500 RPM. -----	91
Figure 3.2.6. A405 for relationship between initial flow rate and the behaviour of sheep RBCs at 900 RPM. -----	93
Figure 3.2.7. Behaviour of eluting sheep RBCs by step flow at 500 RPM. -----	94
Figure 3.2.8. Peak area comparison of PEAK A and PEAK B in 500 RPM and 1000 RPM. -----	96
Figure 3.2.9. Maximum and minimum flow rate for sheep RBCs different rotational speeds (g-field) in Milli-CCC [®] -----	98
Figure 3.2.10. Minimum / maximum flow rate comparison between sheep, hen and guinea pig RBCs -----	100
Figure 3.2.11. Results comparison between sheep blood as sample and fraction from PEAK B as sample. -----	102
Figure 3.2.12. Behaviour of RBCs ghost cells at minimum condition for intact RBCs. -	103
Figure 3.3.1. Relationship between minimum / maximum flow rate of RBCs from different species -----	106
Figure 3.3.2. Relationship between minimum flow rate (1000 RPM) for different species on RBCS -----	107
Figure 3.3.3. Comparisons between V_f and Minimum flow rate shows Minimum flow rates do not fit the calculated V_f . -----	110
Figure 3.3.4. Comparison between Fedotov equation, improved equation and min F. --	115
Figure 3.3.5. Comparison between electrophoretic mobility and alpha in species. -----	117
Figure 4.2.1. Comparisons of elution of PEAK A (non-retained material) between fixed and unfixed sheep RBCs. -----	120
Figure 4.2.2. Comparisons of elution of PEAK A (non-retained material) between fixed and unfixed hen RBCs. -----	121
Figure 4.2.3. Elution of unfixed sheep RBCs by step flow at 1000 RPM. -----	123

Figure 4.2.4. Elution of glutaraldehyde fixed sheep RBCs by step flow at 1000 RPM. -----	124
Figure 4.2.5. Comparison between the elution behaviour of unfixed and glutaraldehyde fixed sheep RBCs in step flow gradient flow modes at 1000 RPM. -----	124
Figure 4.2.6. Elution of unfixed hen RBCs by step flow at 1000 RPM. -----	125
Figure 4.2.7. Elution of glutaraldehyde fixed hen RBCs by step flow at 1000 RPM. ---	125
Figure 4.2.8. Comparison between the elution behaviour of unfixed and glutaraldehyde fixed hen RBCs in step flow gradient flow modes at 1000 RPM. -----	126
Figure 4.2.9. Elution of unfixed sheep RBCs by step flow at 500 RPM. -----	127
Figure 4.2.10. Elution of glutaraldehyde fixed sheep RBCs by step flow at 500 RPM. -	127
Figure 4.2.11. Comparison between the elution of unfixed and glutaraldehyde fixed sheep RBCs in step flow at 500 RPM. -----	128
Figure 4.2.12. Elution of unfixed hen RBCs by step flow at 500 RPM. -----	128
Figure 4.2.13. Elution of glutaraldehyde fixed hen RBCs by step flow at 500 RPM. ----	129
Figure 4.2.14. Comparison between the elution of unfixed and glutaraldehyde fixed hen RBCs in step flow at 500 RPM. -----	130
Figure 4.3.1. Dependence of initial flow rate on rotational speed for fixed and unfixed sheep RBCs. -----	132
Figure 4.3.2. Comparison between Fedotov equation, improved equation and min F. --	132
Figure 4.3.3. The eluted “sticky” fixed hen RBCs. -----	134
Figure 5.2.1. Elution of sheep blood sample in flow gradient. -----	138
Figure 5.2.2. Elution of mixed hen/sheep RBCs sample in flow gradient. -----	139
Figure 5.2.3. Cell number analysis for each fraction from the mixed hen / sheep blood sample elution in flow gradient -----	140
Figure 5.2.4. Elution of hen blood sample by a step increase in flow. -----	142
Figure 5.2.5. Elution of sheep blood sample by a step increase in flow. -----	142

Figure 5.2.6. Comparison between the elution behaviour of hen and sheep RBCs in step flow gradient flow modes. -----	143
Figure 5.2.7. Elution of mixed hen/sheep blood sample by a step increase in flow. ----	143
Figure 5.2.8. Cell number analysis for each fraction in step flow. -----	144
Figure 5.2.9. Elution of hen blood sample by an improved step increase in flow. -----	146
Figure 5.2.10. Elution of sheep blood sample by an improved step increase in flow. ---	146
Figure 5.2.11. Comparison between the elution behaviour of hen and sheep RBCs in improved step flow gradient flow modes. -----	147
Figure 5.2.12. Elution of mixed hen and sheep blood sample by an improved step increase in flow. -----	148
Figure 5.2.13. Cell number analysis for each fraction in improved step flow -----	148
Figure 5.2.14. Cell number analysis for each fraction in improved step flow by different sample loops. -----	150
Figure 5.2.15. Elution of a mixture of unfixed and glutaraldehyde fixed sheep RBCs. --	152
Figure 5.2.16. Comparison of A405 for original fractionated sample. -----	152
Figure 5.2.17. Elution of mixed glutaraldehyde fixed sheep and glutaraldehyde fixed hen. - -----	154
Figure 5.2.18. Cell number analysis for each fraction of eluting a mixture of glutaraldehyde fixed sheep and glutaraldehyde fixed hen RBCs in isotonic buffer. -----	155
Figure 5.2.19. Light microscopy examine for fraction no.7 of elution a mixture of glutaraldehyde fixed hen and fixed sheep RBCs -----	156
Figure 5.2.20. Elution of a mixture of glutaraldehyde fixed sheep and glutaraldehyde fixed hen RBCs by a step increased flow in isotonic buffer with 0.5% Tween® 20 with rotational speed at 500 RPM. -----	156
Figure 5.2.21. Cell number analysis for each fraction of eluting a mixture of glutaraldehyde fixed hen and glutaraldehyde fixed sheep RBCs in step flow by isotonic buffer with 0.5% Tween® 20 -----	157
Figure 5.3.1. Structure of Tween® 20. -----	164

Figure 6.2.1. Absorbance (A405) of fractions PEAK A eluting sheep blood sample in 1.6 mm ID circular column B. -----	170
Figure 6.2.2. A405 of Peak A for eluting sheep blood sample by rectangular column C (2.5 mm × 0.8 mm). -----	171
Figure 6.2.3. A405 of Peak A for eluting sheep blood sample by rectangular column D (0.8 mm × 2.5 mm). -----	171
Figure 6.2.4. Elution of mixed hen/sheep blood sample by a linear increased step flow. -----	173
Figure 6.2.5. The fraction eluted from column B in Figure 6.2.4 using 5 ml/min at 0 RPM shows that the hen and sheep RBCs were still mixed. (100X). -----	174
Figure 6.2.6. Elution of blood sample in column C using a flow gradient. -----	175
Figure 6.2.7. Elution of blood sample in flow gradient by column D. -----	176
Figure 6.2.8. Elution of mixed hen/sheep blood sample by a step increase in flow. -----	178
Figure 6.2.9. Cell number analysis for each fraction from Figure 6.2.8 -----	178
Figure 6.2.10. Comparison between elution of blood sample in species using a flow gradient in rectangular (“flat”) column C. -----	180
Figure 6.2.11. Relationship between maximum flow rate, cell volumes, cell density and elution order. -----	181
Figure 6.2.12. Elution of mixed rabbit/hen blood sample by a step increase in flow. -----	182
Figure 6.2.13. Cell number analysis for each fraction obtained as described in Figure 6.2.12. -----	183

List of Tables

Table 1.1.1. Angular velocities of motors and rotary frames on nonsynchronous CCC. From Kazufusa et al., 2007. -----	9
Table 1.2.1. Mean corpuscular volume or mean cell volume (MCV) for red blood cells in different species. -----	22
Table 1.3.1. Range of biological samples separated by CCC using Aqueous Two-Phase Systems. -----	26
Table 1.3.2. Separations of biological samples using PEG-dextran and PEG-phosphate Aqueous Two-Phase Systems. -----	26
Table 1.3.3. Examples of the use of CCC and CCD machines to separate biological samples using Aqueous Two-Phase Systems. -----	27
Table 1.3.4. Separations of biological samples by CCC in a filed flow fractionation mode in a single phase. -----	27
Table 2.2.1. Parameters of the CCC columns used in this thesis. -----	63
Table 2.2.2. Volume of sample loops and volume ratio to column A. -----	66
Table 2.3.1. List of chemicals and their suppliers used to make isotonic buffer. -----	67
Table 2.3.2. Information of blood samples were applied in this thesis. -----	68
Table 2.3.3. List of chemicals and their suppliers used to make 0.15 M Sodium phosphate buffer, pH 7.4. -----	69
Table 2.3.4. List of chemicals and their suppliers used for cell fixation. -----	70
Table 2.3.5. Information of Tween [®] 20 for hindering cell aggregation. -----	70
Table 2.5.1. Information of Percoll [®] applied for cell density measurement. -----	79
Table 2.5.2. Measured RBCs density in species. -----	80
Table 2.6.1. Information of instruments applied in this thesis. -----	83
Table 3.2.1. A comparison of maximum flow rate and minimum flow rate for sheep RBCs at different rotational speeds -----	98

Table 3.2.2. Minimum flow rate and maximum flow rate for different RBCs in species -	99
Table 3.2.3. Comparison peak area of PEAK A between sheep blood as sample and PEAKB as sample. -----	102
Table 3.3.1. Comparisons of each species of RBCs of measured cell radius with radius calculated to be required for calculated values of V_f to match experimentally determined min flow at different rotational speeds. -----	111
Table 3.3.2. The comparisons of each RBCs in species for theoretical and measured density at different rotational speeds. -----	112
Table 3.3.3. The comparisons of each RBCs in species for theoretical and measurement $r^4\Delta\rho^2$ at different rotational speeds. -----	112
Table 3.3.4 Comparison between V_f and Minimum flow rate for each RBCs at different rotational speed. -----	113
Table 3.3.5. Suggested coefficient α for each RBCs. -----	116
Table 3.3.6. Electrophoretic mobilities and coefficient α of RBCs in species. From Seaman, 1975. -----	117
Table 4.2.1. The minimum flow rate comparison for fixed sheep RBCs and unfixed sheep RBCs at different rotational speeds. -----	121
Table 6.2.1. A comparison of minimum flow rate for sheep RBCs at different rotational speed using column A (ID 1.0mm) and column B (ID 1.6mm) -----	168

Abbreviations & Nomenclature

ATP: Adenosine triphosphate

ATPS: Aqueous Two-Phase Systems

BIB: Brunel Institute for Bioengineering

CCC: Counter-Current Chromatography

CCCD: Centrifugal CounterCurrent Distribution

CCCE: Continuous Counter-Current Extraction

CCD: Counter-Current Distribution

CPC: Centrifugal Partition Chromatography

CPC: Coil Planet Centrifuge

ESR: Erythrocyte Sedimentation Rate

FFF: Field Flow Fractionation

Hct: haematocrit

LLC: Liquid-Liquid partition Chromatography

MCV: Mean Corpuscular Volume or Mean Cell Volume

NSCCC: Non-Synchronous Counter-Current Chromatography

PEG: Polyethylene glycol

PTFE: Polytetrafluoroethylene

RBC: Red Blood Cell

RPM: Revolutions per Minute

TLCCD: Thin layer CounterCurrent Distribution

UV: Ultraviolet

i.d.: inner diameter

o.d.: outside diameter

Chapter 1. Introduction and Literature Review

Countercurrent Chromatography (CCC) is a technique that separates materials by their differential partitioning between two liquid phases. There are essentially two modes of operation: hydrostatic and hydrodynamic which differ in the way one phase is held stationary whilst the other phase flows over it, and the modes of mixing and phase separation that give rise to multiple partition steps (section 1.1.1.2 and section 1.1.1.3). Two-phases system obtained with organic - organic, aqueous - organic and aqueous - aqueous systems have been used to achieve separations of small molecules, protein and bioparticles, such as subcellular organelles (section 1.3.1). In hydrostatic CCC, constant g-field generated by rotation is used to retain stationary phase. Then there is no influence on distribution of stationary phase after flow rate stops (rotation is maintained). In hydrodynamic CCC, fluctuating g-field is used to retain the stationary phase and achieve mixing. In a limited number of studies a single liquid phase has been used in hydrodynamic CCC centrifuges to separate particles of increasing size from nanoparticles, cells, to soil particles (section 1.3).

The aim of this thesis is to study the behaviour of cells in fluctuating g-fields to understand the effects of g forces and flow forces that act on them in order to explore the potential of this mode of CCC operation for cell separation and to highlight general principles of particle fractionation. Erythrocytes have been used as readily available cells (section 1.2)

1.1. Counter-current chromatography (CCC) design and centrifugal force fields (fluctuating g-field)

1.1.1. Countercurrent chromatography (CCC)

As a bridge between equilibrium Countercurrent Distribution (CCD) (Craig & Post, 1949) and conventional liquid-liquid partition chromatography (LLC) (Martin & Synge, 1941), Countercurrent chromatography is a liquid-liquid separation technique in which the stationary liquid phase in the apparatus is retained without using any solid support (Ito & Bowman, 1970). The retention of liquid-stationary phase is achieved by a gravity or centrifugal force in segmented compartments while the mobile phase is pumped through it. (Conway, 1990) The separation is based on partition ratio (K_D) of analyte between the stationary phase and the mobile phase.

Because there is no supporting matrix in CCC, the separation is not distorted by solute adsorption (Conway, 1990) and the sample can be recovered by either elution in the

separation process or clear column process (Berthod et al., 2007). Compared to conventional LLC, CCC provides high stationary phase volumes from 40% to 90% of the column volume (Conway, 1990) which suggests 10% to 60% of column volume is available for sample injection. The liquid-liquid system also enables a choice of either phase as mobile phase.

1.1.1.1. CCC setup

A typical CCC separation system is shown in Figure 1.1.1. Two pumps are required for the CCC system to pump the mobile and stationary phases. A 6-way selection valve injection port with load and injection modes is used for injecting sample. Sample is injected via a sample loop, which is made of a certain length of a PTFE or stainless steel tube, when the injection port is in load mode. Then mobile phase is pumped through the sample loop when the injection port is changed to injection mode flowing the injected sample into the column.

When the mobile phase elutes from the column, it is pumped through a detector connected to a computer for recording the detected signals as chromatograms. A fraction collector is usually used to collect elution fractions after the detector. Compressed nitrogen can be used to clean the column or blow out the phases from the column.

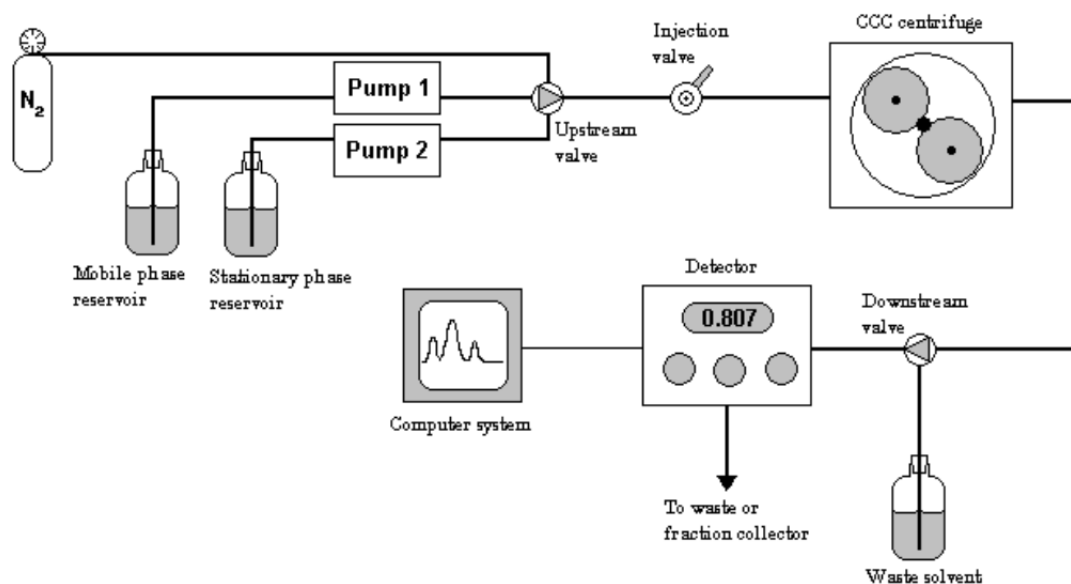


Figure 1.1.1. Schematic diagram of a typical CCC setup. From Garrard et al., 2008.

1.1.1.2. Hydrostatic CCC

In hydrostatic CCC, also called Centrifugal Partition Chromatography (CPC), the stationary phase is retained in a number of chambers serially, which are connected by ducts, under a uniform centrifugal force field generated by rotation around a single axis. The

separation is achieved by the solute distribution while pumping the mobile phase through these chambers serially, which is shown in Figure 1.1.2. The direction of flow should be based on the choice of mobile phase as the flow direction is against the centrifugal force when the mobile phase is upper-phase and the flow direction follows the centrifugal force when the mobile phase is lower-phase. Therefore, the mixing of centrifugal partition chromatography provides is a cascade mixing between stationary and the mobile phases.

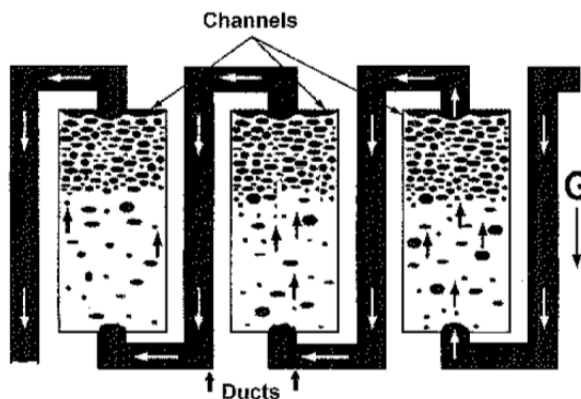


Figure 1.1.2. Schematic of structure and principle of centrifugal partition chromatography. From Berthod, 2002.

1.1.1.3. Hydrodynamic CCC

In contrast to the chambers in hydrostatic CCC, the column of hydrodynamic CCC is a coiled tube (generally PTFE) without rotating seals. Therefore, hydrodynamic CCC does not have the problem of dead area between chambers and the leakage problem associated with the seals in CPC. The rotation of the column is in planetary motion as the tubing wound on supported bobbin rotates around axis of rotation (planet axis) while the whole bobbin rotates around the axis of revolution (solar axis) just as the Earth revolves around the sun (Figure 1.1.3).

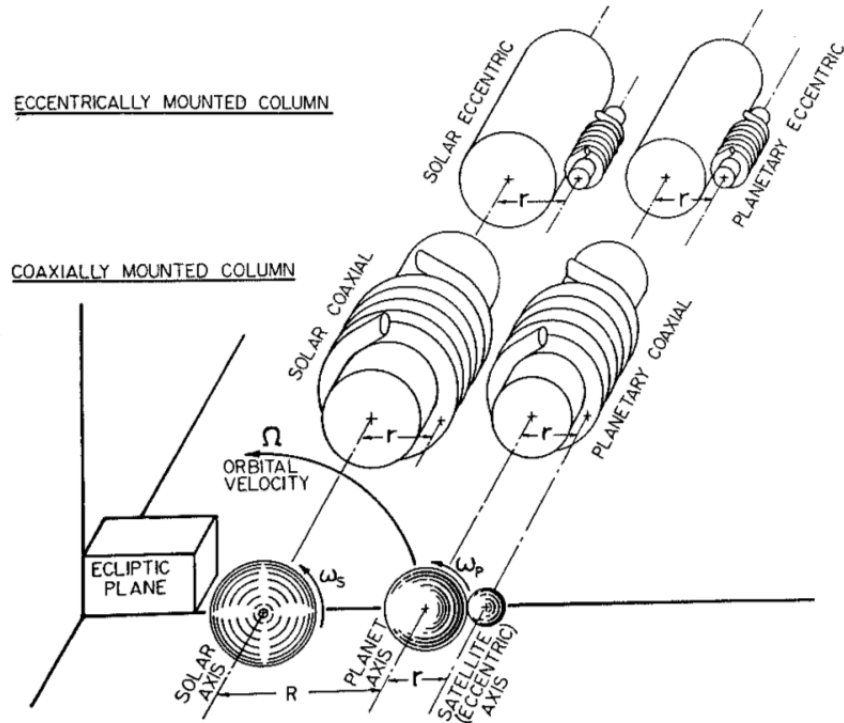


Figure 1.1.3. Countercurrent chromatography configurations having parallel axes. From Conway, 1990.

By combination of different rotation direction and position relationship of bobbin and revolution axis, different type of CCC have been developed (summarised in Figure 1.1.4).

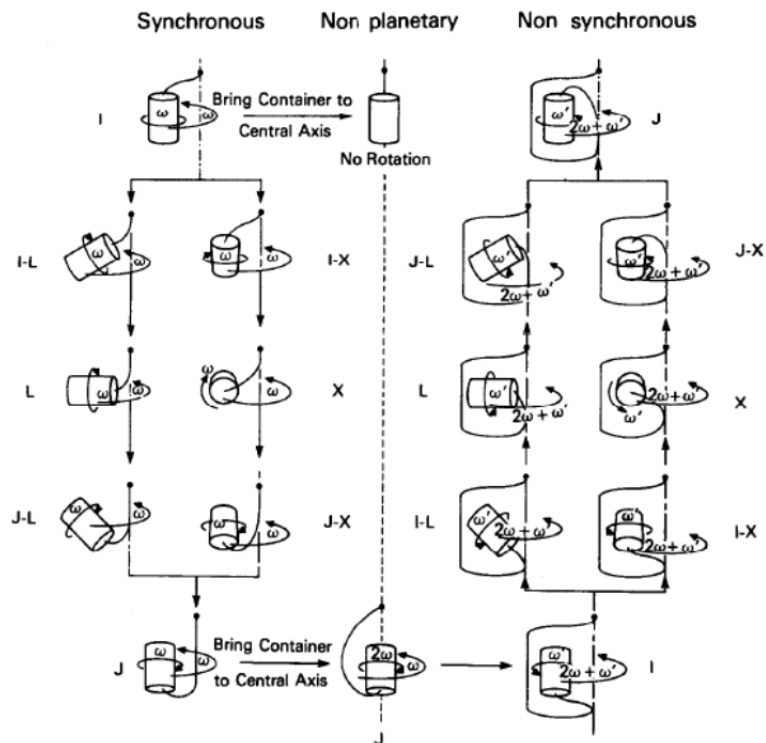


Figure 1.1.4. Rotary seal free flow through centrifuge systems for performing CCC. From Ito, 1991.

Consider the J-type CCC for example (Figure 1.1.5). The bobbin rotates around its own axis and revolves around the centrifuge axis at the same angular velocity (ω) in the same direction (synchronous motion) (Menet & Thiebaut, 1999).

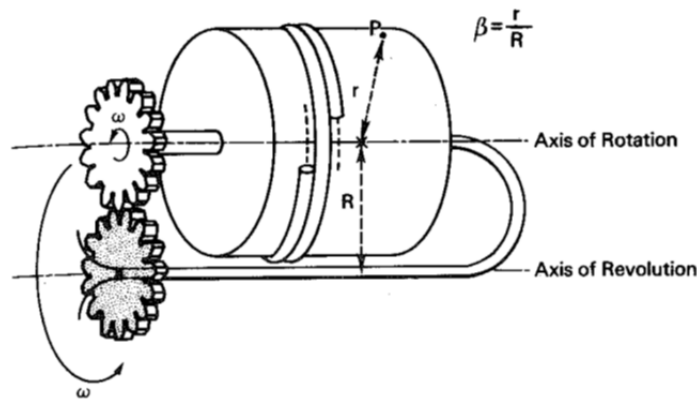


Figure 1.1.5. Design of J-type CCC. From Ito & Conway, 1996.

A special planet gear anti-twisting mechanism is applied in CCC as the white planet gear rotates twice with each circuit (Conway, 1990), as shown in Figure 1.1.6.

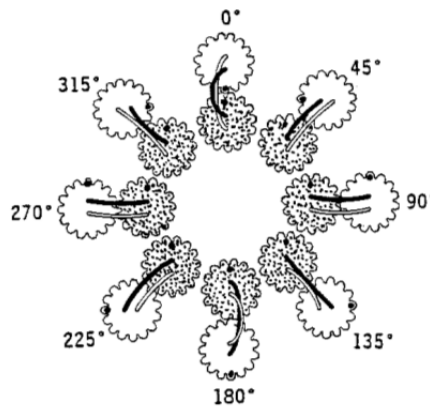


Figure 1.1.6. Schematic illustration of column and antitwisting feed tube motion in the planet gear drive. From Conway, 1990.

The mixing is achieved by this planetary motion. While the stationary phase is retained by the planetary motion and mobile phase is pumping through, the closer side of the column to the axis of revolution generates the mixing area between the 2 immiscible liquid phases and the further side of the column to the axis of revolution generates the settling area of the 2 immiscible liquid phases, as shown in Figure 1.1.7.

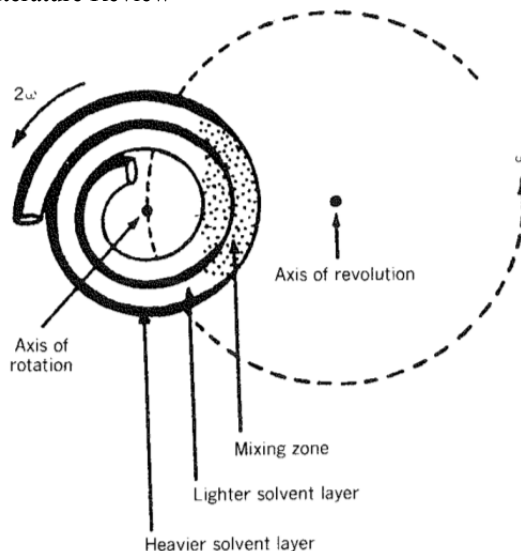


Figure 1.1.7. Solvent distribution in (multilayer) column of CCC. From Ito & Conway, 1996.

This motion creates an Archimedean screw force, which moves all objects of different density toward one end of the column. This end of the column is called head and the other end, the tail (Ito, 2005). When the rotating column is filled with 2 immiscible phases, both of them tend to move to the head of the column. Both the 2 immiscible phases cannot occupy the head of column at the same time it is found that the upper phase occupies the head of the column whereas the lower phase occupies the tail of the column. During the CCC processing, the mobile phase can be pumped in either the head or tail direction. Generally, if lower phase is chosen as the stationary phase, the mobile phase (upper phase) should be pumped from tail to head, and the mobile phase (lower phase) should be pumped from head to tail when the upper phase is the stationary phase to maintain the stationary phases in the column (Grudzień, 2011).

1.1.2. Type of columns

1.1.2.1. Column orientations

The columns of CCC are usually wound of either PTFE or stainless steel tube and the different column designs used in CCC are summarized in Figure 1.1.8.

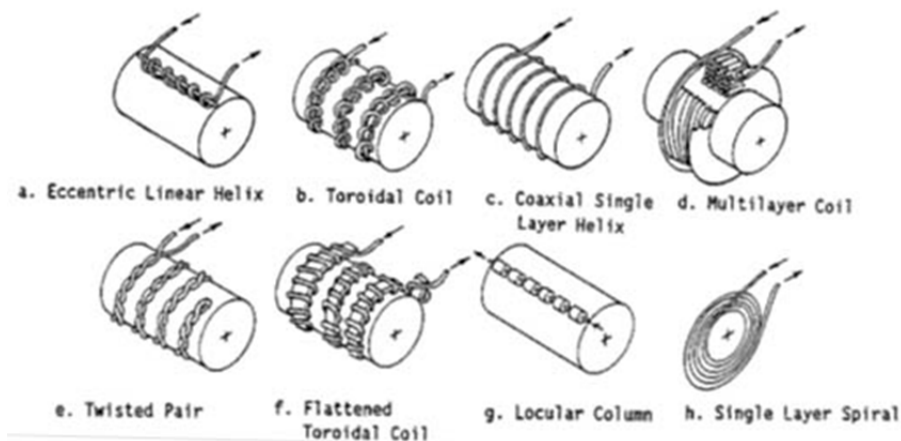


Figure 1.1.8. Columns applied in centrifugal Countercurrent chromatographs. From Conway, 1990.

“Both eccentric (a) and toroidal (b) have a common feature as in each helical turn the two solvent phases are always subjected to an outwardly directed force field where the heavier phases is distributed toward the outer portion and the lighter phase toward the inner portion of each coiled turn, while the 2 phases are mixed back and forth by the fluctuating force field” (Menet & Thiebaut, 1999). Therefore, toroidal columns have features of both hydrostatic and hydrodynamic CCC. They provides vigorous, cascade mixing between the stationary and mobile phase which is especially beneficial if phases of high viscosity such as ATPS are used. They also have the advantage over CPC that columns are easier to clean than the chambers in CPC. However, the retention of the stationary phase in these columns is lower than 50% of the column volume. Both eccentric and toroidal columns have been used for separating polar analytes such as peptides and proteins (Menet & Thiebaut, 1999).

1.1.2.2. Column geometry

Normally the column used in CCC is a circular tube. However, the column can also be made with different shapes (as shown in Figure 1.1.9) which provide different stationary phase retention performance.

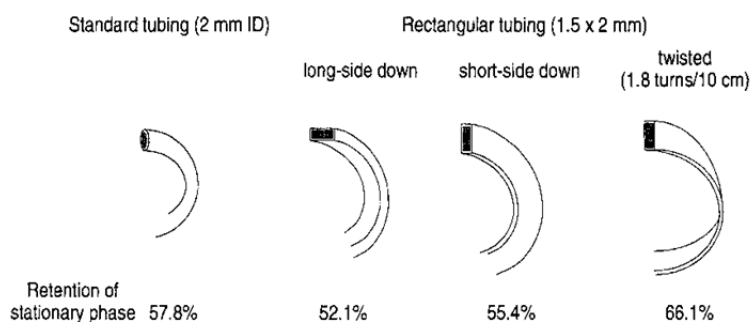


Figure 1.1.9. Different tubing geometry for hydrodynamic CCC. The retention of stationary phase for the phase system Tert-Butyl Methyl Ether (TBME) – n-butanol – acetonitrile – water, 2:2:1:5; less dense layer as stationary phase. From Degenhardt et al., 2001.

1.1.3. Nonsynchronous CCC and Synchronous CCC design

1.1.3.1. Nonsynchronous CCC design

The nonsynchronous CCC introduced in 1979 (Conway, 1990) allows for independent rotation and revolution of the column holder (Ito et al., 1983). This has provided unique separation method for cells and macromolecules (Kazufusa et al., 2007). A cross-sectional view of nonsynchronous CCC is shown in Figure 1.1.10.

Two main rotary structures are shown in Figure 1.1.10: Rotary frame 1 and Rotary frame 2. Frame 1 consists of 3 plates rigidly linked together and directly driven by the main motor (Ito et al., 1983). Frame 2 consists of supports for a pair of rotary shafts, one holding a column holder assembly and the other the counterweight (Ito et al., 1983). As Figure 1.1.10 shows, pulley 5 stops when the side motor stops, which motion is transferred to Rotary frame 2 and results in rotation of rotary frame 2 at $2\omega_1$ (if angular velocity of main motor is ω_2). When side motor has an angular velocity as ω_2 , pulley 4 and pulley 3 rotates at the same rate, and motion is transferred to rotary frame 1 as $\omega_1 - \omega_2$, finally (Ito et al., 1983).

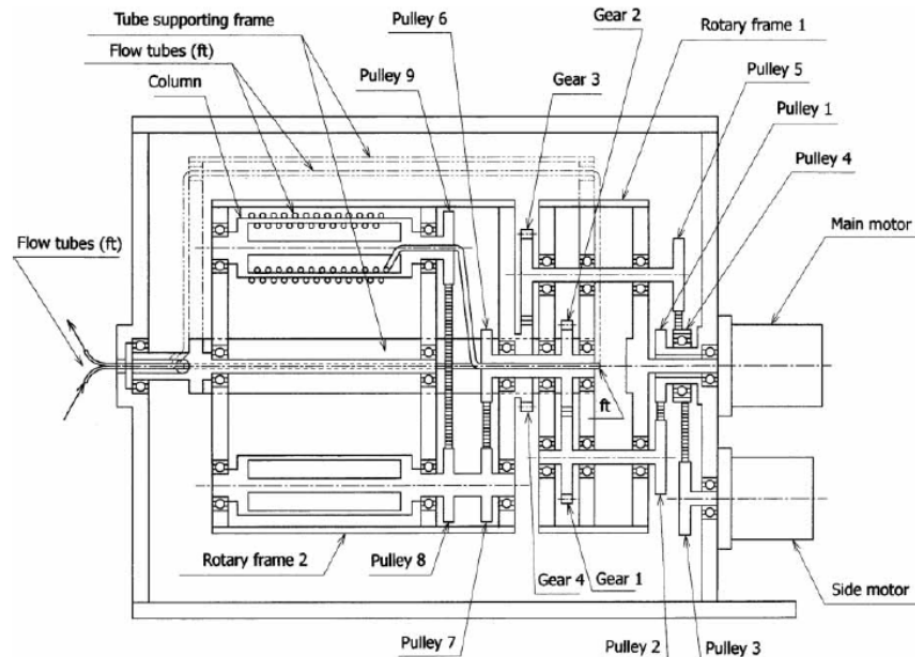


Figure 1.1.10. Cross sectional view of nonsynchronous CCC. From Kazufusa et al., 2007.

A rotation/revolution ratio is shown as below:

$$\frac{r}{R} = -\frac{\omega_2}{2\omega_1 - \omega_2} \quad [\text{Equation 1.1.3.1a}]$$

A revolution mechanism of nonsynchronous CCC and the angular velocities of motors and rotary frames on nonsynchronous CCC are shown in Figure 1.1.11 and Table 1.1.1, respectively.

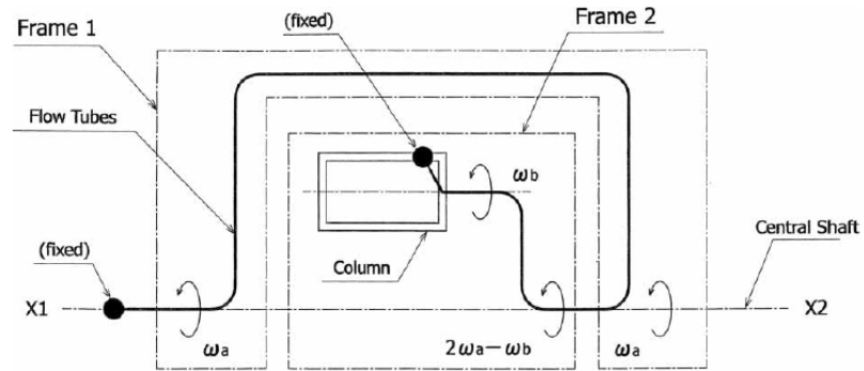


Figure 1.1.11. Revolution mechanism of nonsynchronous CCC. From Kazufusa et al., 2007.

Table 1.1.1. Angular velocities of motors and rotary frames on nonsynchronous CCC. From Kazufusa et al., 2007.

Main motor	Side motor	Rotary frame 1	Rotary frame 2	Column		
				Rotation	Revolution	Total
$+\omega_a$	0	$+\omega_a$	$+2\omega_a$	0	$+2\omega_a$	$+2\omega_a$
0	$+\omega_b$	0	$-\omega_b$	$+\omega_b$	$-\omega_b$	0
$+\omega_a$	$+\omega_b$	$+\omega_a$	$+2\omega_a - \omega_b$	$+\omega_b$	$+2\omega_a - \omega_b$	$+2\omega_a$

Therefore, as long as suitable ω_a and ω_b have been used, any combination of revolutionary and rotational speeds of column holder can be achieved.

1.1.3.2. Synchronous CCC design

By contrast from nonsynchronous CCC, in synchronous CCC, the rates of rotation and revolution are always synchronized, i.e., the column rotates once about its own axis during one revolution around the central axis of the centrifuge (Menet & Thiebaut, 1999). Details of designs of synchronous CCC are summarized in Figure 1.1.12.

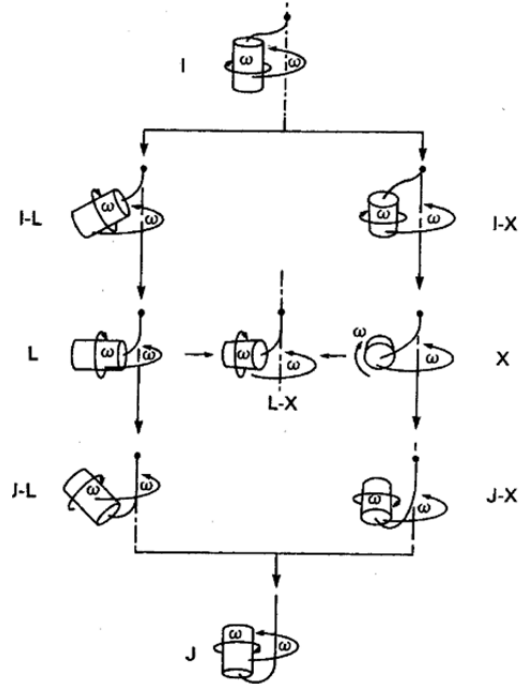


Figure 1.1.12. A series of synchronous seal free flow through CCC designs for performing hydrodynamic CCC in which the holder axis is inclined toward the centrifuge axis to form I-L, L, J-L in the left column and the holder axis is rotated while keeping the same distance to the central axis of the centrifuge to form I-X, X, J-X in the right column. From Yoichi & Ito, 1998.

The 3 relationships between the 2 rotational axes are: parallel (I, J), nonparallel (I-L, L, J-L, I-X, J-X) and crossed axis (X).

In the I-type design the holder rotates around its vertical axis and simultaneously revolves around the central axis of the centrifuge at the same rate but in the reversed directions (Menet & Thiebaut, 1999).

With the exception of the type I-X and J-X designs, prototypes of these centrifuge systems were constructed at the National Institute of Health and J-type and X-L type CCC were found to be most useful in terms of stationary phase retention and partition efficiency (Menet & Thiebaut, 1999).

i. J type CCC design

In 1980s, in order to seek an ideal combination between planet motion pattern and geometric position of columns, Ito developed a high performance CCC (J-type) to provide the same rate and direction of rotation and revolution, which he called “high-speed CCC.”

In order to reduce separation period, a new low volume capacity Milli-CCC[®] device was developed by the Brunel team in 2003 (Lee et al., 2003) with improved mechanical design and construction so that higher rotational speeds were possible enabling higher flow rates

to be used, giving faster separation times. Maximum rotational speed for Milli-CCC[®] J-type is 2100 RPM and stationary phase retention factor higher than 60% could be obtained with 1500 RPM and flow rates of 1 ml/min producing separation of compounds with K_D distribution coefficient of 1 in less than 5 min (Lee et al., 2003). This instrument has also been connected with mass spectrometer (CCC-MS). The cross-section of its rotor is shown in Figure 1.1.13.

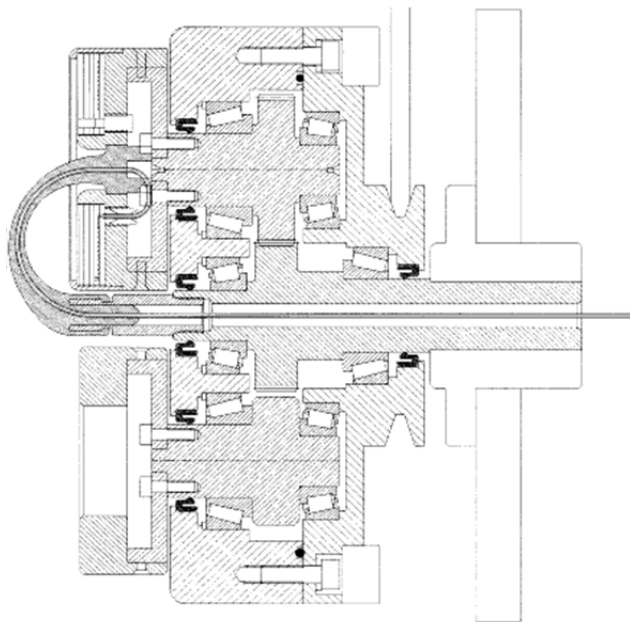


Figure 1.1.13. Cross section of prototype Milli rotor. From Lee et al., 2003.

One feature of this J-type Milli-CCC[®] compared to traditional CCC is its “cantilever” design, which means both bobbin and rotor are mounted on shafts at one end only while traditionally they are mounted on shafts at both ends (Lee et al., 2003).

With its simple design, mechanical reliability and easy maintenance, J-type CCC is the highest selling device in the world since 1980s (Menet & Thiebaut, 1999). However, although J-type CCC has made an important breakthrough by remarkably shortening separation times without sacrificing the partition efficiency (Ito, 1981; Ito et al., 1982), this system has been reported as failing to retain the polymer phase systems which are suitable for partitioning macromolecules (Skuse & Jones, 1992). Therefore, normally J-type CCC is considered to be better used for low molecular weight compounds with organic-aqueous solvent systems for natural and synthetic products. In recent years, ATPS was used successfully for J-type CCC in Brunel Institute for Bioengineering (BIB) (Bourton, 2008; Grudzień, 2011; Fernando, 2011). It suggests with special design for higher rotational speed, the failing retain problem for ATPS in J-type CCC was improved by BIB machines.

ii. X-L type CCC design

As the second most studied hydrodynamic apparatus, X-L type synchronous CPC (Coil Planet Centrifuge) which is also known as cross-axis CCC, is able to retain high viscosity ATPS stably and is applied to separate biological macromolecules and cells. The vertical axis of X-L type CCC and the horizontal axis of the column are always kept perpendicular to each other at a fixed distance (Menet & Thiebaut, 1999). As a synchronous apparatus, X-L type CCC provides the same rotational speed of the column as it revolves around the central axis and the column rotates on its own axis (Menet & Thiebaut, 1999). Depending on the ratio of L (lateral shift) and R (revolution radius), different types of cross-axis CCC can be obtained as shown in Figure 1.1.14.

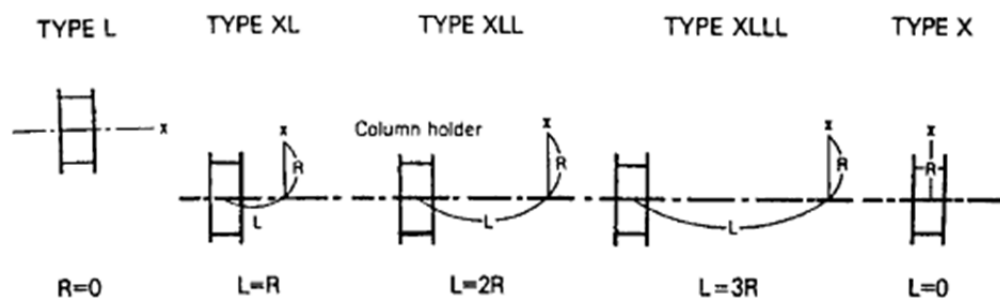


Figure 1.1.14. Orientation of the column holder in five different types of cross-axis CCC. R is the distance between the 2 axes and L is the distance of the lateral shift of the column holder along its axis. From Yoichi & Ito, 1998.

A cross-section view for a type of XLL cross-axis CCC made by Shibusawa is shown in Figure 1.1.15.

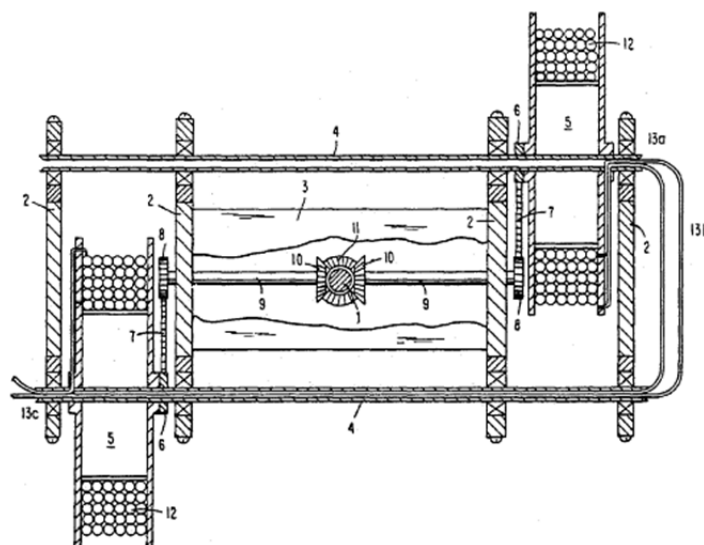


Figure 1.1.15. Cross-section of XLL cross-axis CCC. From Shibusawa et al., 1992.

The reason that different types cross-axis CPC were designed is that the X type CCC provides the most efficient mixing while the L type produces the most stable retention of the stationary phase due to its minimum mixing effects (Yoichi & Ito, 1998). Therefore, by selecting different choices of location of the column holder one can obtain different results for mixing and phase retention. By successful retention of ATPS, cross-axis CPC have been used for separation and purification of protein samples, including lactic acid dehydrogenase, recombinant enzymes, proflin-actin complex (Shibuswa & Ito, 2001).

1.1.4. Principle of hydrodynamic CCC

1.1.4.1. Air, liquid and bead in CCC

The column may be wound as a helical or spiral column (Figure 1.1.16). A slowly rotating column is filled with liquid and containing both an air bubble and a solid bead, both bubble and bead move to the same end of column, which is the head of a column.

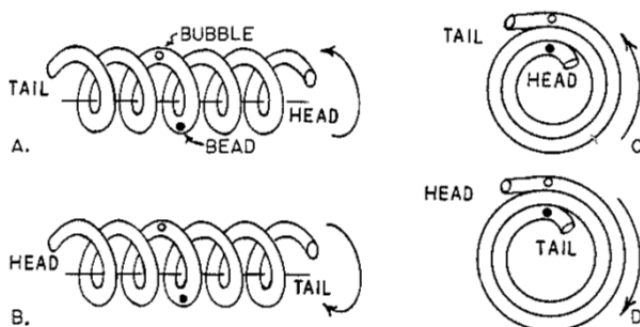


Figure 1.1.16. Characterization of the head and tail of helical and spiral columns. A bubble or bead moves to the head on rotation of the column. From Conway, 1990.

When the rotating column is filled with 2 immiscible phases, a competitive distribution happens between phases as both of them tend to move to the head but they cannot occupy the same position at the same time. Therefore, different distributions of 2-immiscible liquids form based on different rotational speed and design of columns, as shown in Figure 1.1.17 and Figure 1.1.18.

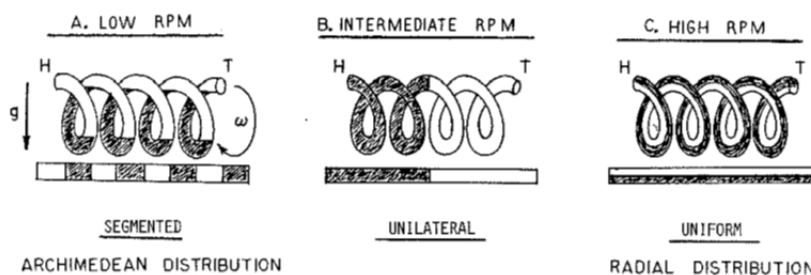


Figure 1.1.17. Distribution of equal volumes of heavy (shaded) and light phases of a two-phase system in a rotating helical column as a function of the rate of rotation. From Conway, 1990.

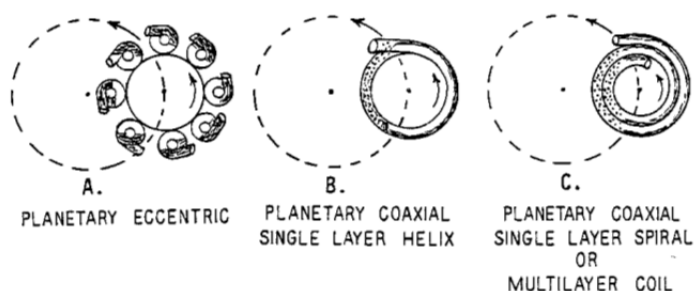


Figure 1.1.18. Distribution of heavy (shaded) and light phases of a two-phase systems in Countercurrent chromatographs at high rate of rotation. From Conway, 1990.

If mobile phase is pumped through the rotating column which is filled with stationary phase, then some of the stationary phases will be displaced until the hydrodynamic equilibrium is obtained. When compounds with different partition coefficients between stationary and mobile phases are injected into this system in the mobile phases, a compound that is only soluble in mobile phase ($K_D = 0$) will elute with the mobile phase and a compound that is only soluble in stationary phase ($K_D = \infty$) will stay in the column.

1.1.4.2. Distribution ratio

Therefore, the retention time of an analyte is based on its affinity to the 2 immiscible liquids system. The distribution constant or partition ratio (K_D) is the ratio of a concentration of an analyte in the stationary phase and the mobile phase at equilibrium. Retention time can be determined from K_D as follows (Grudzień, 2011):

$$R_T = \frac{K_D \cdot V_S + V_M + V_{extra}}{F}; [\text{min}] \quad [\text{Equation 1.1.4.2a}]$$

where R_T is retention time (min); K_D is distribution ratio (ml); V_S is stationary phase volume (ml); V_M is mobile phase volume (ml); V_{extra} is extra column volume (ml); F is mobile phase flow rate (ml/min).

1.1.5. Orbital motion and G field of hydrodynamic CCC

1.1.5.1. β and Orbital motion

The radius ratio β is an important parameter in CCC and is defined as

$$\beta = \frac{r}{R} \quad [\text{Equation 1.1.5.1a}]$$

where r is the distance from the planet axis to the centre of a particular layer of tubing in the column and R is the distance from the revolution axis and rotation axis, as shown in Figure 1.1.5.

With different values of β , different orbits can be obtained as shown in Figure 1.1.19.

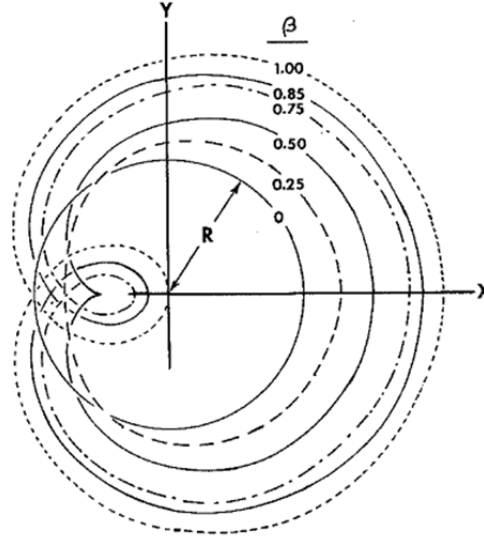


Figure 1.1.19. Orbits of an arbitrary point at various values of β on the planet gear column holder. From Conway, 1990.

1.1.5.2. Direction and magnitude of g-field

The planetary motion provides fluctuating g-fields. Taking J-type CCC as an example, the relationship between angle of g force vector - γ_r (equation 1.1.5.2a) and β value (Figure 1.1.20) and magnitude of g force (F) (equation 1.1.5.2b) (Figure 1.1.21) shows a transition is reached at $\beta = 0.25$. When $\beta = 0.25$, the direction of F changes from -90 to 90° while its magnitude drops to 0 (Conway, 1990).

$$\gamma_r = \tan^{-1}\left(\frac{-\sin\theta}{4\beta + \cos\theta}\right) \quad [\text{Equation 1.1.5.2a}]$$

where γ_r is the angle of g force vector and θ is the rotated angle to initial point.

$$F = R\Omega^2(1 + 8\beta\cos\theta + 16\beta^2)^{0.5} \quad [\text{Equation 1.1.5.2b}]$$

where F is magnitude of the resultant force and Ω is rotational speed of holder (RPM).

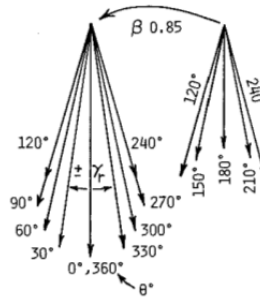


Figure 1.1.20a. Scale drawing of the force vector in different orbital position of the column holder and its angle γ_r . Vectors for reversed motion from 120° to 240° are displaced for clarity. From Conway, 1990.

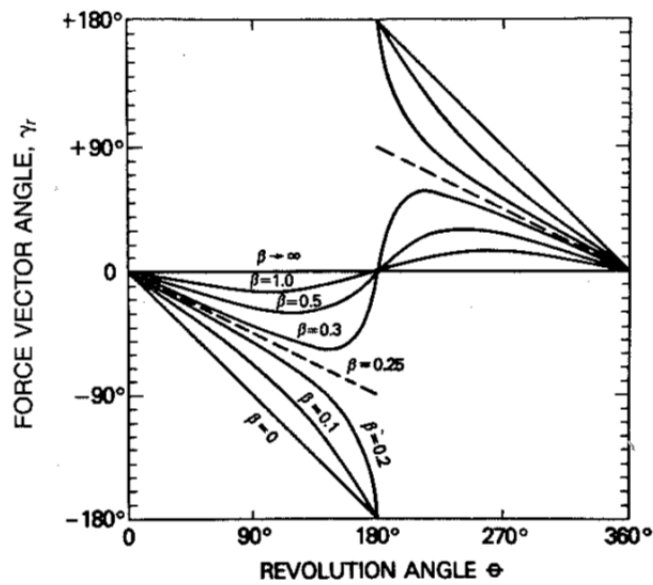


Figure 1.1.20b. Inclination, γ_r , of the force vector, F , to the radius, r , through the arbitrary point P , on the planet gear column holder. γ_r is shown for various β values during one orbit of the holder. From Conway, 1990.

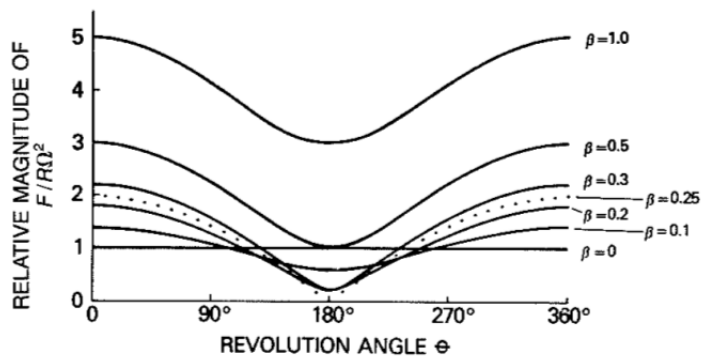


Figure 1.1.21. Magnitude of g force (F) on an arbitrary point P on the planet gear column holder as a function of the revolution angle. From Conway, 1990.

Therefore, in most locations, the vector is directed outwardly from the circle except for $\beta < 0.25$ where its direction is reversed (Menet & Thiebaut, 1999) as shown in Figure 1.1.22.

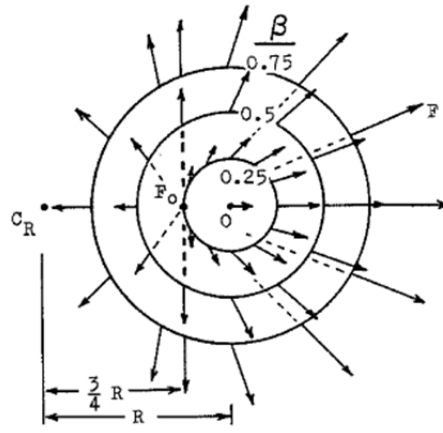
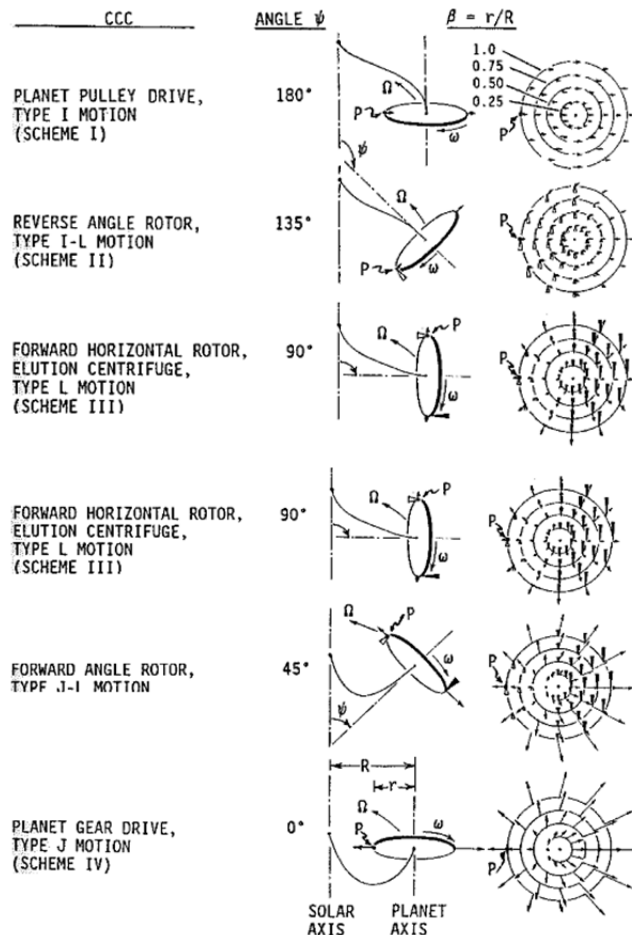


Figure 1.1.22. Relative magnitude and direction of the force vectors at various positions on planet gear column holder. At β below 0.25, the force vectors all face the same direction, and as β is increased beyond 0.25, the fields appears radial. From Conway, 1990.

The g-field for different hydrodynamic CCC design is shown in Figure 1.1.23. For example, the I-type always provides the same g-field directions for different β value. Since the different g-fields directions, the influence of column rotation mode is reported as neither retention nor separation of particles was observed for I-type and only J-type makes it possible to retain particles and selective elution by changing the separation conditions (Katasonova et al., 2003).



1.1.5.3. G-level calculation for CCC in nonsynchronous and synchronous modes

The calculation of g-field in nonsynchronous CCC has been described by van den Heuvel & Konig, (2011) as shown in Figure 1.1.24.

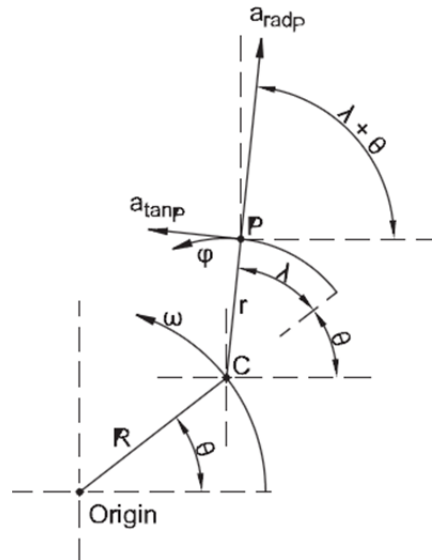


Figure 1.1.24. Motion of nonsynchronous centrifuge rotor. From van den Heuvel & Konig, 2011.

where R is radius of centrifuge rotor with point C as centre of column, θ , λ is displacement angle, ω , φ are rotational speeds. The relationship of rotational speed and g levels follows as:

$$g_{\text{radp}} = \frac{R(\omega^2(\cos(\varphi t) + \beta(\varphi + \omega)^2))}{9.807} \quad [\text{Equation 1.1.5.3a}]$$

$$\text{Max } g_{\text{radp}} = \frac{R(\beta(\varphi + \omega)^2 + \omega^2)}{9.807} \quad [\text{Equation 1.1.5.3b}]$$

$$\text{Min } g_{\text{radp}} = \frac{R(\beta(\varphi + \omega)^2 - \omega^2)}{9.807} \quad [\text{Equation 1.1.5.3c}]$$

$$\text{Mean } g_{\text{radp}} = \frac{R(\beta(\varphi + \omega)^2)}{9.807} \quad [\text{Equation 1.1.5.3d}]$$

$$g_{\text{tanp}} = -\frac{R\omega^2(\sin(\varphi t))}{9.807} \quad [\text{Equation 1.1.5.3e}]$$

where R is radius (m), ω and ϕ are rotational speed (rad/s), β is the diameter ratio between column and rotor and 9.807 is gravitational acceleration (m/s^2) (van den Heuvel & Konig, 2011).

Although the above equations were established for nonsynchronous CCC they can be extended to synchronous CCC: when $\omega = \phi$, the angular velocities of rotor and column are equal and, nonsynchronous CCC becomes a J-type CCC. Similarly when $\omega = -\phi$, nonsynchronous CCC can be considered as I-type CCC. J-type CCC with same β -value or with different β -values and nonsynchronous CCC were calculated and compared with equations (1.1.5.3b) – (1.1.5.3d) (van den Heuvel & Konig, 2011). Therefore, via this calculation method, a relationship between rotational speed and g level has been established.

1.1.5.4. Liquid distribution and phase mixing in the column

The influence of rotation on the liquid flow is important to consider. The Archimedean screw effect generated by the rotation transports the contents of the column towards to the head end of column (Wood, 2010). The dependence of tangential velocity on β -value is shown in Figure 1.1.25.

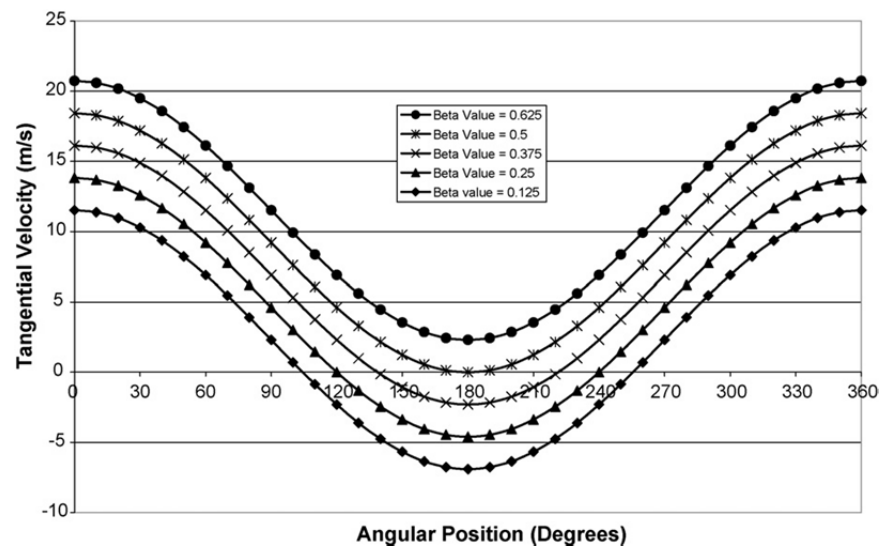


Figure 1.1.25. Variation of the tangential velocity with angular position in the column for J-type centrifuge for a 110 mm rotor radius and a rotational speed of 800 RPM. The dependence of this variation on beta values is shown for beta values from 0.125 to 0.625. From Wood, 2010.

Figure 1.1.25 shows that the direction of the tangential velocity changes when the β -value is smaller than 0.5. Thus when the β -value is greater than 0.5, the Archimedean screw effect is consistent with the upper phase always migrating to the head. Therefore, although the g-field direction does not change if β -value is greater than 0.25 as shown in Figure

1.1.21, from β -value between 0.25 to 0.5, the screw effect pushes the contents to one end but also to the other end when the tangential velocity is negative (Wood, 2010) may lead to a failure of retaining contents. Therefore, a β -value < 0.5 should be avoided.

Figure 1.1.25 shows that the maximum tangential velocity was obtained when the rotation degree is 0° , which is the start position of rotation and also gives the greatest g-field. The minimum tangential velocity was obtained when the rotation degree is 180° which is the position that generates the minimum g-field.

The relationship between mixing zone (the liquid mixing area in two phases system) in the column and the direction and magnitude of g-field (β 0.5-0.85) is shown in Figure 1.1.26.

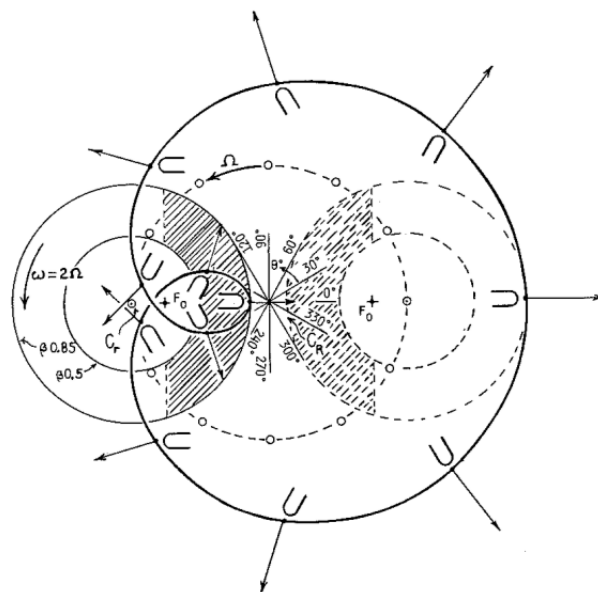


Figure 1.1.26a. Magnitude and direction of the resultant force vectors for $\beta = 0.85$ in the planet gear chromatography and the visually observed mixing zoon in multilayer-coil columns (shaded area). From Conway, 1990.

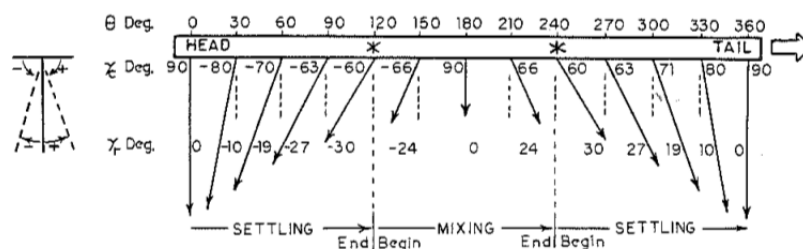


Figure 1.1.26b. The uncoiled column moving in a tailward direction relative to the settling and mixing area. From Conway, 1990.

The mixing zone is the shaded area in Figure 1.1.26. “For counter-clockwise rotation of the apparatus, the force vector swings to the left diminishes the intensity and reaches a maximum γ_r when θ is about 120° . The vector then swings back toward the right, and the

mixing commences at the start of the rightward swing. After the g-field is minimum in magnitude when θ is 180° , the rightward limit of γ_r is reached at θ of 240° where the phase mixing ceases at this point and force vector begins its leftward swing.”(Conway, 1990) (Figure 1.1.26). Thus, Figure 1.1.26 shows the connection between the fluctuating g-field and mixing zone in the column giving more detail than Figure 1.1.7 which describes the mixing zone in the column.

1.2. Introduction of red blood cell

Red blood cells, also known as erythrocytes, often are abbreviated as RBC. In all vertebrates and some invertebrates, these cells contain haemoglobin. RBCs are the largest group of blood cells. Blood can be mainly separated into 3 main parts by centrifugation: an upper liquid component called plasma; a thin cell layer containing white blood cells and platelet, often called the “buffy coat”; and the lowest cell layer of RBCs. RBCs are important for transportation for oxygen through blood in vertebrates. Other blood cells, such as white blood cells, are immune cells. RBCs concentrations are often measured clinically by the haematocrit (hct), which is the percentage of red blood cells in whole blood, determined by centrifuging blood and measuring the volume of the sedimented RBCs and expressing as a % of the whole blood volume.

Mature mammalian RBCs lack a cell nucleus, which means they have no DNA. They also lack mitochondria and all other subcellular structures. They have 2 main metabolic pathways and can synthesize energy (as ATP and reduced coenzymes) from glucose by glycolysis and the hexose monophosphate shunt.

i. Red blood cells for vertebrates

Mammalian red blood cells are biconcave disks. They have nucleus when they are in hematopoietic tissue (as reticulocytes), but on entering the circulation the nucleus is gradually lost. By contrast, RBCs for birds are oval shaped which protrudes to both sides from middle and contain a nucleus.

The size of RBCs varies in different animal species (Klein et al., 1968) as listed in table 1.2.1. Generally, animals with large RBCs have less cells number in unit volume of blood.

Table 1.2.1. Mean corpuscular volume or mean cell volume (MCV) for red blood cells in different species.

Species	Human ^a	Dog ^d	Cat ^d	Rhesus ^d	Baboon ^d	Swine ^d	Sheep ^d
MCV (fL)	80-100	65-80	65-80	72-86	71.2-82.8	50-68	23-48
Species	Cow ^d	Rabbit ^b	Guinea pig ^d	Hamster ^d	Rat ^d	Mouse ^d	Hen ^c
MCV (fL)	40-60	50-75	78-95	67-77	48-70	41-49	133-148

a) From RBC indices, n.d.

b) From Complete blood count and biochemistry reference values in rabbits, n.d.

c) From Nowaczewski & Kontecka, 2012.

d) From Reference values for laboratory animals, n.d.

ii. Red blood cells for human

Human RBCs are biconcave discs with thicker edges and thinner middles, rather like a doughnut but without a hole. This shape provides a large ratio of surface area to volume, which supports O₂ and CO₂ movement inside and outside of the RBCs. It also has excellent flexibility in order to facilitate cell movement through capillaries, particularly in the spleen. Membranes for RBCs contain glycoproteins and glycolipids which show variations for individuals and gives rise to various blood groups.

Adult contains about 2-3E+13 RBCs (female has 4-5 million/mm³ and male has 5-6 million/mm³) (Snyder & Sheafor, 1999). The reason female has less RBCs per volume is due to physiological bleeding in women (menstruations) and the effect of testosterone in men which stimulates erythropoiesis.

iii. Osmotic fragility

Osmotic pressure for RBCs roughly equals osmotic pressure for plasma in normal status, which is very important to maintain shape of RBCs. To maintain the shape and volume of isolated RBCs they must be re-suspended in medium that is isotonic with that of plasma such as 0.85% ~ 0.9% NaCl solution (0.15M NaCl) or 5% glucose solution or 0.3M sucrose solution. A solution of lower osmotic pressure is called a hypotonic solution. This causes RBCs to swell as water enters to equalise the osmotic pressure inside and out. At a critical low tonicity solution, the membrane can expand no more and the cell ruptures with release of haemoglobin, a process called haemolysis. A solution of higher osmotic pressure to plasma is called a hypertonic solution, which can lead to dehydration of the RBC and shrinkage.

The osmotic fragility of RBC is determined by placing RBCs in solutions of decreasing concentrations of NaCl (from 0.85%, 0.8% 0.3% w/w). Some RBCs will begin to rupture at 0.45% solution, and a supernatant after the cell debris is spun down is slightly red. For concentrations lower than 0.35%, all RBCs are broken. Therefore, 0.45% to 0.35% NaCl solution is the range of brittleness (resistance) for normal human RBCs (Blanchette et al., 1995). If RBCs rupture in solution which is higher than 0.45%, it means the RBCs has larger brittleness and smaller resistance; if RBCs rupture in solution which is lower than 0.35%, it means RBCs has larger resistance and smaller brittleness.

iv. Suspension stability at unit g

After mixing blood with an anticoagulant and standing the tube vertically, due to the higher density of the RBCs than the medium, the cells gradually sink. The distance of

sinking in unit time for RBCs is called the erythrocyte sedimentation rate (referred as ESR). The ESR gives an indication of RBC suspension stability. During pregnancy, active tuberculosis, rheumatic fever and suffering cancer, ESR is accelerated. Therefore, ESR helps diagnosis and prognosis on clinical examination.

An important contribution to maintaining a suspension of RBCs is the surface of RBCs which is negatively charged surface, due to the presence of negatively charged sialic acids on surface located glycoproteins and glycolipids. Therefore, RBCs are not easy to agglutinate, and negatively charged RBCs show good suspension stability. If positively charged protein increases in the plasma and is adsorbed by RBCs in plasma, the surface charge is reduced and aggregation of RBCs is promoted, leading to an increase in ESR.

1.3. Behaviour of cell and particle in rotating columned column

1.3.1. Introduction

The cell, as the fundamental functional unit of all known living organisms, is the “building blocks of life”. Organisms such as plants or animals consist of a great number of different kinds of cells (Bauer, 1999). In the “concert” of life, each cell type shows their special features and distinct functions, and understanding of mechanism of life depends on knowledge about each single type of plant and animal cells, therefore, the knowledge of gathering each cell type separately is a permanent task of science (Bauer, 1999).

Compared to chemical molecule separations, cell separation is unique since there are no 2 exactly same cells in the world (Sharpe, 1988). A molecule population can be defined by the same structure, and can be separated from other, different molecules with different structures (Fisher et al., 1998). However, it turns out to be a tricky question when we are trying to define and separate the “same” cell or one “type” of cell from others since there is no cell populations that can be considered as a pure population unless this population includes only one cell (Sharpe, 1988). Therefore, when a cell population is mentioned, the cells which this population includes may share certain features (function, density, etc.), such as T-lymphocytes which can be separated from whole blood. But this population will also include different subsets (Sharpe, 1988) in which different individual cells may also be in different stages of the cell cycle (Sharpe, 1988). Therefore, the character of cell separation is quite different from soluble material separations as it is difficult to define an absolute population or even measure an indisputable purity at all (Sharpe, 1988).

Although different cell separation methods have their own principles, and they may have much better separation performance for certain special cell separations than others, all cell separation methods can be considered as 2 processes: 1) amplify the existing different behaviour for each cells and 2) obtain the desired cells from the rest (Sharpe, 1988). Except separations methods based on DNA content, all cell separation methods either distinguish cells from others by size and/or density or the presence or absence of certain specific cell surface molecules. The former includes centrifugation, unit gravity sedimentation, centrifugal elutriation, field-flow fractionation, etc. and the latter separates cells by aqueous two-phase partition (by ATPS), electrophoresis, affinity chromatography, flow sorting, etc.

Counter-Current Chromatography (CCC) is a form of support free liquid-liquid partition chromatography in which stationary liquid phase is retained in a long tubular column by

gravitational or centrifugal force, while a second immiscible, mobile liquid phase is pumped through the column (Ito, 2007; Shibuswa & Ito, 2001). Since the introduction of CCC in 1970 (Ito, 1991), a range of biological samples has been separated in CCC by using various aqueous two-polymer phase systems (Table 1.3.1):

Table 1.3.1. Range of biological samples separated by CCC using Aqueous Two-Phase Systems.

proteins	Sutherland & Ito, 1978; Ito, 1979; Sutherland, 1985; Shinomiya et al., 2003
lipoproteins	Shibusawa et al., 1995; Shibusawa, 1997
nucleic acids	Ito, 1980; Ito, 1981
polysaccharides	Sutherland & Ito, 1978
bacteria	Sutherland & Ito, 1978; Sutherland & Heywood-Waddington, 1987
cell particles	Ito, 1981; Sutherland & Ito, 1980; Harris et al., 1984; Sutherland & Heywood-Waddington, 1987; Shinomiya et al., 2005; Shinomiya et al., 2007;

The different polymer-phase systems available the PEG [poly(ethylene glycol)]-dextran and PEG-phosphate systems have been most commonly used for partition of biological samples (Table 1.3.2):

Table 1.3.2. Separations of biological samples using PEG-dextran and PEG-phosphate Aqueous Two-Phase Systems.

cells	Harris et al., 1984; Sharpe, 1984; Van Alstine et al., 1985; Pascual et al., 1994; Petrov & Pinaev, 2002
protein	Wilkes et al., 1982; Shibusawa & Ito, 1998; Menet, 2001; Shinomiya et al., 2003; Shinomiya et al., 2007
subcellular organelles	Heywood-Waddington et al., 1986; Sutherland & Heywood-Waddington, 1987;
bacteria	Stendahl et al., 1973; Leive et al., 1984

Separations have been made in a range of CCC and CCD machines (Table 1.3.3):

Table 1.3.3. Examples of the use of CCC and CCD machines to separate biological samples using Aqueous Two-Phase Systems.

CounterCurrent Chromatography (CCC)	Sutherland & Ito, 1978; Sutherland & Ito, 1978; Sutherland & Ito, 1980; Sutherland & Heywood-Waddington, 1987
CounterCurrent Distribution (CCD)	Sancho et al., 1986; Isabel et al., 1998
Thin layer CounterCurrent Distribution (TLCCD)	Sharpe, 1984
Centrifugal CounterCurrent Distribution (CCCD)	Ollero et al., 1994; Perez-pe et al., 2001; Grasa et al., 2005

In addition to the use of two-phase systems, separations have also been achieved by CCC in a single liquid phase, in a field flow fractionation mode (Table 1.3.4).

Table 1.3.4. Separations of biological samples by CCC in a field flow fractionation mode in a single phase.

red blood cell	Ito et al., 1979; Ito et al., 1980; Ito et al., 1983
mast cells	Okada et al., 1996; Shinomiya et al., 2007
components of blood	Shinomiya et al., 2005

Chapter 1.3 mainly reviews the behaviour of cell/particles (Ito et al., 1966; Ito et al., 1983; Fedotov et al., 2000; Katasonova et al., 2003; Fedotov et al., 2010) in CCC by ATPS and single phase, and also includes related performance of cells (Ito et al., 1975; Ito et al., 1977) and a density cell separation method under g-field which has been developed by Ito (Ito & Shinomiya, 2001; Shiono et al., 2005; Shiono et al., 2007).

1.3.2. Cell separation in non-synchronous Counter-Current Chromatography (NSCCC) by aqueous two-polymer phase system (ATPS)

1.3.2.1. ATPS for cell separation and design of CCC for ATPS

“Gentle” separation environment is the essential requirement of cell separation. Mixture of aqueous solutions of two polymers, such as dextran and polyethylene (PEG) above critical concentrations form two-phase systems, in which one phase is rich in dextran, the other rich in PEG. These provides a suitable environment for cell separation (Leive et al., 1984) as they have high water content and have been found to maintain many properties of the biomaterials. The cells and cell organelles are separated by their partition in ATPS, as the separation is based on surface properties rather than merely size and density. The cell separation by ATPS was initially achieved by on Countercurrent distribution (CCD) and successfully separated a wide range of cells (Walter et al., 1985). After CCC was developed, it was used to separate whole cells.

However, although the polymer phase systems provide an ideal environment for live cells, the high viscosity and low interfacial tension between the two phases tend to cause a loss of stationary phase from the column in the J-type CCC (Shibuswa & Ito, 2001) which limits separation performance.

By contrast the cross axis CPC, with column holders at the off-centre position on the rotary shaft (Figure 1.1.4), enables retention of the stationary phase of ATPS (Shibuswa & Ito, 2001). Over the years, various types of cross axis CPC have been developed, including T types X, XL, XLL, XLLL and L (Shibuswa & Ito, 2001) with different ratio of L/R where L is the measure of the lateral shift of the column holder along its axis and R is the distance between the axis of the column and axis of the apparatus (Menet & Thirbaut, 1999). By successful retention of ATPS, cross-axis CPC has been used was used for the separation and purification of protein samples, including lactic acid dehydrogenase, recombinant enzymes and profilin-actin complex (Shibuswa & Ito, 2001).

1.3.2.2. Bacterial cell separation by toroidal column centrifuge

In 1978, Sutherland and Ito reported a separation of two strains of *E. coli* (ATCC 8739 & ATCC 11303) by ATPS (Sutherland & Ito, 1978, Sutherland et al., 1987). They used a toroidal column CCC with a 200-coiled column of 1-mm i.d. PTFE tubing. The basic phase system used consisted of 5% (w/w) dextran 500, 4% (w/w) PEG 6000, and 0.01M potassium phosphate (pH 6.9) (Sutherland et al., 1987).

The partition of the two strains of *E. coli* is shown in Figure 1.3.1.

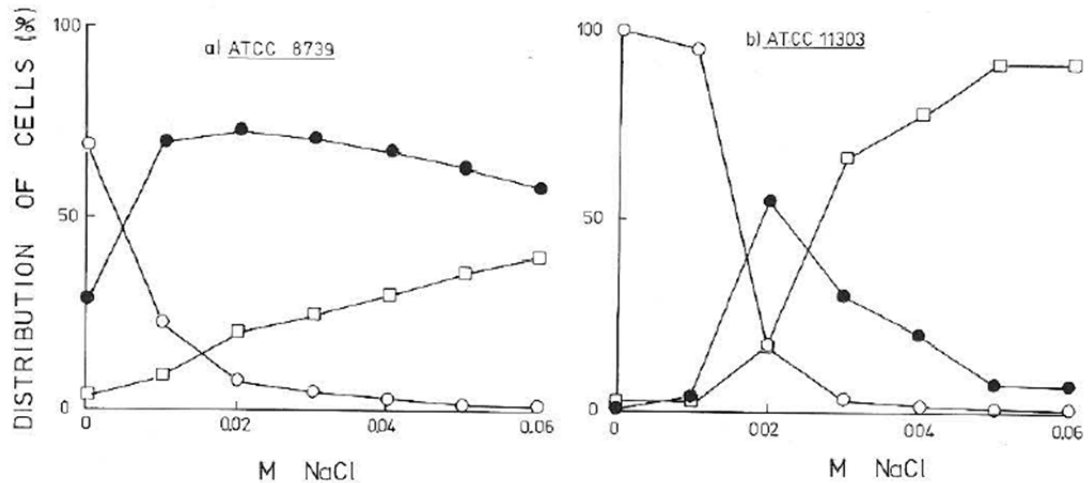


Figure 1.3.1. The distribution of two different strains of *E. coli* in a two-phases polymer system, where (○) in upper phase; (●) at interface; (□) in lower phase. From Sutherland et al., 1987.

As Figure 1.3.1 shows, both strains were partitioned towards the upper phase at zero NaCl concentration. As the NaCl concentration was increased ATCC 8739 partitioned predominantly toward the interface at a concentration greater than 0.005M whereas ATCC 11303 required NaCl concentration of 0.015M to cause it to move to the interface (Sutherland et al., 1987).

This difference in sensitivity to NaCl concentration was exploited in the method developed by using a gradient of increasing NaCl concentration ATCC 8739 was retained in column when a NaCl concentration of 0.06M was used (Sutherland et al., 1987). The column was filled with the heavier dextran phase at 0.02M NaCl concentration and the centrifuge rotated at 750 RPM with a column rotation of 5.25 RPM initially. Concentration was then decreased to 0M gradually (Figure 1.3.2) while the mixture of two *E. coli* strains was injected with mobile phase while the flow rate was 14 ml/h (0.23 ml/min) (Sutherland et al., 1987). The separation obtained is shown in Figure 1.3.2 and the reproducibility of CCC

run results for both two strains separation result was 93% when rerun separately (Sutherland et al., 1987).

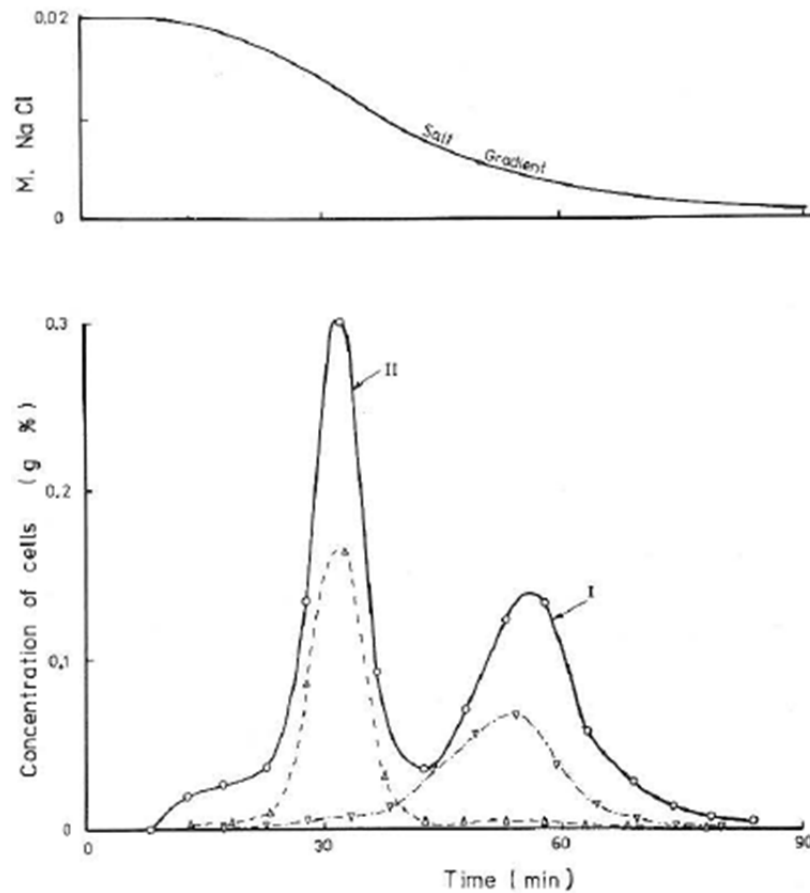


Figure 1.3.2. A gradient separation of a mixture of two strains of E.coli cells, where (○) mixture of ATCC 8739 (I) and ATCC 11303 (II); (▽) rerun of I; (△) rerun of II. From Ref Sutherland et al., 1987; Sutherland & Ito, 1978.

1.3.2.3. Erythrocyte separation by Nonsynchronous CCC

In 1980, Sutherland and Ito reported separations of dog/human/sheep red blood cells in a nonsynchronous flow through coil plant centrifuge (the same machine was used in 1.3.2.2) (Sutherland & Ito, 1980). A cross-sectional view of this machine is shown in Figure 1.3.3. The separation column was prepared using an 18-m-long, 1mm i.d. PTFE tube, wound onto 6-mm o.d. cores, giving about 600 turns with a total capacity of 16.2 ml (Sutherland & Ito, 1980).

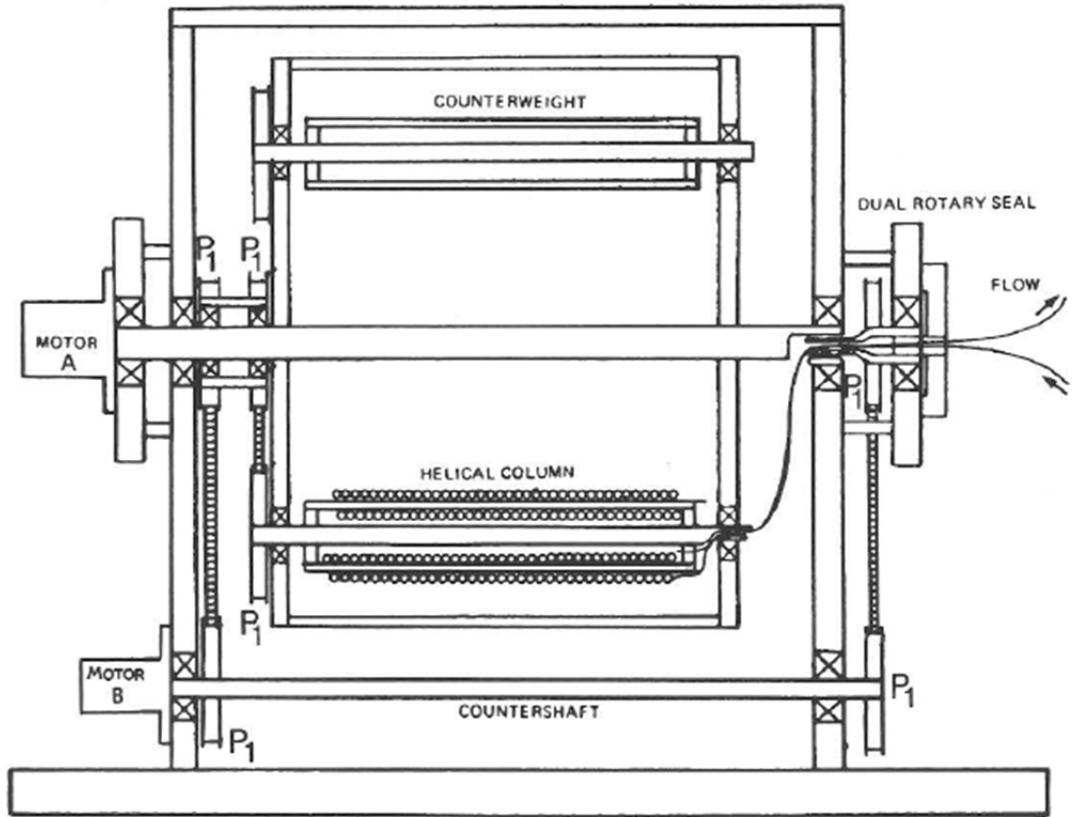
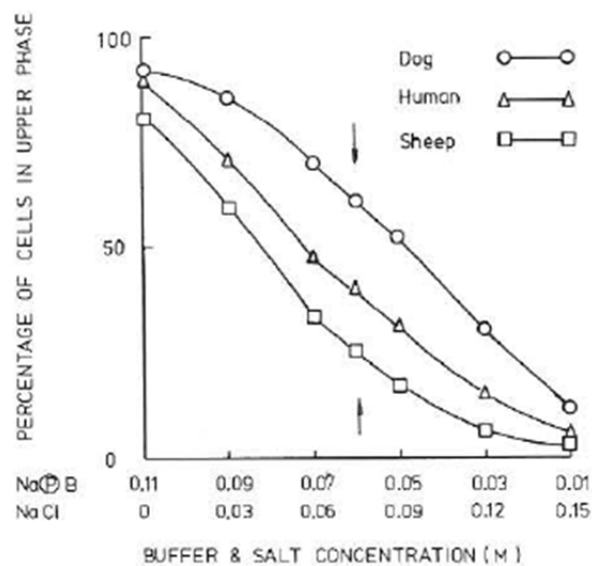


Figure 1.3.3. Cross-sectional view of the nonsynchronous flow through coil planet centrifuge. From Sutherland & Ito, 1980.

Partition is ATPS formed by PEG 6000 and dextran 500 in isotonic phase systems of varying composition of sodium phosphate buffer and NaCl showed that a composition of 0.06M phosphate and 0.07M NaCl gave the largest differences in the distribution of RBCs between the phase with top (PEG) phase partitions of 61% dog, 40% human and 25% sheep (Figure 1.3.4) and was used to separate dog and sheep RBC, and dog and human RBC.



T, the column was filled with the stationary phase (heavier dextran rich phase) with the centrifuge stationary while the centrifuge was then started with revolution 750 RPM (motor A) and rotation at 10 RPM (with motor B at 740 RPM) (According to the design (Figure 1.3.3), if motor (A) rotates at (Ω) and motor (B) at (ω), the helical column will rotate at ($\Omega-\omega$)) (Sutherland & Ito, 1980). About 1 ml of mobile phase (the PEG-rich lighter phase) was pumped into the column and rotation stopped during sample injection, then restarted. The flow was then allowed to continue for about 1ml after elution, when the centrifuge (motor A) was stopped and the column contents pumped out with the column (motor B) rotating at about 60 RPM. The separations of sheep and dog RBCs and human and dog RBCs separation are shown in Figure 1.3.5 and Figure 1.3.6, respectively A flow rate of 14 ml/min was used for the sheep/dog RBC separation but this was reduced to 7 ml/min for the dog/human RBC separation as their partitions were closer, and the lower flow rate was used to increase the retention of stationary phase, with consequent increased resolution (Sutherland & Ito, 1980). For erythrocyte separation, the mobile phase pumping process was stopped before elution and the column contents were pumped out (Sutherland et al., 1987). They also noticed the peaks would spread out when the elution process was extended and explained it as sedimentation effects in the outlet tubing.

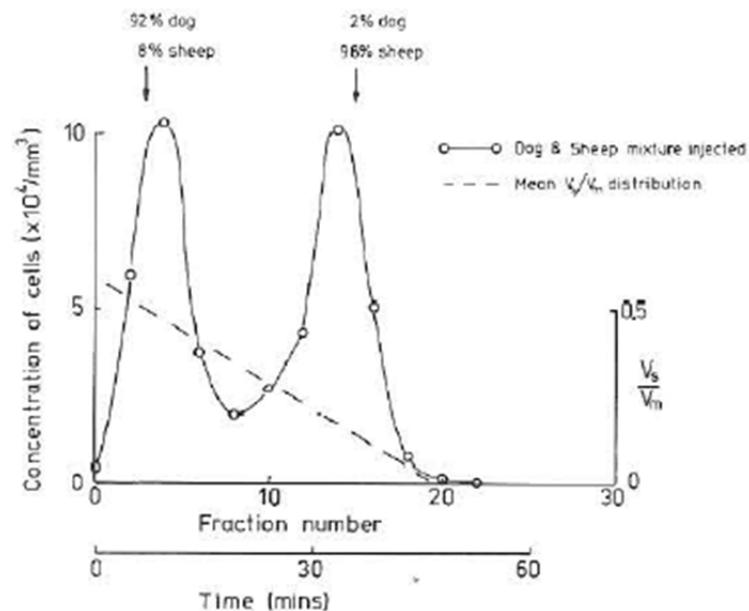


Figure 1.3.5. Results of sheep/dog RBCs separation. Separation of a 20% mixture of packed sheep and dog RBCs using 5% (w/w) Dextran 500 – 4% (w/w) PEG 6000 at 0.075M NaCl phase system. The flow rate was 14 ml/h with a centrifuge speed of 740 RPM and column rotation 10 RPM. Fractionated samples were collected per 2.5 min. From Sutherland & Ito, 1980.

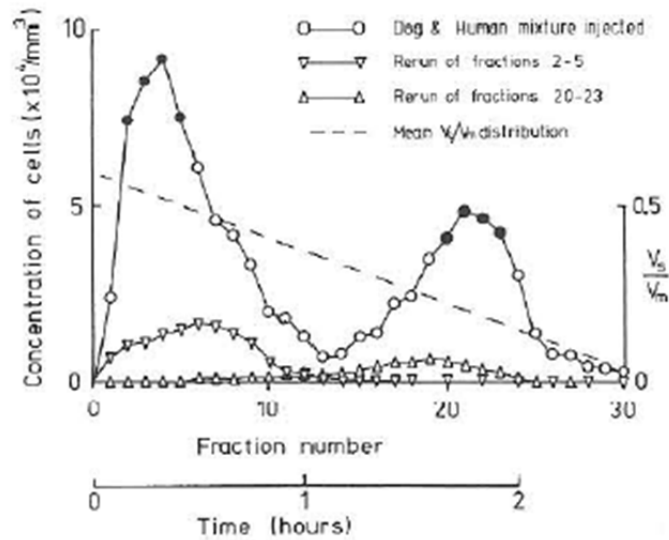


Figure 1.3.6. Results of human/dog RBCs separation. Separation of a 20% mixture of packed human and dog RBCs using 5% (w/w) Dextran 500 – 4% (w/w) PEG 6000 at 0.075M NaCl phase system. The flow rate was 7 ml/h with a centrifuge speed of 740 RPM and column rotation 10 RPM. Fractionated samples were collected per 5 min. From Sutherland & Ito, 1980.

Both results show successful separations of the RBCs mixture as Figure 1.3.5 shows 92% of cells eluted first peak were dog RBCs and 98% of cells retained sheep RBCs and the separation of dog and human RBCs was confirmed by the eluting peaks in the mixture occurring in similar positions to those obtained with dog and human RBCs run separately.

The same machine was applied to separate human/sheep RBCs in single phase and the comparison and discussion will be continued when introducing cell separation by CCC in single phase.

4 years later after Sutherland and Ito reported their erythrocyte separation, in 1984, Harris et al. (1984) reported studies made on repeating this sheep/dog RBCs separation. The same machine and revolution/rotational speed were used for both two RBCs separations, while the flow rate for the studies by Harris et al. was 8 ml/h which was much slower than the flow rates of 14 ml/h used earlier by Sutherland and Ito. Except the basic ATPS (5% (w/w) Dextran 500 – 4% (w/w) PEG 6000), latter (Harris et al.) used 0.07M phosphate and 0.06M chloride (Harris et al., 1984) instead of 0.075M NaCl (Sutherland & Ito, 1980). The results of these two sheep/dog RBC separations are shown in Figure 1.3.7.

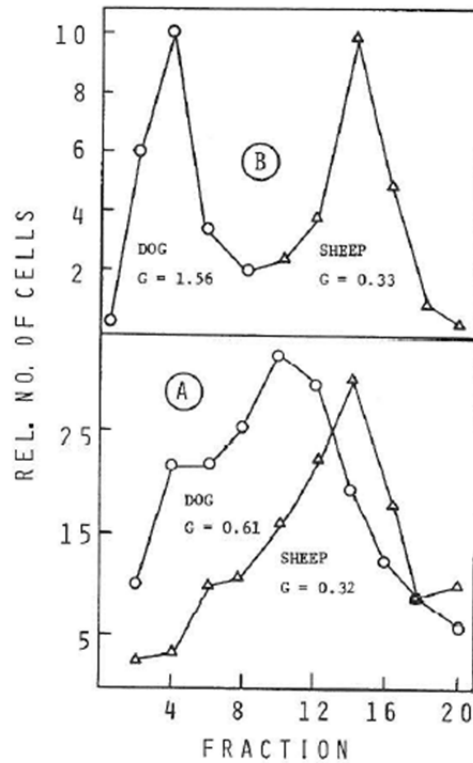


Figure 1.3.7. Separation results of fresh sheep/dog RBCs as done by Sutherland & Ito (B) Separation of a 20% mixture of packed sheep and dog RBCs using 5% (w/w) Dextran 500 – 4% (w/w) PEG 6000 at 0.075M NaCl phase system. The flow rate was 14 ml/h with a centrifuge speed of 740 RPM and column rotation 10 RPM. Fractionated samples were collected per 2.5 min and Harris et al. (A) Separation of a mixture of sheep and dog RBCs using 5% (w/w) Dextran 500 – 4% (w/w) PEG 6000 at 0.07M phosphate and 0.06M chloride. The flow rate was 8 ml/h with a centrifuge speed of 740 RPM and column rotation 10 RPM. From Harris et al., 1984.

Interestingly Sutherland and Ito obtained the better separation. Harris et al. (1984) discussed the reason of those difference as Sutherland and Ito's phase system (4.7/3.8) (as water content of polymers in Sutherland and Ito experiment was not accounted for their preparation of 5/4 system (Harris et al., 1984)) was nearer the critical point than Harris et al. (5/4) (Harris et al., 1984). Also, in Sutherland and Ito's paper, they used flow rate as 14 ml/h to obtain a better retention while the flow rate for Harris et al. was 8 ml/h, which suggests the separation was sensitive to operational conditions.

1.3.2.4. *S. typhimurium* separation by Nonsynchronous CCC

In 1984, Leive et al. reported a separation between *Salmonella typhimurium* G30 containing long chain LPS (Lipopolysaccharide) from those containing short chain LPS by CCC (Leive et al., 1984) *S. typhimurium* cultured in the presence of galactose, makes a normal lipopolysaccharide; whereas in its absence, it makes a short chain terminated at the point of addition of the first galactose in the molecule (Ito et al., 1983). Bacteria with these

different lipopolysaccharides show different partition (Ito et al., 1983). The machine used was prepared from 1 mm i.d. PTFE tubing by winding onto 6 units of 20 cm long, 0.6 cm o.d. stainless steel pipe cores in a series to make about 600 helical turns with a total capacity of approximately 15 ml (Leive et al., 1984). In the experiment, the polymer phase system was 6.2% (w/w) dextran 500, 4.4% (w/w) PEG 6000, 0.5M Tris-chloride (pH 7.0), 10mM potassium phosphate (pH 7.0), and 0.01% sodium azide (Ito et al., 1983; Leive et al., 1984).

Different to typical Countercurrent Chromatography operation, Leive et al. filled the column with equal amounts of the upper and lower phases by 20 ml syringe (10 ml of each phase) initially and then the sample suspension in equal amounts of two phases was injected into the column (Leive et al., 1984). Then the upper mobile phase was pumped at 8.5 ml/h while the column was rotated at 600 RPM for revolution with 5 RPM rotation (Leive et al., 1984), and the contents in column were eluted after 30 fractions by syringe with equal volume mixture of the two phases (Leive et al., 1984). Their separation results are shown in Figure 1.3.8.

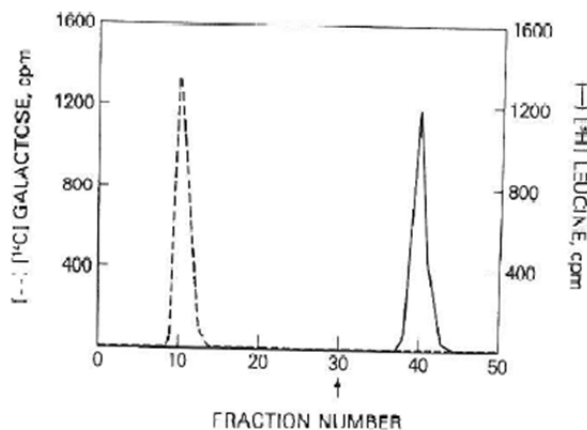


Figure 1.3.8. Separation of cells of *S. typhimurium* G30 containing long/short chain LPS. Separation by using 6.2% (w/w) dextran 500, 4.4% (w/w) PEG 6000, 0.05M Tris-chloride (pH 7.0), 10mM potassium phosphate (pH 7.0), and 0.01% sodium azide. 1 ml sample suspension in equal amounts of the two phases was injected into the column after the column was filled with the upper and the lower phases equally. Then set the revolution as 600 RPM with rotation was 5 RPM and pumping the upper mobile phase at 8.5 ml/h. Fractionated sample was collected 1 ml per tube. From Leive et al., 1984.

This method completely separated long chain LPS bacteria cells from the short chain LPS bacteria as the left peak was long chain bacteria while the right peak was short chain bacteria with resulting in near 100% cell recovery (Leive et al., 1984).

A similar separation was achieved by Ito et al., (1983) using the same 2 phases system (6.2% (w/w) dextran 500, 4.4% (w/w) PEG 6000, 0.05M Tris-chloride (pH 7.0), 10mM

potassium phosphate (pH 7.0), and 0.01% sodium azide) and operation, but the column was rotated at 1000 RPM with column rotation of 5 RPM under 8.5 ml/h flow rate (Figure 1.3.9).

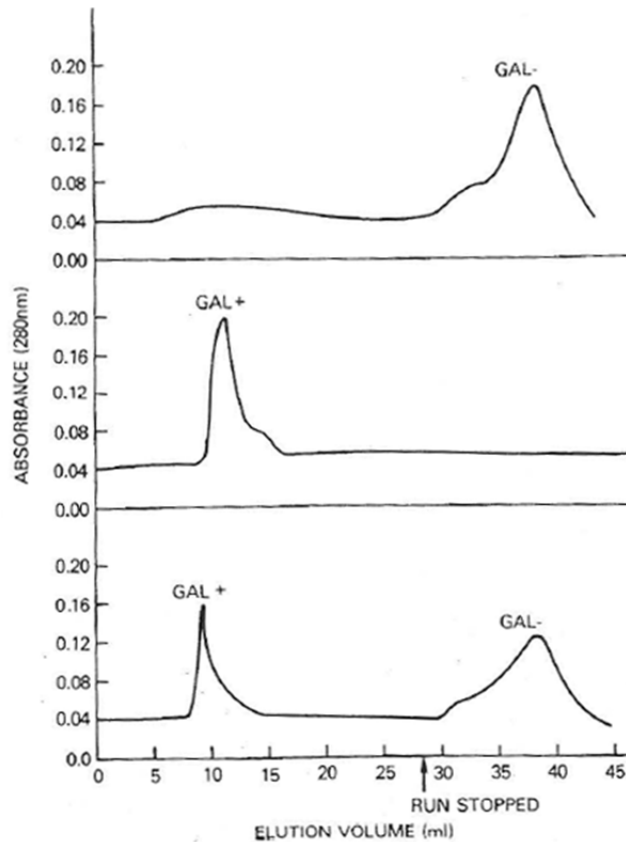


Figure 1.3.9. Separation of *S. typhimurium* strain on the polymer phase system with the nonsynchronous flow through coil planet centrifuge. 6.2% (w/w) dextran 500, 4.4% (w/w) PEG 6000, 0.05M Tris-Cl (pH 7.0), 10mM potassium phosphate (pH 7.0), and 0.01% sodium azide. 1 ml of mixture of galactose(+) and galactose(-) sample suspension in upper phases was injected into the column at 8.5 ml/h after the column was filled with the upper and the lower phases equally. Then set the revolution as 1000 RPM with rotation was 5 RPM. From Ito et al., 1983.

S. typhimurium cultured on the galactose deficient media (gal-) distributed at the interface or the lower stationary phase, therefore retained in the column (top). The same strain of cells cultured on galactose containing media (gal+) develops lipopolysaccharide outer layer which alters their partition behaviour so that they distribute in the upper mobile phase, and therefore are eluted from the column (Figure 1.3.9 middle). Figure 1.3.9 (lower) also shows that the two forms of *S. typhimurium* could be separated into two peaks as when they run separately (top & middle) (Ito et al., 1983).

1.3.3. Cell separation in non-synchronous Counter-Current Chromatography (NSCCC) by single phase

1.3.3.1. Erythrocyte separation

In 1979, Ito et al. reported a sheep/human RBCs separation by nonsynchronous CCC in a single phase (isotonic buffer) (Ito et al., 1979). The machine used was the same machine as shown in Figure 4 but with a different column which was prepared from 6 m long, 1 mm i.d. PTFE tube coiled onto 6 mm o.d. cores, making about 200 helical turns with a total capacity of 5.2 ml (Ito et al., 1979). Isotonic buffered saline solution (pH 7.4) was prepared by dissolving NaCl 90g, Na₂HPO₄ 13.65 g, and NaH₂PO₄·H₂O 2.15 g in 1 L of distilled water and diluted 85 ml of this solution with distilled water to final volume to 1L (Ito et al., 1979). During the separation process, the revolution was 520 RPM (50 g) with 3.6 RPM for column rotation, while the flow rate was 3.6 ml/h (0.06 ml/min) (Ito et al., 1979). The result of this separation is shown in Figure 1.3.10.

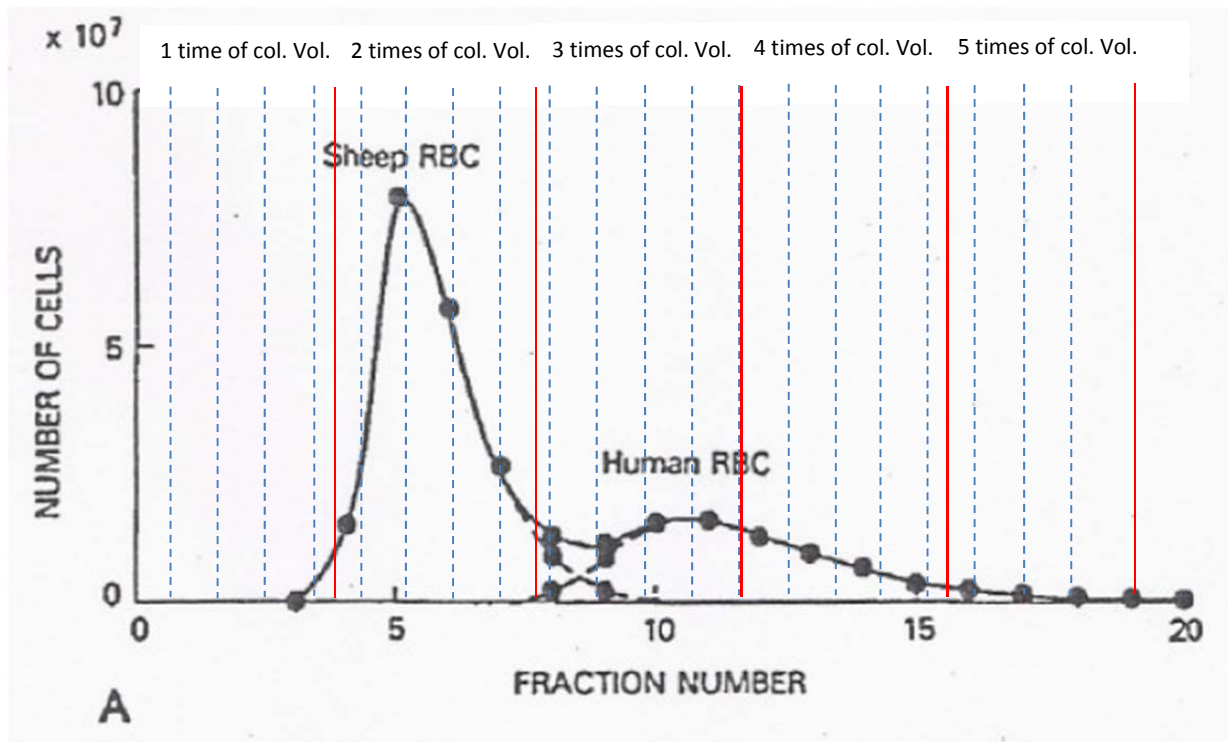


Figure 1.3.10. Separation of human and sheep erythrocytes. Equal amounts of sheep and human cell suspensions were mixed into 0.2 ml was injected into column by isotonic buffer at 520 RPM with rotation at 3.6 RPM and 3.6 ml/h. Fractionated samples were collected 1.2 ml/tube. Total volume was 5.2 ml with 1 mm i.d. From Ito et al., 1979. The positions of fractions in terms of column volumes have been added.

In Figure 1.3.10, the solid line indicates total cell population while the dotted lines represent human and sheep cell population in the fractions between the two peaks (Ito et al., 1979). As the fractionated sample was collected 1.2 ml/tube, the column volume was calculated easily as shown in Figure 1.3.10. As described by them, some human cells that still remained in the column tube after 20 fractions were the greatest size (Ito et al., 1979).

The sheep RBCs were eluted from the 4th to 10th fraction, therefore, the sheep RBCs were not sedimented or even retained during the process while the human RBCs which were eluted from 8th fraction which means human RBCs were retained 1 column volume in the column.

Compared to the results from Figure 1.3.5 which separated sheep/dog RBCs (dog RBC has similar size as human RBCs), this single phase separation is based on the size, density, and shape of cells with larger cells being retained due to the inertia effects (Sutherland & Ito, 1980). Therefore, the smaller sheep RBCs were eluted quicker than human RBCs, while in ATPS, the sheep RBCs partition more toward the interface and are retained longer while dog RBCs eluted first (Sutherland & Ito, 1980).

Interestingly, in 1980, Ito et al. reported another sheep/human RBCs separation by nonsynchronous flow through coil planet centrifuge (Ito et al., 1980). The sketch of their machine is shown in Figure 1.3.11.

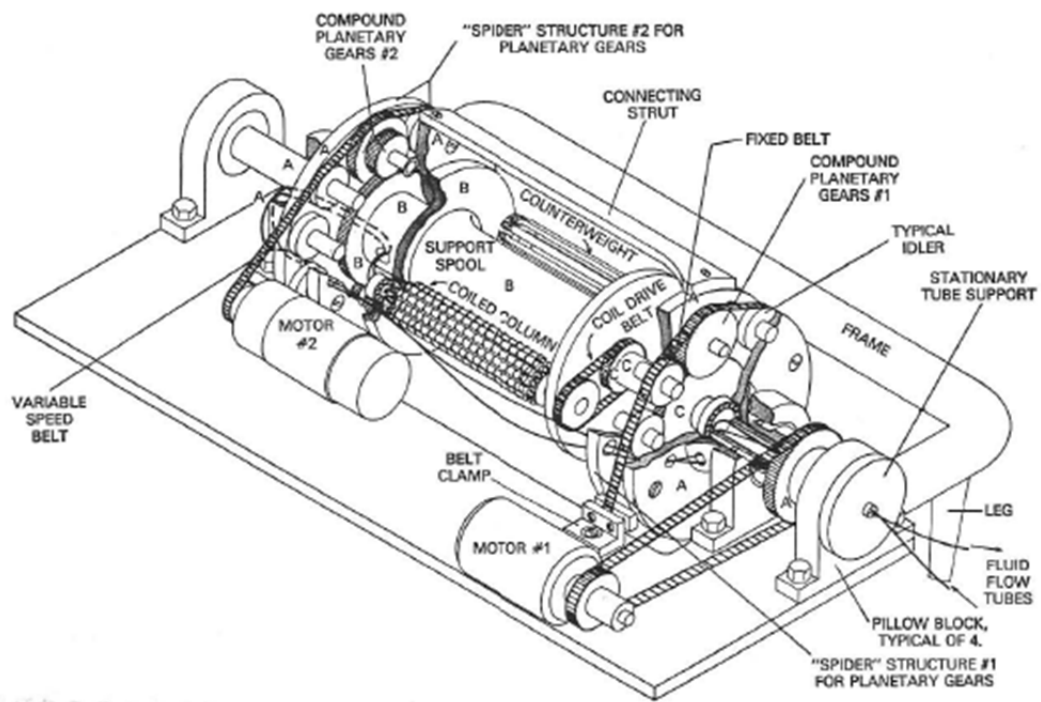


Figure 1.3.11. Sketch of nonsynchronous flow through coil planet centrifuge. From Ito et al., 1980.

Different to the similar sheep/human RBCs separation 1 year earlier (Ito et al., 1979), the separation column was prepared by winding 0.55 mm i.d. PTFE tubing onto 6 units of stainless steel tubes (0.68 cm o.d. and 20 cm long) and the tail of first unit bridges to the head of second unit (Ito et al., 1980), which actually should be eccentric column as classification of CCC columns as shown in Figure 1.1.8. The entire column consisted of 1200 helical turns with a total capacity of about 6 ml (Ito et al., 1980).

In this study there were slight changes to the conditions used in 1979: revolution was set to 800 RPM with 10 RPM rotation while flow rate was 5 ml/h (Ito et al., 1980). The result is shown in Figure 1.3.12.

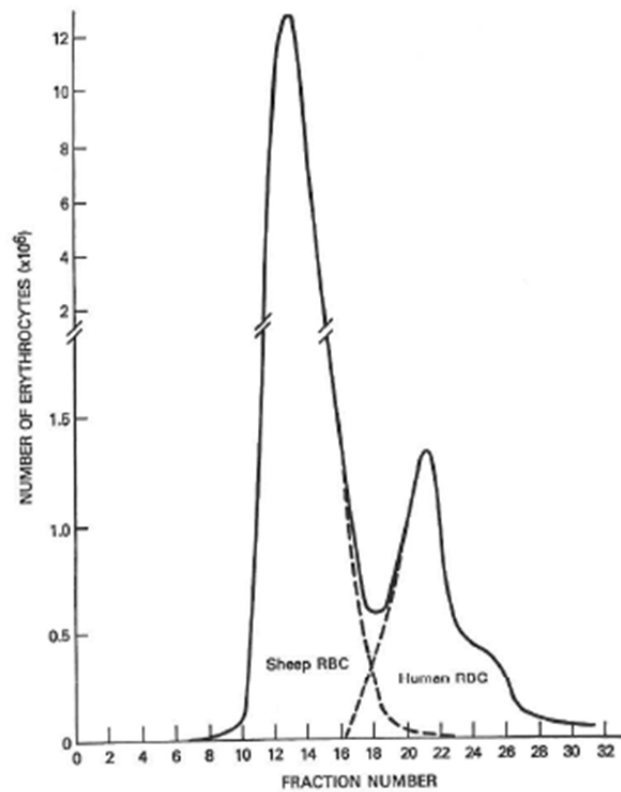


Figure 1.3.12. Separation of human and sheep erythrocytes. Equal amounts of sheep and human cell suspensions were mixed into 0.2 ml was injected into column by isotonic buffer at 800 RPM with rotation at 10 RPM and 5 ml/h. Fractionated samples were collected 0.8 ml/tube. Total volume was 6 ml with 0.55 mm i.d. From Ito et al., 1980.

Comparing Figure 1.3.10 and Figure 1.3.12, some features are similar as sheep RBCs were eluted first at 1 column volume (0.8 ml/tube) with an overlap area between two peaks. As the description of Ito et al. (1980), when the rotational speed of the column and/or the applied flow rate are below the optimal range, cells are retained at the beginning portion of the column. But in this study, they also described poor sample recovery problem that was caused by the adhesion of cells to the internal surface of the tube, which tends to retain the cells in the column almost permanently (Ito et al., 1980). However, in the separation in 1979, the recovery was not described, only that the largest human RBCs were retained in column after 20 fractions (Ito et al., 1979). If compare the number of revolution/rotational speed only, the Ito et al. (1979) study applied 520 RPM with 3.6 RPM with a flow rate of 5 ml/min while the Ito et al. (1980) study used 800 RPM with 10 RPM, and the flow rate was 3.6 ml/h. It is a bit difficult to explain why the latter operating conditions gives rise to

adhesion given the lack of detailed data, however, as they described, the result in their paper did show a similar separation.

The research of behaviour of sheep/human RBCs in nonsynchronous CCC was continued, in 1983, Ito et al. showed a comparison of the relationship between flow direction and rotation direction on this separation which is shown in Figure 1.3.13.

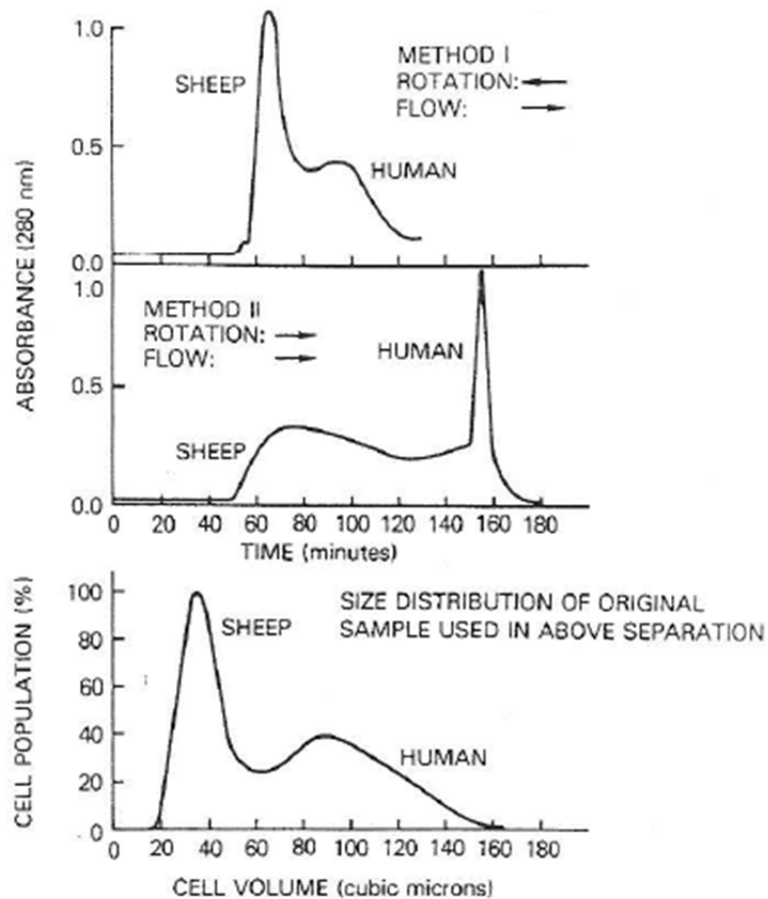


Figure 1.3.13. Separation of human and sheep erythrocytes by elutriation with the nonsynchronous flow through coil planet centrifuge. Equal amounts of sheep and human cell suspensions were mixed into 0.2 ml was injected into column by isotonic buffer at 1000 RPM with rotation in either direction (12.5 RPM and 22 ml/h in Method I; 4 RPM and 45 ml/h in Method II). From Ito et al., 1983.

Obviously, the top result is the typical sheep/human RBCs separation as results shown in 1979 and 1980 in which the small sheep RBCs were eluted with a sharp peak which was followed by a broader peak of the larger human RBCs. However, in Method 1 the coiled column was slowly rotated (12.5 RPM) in such a direction that the cells were held back toward the inlet of the column against the flowing stream (22 ml/h) (head-tail elution) (Ito et al., 1983). An interesting results is shown in the Method 2 when the rotational direction of the coiled column was reversed so that all cells are slowly carried toward the outlet of the column by rotation (4 RPM) while the flowing stream (45 ml/h) further promotes the

traveling rate of the smaller cells (tail-head elution) (Ito et al., 1983) which gives a broad peak of sheep RBCs and a sharp peak of human RBCs (Ito et al., 1983).

1.3.3.2. Rat liver cell and mast cell separation

The method of cell separation in single phase was also applied to other cells such as rat liver cells (Ito et al., 1983) and mast cells (Okada et al., 1996), which are shown in Figure 1.3.14 and Figure 1.3.15, respectively.

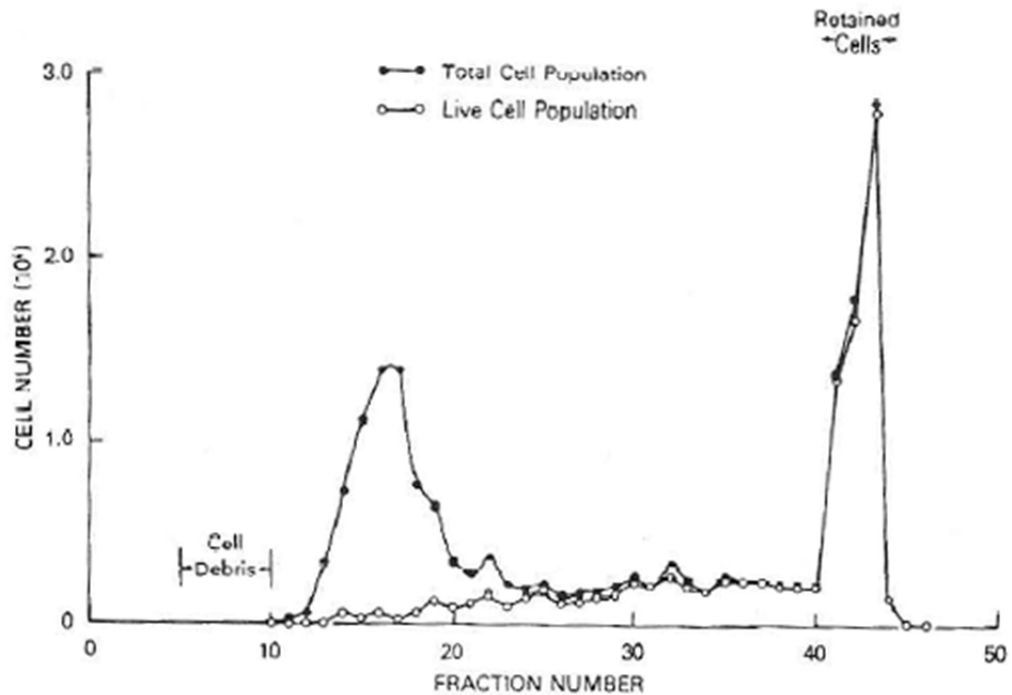


Figure 1.3.14. Elutriation of rat liver cells with the nonsynchronous flow through coil planet centrifuge. Damaged cells were eluted first as a sharp peak while most of the viable cells were retained in the coiled column. From Ito et al., 1983. Detailed operational conditions were unclear.

The separation of liver cells (Figure 1.3.14) gave one low broad peak while a large population of the cells were retained in the column. The rye test showed the broad peak includes damaged cells and the rest were mostly viable and increased in size with the fraction number (Ito et al., 1983). Furthermore, the retained cells were the largest in size and the last few fractions consisted of aggregated cells probably resulting from incompleteness of the digestion of the hepatic cords required to generate a single cell suspension (Ito et al., 1983). They confirmed that the cell damage existed before being subjected to centrifuge (Ito et al., 1983).

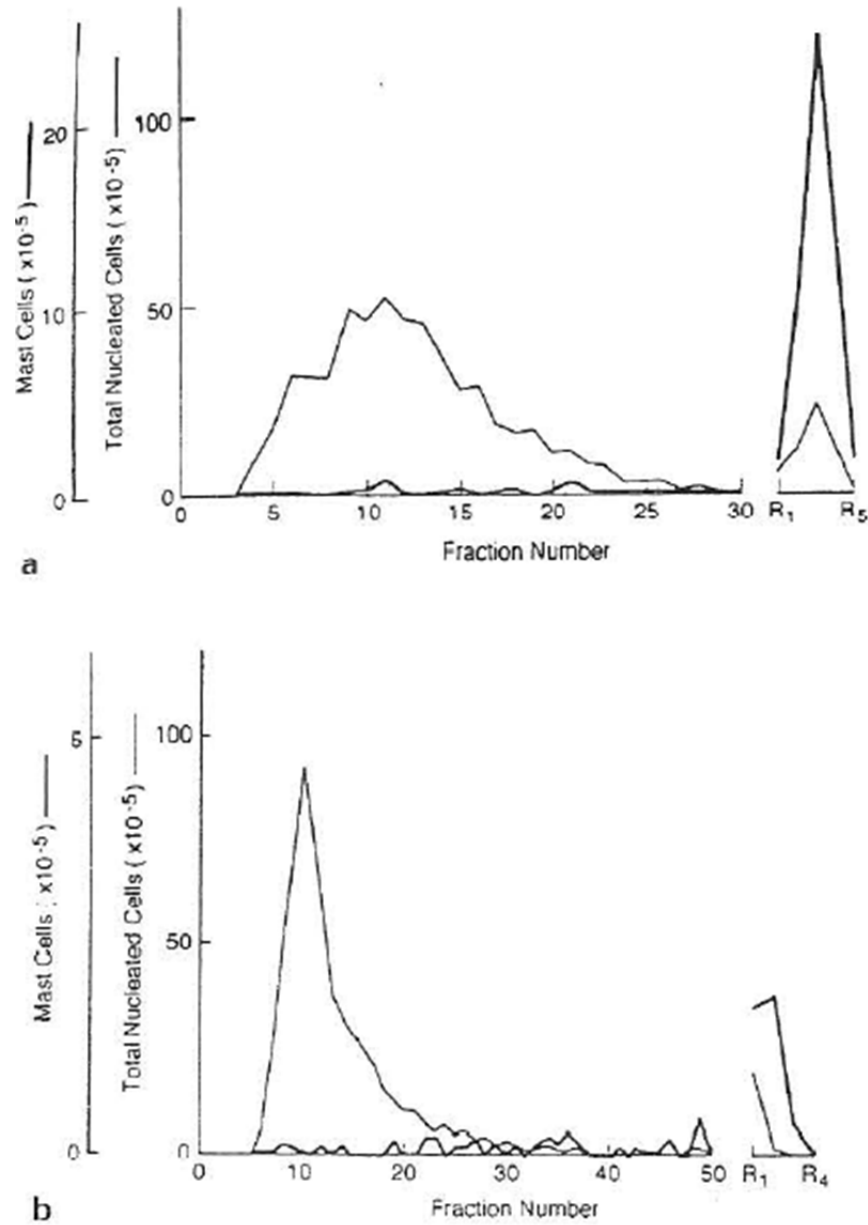


Figure 1.3.15. Separation of mast cells from other leukocytes. Cells were suspended in the RPMI 1640 medium (containing 4mM L-glutamine, 50 μ M 2-mercaptoethanol) at a concentration of 2-3E+7 cells/ml were injected at a centrifugal field of 90g and 0.29 ml/min. Where (a) rat mast cell separation; (b) mouse mast cell separation. And fractionated sample was collected as every 10 (a) and 5 (b) min, while R = fractions flowed out after centrifugation. From Okada et al., 1996.

The mast cells (with a high density: over 1.085 g/ml) separation reported by Okada et al. (1996) is different from all the cell separations described above in that, the single phase was not isotonic buffer but RPMI 1640, supplemented with 50% heat-inactivated FCS and 0.32% sodium citrate. The CCC machine they used is an improved design for cell separation as no rotary seal is required and the separation can be performed without a risk of leakage and contamination. The column was prepared by winding a 12- or 18-m long Teflon tube onto the holder with a diameter of either 20 or 6 mm Teflon tubes with i.d. of 1.6 or 0.9 mm were tested. The flow rate was 0.29 ml/min during the separation process.

They report that the coiled column wrapped on the holder with a diameter of 6 mm (480 helical turns) gave better separation than a 20-mm holder (260 helical turns), and over 99% pure rat mast cells were obtained reproducibly with reasonable yields.

Shinomiya et al. (2005) have also reported a new mast cell separation with the multilayer column). One of their results is shown in Figure 1.3.16.

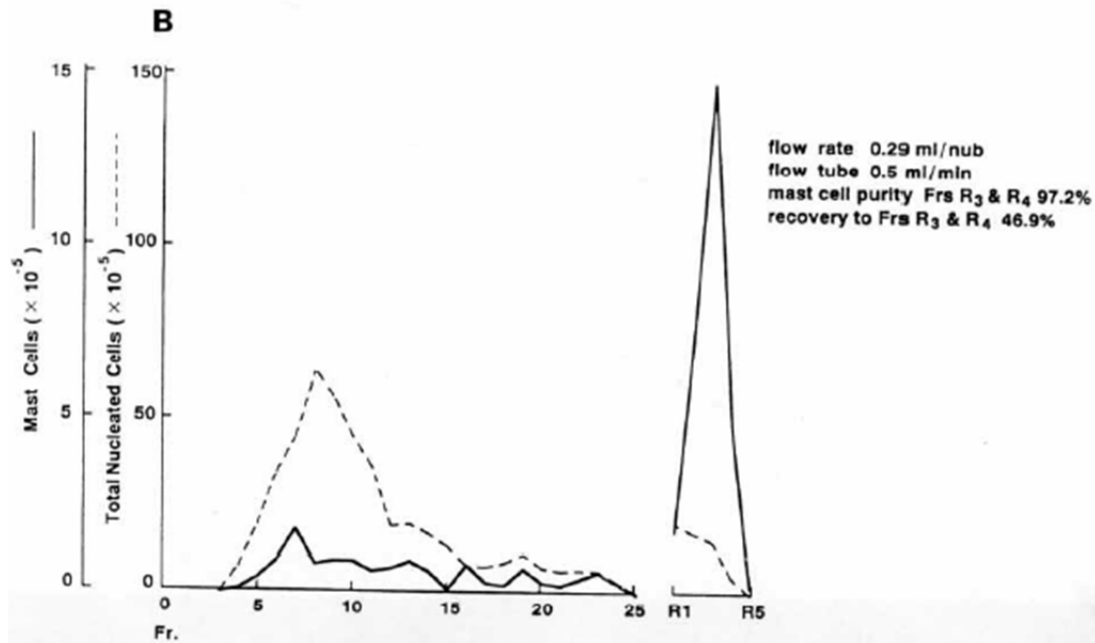


Figure 1.3.16. Elution of rat mast cells using nonsynchronous CPC with multilayer column. Rat mast cells were suspended in RPMI 1640 + 10% FCS were injected at 800 RPM with rotation as 5 RPM and 0.29 ml/min. Total volume was 12.5 ml with 0.9 mm i.d. From Shinomiya et al., 2005.

While Figure 1.3.16 generally repeated result from Figure 1.3.15 as retaining mast cells to the last peak.

1.3.3.3. Blood cell components separation

Recently, Shinomiya et al. (2005) reported elutriation of blood cell components and mast cells by nonsynchronous coil planet centrifuge using both eccentric column and multilayer column assemblies. “The eccentric column assembly was prepared by winding, 0.8 mm i.d. Teflon tubing onto a set of 20 cm × 6 mm o.d. aluminium pipes, making a series of tight left-handed columns. 11 column units were arranged symmetrically around the holder hub of 6 cm o.d. in such a way that the axis of each column unit was parallel to the holder axis. The total column capacity was 20 ml. The multilayer column was prepared by winding 0.9 mm i.d. Teflon tubing (18 m long, 260 turns) onto the holder with a diameter of 20 mm. The total capacity was 12.5 ml).

The effect of revolution and rotation on the separation of sheep blood cell components in isotonic buffer using the eccentric column was studied using revolution at 800 RPM with rotation at 10 RPM while flow rate was 0.4 ml/min (Figure 1.3.17).

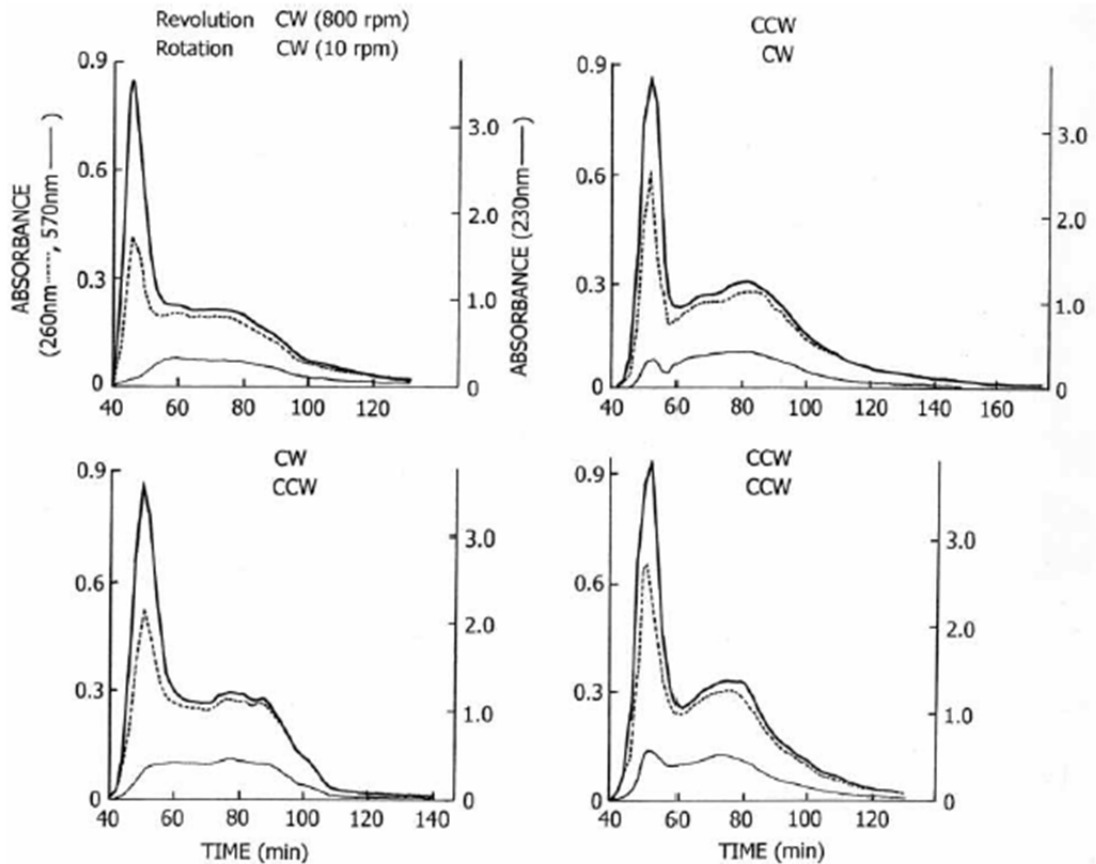


Figure 1.3.17. Effects of revolution and rotation on the separation of sheep blood cell components using nonsynchronous CPC and eccentric column assembly. Sheep blood mixed with equal volume of Alsever's solution (500 μ L) was injected by isotonic phosphate buffer solution (pH 7.4) at 800 RPM with rotation as 10 RPM and 0.4 ml/min. Fractions were collected 0.8 ml/tube. From Shinomiya et al., 2005.

As Figure 1.3.17 shows, changing the revolution and rotational direction gave similar results as blood was partially separated into two main peaks. It is an interesting result when it is compared to results in Figure 1.3.13, where flow direction was not changed but the direction of rotation was changed. As described with respect to Figure 1.3.13, the change of rotational direction changes the movement of cells towards inlet or outlet and the results in Figure 1.3.13 shows a peak shape change. By contrast in Figure 1.3.17, although the rotational direction changed, the change of peak shape was not as significant as Figure 1.3.13.

The process of separating sheep blood cell components by a changing rotational speed was then examined. This was set to 0 RPM initially and increased to 10 RPM gradually

Chapter 1. Introduction and Literature Review
 (Shinomiya et al., 2005). Revolution at 1000 RPM, 900 RPM, and 800 RPM were tested and gave similar results. Figure 1.3.18 shows results for 1000 RPM as an example.

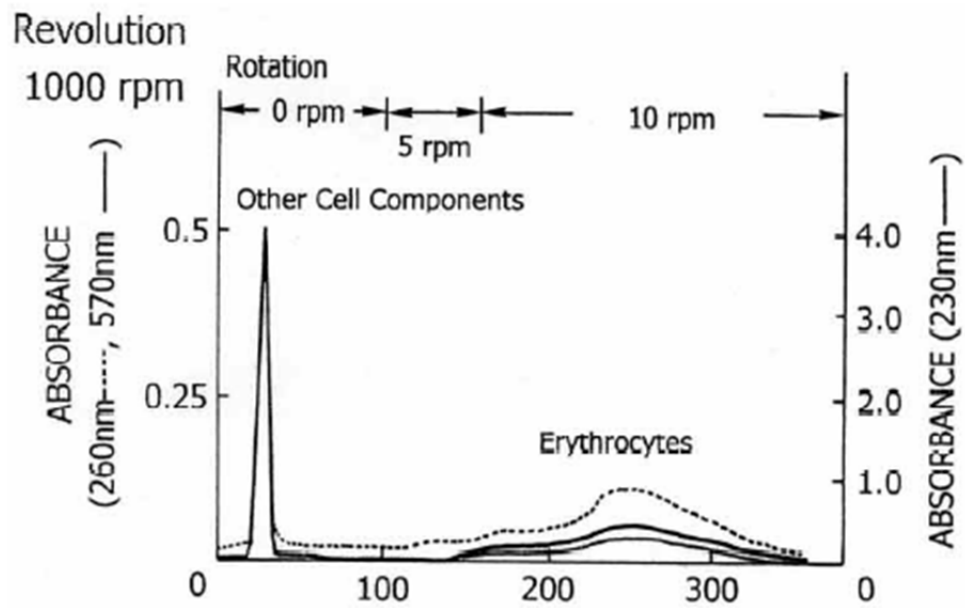


Figure 1.3.18 Effect of increasing rotational speed on the separation of sheep blood components using nonsynchronous CPC. Sheep blood mixed with equal volume of Alsever’s solution (500 μ L) was injected by isotonic phosphate buffer solution (pH 7.4) at 10000 RPM (counter-clockwise direction) with increasing rotation from 0 RPM – 10 RPM (clockwise direction) and 0.4 ml/min. Fractions were collected 0.8 ml/tube. From Shinomiya et al., 2005.

As Figure 1.3.18 shows, the fractions from the first sharp peak consisted of plasma proteins and cells, such as platelets and leukocytes free of erythrocytes while retaining erythrocytes in the column until the column rotation rate was increased to 10 RPM. A similar result obtained with human blood is shown in Figure 1.3.19.

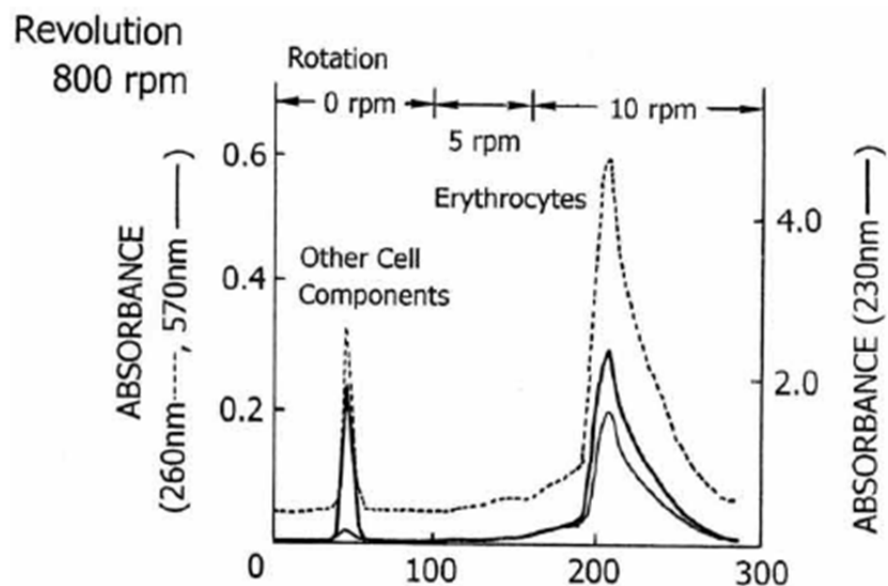


Figure 1.3.19. Effect of increasing rotational speed on the separation of human blood cell components using the nonsynchronous CPC (Coil Planet Centrifuge). Human blood mixed with equal volume of Alsever's solution (500 μ L) was injected by isotonic phosphate buffer solution (pH 7.4) at 10000 RPM (counter-clockwise direction) with increasing rotation from 0 RPM – 10 RPM (clockwise direction) and 0.4 ml/min. Fractions were collected 0.8 ml/tube. From Shinomiya et al., 2005.

These cell separation methods in nonsynchronous CCC for blood cell components have been very important in changing of thinking about separation modes because they made use of retaining the cells on purpose, whilst other separation modes tried to avoid retention. As mentioned above, a low rotational speed or low flow rate causes cells to be retained. Then, by only changing the rotational speed, the behaviour of RBCs is changed from retaining to eluting.

1.3.4. Particle separation by CCC

1.3.4.1. Particle separation by 2 phases system

i. Lipoprotein separation by cross-axis CCC via ATPS

Biological particles such as high- and low- density lipoprotein (HDL & LDL) have been separated from human serum by ATPS systems using X-L type cross-axis CCC (Shibusawa et al., 1995; Shibusawa, 1997) (Figure 1.3.20). The separation column was formed by winding 2.6 mm ID PTFE as a single-layer column with 60 ml capacity. 16% (w/w) PEG 1000 and 12.5% (w/w) dibasic potassium phosphate (pH 9.2) was the ATPS. (Shibusawa, 1997).

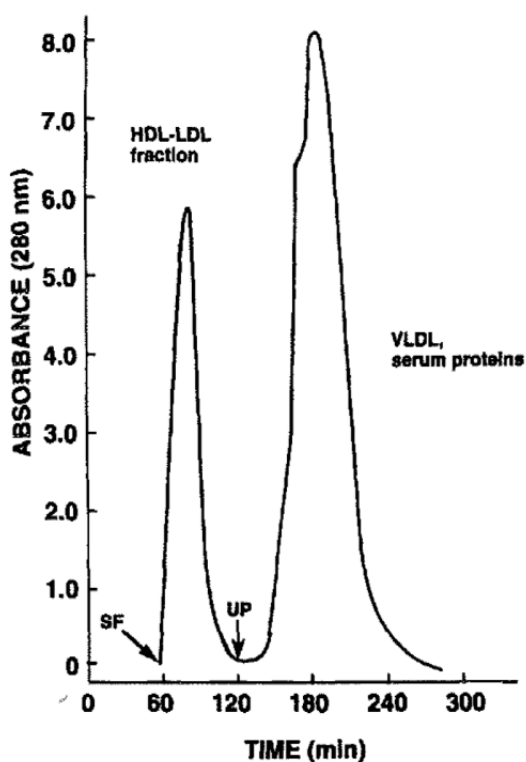


Figure 1.3.20. X-L type Countercurrent chromatography separation of HDL and LDL from human serum with ATPS. 4 ml of human serum in which 0.9 g of PEG 1000 and 0.7 g of dibasic potassium phosphate were dissolved; solvent system: 16% (w/w) PEG 1000, 12.5% (w/w) dibasic potassium phosphate at pH 9.2; mobile phase: lower phase; flow rate: 0.5 ml/min; rotation speed: 500 RPM. SF: solvent front; UP: starting point of the reversed elution mode with the upper mobile phase. From Shibusawa, 1997.

“The separation was performed at 500 RPM using lower phase as mobile phase where both HDLs and LDLs were eluted together near the solvent front (SF)” (Shibusawa, 1997). Other proteins (very low density lipoprotein/VLDLs and serum proteins) were retained until the pumping of upper phase in the reverse direction (Shibusawa, 1997).

ii. Trace element separation by 2 phases system

Trace elements have been reported to be separated by CCC with single layer vertical coiled column in 2002 (Spivakov et al., 2002; Fedotov, 2002). This separation/extraction of dissolved geological samples (complex matrices) was achieved by retention of 0.1 M tetraoctylethylenediamine in chloroform as stationary phase at 450 RPM using different mobile phases (Spivakov et al., 2002) as shown in Figure 1.3.21.

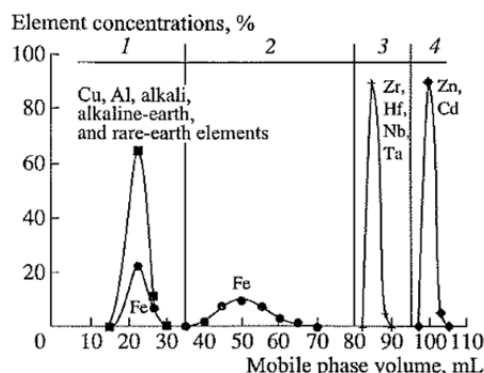


Figure 1.3.21. Group preconcentration and recovery of Zr(IV), Hf(IV), Nb(V), and Ta(V) in the 2 phases liquid system. Mobile phase: (1) 0.1M HCL+0.01M H₂C₂O₄, (2) 0.1M HCL+5% ascorbic acid, (3) 2.0M HCL, (4) 1.0M HNO₃; mobile phase flow rate: 1 ml/min. Rotational speed: 450 RPM. From Spivakov et al., 2002.

1.3.4.2. Particle separation by single phase

In addition to cells, particles separation by CCC in a single phase has also been reported (Ito et al., 1983; Katasonova et al., 2003; Fedotov et al., 2005; Fedotov et al., 2000; Fedotov et al., 2010). In 1983, Ito introduced the principle of particles separation with a rotating coiled tube (Ito et al., 1983) which is shown in Figure 1.3.22.

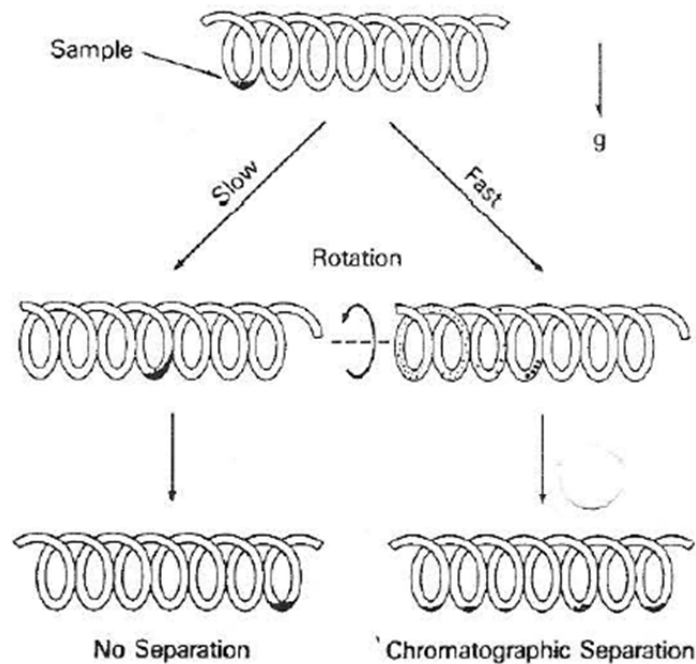


Figure 1.3.22. Principle of particle separation with a rotating coiled tube in a single phase. The coil was filled with water and particles were introduced from tail end. A slow rotation carried all particles to head end with no separation. When the rotational speed was increased, the larger particles moved faster than smaller particles to achieve the particles separation. From Ito et al., 1983.

As illustrated in Figure 1.3.22, the column is initially filled with water and then sample particles are introduced at the tail (top), followed by the rotation of the column. Under a slow rotation (left), all particles always stay together at the bottom of the column and move toward the head of the column at a uniform rate of one helical turn per one rotation of the column which could not give rise to separation of different particles (Ito et al., 1983). When the rotational speed is increased (right), the particles fail to remain at the bottom of the column and they are consequently retarded in their different movement speed toward the head of column which depends on the sedimentation rate of the particles, as the larger particles move faster than the smaller particles and the particles are chromatographically separated along the length of the column according to their relative size and density (Ito et al., 1983). The fractionation of the particles becomes possible by introducing continuous flow through the column during separation (Ito et al., 1983).

In 2003, Fedotov et al. reported studied on the relationship between β value and tubing material and the retention in the column of solids (Soil contained silt, clay, and sand fractions – colloids and solid particles from 0.1 μm to 250 μm) (Fedotov et al., 2003), which is shown in Figure 1.3.23.

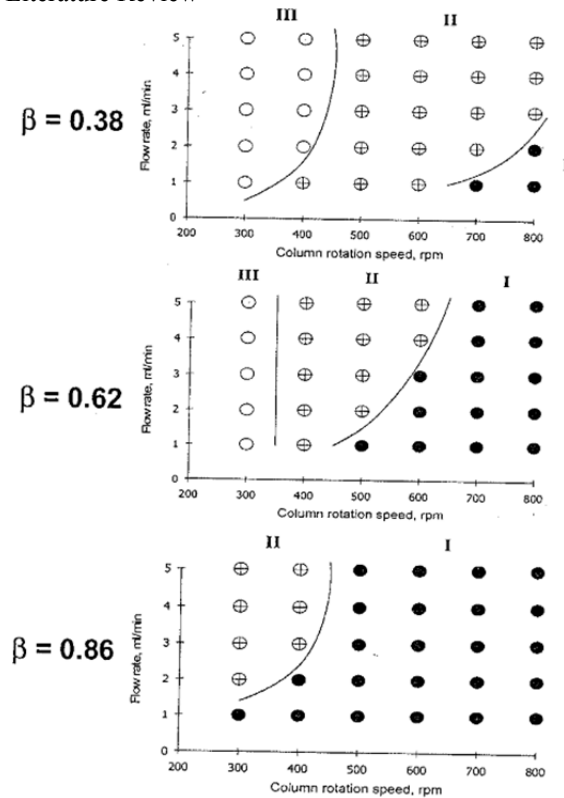


Figure 1.3.23. Retention of a solid sample in PTFE columns with different β values. And the effect of column rotation speed and mobile phase flow rate. Key: ●, soil sample is completely retained in the column; ⊕, colloidal sub-micron particles can be eluted; ○, colloidal and fine solid particles can be eluted. The soil sample (Soil contained silt, clay, and sand fractions – colloids and solid particles from 0.1 μm to 250 μm) (up to 5 g) (was stirred in distilled water to obtain 25 ml of suspension) was pumped to column at 15 ml/min. From Fedotov et al., 2003.

Results in Figure 1.3.23 were obtained from J-type CCC with 3.2 mm ID column under $\beta = 0.32$; $\beta = 0.62$; $\beta = 0.86$, respectively. It shows with increasing of rotational speed, the easier retention of solids was; and the colloidal submicron particles were easier to be eluted than fine solid particles. Increasing the β value made a smaller area of Zone III (all solids eluted) (Fedotov et al., 2003) and higher β value was used to obtain better retention of solid by “pressing” fine particles to the outer tube wall (Fedotov et al., 2003). This report also described the difficulty of removing soil sample in stainless steel columns.

In 2000, Fedotov et al. reported latex beads separation and separation of humic substance and quartz particles by coiled tube field flow fractionation (CTFFF) which is a rotating coiled tube (Fedotov et al., 2000) which is shown in Figure 1.3.24 and Figure 1.3.25, respectively.

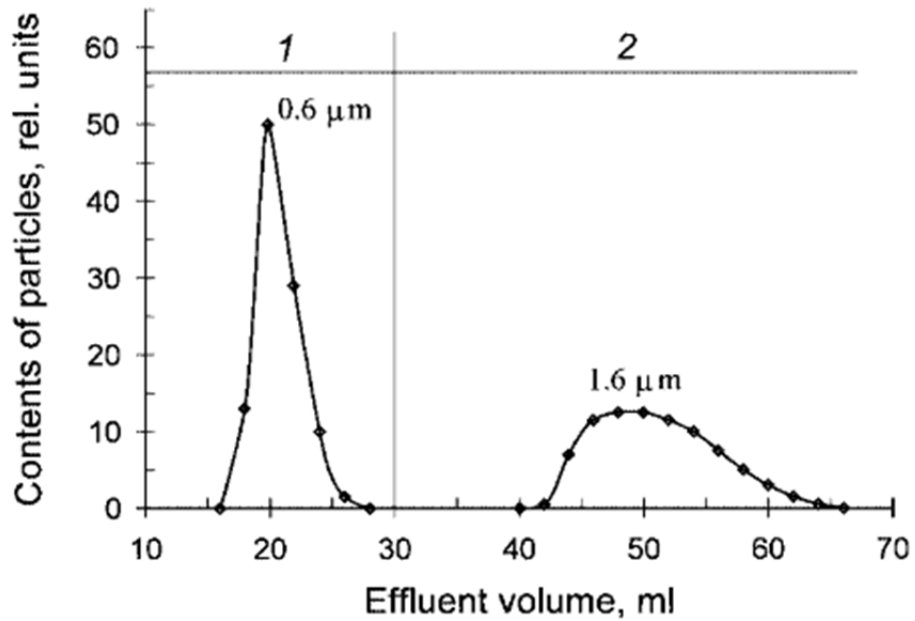


Figure 1.3.24. Separation of latex beads. Mixture of colored latex beads (yellow, 0.6 μm and rose, 1.6 μm) in 1 ml water was injected to column at 800 RPM 0.5 ml/min by water. The elution was changed to 0 RPM and 2 ml/min after 30 effluent volumes. Total volume was 17 ml (single layer column) and 1.5 mm i.d. with revolution radius $R = 85$ mm and rotation radius $r = 35$ mm. From Fedotov et al., 2000.

As described, at stage 1, rotational speed was 800 RPM with flow rate was 0.5 ml/min and at stage 2, rotational speed was 0 RPM with flow rate was 2 ml/min (Fedotov et al., 2000). This is different from the principle of particles separation in Figure 1.3.22 which requires both ends of the column being closed. In Figure 1.3.24 there is flow through the column. However, as described in Figure 1.3.22, the larger particles move faster and the result of Figure 1.3.24 shows that the smaller particles (0.6 μm) moved faster with the larger particles (1.6 μm) being retained.

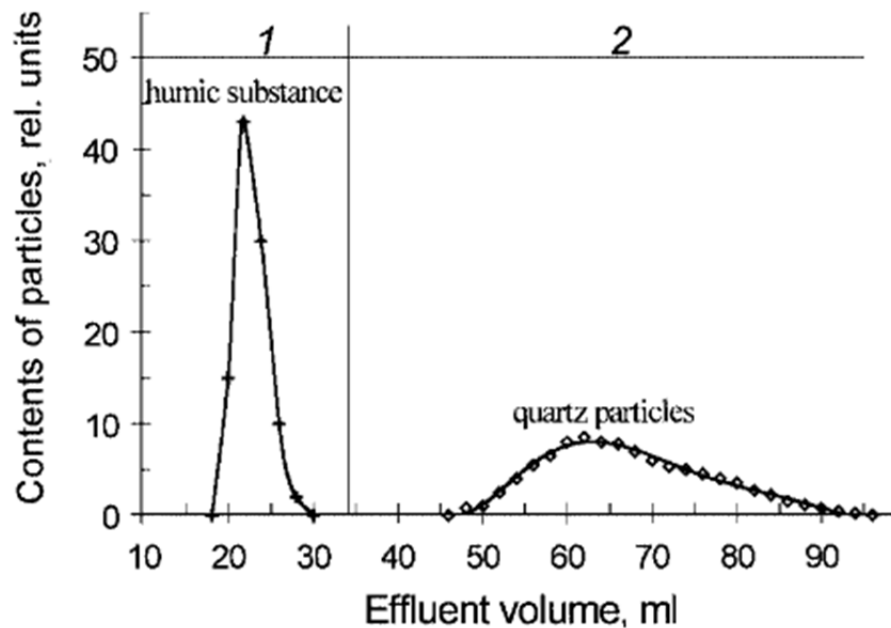


Figure 1.3.25. Separation of humic substance and quartz particles. Mixture of humic acid sodium salt (10 mg) and quartz sand (10 mg) in 2 ml of 0.01 mol/l aqueous ammonium chloride solution. Sample was injected to column at 115 RPM and 0.15 ml/min by 0.01 mol/l ammonium chloride aqueous solution. Then changed to 0 RPM and 15 ml/min. From Fedotov et al., 2000.

A similar result is shown in Figure 1.3.25 for the separation of humic substance and quartz particles (sizes are unclear). At stage 1 rotational speed was 115 RPM with flow rate of 0.15 ml/min and at stage 2, rotational speed was 0 RPM with a flow rate of 15 ml/min to elute the quartz particles pressed on the tube wall (Fedotov et al., 2000). As in Figure 1.3.24, the larger size particles not only move faster but also retained on the tube wall which makes them difficult to remove.

In 2002, a separation of silica gel particles and separation of quartz sand particles by J-type CCC was reported (Katasonova et al., 2003), shown in Figure 1.3.26 and Figure 1.3.27, respectively.

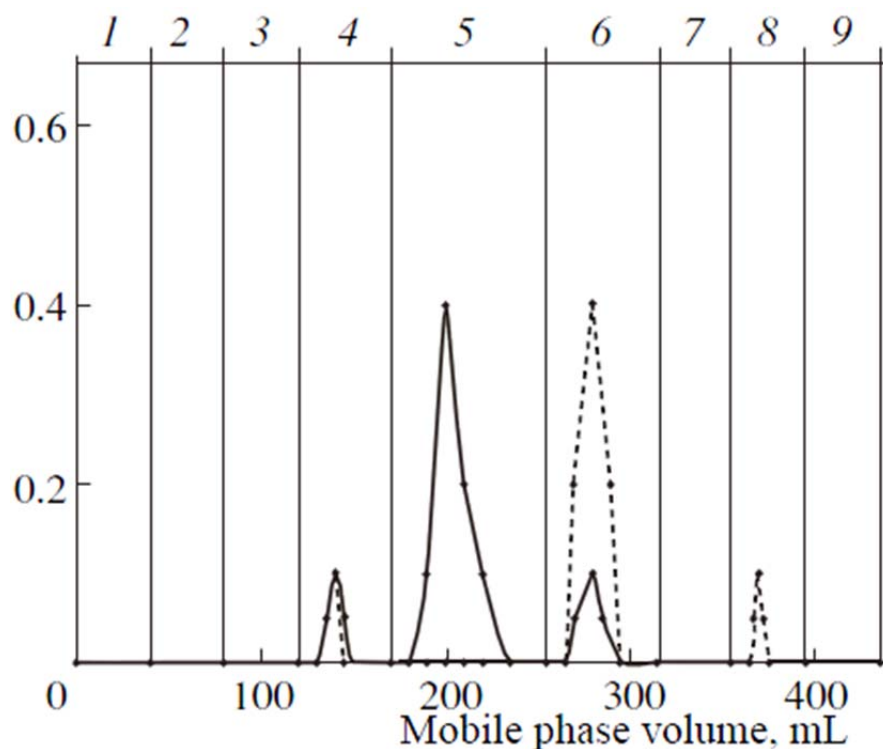


Figure 1.3.26. The fractionation of model silica gel samples. A mixture of 10 μg Silasorb-300 + 10 μg Silasorb-600 in 5 ml of water was injected to column at 70 RPM and 0.29 ml/min and then steps of 0.35, 0.67, 1 (particles 1-2 μm), 1.67 (5 μm), 3.5 (10 μm), 6.7, 10 (>10 μm), and 15 ml/min at 70 RPM. From Katasonova et al., 2003.

The separation of Figure 1.3.26 was under rotational speed of 70 RPM with initial flow rate of 0.29 ml/min. Gradually increased flow to 15 ml/min eluted 2 μm particles with 1 ml/min (4); eluted 5 μm particles with 1.67 ml/min (5); eluted 10 μm particles with 3.5

ml/min (7) and eluted particles greater than 10 μm using 10 ml/min (8) (Spivakov et al., 2002; Katasonova et al., 2003).

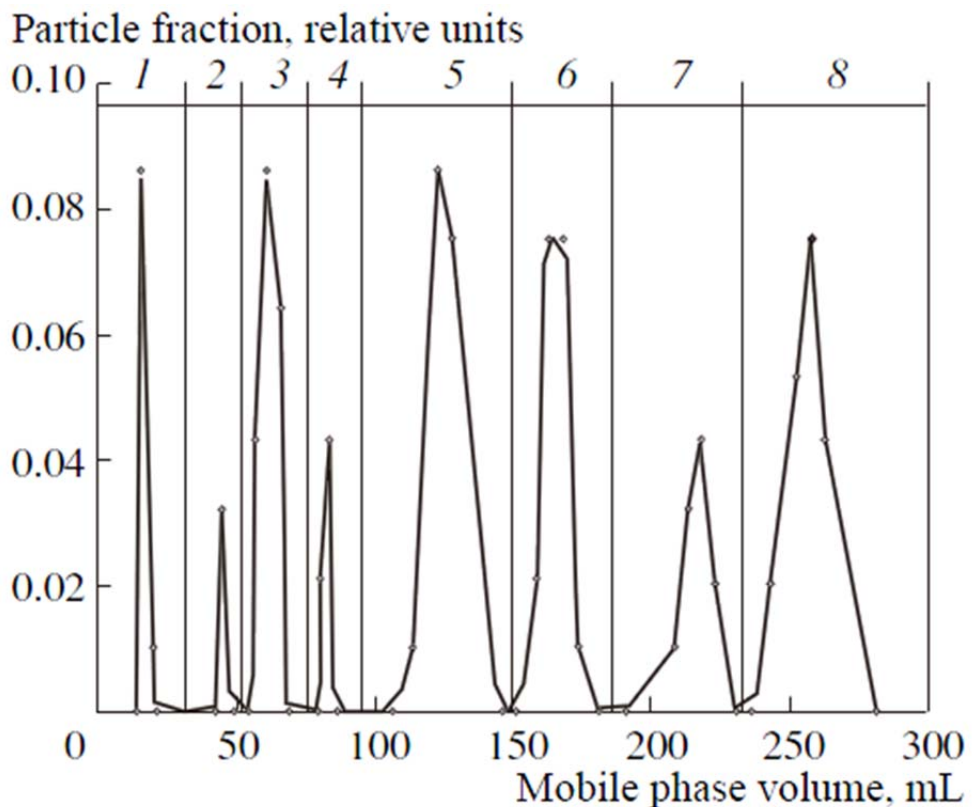


Figure 1.3.27. The fractionation of quartz sand. Quartz sand sample (10 μg in 5 ml of water) was injected to column at 70 RPM and 0.15 ml/min and then steps to 0.35 (1-2 μm), 0.67 (2-3 μm), 1 (3-4 μm), 3.5 (5-7 μm), 6.7 (7-8 μm), 10 (10 μm) and 15 ml/min (> 10 μm) at 70 RPM. From Katasonova et al., 2003.

Similar (Figure 1.3.27) to Figure 1.3.26, gradually increasing flow rate was applied with rotational speed at 70 RPM (Katasonova et al., 2003). The result shows that the larger particles were the easier to retain in the column and a higher flow rate was required to elute them. The influence of rotational speed was reported: the high density particles (> 2 g/cm^3) were easier to retain in the column therefore low rotational speed was required to separate them for low density particles (1.2-1.4 g/cm^3) high rotational speed were required as these particles were easier to be eluted with no retention under low rotational speed (Katasonova et al., 2003). The influence of initial flow rate and inner diameter were also discussed in their paper (Katasonova et al., 2003). And a mathematical simulation of solid particle motion in the carrier liquid flow in a rotating coiled column was reported (Fedotov et al., 2005). This equation is discussed in details in chapter 8.

In 2010, separation of different size nano- and microparticles was reported (Fedotov et al., 2010) using “a model planetary centrifuge equipped with a vertical conoidal drum with two symmetric shoulders contributing to the retention of small particles” with 1.5 mm i.d.

PTFE tube, total volume was 10 ml (R was 9 cm with radius of rotation in the top part was 2.5 cm and radius of rotation in the bottom part was 5.5 cm (Fedotov et al., 2010) which is shown in Figure 1.3.28.

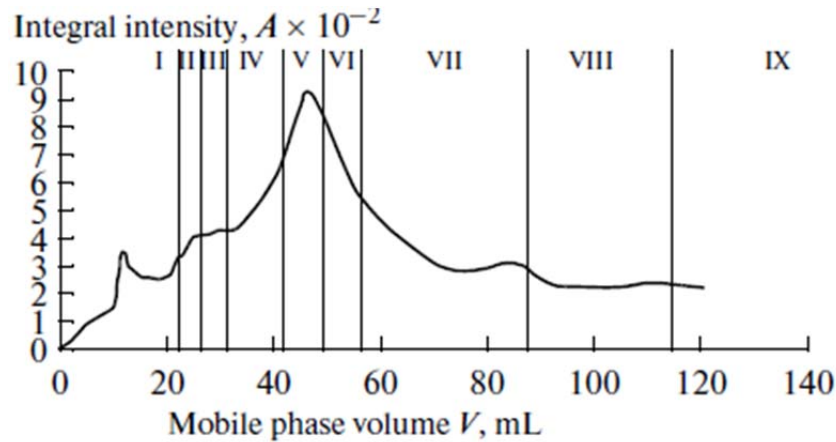


Figure 1.3.28. Fractionation of a mixture of standard sample of silica gel (“150 nm”, “400 nm”, “900 nm”) in a conoidal rotating coil column eluted by deionized water. The mixture was injected to column at 800 RPM and 0.1 ml/min and the directions of pumping the mobile phase and column rotation coincide. Then the flow rate steps to 0.15, 0.3, 0.5, 0.7, 1.0, 2.7, 3.7 and 5 ml/min. From Fedotov et al., 2010.

From I to V, the fractionated samples included 100-150 nm particles; ~350 nm particles distributed in IV & VII; 720-760 nm particles were eluted in V to IX (Fedotov et al., 2010). Therefore, the elution order also follows particle size as smaller size particles were eluted easier and bigger size particles were retained easier. However, although some separation was achieved the fractionated results show different size of particles were only partly separated as in some fractionated samples, such as IV, V, VI, the particles of different sizes were eluted mixed. Compared to other particles separation above, this nano- microparticles separation based on increasing the flow rate generates a board peak but not different separated peaks for each particles size. These separations were all based on increased flow rate (step flow). Different results of combination of rotational direction and pumping direction were also reported. When rotational direction was opposite to mobile phase direction, no peaks were registered and the above separation was achieved when rotational direction and mobile pumping direction coincided (Fedotov et al., 2010).

1.3.5. Related applications of similar mechanism on cells by Ito et al

In 1977, Ito et al. reported an application for coiled column in unit gravity for osmotic fragility test of erythrocytes (Ito et al., 1977). The principle of it was based on the movement speed of RBCs is much slower than that of the solution (the average moving

rate of the RBCs is approximately 1/10 of the gradient flow (Ito et al., 1977)) The 0.85mm i.d. 175cm long with 1ml capacity was orientated horizontally, so that plasma, haemoglobin, and anything less affected by gravity will flow rapidly through the tube with a good retention of RBCs (Ito et al., 1977). Therefore, when a saline solution with a decreasing osmotic gradient is pumped through the tube, the new released haemoglobin from haemolysed cells will be eluted out of column while still retaining intact RBCs in column (Ito et al., 1977). They measured and reported osmotic fragility changes between different blood samples which can be a useful diagnostic parameter for spherocytosis and other haematological disorders (Ito et al., 1977).

In 1975, Ito et al. introduced a flow through centrifuge applied to plasmapheresis (Ito et al., 1975) as shown in Figure 1.3.29.

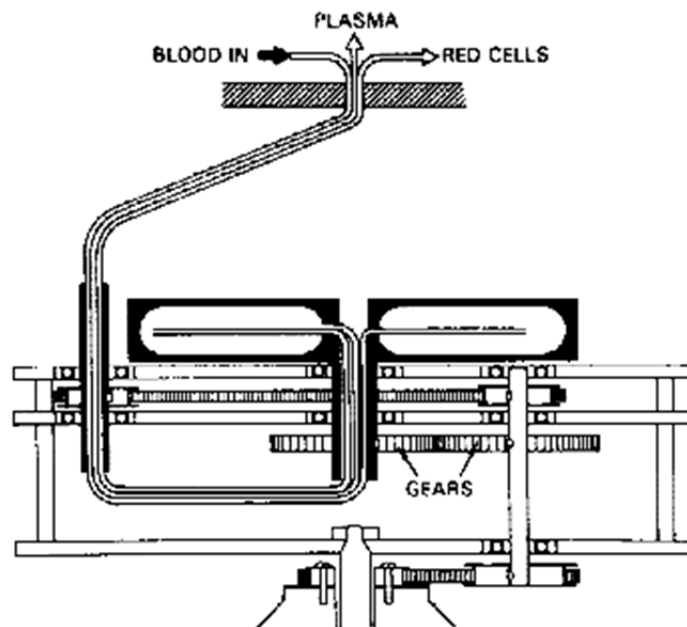


Figure 1.3.29. Design of the flow through centrifuge. The frame of the centrifuge body consisting of three horizontal plates carries three rotary structures – central bowl, countershaft (right), and tube – supporting hollow shaft (left). From Ito et al., 1975.

They reported plasma free of RBCs was collected at 12 ml/min at 1000 rev/min or 18 ml/min at 1300 rev/min with no evidence of RBCs hemolysis (Ito et al., 1975) which can be applied to plasmapheresis, cell washing and elutriation, zonal centrifugation and counter current chromatography (Ito et al., 1975).

In 2001, Ito & Shinomiya introduced a continuous flow cell separation method based on density (Ito & Shinomiya, 2001). The separation centrifuge and its principle are shown in Figure 1.3.30.

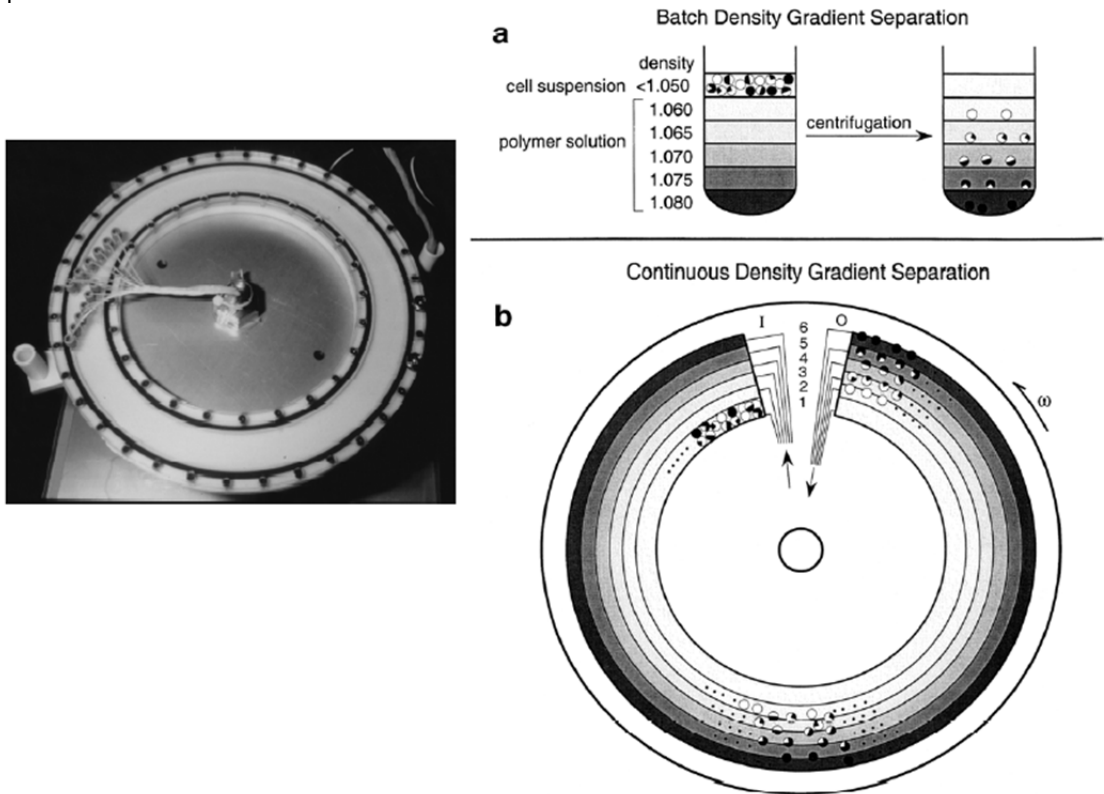


Figure 1.3.30. Photograph of the separation centrifuge (left) and conventional batch density gradient separation and proposed continuous method for cell separation by density gradient centrifugation for continuous separation. From Ito & Shinomiya, 2001.

As Figure 1.3.30 shows, a set of density media based on Percoll (the Percoll stock (density = 1.13 g/ml) was diluted to five media) is continuously pumped through inlet 2-6 and the sample cell pumped from inlet 1 while the cells are distributed in the corresponding density layers before reaching the outlet of channel under adjusted centrifugal force and flow rate (Ito & Shinomiya, 2001). The density layer and human buffy coat separation results are shown in Figure 1.3.31 and Figure 1.3.32.

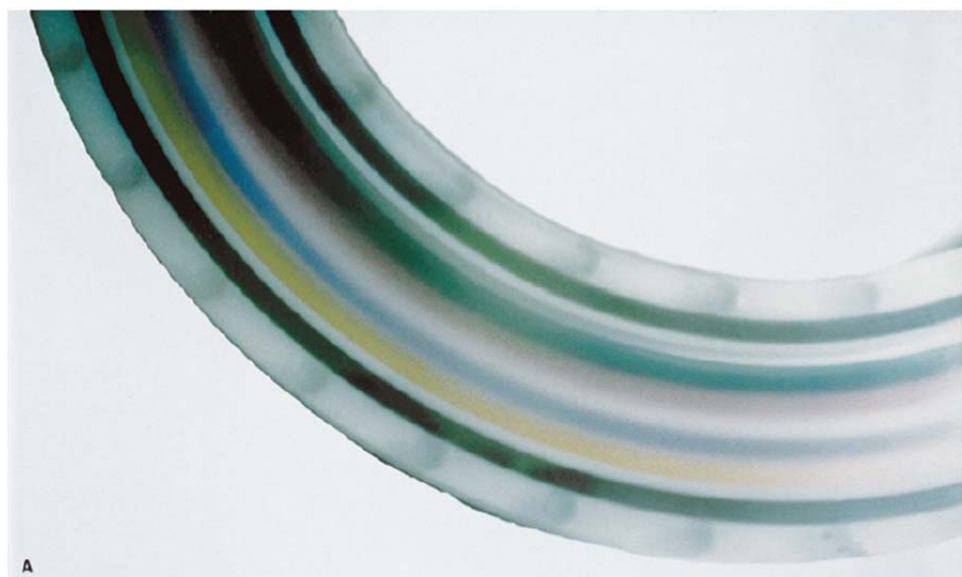


Figure 1.3.31. Stroboscopic observation of the separation column with coloured percoll layers. This is in the continuous method as shown in Figure 1.3.30. From Ito & Shinomiya, 2001.

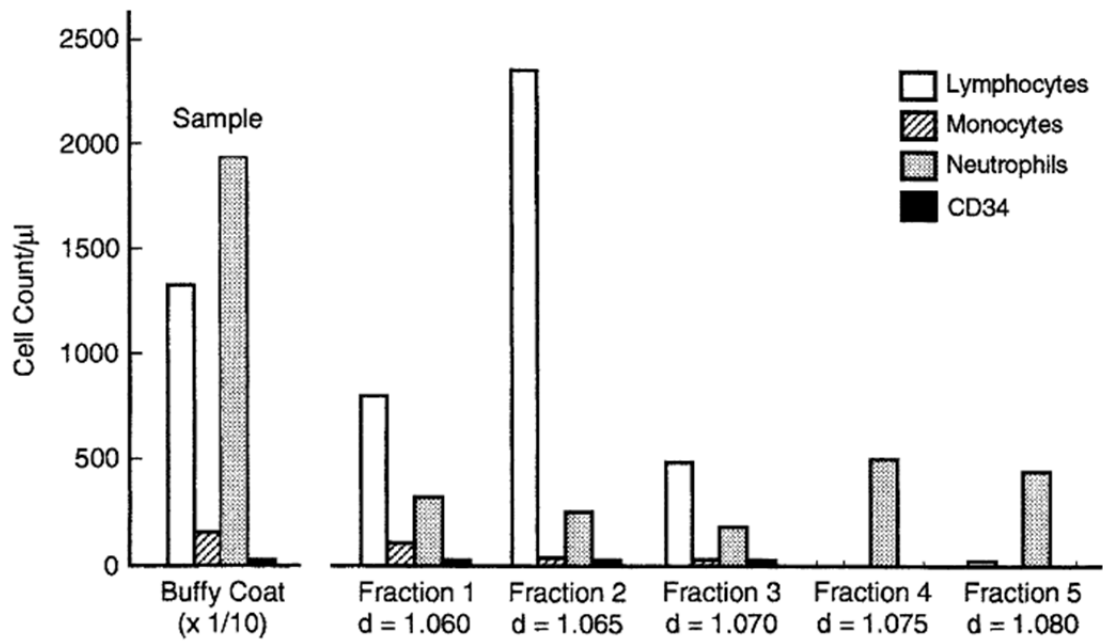
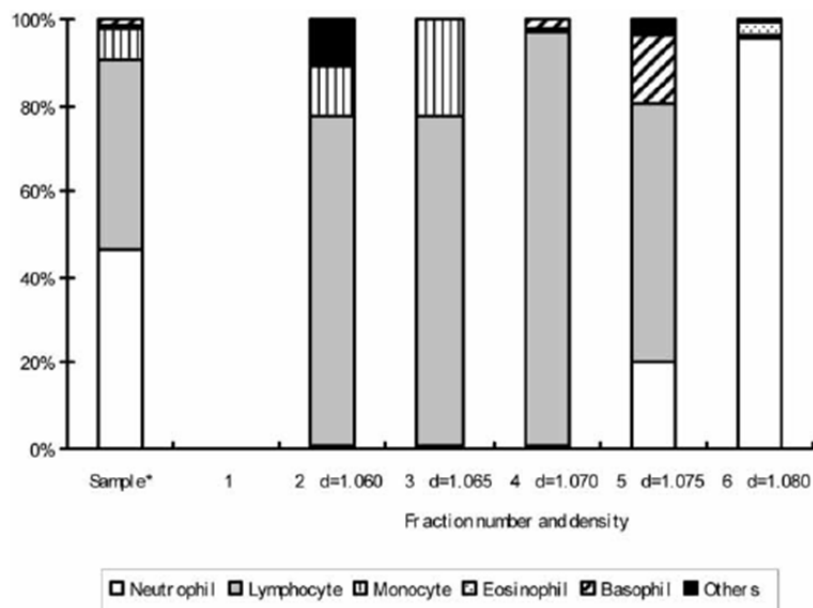


Figure 1.3.32. The result of separation of human buffy coat by the continuous density gradient centrifugal method of Figure 1.3.30. From Ref Ito & Shinomiya, 2001.

As they reported for Figure 1.3.31, the coloured density layers were well preserved even at a small density difference of 0.001 g/cm^3 between neighbouring layers (Ito & Shinomiya, 2001) and successfully separated buffy coat as shown in Figure 1.3.32 (Ito & Shinomiya, 2001).

In 2005, Shiono et al. repeated the buffy coat separation with the same machine (Shiono et al., 2005) and methodology which is shown in Figure 1.3.33.



Chapter 1. Introduction and Literature Review

Figure 1.3.33. Different leukocyte populations in each fraction obtained from buffy coat. Many lymphocytes were found in fraction 3 and 4; a number of neutrophils were in fraction 6 and CD34-positive cells, which are believed to be stem cells, were concentrated in fraction 2. The same method from Figure 1.3.32. From Shiono et al., 2005.

By this method, they also separated and collected cultured mast cells (Figure 1.3.34). Fraction 2 (density 1.065 g/ml) included 3.5% mast cells and fraction 6 (density 1.085 g/ml) included 90.4% mast cells (Shiono et al., 2005).

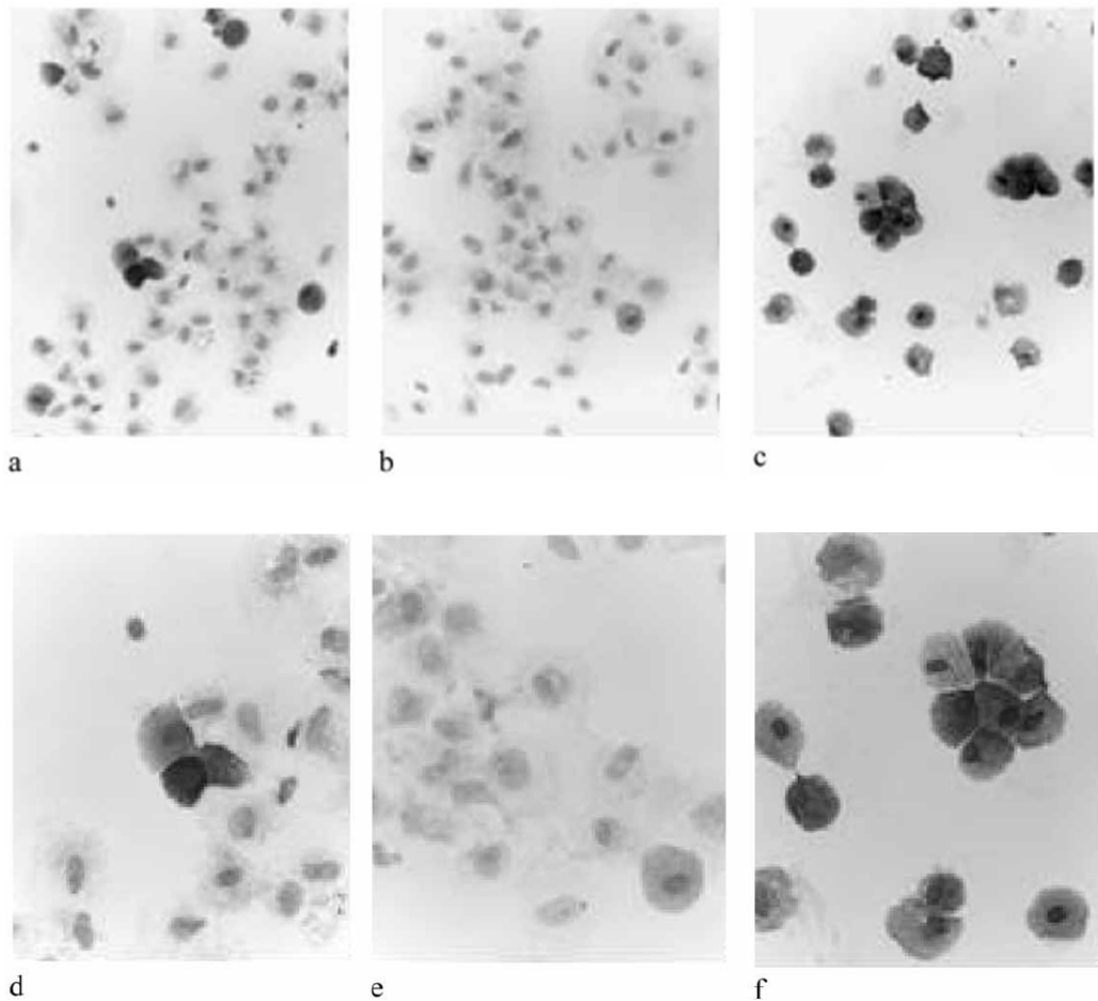


Figure 1.3.34. Separation of cultured human mast cells. (a, d), Co-cultured cell suspension (mast cell: 10.9%) (b, e) fraction 2 (density: 1.065 g/ml, mast cells 3.5%). (c, f) fraction 6 (density:1.085 g/ml, mast cells: 90.4%). The same density difference separation as Figure 1.3.30. From Shiono et al., 2005.

In 2007, Shino et al. (2007) also reported a colony forming cell assay for human hematopoietic progenitor cells harvested by the same machine under similar conditions as shown in Figure 1.3.35. What is particularly important about these results is that cells harvested by the method still retain the ability to proliferate, indicating they can be recovered without loss of their native functions.

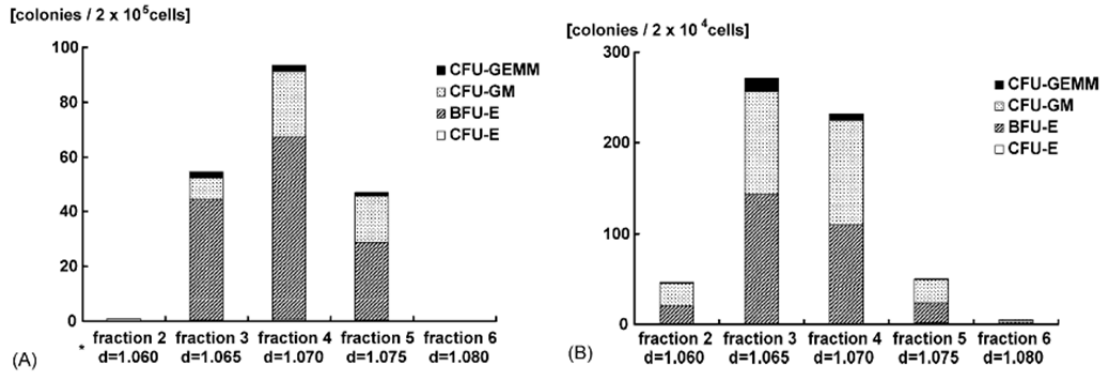


Figure 1.3.35. Progenitor frequencies in peripheral blood (A) and umbilical cord blood (B). Application of method in Figure 1.3.30. From Shiono et al., 2007.

1.3.6. Conclusion

With the developing of Countercurrent Chromatography, whole cells/particles separation by CCC has been researched step by step. Generally, there are two methods to separate cells: 1) ATPS of different type of cells and 2) using a single phase which separates by size, density or shape. The former is similar to Countercurrent Distribution and the latter can be compared with elutriation and field-flow fractionation. Red blood cells as model has been the most researched for the cell separation and successful separations have been reported for both ATPS and single phase. In addition, other cells such as bacteria and mast cells have also been studied and separations of latex particles and quartz sand have been reported in a single phase. The unique part of this technique is the fluctuating g-field which is generated by the column rotation, however, the design of how the column rotates is also a key part to separate cell. As reported, as J-type CCC does not provide a good retention of ATPS, cross axis machine and Brunel machines have been suggested and applied. By contrast, J-type CCC retains particles well for single phases while I-type CCC does not provide this performance. No matter which method is used to separate the cells, the revolution/rotational speed and flow rate are the key factors to influence the separation, and the revolution/rotational direction and flow direction also change the separation behaviour of cells. One simulation has also been reported for the behaviour of cells/particles in such a rotating coiled column.

1.4. Discussion and Conclusion

In this chapter, the development and different types of Counter-Current chromatography centrifuges were introduced. J-type CCC, one of the designs to provide the same rotation and revolution, was focused on as its large applications. The special design generates Archimedean screw effect and a fluctuating g-field which can be changed by changing rotational speed and the design of column. Both features which are generated by the planet rotation may influence the behaviour of RBCs in the system. Therefore, to analyse the behaviour of RBCs 2 main aspects of control are operational conditions and constructive conditions. The former includes the pumping flow rate and rotational speed, and the latter includes columns design, tubing choice and instrument mode.

Milli-CCC[®] is a commercially available Counter-Current Chromatography centrifuge developed by Brunel Institute for Bioengineering based on a prototype which has also been described here. With established commercial coiled column design standard and temperature control system, Milli-CCC[®] was chosen as the experimental CCC centrifuge to research and develop a novel function on cell separation application by this commercial separation system.

According to previous researches on ATPS and single phase cell separation by non-synchronous CCC and synchronous CCC, cells retention was a problem which always tried to avoid and sometimes the sedimentation of RBCs was difficult to remove which decreased the recovery of cell sample and lead to failure of cell separation directly. However, as to the non-synchronous CCC is not commercially available yet and the J-type provides poor retention on ATPS, single phase was chose in this thesis. All previous studies of cell separation in single phase have been achieved by non-synchronous CCC in extending this work to the Milli-CCC there was a need to research and overcome the problem of sedimentation or to seek a method to convert this disadvantage to a feature to achieve the proposed separation of cells. This has been the challenge and task for the project in this thesis.

Although Milli-CCC[®] had been used in BIB to research latex particle separations (Hagedoorn, 2013) previously, cells had not been studied. As examples of particles their behaviour has been examined and compared with other particle separations by the same system, to seek how behaviour of cells fits in and different to behaviours of other particles.

Red blood cells were chosen as model since they are readily available well characterised cells. RBCs of different species provide a range of cells with different sizes, different

densities and different membrane and surface properties. Therefore, RBCs are ideal model to be applied to research and establish the cell separation method. According to cell biology and rheology studies, different from polymer particles, cells require isotonic environments. RBCs also have special different shapes in species with features of aggregation and deformation, which lead the health and diseased RBCs behave different in rheology. Therefore, the physical and physiological properties of RBCs must be considered in the research of cell separation, especially deformation, which is the important property for RBCs.

In conclusion, to research and develop cell separation function of the commercial Milli-CCC[®] centrifuge, besides of the CCC centrifuges aspects of operational condition and instrument constructive condition, the properties of RBCs themselves should also be included, to seek the successful cell separation.

Aims and Objectives

The aim of the research project presented in this thesis was to develop a cell separation methodology using the commercial Milli-CCC[®] centrifuge system by researching the influence of operational condition, instrument constructive aspects and cell special properties.

The objectives to attain this aim were as follows, presented in this thesis in the experimental Chapters 3- 6.:

1) Establishment research method of fundamental behaviour of RBCs in fluctuating g-field (Chapter 3)

- To seek a standard method in order to describe and analyse the fractions obtained by CCC process.
- To research and understand the relationship between operational conditions and fundamental behaviour of RBCs in the fluctuating g-field, especially for the reasons and requirements of cell sedimentation in order to seek potential design of cell separation method.

2) Research of the influence of cell deformability on behaviour of RBCs in fluctuating g-field (Chapter 4)

- To research the contribution of the one of the important RBCs properties – deformability on the behaviour of RBCs sedimentation and elution by using cell fixation method.

3) Development of flow cell separation method (Chapter 5)

- To develop methods to determine the potential cell separation operation conditions.
- To research and develop the method of cell separation via the commercial Milli-CCC[®] centrifuge system by controlling pumping flow rate and rotational speed.
- To solve the problems which arise from cell sedimentation and are generated during cell elution and also to research the method to convert those disadvantages as controllable factors during the cell separation process.
- To seek the method to separate RBCs with different deformabilities.
- To compare the effect of surfactant added to buffer on fixed RBCs separation.

4) Research of the influence of tube shape on behaviour of RBCs in fluctuating g-field (Chapter 6)

Chapter 1. Introduction and Literature Review

- To research the influence of tube shape on the fundamental behaviour of RBCs by a broader ID column and changing the traditional circular tube to the rectangular tube. Also to compare the different effects by 2 rectangular column designs.
- To seek separation conditions methods by applying the established separation condition determine method in chapter 4.
- To compare the separation results by circular and rectangular tubing.

Chapter 2. Experimental set up, methods and materials

2.1. Introduction

In this chapter, the experimental system set up and general experimental methods related to this thesis are described.

2.2. Countercurrent chromatography (CCC) experimental set up

2.2.1. CCC centrifuge

Generally, the experiments were performed in CCC centrifuge. The inlet of the CCC instrument was connected to a piston pump via a sample injection port with sample loop and the outlet was connected to a UV detector followed by a fraction collector. A computer was connected to UV detector for signal collection. All instruments were connected by using 0.8 mm bore PTFE tubing.

2.2.1.1. J type CCC

The experiments were performed by J-type CCC which a prototype machine of Milli-CCC[®]. This machine was designed and made by the Brunel Institute for Bioengineering (Brunel University, Uxbridge, UK) with especial cantilever design as introduced in 1.1.3.2.i (Lee et al., 2003). The rotor radii (R) was 50 mm and the planet radii (r) was different for different columns. The centrifuge provided 500 – 2100 RPM while rotating in clockwise direction or counter-clockwise direction. Except for special experimental designs, the centrifuge rotated clockwise when the coil was filled with isotonic buffer or buffer.

The inlet of the CCC instrument was connected to a Gilson 307 pump (with a 25 ml head) (Gilson Inc, Middleton, WI, USA) via a three way valve and sample injection port. A HAAKE WKL 26 thermostat (Fisher Scientific, Waltham, MA, USA) was used to keep the coil in the CCC instrument at 15°C.

2.2.1.2. CCC column

The CCC columns, made at the Brunel Institute of Bioengineering, were made of PTFE tube. Table 2.2.1 shows the information of the columns used.

Table 2.2.1. Parameters of the CCC columns used in this thesis.

Column	Shape	Size (mm)	Total volume of column (ml)	Length of column (m)	R (mm)	r (mm)	Beta
A	circular	1.0	8.2	11.05	50	34.25-39	0.685-0.78
B	circular	1.6	20.4	10.16	50	28.1-37.7	0.56-0.75
C	rectangular	2.5 × 0.8	25.8	12.91	50	25.0-37.0	0.5-0.74
D	rectangular	0.8 × 2.5	29.2	14.61	50	25.2-37.2	0.5-0.74

The illustrations of column B, C, and D are shown in Figure 2.2.1.

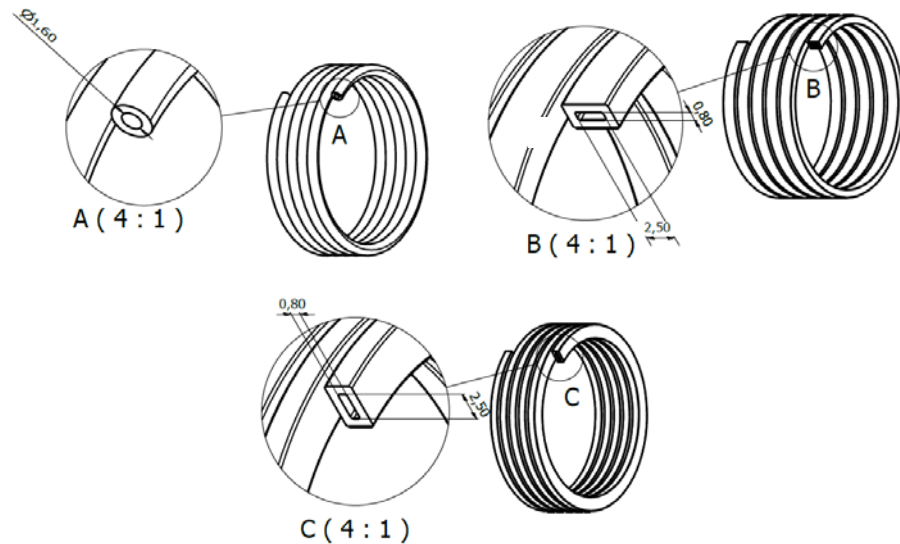
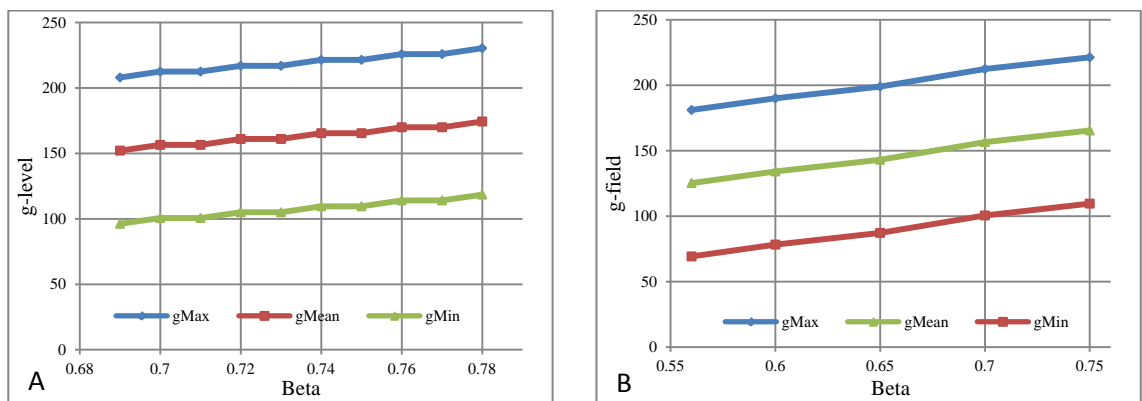


Figure 2.2.1.a. Column B with 1.6 mm-i.d. circular tube; 20.4 ml (10.16 m); $\beta=0.56-0.75$.

Figure 2.2.1.b. Column C with 2.5 mm × 0.8 mm rectangular tube (6 layers); 25.8 ml (12.91 m); $\beta=0.5-0.74$.

Figure 2.2.1.c. Column D with 0.8 mm × 2.5 mm rectangular tube (4 layers); 29.2 ml (14.61 m); $\beta=0.5-0.74$.

The g-field (van den Heuvel & Konig, 2011) comparison between the 4 columns is shown in Figure 2.2.2.



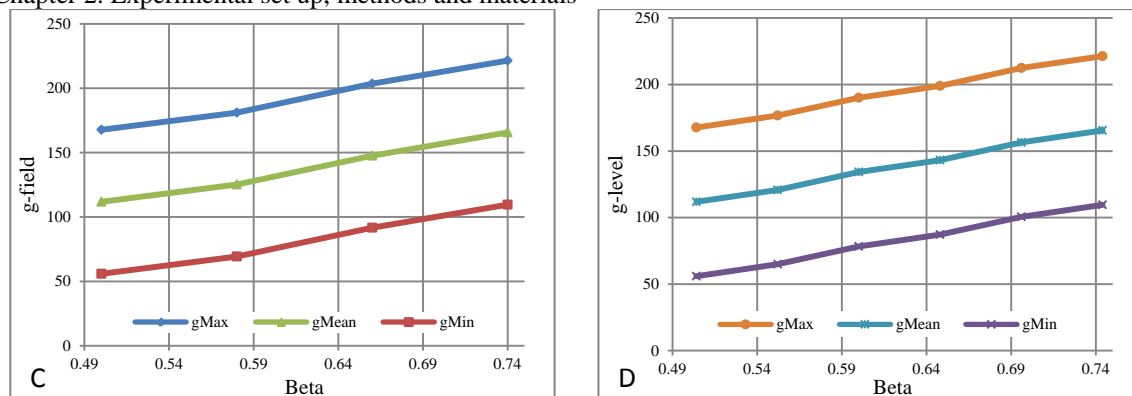


Figure 2.2.2. G-field comparison between 4 applied columns in this thesis derived by method of van den Heuvel & Konig (2011). A) Column A; B) Column B; C) Column C; D) Column D. Column A has the steadiest g-field; the column B has the middle value g-field; column C and D provides the similar g-field.

Figure 2.2.2 shows the different g-fields of 4 applied columns in this thesis which are generated by their different β value. Column A provides the least g-field change as the difference of its β is small. Column B, C and D have the same largest β thus the g-field in the periphery of these 3 columns are the same. Column C and D provide the greatest g-field change from periphery to centre.

2.2.1.3. CCCE Cantilever CCC

CCCE cantilever centrifuge has an especial design as the coil and the counterbalance can be seen through the Perspex front cover. The rotating column was also visualised by Cannon IXUS 990 IS digital camera.

The CCCE coil was wound on an aluminium disk in 5.5 loops by 2.2 m PTFE tubing with an internal diameter of 5 mm to provide 42 ml column volume. The distance between the planetary axis and centre of rotation (R) was 101.6 mm and the β value from 0.55 – 0.85. During the experiment, the cantilever centrifuge was arranged horizontally, therefore, the coil was also rotating in the horizontal plane. The illustration of the special centrifuge with the CCCE coil is shown in Figure 2.2.3.

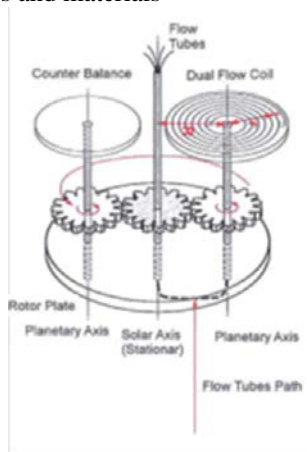


Figure 2.2.3. Illustration of CCCE cantilever centrifuge with coil rotating in horizontal plane. From van den Heuvel & Sutherland, 2007.

2.2.2. Sample loop

The sample loop port provides injection of a fixed volume of sample into the column. The sample loops in this thesis were made by 0.8 mm bore PTFE tube with different volumes. The different sample loops are shown in Table 2.2.2.

Table 2.2.2. Volume of sample loops and volume ratio to column A.

Sample loop	Volume (ml)	Volume ratio to column A (%)
A	0.32	4%
B	0.73	9%
C	1.52	19%
D	4.05	50%

The volume of sample loop was measured by the weight difference before and after a loop was entirely filled with water divided by density of water. The loop was flushed with water then acetone to remove dirt and then the remaining water and acetone were blown out by pumping through compressed air. The volume was taken as the average between 3 measurements.

2.2.3. UV detector and the signal recorder

The outlet of CCC instrument was connected to a Knauer K-2501 UV detector at 405 nm (with a preparative cell) (Knauer, Berlin, Germany) with a computer connected. The recording software was programmed by Brunel Institute for Bioengineering. The mobile phase passed through the UV detector and the signal was recorded as a chromatogram while the data was saved as .csv format file. The chromatogram recording was started when the start button was clicked manually after a sample injection.

2.2.4. Fraction collector

The UV detector followed by a Gilson 201 fraction collector (Gilson Inc, Middleton, WI, USA) for 1 or 2 ml per tube fractions. For 50 ml per tube fractions, Gilson 202 fraction collector was chosen to follow the UV detector (Gilson Inc, Middleton, WI, USA).

2.3. Materials and Buffer preparation method

2.3.1. Isotonic buffer

2.3.1.1. Isotonic buffer preparation

Isotonic buffer was the liquid in most of CCC centrifuge experiments in this thesis and provided an isotonic environment for the RBCs to minimise lysis in the flow studies. A preparation method for isotonic buffer in this report is listed below:

1. Weigh 9 g NaCl, 1.36 g Na₂HPO₄, 0.2 g NaH₂PO₄·H₂O into flask via Sartorius 1601A MP8-1 Balance: d = 0.1 mg (SARTORIUS, Germany) and Sartorius CP2202S Balance: d = 0.01 g (SATORIUS, Germany)
2. Add 100 ml of distilled H₂O and then fully mix and dissolve solute
3. Take 85 ml of solution and add in 915 ml distilled H₂O to dilute to 1 L isotonic buffer
4. Make sure pH is 7.4 and then store at 4°C ready to use

The information of chemicals used for isotonic buffer is shown in Table 2.3.1.

Table 2.3.1. List of chemicals and their suppliers used to make isotonic buffer.

Chemicals used for isotonic buffer	CAS	Supplier
NaCl	7647-14-5	Fisher Scientific
Na ₂ HPO ₄	7558-79-4	Fisher Scientific
NaH ₂ PO ₄ ·H ₂ O	7558-80-7	Fisher Scientific

2.3.1.2. Testing of isotonic buffer for RBC studies

The isotonic buffer was always checked to ensure it had been prepared correctly and did not lyse red cells as follows.

1. Prepare 10 centrifuge tubes (1 ml), and number them from 1 to 10.
2. Add 0.5 ml sheep blood sample to each tube.
3. For 5 of tubes, add 0.5 ml H₂O, while adding 0.5 ml buffer to the left 5 tubes.
4. After fully mixed for 30 mins, pipette 400 µl from each mixed sample to 96 wells

Chapter 2. Experimental set up, methods and materials

plate (Disposable polystyrene Microtiter plates, Thermo electron corporation, MA, USA) to prepare read optical density by BIOHIT ELX800 plate reader (BIOHIT BioTek Instruments, Finland).

5. Then centrifuge the left mixed sample at 3000 RPM for 10 mins by SANYO S693/03/515 Micro centrifuge (SANYO Electric Co., Ltd., Japan).
6. Pipette 400 μ l supernatant from each sample to 96 wells plate.
7. Read absorption value was at 405 nm. Plot results to graph by number of tube as horizontal axis and absorption value as vertical axis.

The information of blood samples were applied in this thesis is shown in Table 2.3.2.

Table 2.3.2. Information of blood samples were applied in this thesis.

Blood Sample	Supplier
sheep blood in Alsevers (before March 31 2013)	Harlan (Laboratories Ltd., Belton, Leicestershire LE12 9TE, UK)
rat blood in Alsevers	Harlan (Laboratories Ltd., Belton, Leicestershire LE12 9TE, UK)
mouse blood in Alsevers	Harlan (Laboratories Ltd., Belton, Leicestershire LE12 9TE, UK)
dog blood in Alsevers	Harlan (Laboratories Ltd., Belton, Leicestershire LE12 9TE, UK)
sheep blood in Alsevers (after March 31 2013)	TCS (TCS Biosciences Ltd., Botolph Claydon, Buckingham MK18 2LR, UK)
hen blood in Alsevers	TCS (TCS Biosciences Ltd., Botolph Claydon, Buckingham MK18 2LR, UK)
rabbit blood in Alsevers	TCS (TCS Biosciences Ltd., Botolph Claydon, Buckingham MK18 2LR, UK)
guinea pig blood in Alsevers	TCS (TCS Biosciences Ltd., Botolph Claydon, Buckingham MK18 2LR, UK)
horse blood in Alsevers	TCS (TCS Biosciences Ltd., Botolph Claydon, Buckingham MK18 2LR, UK)

*Alsevers is an isotonic saline/glucose solution containing citrate used to collect and store blood. The citrate prevents coagulation and the glucose maintains ATP levels for some time during storage.

The result of isotonic buffer test is shown in Figure 2.3.1.

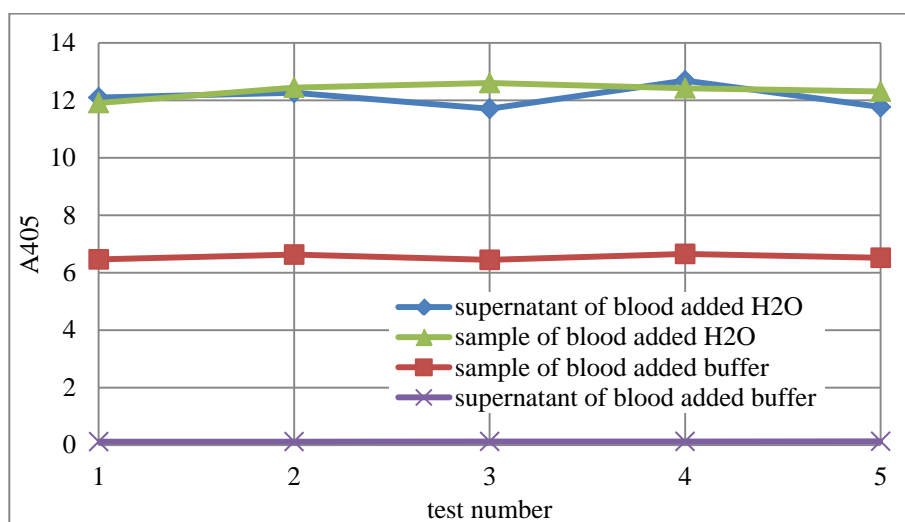


Figure 2.3.1. Isotonic buffer safety test. Comparison between sheep blood re-suspended by isotonic buffer and sheep blood re-suspended by H₂O shows absorption value for sample and supernatant kept the same

Chapter 2. Experimental set up, methods and materials
when blood re-suspended by H₂O while the supernatant of isotonic buffer re-suspended by blood decreased to 0 after centrifugation.

The objective of this test was to check whether sheep RBCs lyse in water and isotonic buffer. Figure 2.3.1 shows that the absorption values of supernatant for sheep blood samples prepared with adding H₂O were as high as its sample absorption values (were around 12). On the contrary, absorption values of supernatant for sheep blood samples prepared with adding isotonic buffer kept in low level (were nearly 0) while its sample absorption values were much higher (i.e. around 6.3).

This shows that the RBC lyses when suspended in H₂O but no lysis in isotonic buffer, therefore the isotonic buffer kept isotonic environment for cells.

2.3.2. Cell fixation solution preparation

Cell fixation was applied to fix the shape of RBCs by glutaraldehyde as the aldehyde group can combine with amino groups of cell surface proteins to form a cross link bridge. Compared to formaldehyde fixation, glutaraldehyde fixation provides more rigid fixed cell as its greater length and 2 aldehyde groups allows it to link a distant pair of proteins molecules.

Instead of isotonic buffer, 0.15M Sodium phosphate buffer, pH 7.4 was applied in cell fixation. This isotonic buffer was prepared as follows.

1. Dissolve 2.04 g KH₂PO₄ in 100 ml distilled water to prepare 0.15M KH₂PO₄.
2. Dissolve 2.13 g Na₂HPO₄ in 100 ml distilled water to prepare 0.15 M Na₂HPO₄.
3. 0.15M Sodium phosphate buffer, pH 7.4 (100 ml) was prepared by mixing 24 ml 0.15M KH₂PO₄ and 76 ml 0.15 M Na₂HPO₄.
4. Adjust pH if necessary.

The information of chemicals used for 0.15M Sodium phosphate buffer, pH 7.4 is shown in Table 2.3.3.

Table 2.3.3. List of chemicals and their suppliers used to make 0.15 M Sodium phosphate buffer, pH 7.4.

Chemicals used for Sodium phosphate buffer	CAS	Supplier
Na ₂ HPO ₄	7558-79-4	Fisher Scientific
KH ₂ PO ₄	7778-77-0	Fisher Scientific

The fixation process is an irreversible change. Because any remaining glutaraldehyde may generate cross link bridge between cells, fixative was neutralised by adding a 2 molar excess of glycine.

The information of chemicals used for cell fixation is shown in Table 2.3.4.

Table 2.3.4. List of chemicals and their suppliers used for cell fixation.

Chemicals used for cell fixation	CAS	Supplier
glutaraldehyde solution (70% v/v, double distilled)	111-30-8	SIGMA-ALDRICH
Glycine	56-40-6	SIGMA-ALDRICH

2.3.3. Surfactant (Tween[®] 20) added isotonic buffer preparation

Tween 20 was used to hinder the RBC aggregation that occurred under certain conditions in the flow separation of fixed RBCs .

The concentration of Tween[®] 20 applied in this thesis was from 0.05% to 0.5%, v/v, by mixing certain volume of Tween[®] 20 with isotonic buffer. The information of Tween[®] 20 is shown in Table 2.3.5.

Table 2.3.5. Information of Tween[®] 20 for hindering cell aggregation

Chemicals used for hindering cell aggregation	CAS	Supplier
Tween [®] 20	9005-64-5	ACROS ORGANICS

As Tween[®] 20 caused the lysis of unfixed RBCs, it was only applied to fixed RBCs experiment.

2.4. Blood sample preparation methods

2.4.1. Blood sample wash method

In order to obtain RBCs sample, a preparation method was used to remove blood plasma, white blood cells and platelet, etc., which is listed as below:

1. Prepare 2 clean centrifuge tubes (2 ml), loose caps.
2. Pipette certain volume (e.g. 1 ml) blood sample to first centrifuge tube.
3. Balance centrifuge with the other tube using the same volume of H₂O.
4. Centrifuge blood sample at 3000 RPM for 10 mins.
5. Remove and dispose of supernatant in Virkon and then add isotonic buffer to same volume (e.g. 1 ml) as the other centrifuge tube.

6. Fully mix buffer and blood cells to wash.
7. Centrifuge washed sheep blood sample again at 3000 RPM for 10 mins.
8. Pipette supernatant away and dispose with Virkon.
9. Add isotonic buffer to wanted volume to prepare washed blood sample (usually recovered to the original volume as pipette in step 2).

The process should be repeated if necessary.

This procedure can also be used to prepare RBCs sample by certain haematocrit (hct) by before the last step reading volume of sedimented RBCs (pellet), then adding required volume of buffer to prepare the required haematocrit. (e.g. if cell volume was 1ml and concentration of blood cell sample required was 20% hct, then add to 5 ml with isotonic buffer).

2.4.2. Red blood cell fixation method

2.4.2.1. Cell fixation method

In order to obtain rigid RBCs glutaraldehyde was applied for cell fixation and glycine solution was applied to inactive the fixation reaction. A detailed procedure of cell fixation by glutaraldehyde is listed below:

1. 1 ml blood in Asevers was spun down (3000 RPM, 10 mins), supernatant removed and the pellet re-suspended in 0.15M sodium phosphate buffer, pH 7.4 and re-spun. This was repeated 3 times and the cells re-suspended to 0.5 ml.
2. 0.5 ml sodium phosphate buffer containing 2% glutaraldehyde (70% (v/v), double distilled) was added to re-suspended RBCs sample by giving a final glutaraldehyde concentration of 1%.v/v.
3. After 10 mins fixation process, glycine solution (2 molar excess) was added to the fixed RBCs sample to inactive the glutaraldehyde.
4. After 30 mins, the fixed RBCs solution was spun down (3000 RPM, 10 mins), supernatant removed and the pellet re-suspended in isotonic buffer to 1 ml.

2.4.2.2. Cell fixation result test

Successful fixation of the fixed RBCs was confirmed by re-suspending fixed cells in H₂O. After centrifugation, for unfixed cells, a clear red colour supernatant of released haemoglobin (Hb) was obtained whereas with fixed cells there was no red colour in its supernatant. A detailed procedure of cell fixation result test is listed as below:

Chapter 2. Experimental set up, methods and materials

1. Prepare 10 centrifuge tubes (1 ml), and number them from 1 to 10.
2. Add 0.5 ml sheep blood sample to each tube.
3. For 5 of tubes, add 0.5 ml H₂O, while fixing the RBCs to the left 5 tube as described method in 2.4.2.1 but added H₂O to 1 ml instead of isotonic buffer in last step.
4. After the cell fixation and re-suspension, pipette 400 µl each mixed sample to 96 wells plate to prepare read optical density by plate reader.
5. Then centrifuge left mixed sample at 3000 RPM for 10 mins.
6. Pipette 400 µl supernatant of each sample to 96 wells plate.
7. Read absorption value was at 405 nm. Plot results to graph by number of tube as horizontal axis and absorption value as vertical axis.

The result of cell fixation result test is shown in Figure 2.4.1.

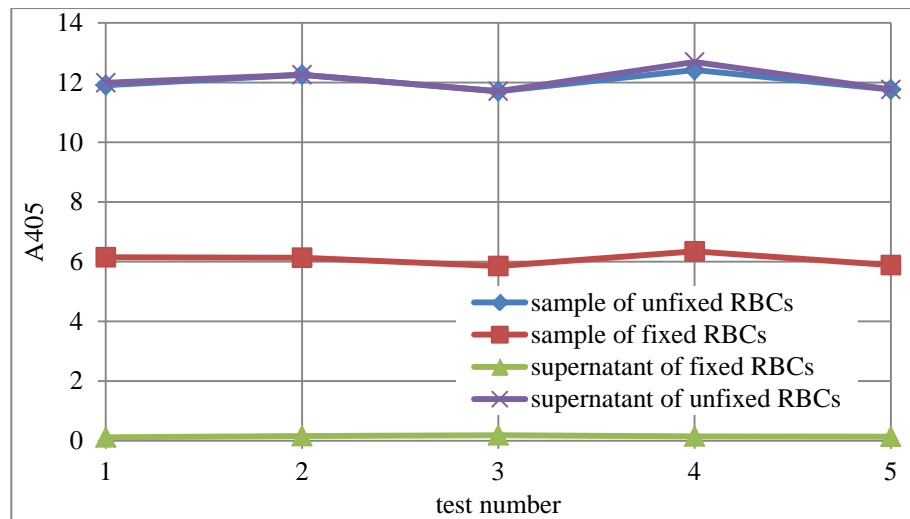


Figure 2.4.1. Cell fixation results test. The result of sheep RBCs fixation results test shows the supernatant value of fixed sheep RBCs dropped to 0 while the supernatant value for unfixed sheep RBCs was as high as its sample value.

From Figure 2.4.1, it shows after the cell fixation, RBCs cannot lyse in H₂O while the unfixed broke and released Hb. Therefore, the cell fixation was successful.

Alos fixed cells were checked by light microscopy using a SW-107 biological microscope (PaiVeiDi tech. Ltd., Beijing, China) to confirm their shape was unaltered and there was no cross link bridge between cell to cells. Figure 2.4.2 shows results for fixed sheep and hen cells compared with unfixed cells (Figure 2.4.3)

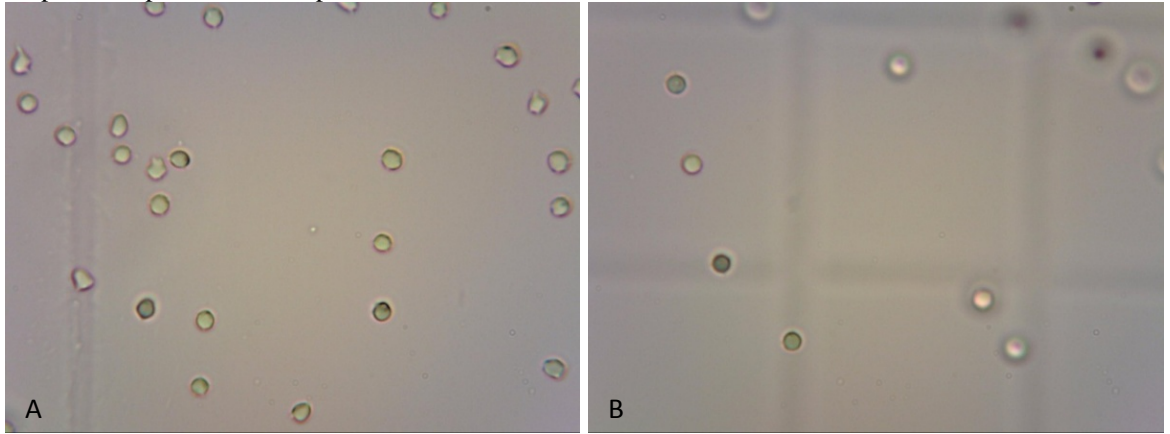


Figure 2.4.2. A) Light micrograph of unfixed sheep RBCs (left); B) Light micrograph of glutaraldehyde fixed sheep RBCs (right) (400X).

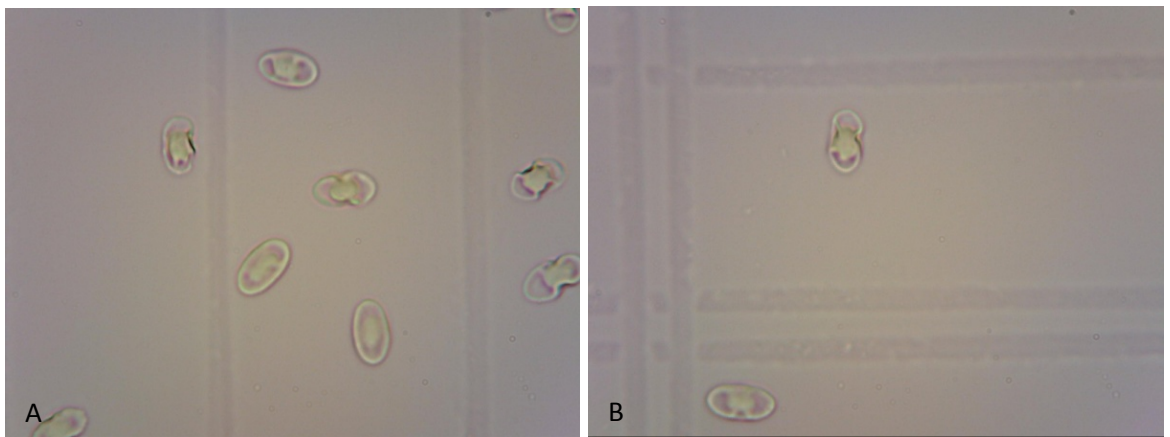


Figure 2.4.3. A) Light micrograph of unfixed hen RBCs (left); B) Light micrograph of glutaraldehyde fixed hen RBCs (right) (400X).

Figure 2.4.2 and Figure 2.4.3 show that, although a slight shrinkage was observed on fixation, generally the shape and size of sheep/hen RBCs did not obviously change. In particular the oval shape of hen RBCs was preserved. In addition both sheep and hen fixed RBCs when re-suspended in water showed no release of haemoglobin, confirming that fixation was successful.

2.4.3. Sheep RBCs ghost cell preparation

RBCs ghost cells, which is the RBCs membrane that remains intact after haemolysis, has the size between free Hb and intact RBCs. Since the blood sample also includes RBCs membrane fragments, therefore, the behaviour of sheep RBCs ghost cell was examined. A detailed procedure to prepared ghosts cell result is listed as below:

1. 2 ml sheep blood sample was pipetted to centrifugal tube then centrifuged at 3000 RPM for 10 mins.

2. The sedimented sheep RBCs (pellet) were lysed by re-suspending in deionised water to 2 ml after supernatant removed.
3. The lysis sheep RBCs sample was washed 3 times as described in 2.4.1.
4. The sedimented sheep RBCs ghost cell (pellet) was re-suspended by isotonic buffer to 2 ml after the free Hb (supernatant) removed.

The light micrograph of sheep RBCs ghost cells was obtained by biological microscope as shown in Figure 2.4.4.



Figure 2.4.4. Light micrograph of prepared sheep RBCs ghost cell by biological microscope (400X).

2.5. Analytical methods

2.5.1. Fractionated sample analyse method

A method for analysing fractionated sample was developed to obtain absorption value at 405 nm by plate reader. The presence of RBCs in fractionated samples was demonstrated by measuring the absorbance at 405 nm before and after centrifugation of eluted fractions. If cells are present, the absorbance before centrifugation will have a contribution to absorbance from the cells scattering light as well as absorbance from any Hb present. After centrifugation the absorbance will be due only to any free Hb present. This method was used to analyse ratio of RBCs and free Hb in each sample fraction, which is listed as below:

1. Pipette 400 μ l of each sample fraction to 96 wells plate after fully mixed to avoid sedimented red blood cells exist.
2. Centrifuge the remaining sample at 3000 RPM for 10 mins.
3. Pipette 400 μ l of supernatant for each sample fraction to 96 wells plate.
4. Sit 96 wells plate to spectrophotometer to read A405 required filter.
5. Collect data and plot graph by fraction number as horizontal axis and absorption value of analyses for blood cell fraction as vertical axis.

2.5.2. Peak area measure method

Peak area is an important index of chromatogram to measure a signal peak, which is applied to compare ratio for single peak or compare concentration of same peak in different samples. As the software which was used to collect the UV signal does not have a function for peak area calculation, a method for determining peak area by Origin8 was applied to check peak area of UV signals, which is listed as below:

1. Import data in Origin8, then choose needed data column to plot graph
2. Choose analysis – mathematics – integrate – open Dialog – input
3. Set 2 arrows to beginning and the end of target peak/area, then click OK
4. Peak area and others information will be showed on Results Log

2.5.3. Cell size measurement method

Cell size is an important piece of for this thesis. A cell size measurement method was created by combining to use ImageJ software (Downloaded from: <http://imagej.nih.gov/ij/download.html>) and a stage micrometer (Pyser-SGI Ltd., UK). The principle of this measurement method is based on the distance of pixels keeps same between different light micrographs. As the light micrographs were obtained under same condition with the same pixels, the measurements are valid.

1. Take the picture for stage micrometer, sheep RBCs and hen RBCs by light biological microscope at the same enlarge times, respectively.
2. Open the picture of stage micrometer in ImageJ, and choose “straight” tool to draw a line equals to 100 μm . Then choose analyze – Set scale, then define “known distance” as 100 and “unit of length” as μm – click “global”.
3. Open picture of sheep RBCs and hen RBCs, and choose “straight” tool to draw a line equals to cell size. Then choose analyze – tools – scale bar to measure the cell size.

The picture of stage micrometer is shown in Figure 2.5.1.

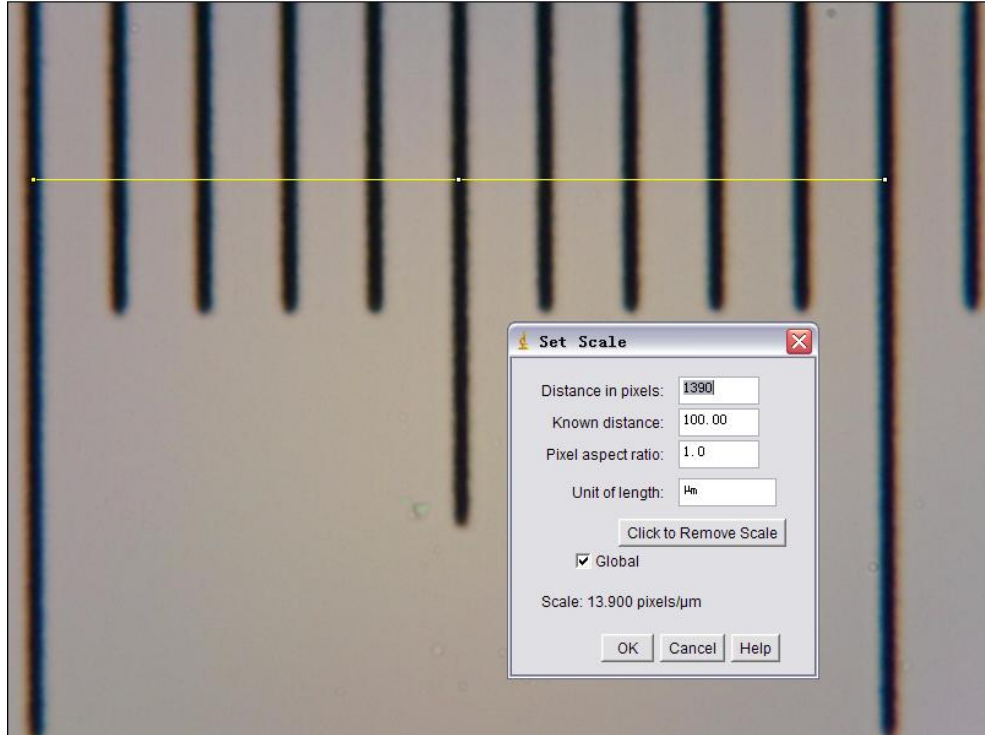


Figure 2.5.1. The defined distance from light micrograph of stage micrometer (400X). As this stage micrometer was 1 mm divided into 0.01 mm each scaled distance, therefore, the distance for 10 scales was 100 μm . The pictures of measurement of sheep and hen RBCs from light micrographs are shown in Figure 2.5.2.

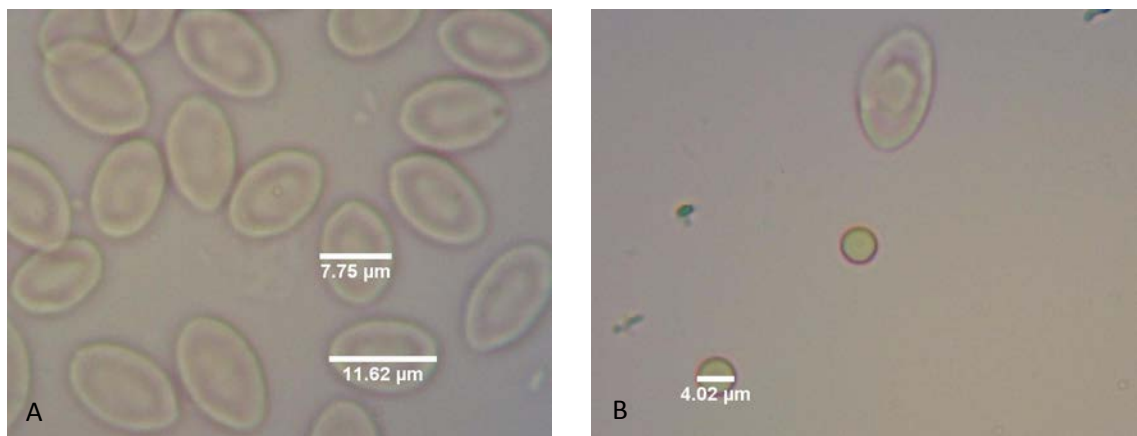


Figure 2.5.2. The measurement of sheep RBCs size from light micrographs (400X) (A) and the measurement of length and width of hen RBCs (400X) (B) shows the sheep RBCs are round with diameter as 4.02 μm and hen RBCs are oval shape with width as 7.75 μm and length as 11.62 μm .

Figure 2.5.2 shows the size difference between sheep RBCs and hen RBCs as hen RBCs are much bigger than sheep RBCs with different length and width while sheep RBCs are round with constant diameter.

Figure 2.5.3 shows the measured diameters of different RBCs in species.

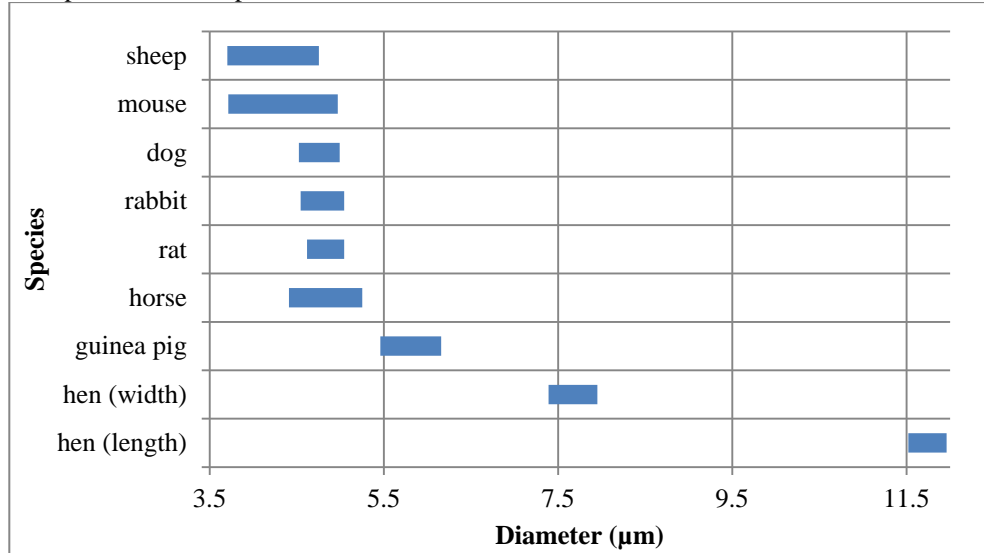


Figure 2.5.3. The diameters of different RBCs in species measured by microscope. From small to big, order of diameter in average is sheep (4.23 µm); mouse (4.34 µm); dog (4.76 µm); rabbit (4.79 µm); rat (4.83 µm); horse (4.83 µm); guinea pig (5.81 µm); hen width (7.75 µm)/hen length (11.74 µm).

There may be limitations to this method of measurement, and therefore these values may differ from actual values. However, the method does show systematic differences in diameter and size order for the RBCs used in this study.

The mean cell volume (MCV) and calculated diameter of above RBCs in species was also measured by Multisizer™ 4 coulter counter (Beckman Coulter (UK) Ltd., United Kingdom) as shown in Figure 2.5.4 and Figure 2.5.5, respectively.

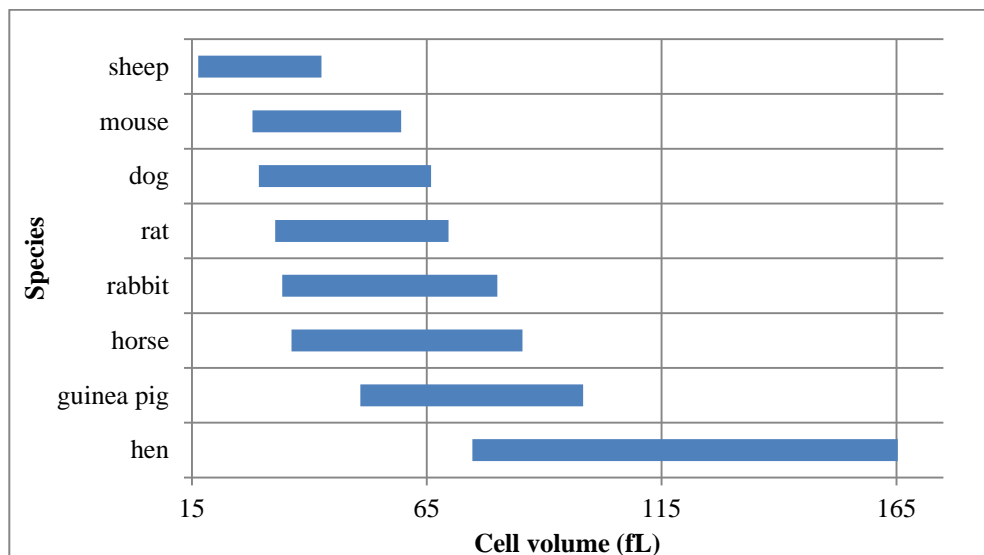


Figure 2.5.4. Cell volumes of different RBCs in species (coulter counter). The mean cell volume (MCV) of different RBCs in species measured by coulter counter. From small to big, order of MCV in average is sheep (28.03 fL); mouse (44.15 fL); dog (46.66 fL); rat (51.38 fL); rabbit (52.67 fL); horse (55.6 fL); guinea pig (71.32 fL); hen length (115.8 fL).

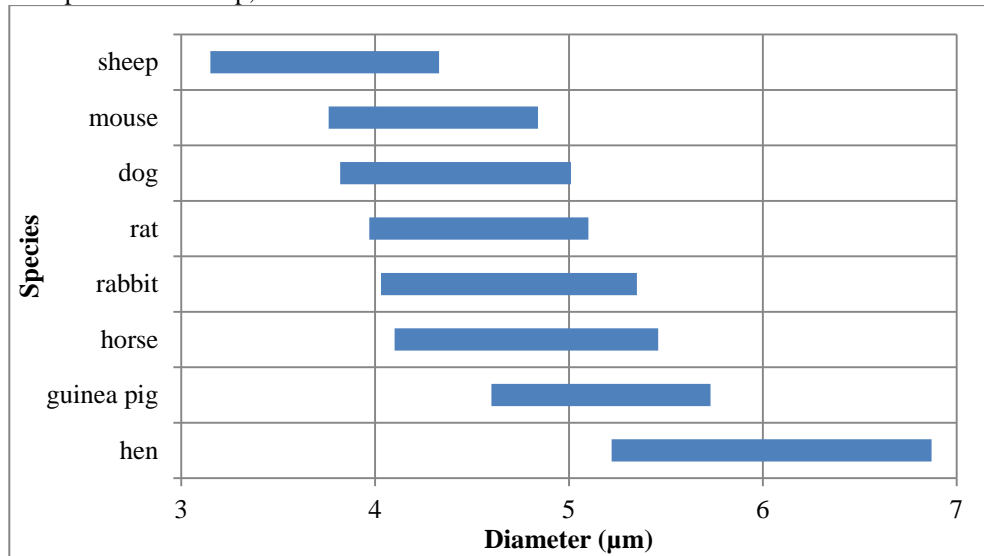


Figure 2.5.5. Cell diameters of different RBCs in species (coulter counter). From small to big, order of diameter in average is sheep (3.69 µm); mouse (4.28 µm); dog (4.36 µm); rat (4.45 µm); rabbit (4.57 µm); horse (4.64 µm); guinea pig (5.06 µm); hen (5.5 µm). (The diameters are calculated assuming as sphere.)

By comparing Figure 2.5.3 to Figure 2.5.5 as shown in Figure 2.5.6, the diameter of these species of RBCs were in close agreement. The particular exception is hen RBC, but of course these are oval shaped cells, with diameters not readily calculable from Coulter volume measurements by assuming as sphere. Therefore, Coulter counter gave only 1 value for hen RBCs and microscope measured both length and width values. The calculation also made smaller diameter values than microscope measured as shape of RBCs is disk but not ball. However, compare to limited measured values by microscope, Coulter counter gave a board measurement range Generally, the order of sizes is similar by both microscope and coulter counter measurement with the exception of rabbit and rat RBCs, which are very similar in size anyway.

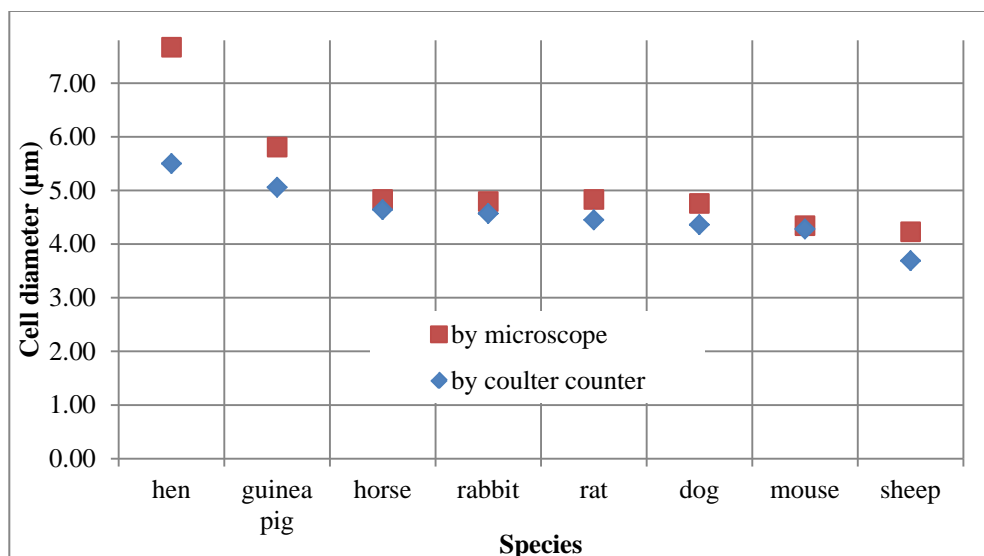


Figure 2.5.6. The comparison of cell diameters measured by microscope and coulter counter. Data (average value) was taken from Figure 2.5.3 and Figure 2.5.5 (hen RBCs diameter was width), which shows the similarity of diameter value between the 2 measurements.

A comparison of cell volumes between measured by coulter counter and from literatures is shown in Figure 2.5.7.

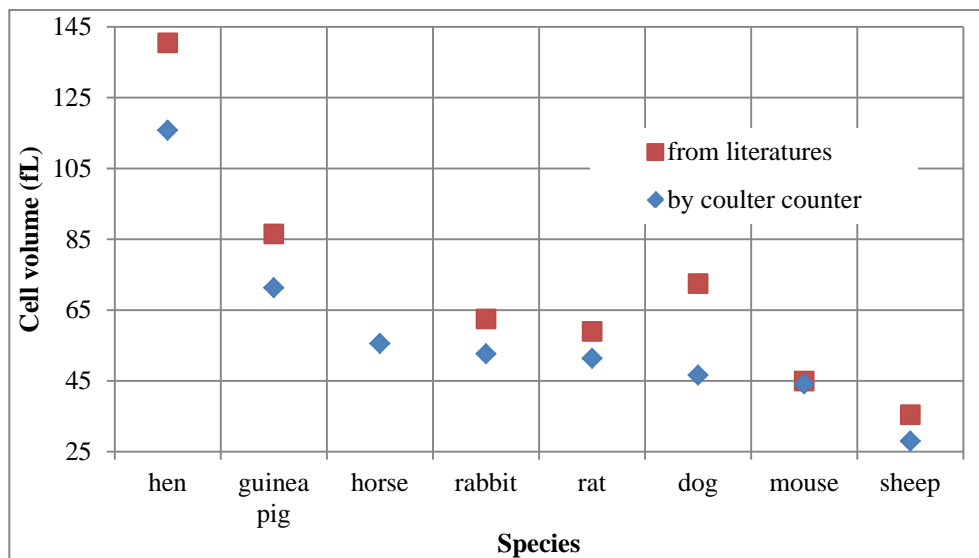


Figure 2.5.7. The comparison of cell volumes measured by coulter counter and are from literatures. Data (average value) was taken from Figure 2.5.4 and Table 1.2.1, which shows the similarity and difference of cell volumes between measurement and literatures.

Figure 2.5.7 shows the value from measurement and literatures are generally similar, at least most of their order (except dog RBC).

Therefore, after the comparisons of cell diameters and cell volumes measured by different methods and data from literatures, the method in this thesis were validated

2.5.4. Cell density measurement

Cell density was measured by Percoll[®]. The information of Percoll[®] applied in this thesis is shown in Table 2.5.1.

Table 2.5.1. Information of Percoll[®] applied for cell density measurement.

Chemical used for RBCs density measurement	Lot	Supplier
Percoll [®]	SLBF9323V	SIGMA-ALDRICH

The measurement method is listed below:

1. Diluted 9 parts of Percoll with adding 1 part of 1.5 M NaCl or 2.5 M sucrose to

Chapter 2. Experimental set up, methods and materials

stock isotonic Percoll (SIP). Solutions of SIP are diluted to lower densities by adding 0.15 M NaCl or 0.25 M sucrose.

2. Adding 2 μ L blood to certain density SIP solution then centrifuged under 13000 RPM (6,613g – 11,336g) for 10 mins with the same density SIP solution together as control.
3. As cells sediment where their density layer is, therefore, then measure the refractive index of this density layer from control.
4. Read density from Figure 2.5.8.

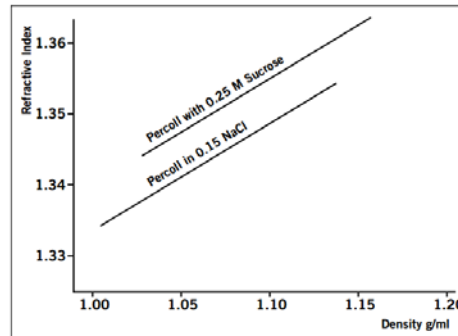


Figure 2.5.8. Relationship between refractive index and SIP density. From Percoll-methodology and applications, n.d..

The densities of RBCs used in this thesis as measured by this method are shown in Table 2.5.2.

Table 2.5.2. Measured RBCs density in species.

species	hen	horse	dog	sheep	rat	guinea pig	mouse	rabbit
density (g/ml)	1.0648	1.0500	1.0474	1.0461	1.0447	1.0415	1.0362	1.0296

Due to the imprecision of this measurement method, the measured values might be different to the real values, however, Table 2.5.2 shows the density difference and a general density order of applied RBCs.

2.5.5. Cell number counting method

Cell number counting is the important method to analyse fractions and evaluate the results of separation. Haemocytometer was applied in this thesis to achieve the cell number counting.

The design of haemocytometer used is shown in Figure 2.5.9.

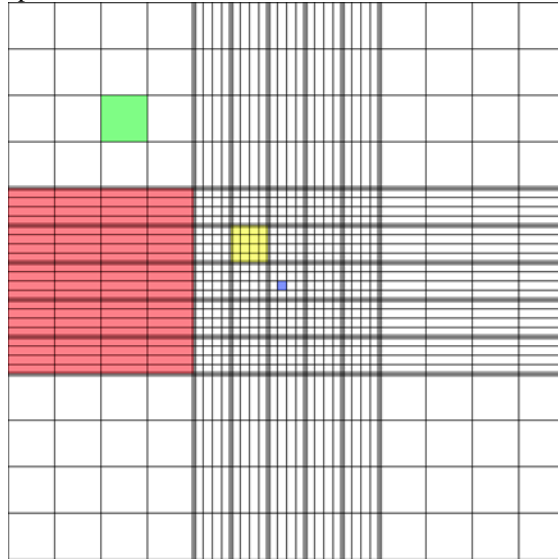


Figure 2.5.9. Illustration of haemocytometer applied in this thesis, where 1 mm^2 is divided into 400 blue squares.

Each red square is $1 \text{ mm} \times 1 \text{ mm}$, with the height as 0.1 mm , the volume of the central 5×5 yellow squares is $0.1 \mu\text{L}$. When counting, 5 yellow squares are counted which are top-left; top-right; central; bottom-left; bottom-right. Therefore, if the average of cell number for the 5 squares is N , then the cell number / mL follows the equation below:

$$\text{Cell number/mL} = N \times 25 \times 10 \times 10^3 \quad [\text{Equation 2.5.5a}]$$

The principle of counting cells in the square was only to count cells that were completely in the square. However, no matter which principle was chosen, it must be consistent through the whole experiment.

2.6. Discussion and Conclusion

To achieve the research and development of fundamental behaviour of RBCs and the cell separation method by Milli-CCC[®], the influence of 3 aspects should be investigated as 1) Operational conditions; 2) Instrument constructive conditions; 3) Cell properties. The methods used prepared in this thesis have been described and where necessary, validated in this chapter.

1) Preparation for investigation of operational conditions influence

The operational conditions include pumping flow rate and rotational speed. For all experiments, all different solutions were pumped by piston pump and the adjustable rotational speed was provided by Milli-CCC[®] and CCCE cantilever centrifuge. The

different injection volumes of blood samples were achieved by preparing different sample loops which provides injection volumes equal to 4% - 50% of column volume.

Due to the limited choices of filters for plate reader, 405 nm was chosen as the wavelength as it provided the highest OD value. Therefore, the UV detector was unified to 405 nm during the detection of CCC process.

2) Preparation for investigation of instrument constructive conditions influence

The different shapes of coiled tubes used were introduced in 2.2.1.2 which were made as the column standard for Milli-CCC[®]. The 4 columns applied in this thesis had similar β value which provided the opportunity to compare different cell behaviours which are only influenced by differences in a) inner diameters, b) tube shapes, and c) different geometry directions. Due to the commercial and standard of instrument and column making, the research results are not limited by special instruments or columns but can be applied for all Milli-CCC[®] centrifuges broadly.

3) Preparation for investigation of cell properties influence

For all above experiments in this thesis, a biocompatible environment for RBCs during CCC process was an essential requirement. Safety test for isotonic buffer is necessary to check whether it can ensure no damage on RBCs which was shown in Figure 2.3.1.

In order to investigate one of the cell properties – deformability, cell fixation by glutaraldehyde was applied to change the flexibility of RBCs. 2.4.2.2 has shown the success of the fixation as fixed RBCs cannot be lysed by H₂O. For the other cell properties – aggregation, surfactant – Tween[®] 20 was added to isotonic buffer in order to hinder the cell aggregation between fixed cells. Therefore, the comparison between aggregated and non-aggregated cells can be achieved.

In order to investigate the behaviour difference between cell fragments and intact RBCs, RBCs ghost cells were also prepared as in 2.4.3. Other necessary methods to support the research such as size and density measurement were also developed, described in section 2.5.3 and section 2.5.4.

The information of instruments applied in this thesis is summarized in Table 2.6.1.

Chapter 2. Experimental set up, methods and materials
 Table 2.6.1. Information of instruments applied in this thesis.

Instrument	P/N	Manufacturer
Countercurrent Chromatography	Milli-CCC®	Brunel Institute for Bioengineering, Brunel University, Uxbridge, UK
Piston pump	Gilson 307	Gilson Inc, Middleton, WI, USA
Thermostat	HAAKE WKL 26	Fisher Scientific, Waltham, MA, USA
UV detector	Knauer K-2501	Knauer, Berlin, Germany
Fraction collector A	Gilson 201	Gilson Inc, Middleton, WI, USA
Fraction collector B	Gilson 202	Gilson Inc, Middleton, WI, USA
Balance A	Sartorius 1601A MP8-1	SARTORIUS, Germany
Balance B	Sartorius CP2202S	SARTORIUS, Germany
Plate reader	BIOHIT ELX800	BIOHIT BioTek Instruments, Finland
Disposable polystyrene Microtiter plates (96 wells)	S2524208	Thermo electron corporation, Milford, MA, USA
Micro centrifuge	SANYO S693/03/515	SANYO Electric Co., Ltd., Japan
Biological microscope	SW-107	PaiVeiDi tech. Ltd., Beijing, China
Coulter counter	Multisizer™-4	Beckman Coulter (UK) Ltd., UK

Chapter 3. Fundamental behaviour of red blood cells in fluctuating g-field

3.1. Summary

The primary aspect researched in this chapter was to define the operational conditions that influenced the behaviour of red blood cells flowing in a single phase of isotonic buffer in a rotating coil in a Milli-CCC[®] centrifuge. These conditions were flow rate, direction, and rotational speed / direction.

Conditions were established at which all cells were retained in the coil (minimum operating conditions) and at which all cells were not retained and were eluted in the column volume (maximum operating conditions).

These fundamentals of behaviour were established using sheep RBCs, and were then extended to 7 other species of RBC: hen, guinea pig, horse, rat, rabbit, dog, and mouse, all of which showed differences in both the minimum and maximum operating conditions.

Retained cells could be eluted by altering the operational conditions of flow and/or rotational speed and this will be developed as a method for cell separations in subsequent chapters based on the cell specific difference that have been established for the minimum and maximum operating conditions.

The minimum operating conditions are influenced by cell size but not by cell density for the series of RBCs studied. By contrast maximum operating conditions are not influenced by cell size.

The dependence on flow rate and rotational speed of the coil (g-field) of the initial operating conditions required to retain cells in the CCC coil has been shown to be modelled by a theoretical equation for particles in fluctuating g-fields reported by Fedotov et al (2003), provided a correction factor, α , is included. This factor varies for the 8 different species of RBCs studied, and there are some indications that this might relate in part at least to cell surface charge. Chapter 4 shows that membrane deformability may also have a role in cell behaviour in rotating coils.

3.2. Experimental

3.2.1. Sheep RBCs behaviour in CCCE cantilever

3.2.1.1. Introduction

In order to research the behaviour of sheep RBCs in the fluctuating g-field without flowing, CCCE cantilever was applied as the column of this instrument was visible via its Perspex front cover. Therefore, it was suitable to observe the result during and after the rotation. In order to eliminate the influence of earth gravity, the CCCE cantilever was arranged horizontal so that the CCCE column was horizontal. A detailed procedure of rotation without flowing experiment is listed as below:

3.2.1.2. Method

Instrument set up: CCCE cantilever CCC (described in 2.2.1.3); 0.32 ml sample loop.

1. Isotonic buffer was pumped to fill the column of CCCE cantilever CCC.
2. Sheep RBCs were washed 3 times (as the method described in 2.4.1) before they were pumped to the middle of the coil by isotonic buffer at 5 ml/min with no rotation.
3. Then the column started to rotate in 250 RPM, clockwise direction for 12 hours with no isotonic buffer pumping. Outlet end of column was opened and the other end was in isotonic buffer while both of them were placed higher than column.
4. Pictures were obtained before and 30 mins later after the rotation.

Above process was repeated rotating in counter-clockwise direction and results are shown in section 3.2.1.3.

3.2.1.3. Results

The position of blood sample before and 30 mins later after the rotation in clockwise direction is shown in Figure 3.2.1.

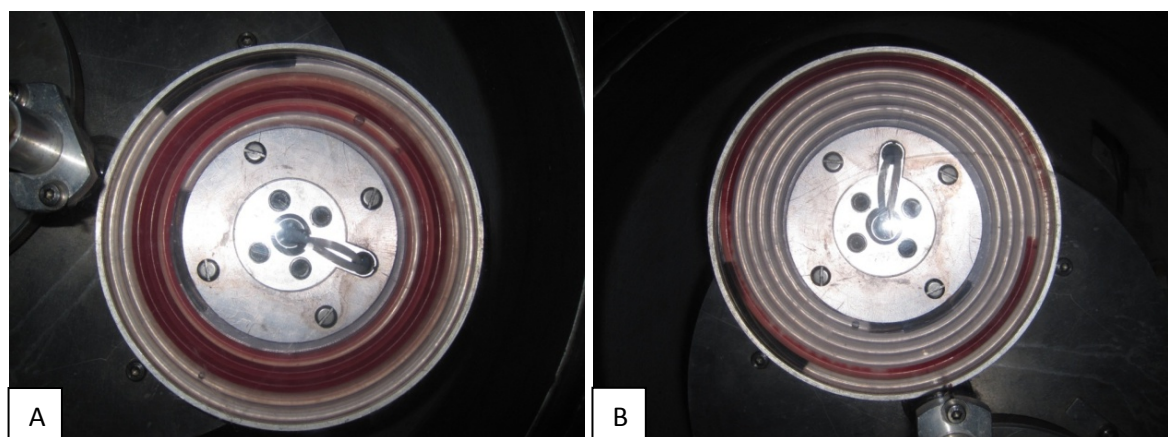


Figure 3.2.1. Behaviour of sheep RBCs in CCCE cantilever (clockwise direction). A) Position of blood sample before the clockwise rotation at 250 RPM for 12 hr. B) Position of blood sample 30 mins after the

Chapter 3. Fundamental behaviour of red blood cells in fluctuating g-field
clockwise rotation had ceased. 0.32 ml of sheep blood sample washed and re-suspended in isotonic buffer was injected into CCCE coil (42 ml; 5 mm ID) at 250 RPM for 12 hours with no isotonic buffer pumping.

Figure 3.2.1 shows after rotation in clockwise direction, with no liquid flow, the RBCs moved from the middle of coil to the periphery of the coil, which was the tail.

The behaviour of sheep RBCs before and after the rotation for 12 hours in a counter-clockwise direction is shown in Figure 3.2.2.

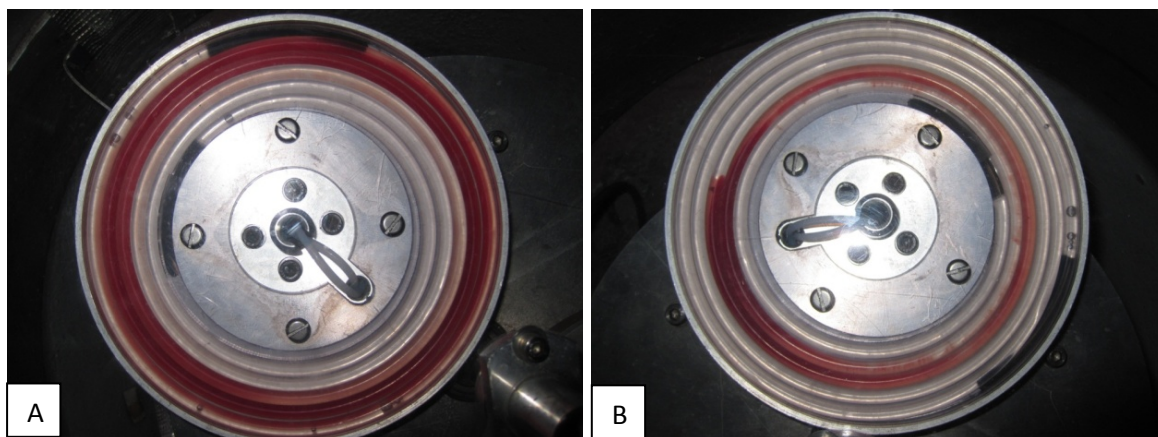


Figure 3.2.2. Behaviour of sheep RBCs in CCCE cantilever (counter-clockwise direction). A) Position of blood sample before the counter-clockwise rotation at 250 RPM for 12 hours. B) Position of blood sample 30 mins after the counter-clockwise rotation had ceased. 0.32 ml of sheep blood sample washed and re-suspended in isotonic buffer was injected into CCCE coil (42 ml; 5 mm ID) at 250 RPM for 12 hours with no isotonic buffer pumping.

Figure 3.2.2 shows after the rotation in counter-clockwise direction, the RBCs moved from the middle of coil to the centre of the coil which is the tail.

3.2.2. Relationship between pumping direction and rotational direction

3.2.2.1. Introduction

Because the CCC column may rotate in clockwise direction and counter-clockwise direction, and the pumping direction can also be from head to tail direction or tail to head direction, there are 4 combinations to operate the CCC. In order to research the difference and the similarity of RBCs behaviours in these 4 combinations, Milli-CCC[®] and column A was applied in this study.

3.2.2.2. Method

Chapter 3. Fundamental behaviour of red blood cells in fluctuating g-field
Instrument set up: Milli-CCC[®] (described in 2.2.1.1) with column A (described in 2.2.1.2),
0.32 ml sample loop; column temperature as 15 °C.

1. Column of CCC instrument was filled with isotonic buffer.
2. The column in the CCC instrument rotated in either clockwise direction or counter-clockwise direction at an initial rotational speed as 1000 RPM.
3. Sheep blood (sample included: around 5.03E+10 sheep RBCs) was injected through the sample injection port into the coil under an initial flow rate as 0.5 ml/min in either the tail to head direction or head to tail direction.
4. Isotonic buffer was pumped for $2 \times$ column volumes through the coil and the eluting components were collected in fractions as 1 ml/tube.
5. From No.10 to No.17 fractions were analysed in a plate reader at 405 nm before and after centrifugation (as described in 2.5.1).

Results are shown in section 3.2.2.3.

3.2.2.3. Results

The objective of 3.2.2.3 is to examine how sheep RBCs behaved in the coil when there was liquid flow, and the influence of pumping direction and rotational direction on this behaviour. A comparison of the 4 different elutions that are possible is summarized in Figure 3.2.3.

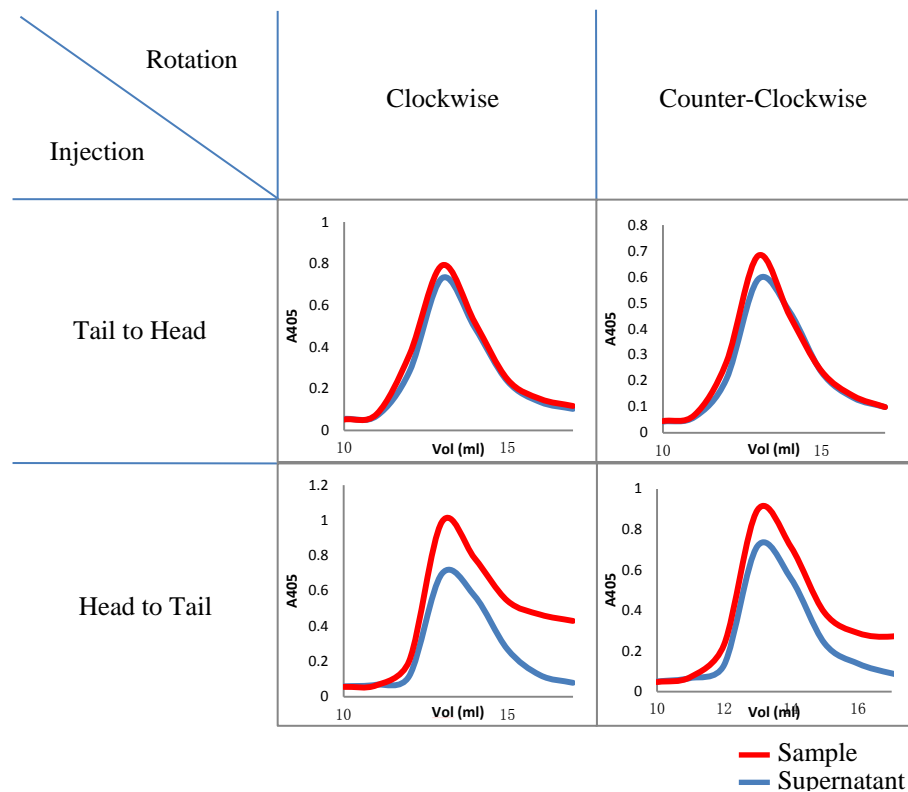


Figure 3.2.3. Comparison of the 2nd column volume elution components between 4 operation combinations of flow direction (head to tail and tail to head) and coil rotation (clockwise and counter-clockwise). Clockwise rotation + pumping from tail to head and counter-clockwise rotation + pumping from tail to head show similar behaviour whereas; counter-clockwise rotation + pumping from head to tail and clockwise rotation + pumping from head to tail both show a different behaviour but similar to each other. 0.32 ml of sheep blood sample was injected to CCC coil (Column A: 8.2 ml; 1 mm ID) at 1000 RPM at 0.5 ml/min. Fractions were collected 1 ml/tube. Fractionated samples were analysed by plate reader before (sample value) and after (supernatant value) centrifugation (3000 RPM; 10 mins).

Figure 3.2.3 shows there were 2 different types of elution results when the absorbance of the fractions eluted were measured (in a plate reader), before and after centrifugation. The first type of elution was obtained with clockwise rotation + tail to head pumping and also with counter-clockwise rotation + tail to head pumping. This elution result was characterised, the sample absorbance (such as 16th fractionated sample in these 2 operational condition combinations) always being equal to the absorbance of that of the supernatant, indicating that this fractionated sample contained Hb only. In the second type of elution result obtained by counter-clockwise rotation + head to tail pumping or clockwise rotation + head to tail pumping, the absorbance of fractions did not equal that of the supernatant after centrifugation (such as 16th fractionated sample in these 2 operational condition combinations). Therefore, for this second type of elution, some RBCs were eluting as well as Hb, in contrast to the first type of elution for which all absorption values of the fractions were due to free Hb.

Therefore, Figure 3.2.3 shows that by only changing the rotational direction and the pumping direction, the behaviour of RBCs was influenced. Generally, injecting from tail to head retains sheep RBCs, whereas, injecting from head to tail elutes sheep RBCs.

3.2.3. The effect of flow rate and rotational speed on the behaviour of sheep RBCs in Milli-CCC®

The general behaviour observed when RBCs are injected into the column of the Milli-CCC at a particular rotational speed (RPM) is that a peak elutes at about 1 column volume which contained free haemoglobin and some cells that had not been retained in the column. This has been called PEAK A. On increasing the flow rate the cells that had been retained in the column could be eluted. This peak is called PEAK B. In some operational modes elution of PEAK B was achieved by reducing the RPM as well as increasing the flow.

The following experiments describe how the operating conditions of initial flow rate and rotational speed influence the retention of sheep RBCs within the coil leading to defining

Chapter 3. Fundamental behaviour of red blood cells in fluctuating g-field conditions of flow and rotational speed that retained sheep RBCs in the column completely, and how these needed to be altered to elute the cells completely from the column. Similar studies performed on other species of RBCs (described in 2.5.3) characterised different conditions of flow and rotational speed that enabled conditions to be defined to separate mixtures of these cells.

3.2.4. Behaviour of sheep RBCs in Milli-CCC[®]: Increasing flow rate decreases retention of cells in the column

3.2.4.1. Introduction

A method was developed to investigate influence of different flow rates on the performance of sheep RBC in 500 RPM. The objective of this study was to study the influence of the initial flow rate used to load the cells on the retention of cells in the column.

3.2.4.2. Method

Instrument set up: Instrument set up: Milli-CCC[®] (described in 2.2.1.1) with column A (described in 2.2.1.2) rotating in clockwise direction; pumping from tail to head direction; 0.32 ml sample loop; column temperature as 15 °C.

1. Set rotational speed at 500 RPM.
2. Sheep blood sample (sample included: around 5.03×10^{10} sheep RBCs) was pumped into column via injection port using an initial flow rate of 1 ml/min.
3. Change flow rate to 5 ml/min, rotational speed at 500 RPM after value returns to base line.
4. Collect sample fractions (1 ml/fraction) to read A405 for both sample and supernatant (described in 2.5.1), and then plot graph by volume as horizontal axis and absorption value as vertical axis.

This experiment was repeated with initial flow rate as 2 ml/min and 3.25 ml/min. Results are show in section 3.2.4.1c.

3.2.4.3. Results

Figure 3.2.4 shows the elution of PEAK A at three different initial flow rates (1, 2 and 3.5 ml/min). PEAK A eluted at about 8.2 ml, which is the column volume of this coil. PEAK A thus contains material (cells and free haemoglobin) that is not retained in the column.

Once the elution of PEAK A was complete – when the absorbance had returned to baseline- the flow rate was increased to 5 ml/min. This eluted PEAK B, which was material that had been retained in the column under the initial flow conditions.

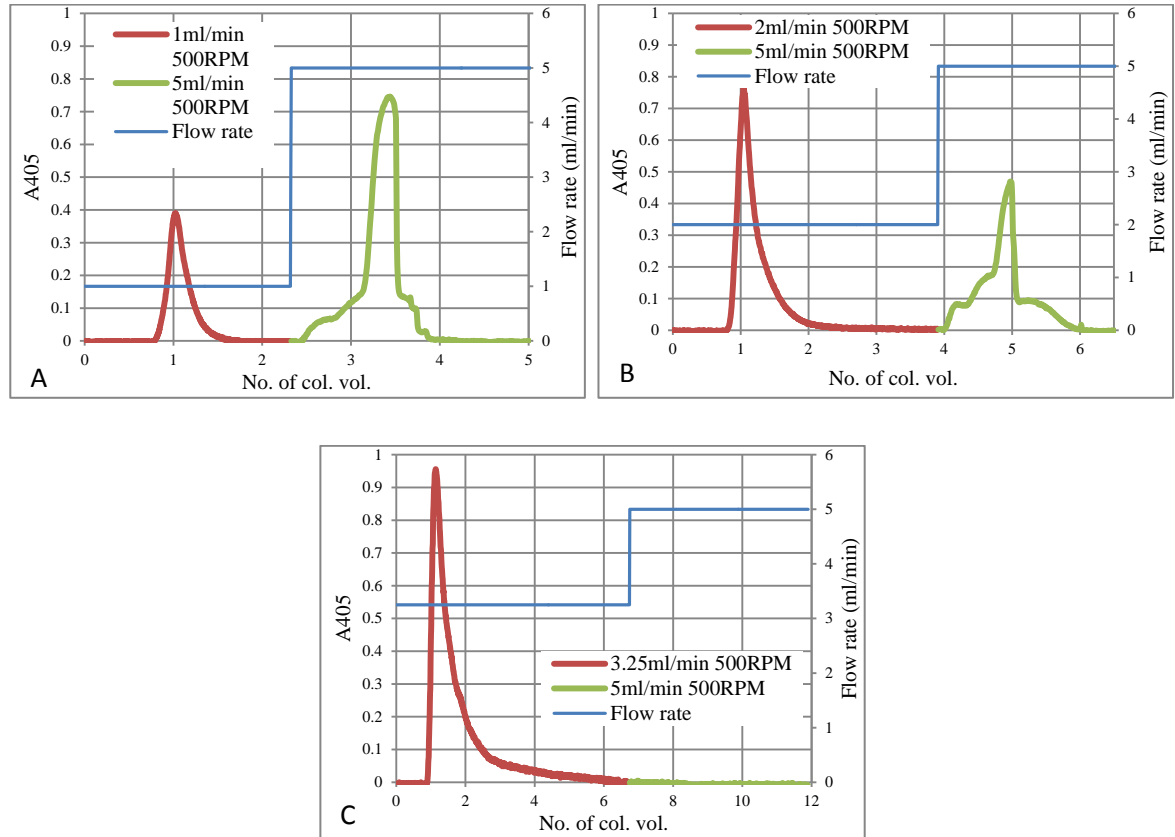


Figure 3.2.4. Relationship between initial flow rate and the behaviour of sheep RBCs at 500 RPM. A) Sheep blood was injected in 1 ml/min. B) Sheep blood was injected in 2 ml/min C) Sheep blood was injected in 3.25 ml/min. 0.32 ml of sheep blood sample injected to CCC coil (Column A: 8.2 ml; 1 mm ID) from tail to head at 500 RPM. Eluent monitored at 405 nm. Operation condition changed to 5 ml/min, 500 RPM to eluted retained sheep RBCs after initial flow rate elution finished.

Figure 3.2.4, shows that increasing the initial flow from 1 to 2 ml/min increased the relative size of PEAK A whilst decreasing the relative size of PEAK B. An initial flow rate of 3.25 ml/min resulted in no PEAK B being detected, indicating no material was retained, all being eluted as PEAK A.

Figure 3.2.5 shows that absorption values of collected fractions at 405 nm for the 3 initial flow conditions of 1, 2 and 3.25 ml/min at 500 RPM.

Chapter 3. Fundamental behaviour of red blood cells in fluctuating g-field

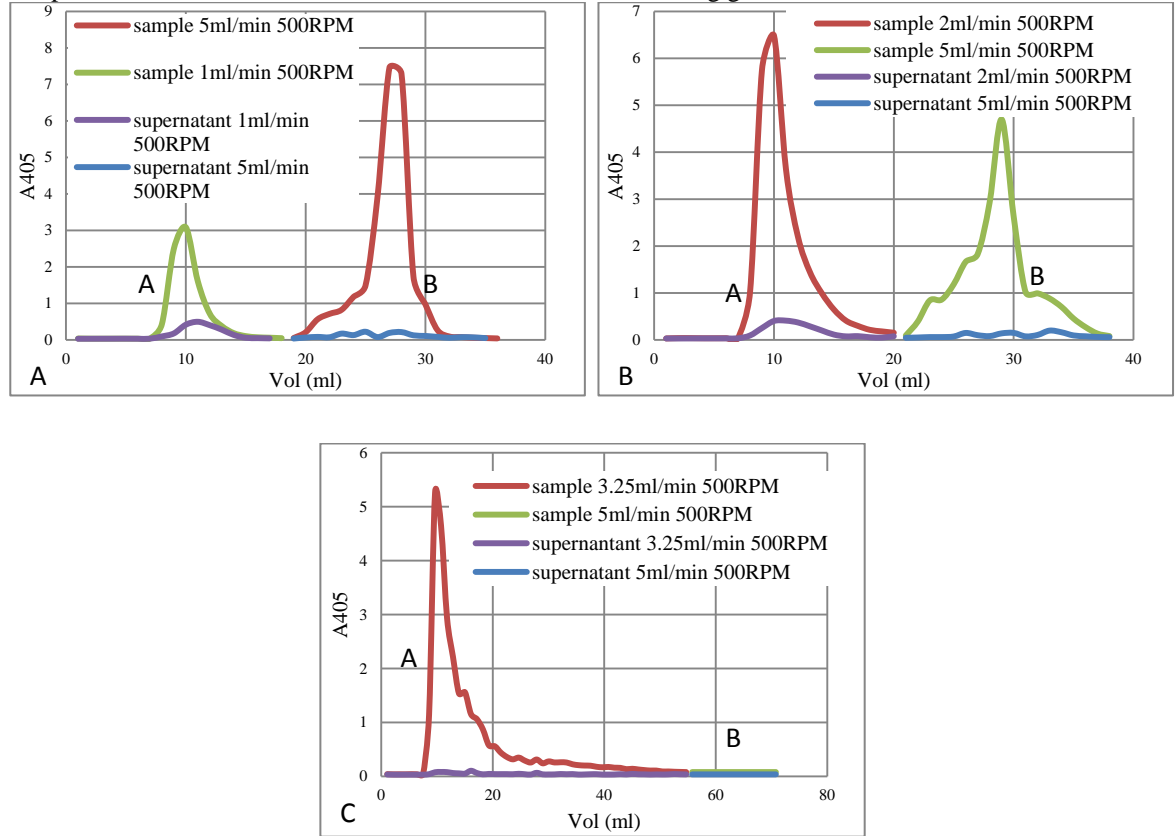


Figure 3.2.5. A405 analyses for relationship between initial flow rate and the behaviour of sheep RBCs at 500 RPM. A) Sheep blood was injected by 1 ml/min. B) Sheep blood was injected by 2 ml/min C) Sheep blood was injected by 3.25 ml/min. 0.32 ml of sheep blood sample injected to CCC coil (Column A: 8.2 ml; 1 mm ID) from tail to head at 500 RPM. Fractions were collected 1 ml/tube. Fractionated samples were analysed by plate reader before (sample value) and after (supernatant value) centrifugation (3000 RPM; 10 mins) (described in 2.5.1).

The absorbance of PEAK A decreased on centrifugation confirming it was composed principally of intact (sedimentable) cells. A relatively small, but significant residual absorbance of the supernatant indicated the elution of free (non-sedimentable) haemoglobin. By contrast the absorbance of PEAK B was reduced to virtually zero on centrifugation, indicating it contained only sedimentable cells, and not free haemoglobin. Importantly PEAK B, the cells retained in the column initially, showing that conditions selected (5 ml/min at 500 rpm) were such that no cells could be retained, and all were eluted.

3.2.5. Behaviour of sheep RBCs in Milli-CCC®: decreasing flow rate increases retention of cells

3.2.5.1. Introduction

In 3.2.4 it was found that a higher initial flow rate resulted in fewer cells being retained in the column, shown as a relatively larger PEAK A containing cells (non-retained components) and a smaller PEAK B. The objective of this section was to establish if reducing the flow rate would lead to the retention of all the cells.

A detailed method is listed as below in which flow rates of 0.8, 1 and 1.25 ml/min were used in the coil rotated, in this study, at 900 RPM.

3.2.5.2. Method

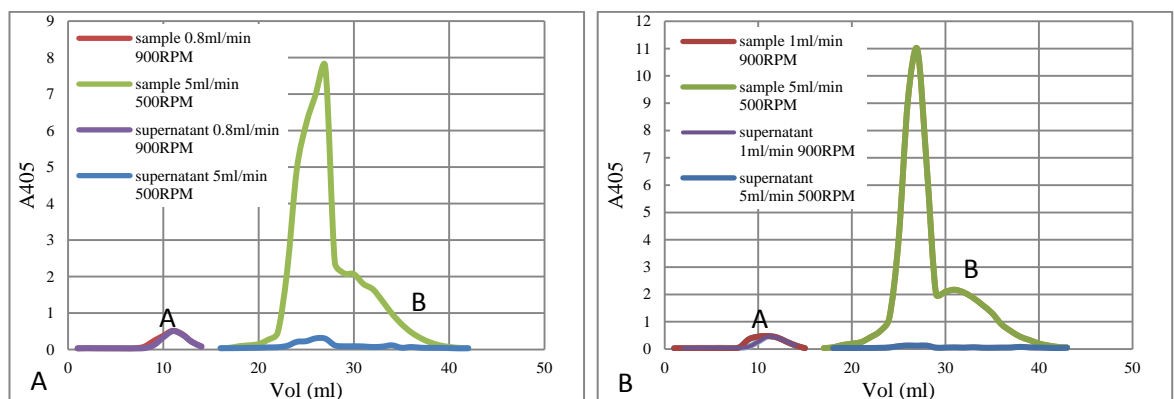
Instrument set up: Instrument set up: Milli-CCC[®] (described in 2.2.1.1) with column A (described in 2.2.1.2) rotating in clockwise direction; pumping from tail to head direction; 0.32 ml sample loop; column temperature as 15 °C.

1. Set rotational speed at 900 RPM.
2. Sheep blood sample (sample included: around $5.03E+10$ sheep RBCs) was pumped into column via injection port using an initial flow rate of 0.8 ml/min.
3. Change flow rate to 5 ml/min, rotational speed as 500 RPM after value returns to base line.
4. Collect sample fractions (1 ml/fraction) to read A405 for both sample and supernatant (described in 2.5.1), and then plot graph by volume as horizontal axis and absorption value as vertical axis.

The experiment was repeated with initial flow rate at 1 ml/min and 1.25ml/min. Results are shown in section 3.2.5.3.

3.2.5.3. Results

Absorption values of fractions are shown in Figure 3.2.6 before and after centrifugation.



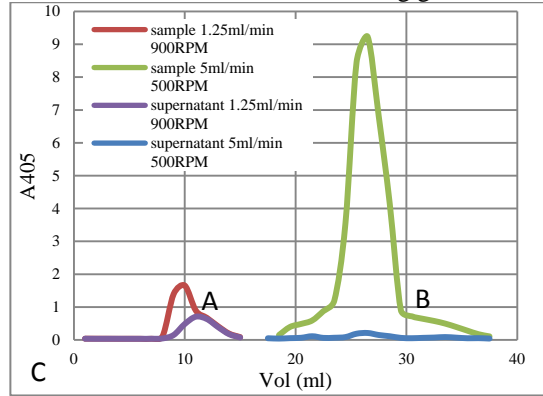


Figure 3.2.6. A405 for relationship between initial flow rate and the behaviour of sheep RBCs at 900 RPM. A) Sheep blood was injected by 0.8 ml/min. B) Sheep blood was injected by 1 ml/min C) Sheep blood was injected by 1.25 ml/min. 0.32 ml of sheep blood sample injected to CCC coil (Column A: 8.2 ml; 1 mm ID) from tail to head at 900 RPM. Fractions were collected 1 ml/tube. Fractionated samples were analysed by plate reader before (sample value) and after (supernatant value) centrifugation (3000 RPM; 10 mins) (described in 2.5.1).

Figure 3.2.6 shows that with initial flows of 0.8 and 1 ml/min, fractions comprising PEAK A showed the same value of absorbance before and after centrifugation, indicating that PEAK A contained only non-sedimentable free haemoglobin, and no RBCs. The RBCs loaded were only eluted when the flow rate was increased to 5 ml/min as PEAK B, which was confirmed to contain only cells and no free haemoglobin by the absence of absorbance after centrifugation. By contrast with an initial flow of 1.25 ml/min absorbance of PEAK A was decreased significantly (ca 50%) on centrifugation. This indicated that at this flow rate some of the RBCs were not being retained in the column. Thus that free Hb is eluted in PEAK A whilst all of the sheep RBCs are retained at 0.8 ml/min (Figure 3.2.6.a) but on increasing the flow to 1.25 ml/min, some intact cells are eluted in PEAK A (Figure 3.2.6.c) and not retained.

This shows that a critical initial flow rate must not be exceeded for all the cells loaded to be retained in the column. Subsequent experiments show that this flow rate increases with increasing rotational speed.

3.2.6. Behaviour of sheep RBCs in Milli-CCC[®]: Flow rate required to elute retained cells. Introduction of “step flow”

3.2.6.1. Introduction

Preliminary work had shown that sheep RBCs that were retained in the column could be eluted with a flow rate of 5 ml/min at 500 RPM and these conditions were used in sections 3.2.4 and 3.2.5. In this section cells were retained completely at 1 ml/min and then the flow

Chapter 3. Fundamental behaviour of red blood cells in fluctuating g-field rate was increased stepwise to determine if there was a critical the flow rate at which cells were eluted. A detailed method is listed as below:

3.2.6.2. Method

Instrument set up: Instrument set up: Milli-CCC[®] (described in 2.2.1.1) with column A (described in 2.2.1.2) rotating in clockwise direction; pumping from tail to head direction; 0.32 ml sample loop; column temperature as 15 °C.

1. Set rotational speed as 500 RPM.
2. Sheep blood sample (sample included: around 5.03×10^{10} sheep RBCs) was pumped into column via injection port using an initial flow rate of 1 ml/min; increase 1 ml/min per $3 \times$ column volumes until 5 ml/min (if no components are eluted in the $3 \times$ column volumes).
3. Collect data by UV detector to plot graph by volume as horizontal axis and voltage as vertical axis.

Results are shown in section 3.2.6.3.

3.2.6.3. Results

The behaviour of sheep RBCs retained in coil at 1 ml/min at 500 RPM followed by a step increased flow rate is shown in Figure 3.2.7.

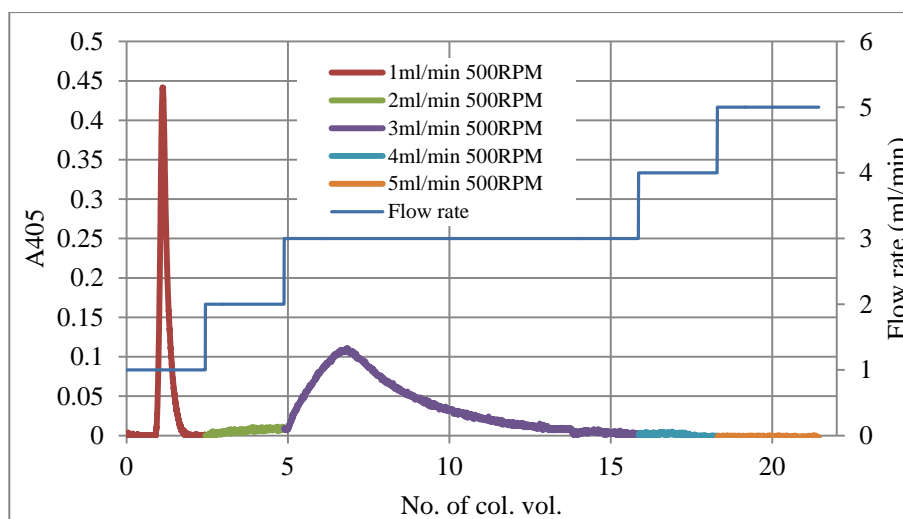


Figure 3.2.7. Behaviour of eluting sheep RBCs by step flow at 500 RPM. 0.32 ml of sheep RBC was injected into CCC coil (Column A: 8.2 ml; 1 mm ID) at 500 RPM at 1 ml/min. Eluent monitored at 405 nm. Flow rate was increased to 2 ml/min and then in steps of 3, 4 and 5 ml/min if no components were eluted within $3 \times$ column volumes (kept the flow rate if components were eluting).

Figure 3.2.7 shows PEAK A eluting at the column volume at flow of 1 ml/min. Increasing the flow to 2 ml/min, gave a slight indication of cells eluting but little elution occurred even after several column volumes. But at 5 column volumes when the flow was increased to 3 ml/min, elution of cells occurred slowly, with a distinct peak of elution, and in this case was completed after ca 10 column volumes. No more cells were eluted even when the flow was increased to 4 and then 5 ml/min. This demonstrated that the sheep RBCs retained in the coil under the initial conditions of 1 ml/min required a critical, higher flow rate to elute them, in this case 3 ml/min. This also confirmed the use of 5 ml/min in the previous experiments to elute all retained cells.

3.2.7. Behaviour of sheep RBCs in Milli-CCC[®]. Detailed analysis of retention of cells in coil on flow rate at two different rotational speeds. Reproducibility of recovery of cells

3.2.7.1. Introduction

Previous experiments had shown that the initial flow rates used to load the cells into the coil influenced the degree to which the cells were retained or eluted at the column volume. This section describes a detailed analysis of the effect of flow rate on retention at two different rotations speeds 500 and 1000 RPM coupled with an analysis of recovery of material either in PEAK A or PEAK B. Cells were loaded at a range of flow rates and after PEAK A had eluted, PEAK B was eluted at 500 RPM and a flow of 5 ml/min. A detailed method is listed as below:

3.2.7.2. Method

Instrument set up: Instrument set up: Milli-CCC[®] (described in 2.2.1.1) with column A (described in 2.2.1.2) rotating in clockwise direction; pumping from tail to head direction; 0.32 ml sample loop; column temperature as 15 °C.

1. Set rotational speed as 500 RPM.
2. Sheep blood sample was pumped into column via injection port using an initial flow rate of 0.5 ml/min.
3. After absorbance value returns to base line (elution of PEAK A complete) change flow rate to 5 ml/min, rotational speed as 500 RPM to elute PEAK B.
4. Collect data by UV detector then import to Origin8 to calculate peak area (as described in 2.5.2).

This experiment was repeated using initial flow rates of 1, 1.5, 2, 2.5, 3 and 3.25 ml/min all at 500 RPM, and also performed at 1000 RPM for initial flow rate of 3, 4, 5, 6, 7, 8, 9, 12, 14, 15 and 16 ml/min.

The peak area was calculated for each flow rate for 500 RPM and 1000 RPM, and then plotted against the initial flow rate (Figure 3.2.8).

3.2.7.3. Results

Figure 3.2.8 shows the relative areas of PEAK A (eluted cells and free haemoglobin) and PEAK B (retained cells) under a range of flow rates at 500 RPM and 1000 RPM .

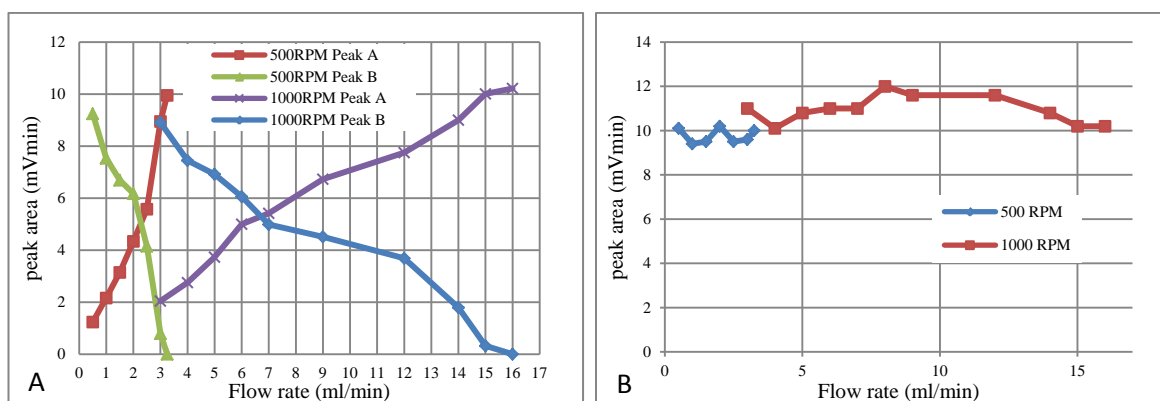


Figure 3.2.8. Peak area comparison of PEAK A and PEAK B in 500 RPM and 1000 RPM. A) Comparison of PEAK A and PEAK B; B) Comparison of sum of PEAK A and PEAK B. 0.32 ml of sheep blood sample was injected to CCC coil (Column A: 8.2 ml; 1 mm ID) from tail to head at 500 RPM or 1000 RPM at different initial flow rate. Eluent monitored at 405 nm. For 500 RPM, the initial flow rate was selected as 0.5, 1, 1.5, 2, 2.5, 3 and 3.25 ml/min; for 1000 RPM, the initial flow rate was selected as 3, 4, 5, 6, 7, 8, 9, 12, 14, 15 and 16 ml/min. Peak area was analysed as described in 2.5.2. Operation condition changed to 5 ml/min, 500 RPM to eluted retained sheep RBCs after initial flow rate elution finished. Different sheep RBCs samples were used for runs at 500 and 1000 RPM.

At 500 RPM and 0.5 ml/min PEAK A is relatively small compared with PEAK B indicating that most, if not all, of the cells are retained. Increasing the flow to 3.25 ml/min progressively reduced the retention of cells (PEAK B) with a concomitant increase in PEAK A, non-retained cells. A similar behaviour is seen at 1000 RPM but in this case a flow rate of 16 ml/min (ca 5 times higher) was required to ensure that no cells were retained.

Figure 3.2.8 shows that at both 500 and 1000 RPM that as PEAK A increases PEAK B decreases. Importantly, the sum of the areas of PEAK A and PEAK B in the 7 runs at different flow rates at 500 RPM and the 11 runs at 1000 RPM were closely similar. This

Chapter 3. Fundamental behaviour of red blood cells in fluctuating g-field demonstrates the reproducibility of the process of retaining and eluting cells in the column. In these 18 runs there is no evidence of altered recovery.

3.2.8. Behaviour of RBCs from sheep and 8 other animal species in Milli-CCC[®]. The concept of maximum flow rate and minimum flow rate and their determination at different initial rotational speeds

3.2.8.1. Introduction

The initial studies described above led to the concept of a minimum operational condition at which all the cells would be retained in the column and a maximum operational condition when all cells could be eluted out of the column. Each of these conditions depended on both the initial flow rate and rotational speed. Thus for different rotational speeds, there is a minimum flow rate and maximum flow rate. In this section a method is developed to measure the minimum flow rate and maximum flow rate for different initial rotational speeds.

This provided graphs of minimum and maximum flow rates against rotational speed (this expressed in terms of the g-value generated) which were characteristic of sheep RBCs. This method was later extended to other species of RBCs (hen; guinea pig; horse; rat; rabbit; dog; mouse) in section 3.2.8.3 providing a quantitative index of performance of different RBCs in this Milli-CCC column.

A detailed method is listed as below:

3.2.8.2. Method

Instrument set up: Instrument set up: Milli-CCC[®] (described in 2.2.1.1) with column A (described in 2.2.1.2) rotating in clockwise direction; pumping from tail to head direction; 0.32 ml sample loop; column temperature as 15 °C.

1. Set rotational speed as 500 RPM.
2. Sheep blood sample was pumped into column via injection port by certain value as initial flow rate.
3. Change flow rate to 5 ml/min, rotational speed as 500 RPM after isotonic buffer was pumped 2 × column volumes.
4. Collect sample fractions (1 ml/fraction) to read A405 for both sample and supernatant (described in 2.5.1), and then plot graph by volume as horizontal axis and absorption value as vertical axis.

5. If PEAK A contains intact sheep blood cells, adjust suitable initial flow rate in step 2 and repeat experiment again.
6. Repeat above steps until determine minimum flow rate (PEAK A does not contain intact blood cells) and maximum flow rate (there is no PEAK B) for each rotational speed.
7. Draw a table for above data and plot graph flow rate (ml/min) against rotational speed, converted to average g values.

This experiment was repeated by for rotational speeds of 600, 700, 800, 900 and 1000 RPM.

3.2.8.3. Results

The results for maximum flow rate and minimum flow rate for different rotational speeds for sheep RBCs are shown in Figure 3.2.9 and Table 3.2.1, which shows the maximum, mean and minimum g-values that have been calculated for the range of rotation speeds used (500 - 1000 RPM) using the method reported by van den Heuvel and Koenig (2011) and the column details for column A (8.2 ml) in Table 2.2.1.

Table 3.2.1. A comparison of maximum flow rate and minimum flow rate for sheep RBCs at different rotational speeds in Milli-CCC (Column A: 8.2 ml; 1 mm ID).

Rotational speed (RPM)	Maximum g (m/s^2)	Mean g (m/s^2)	Minimum g (m/s^2)	Max Flow rate (ml/min)	Min Flow rate (ml/min)
500	60.9	47	33	3.25	0.11
600	87.8	67.6	47.5	4.25	0.16
700	119.4	92.1	64.7	6.2	0.22
800	156	120.2	84.4	8	0.3
900	197.5	152.2	106.9	10.45	0.36
1000	243.8	187.9	131.9	16.1	0.45

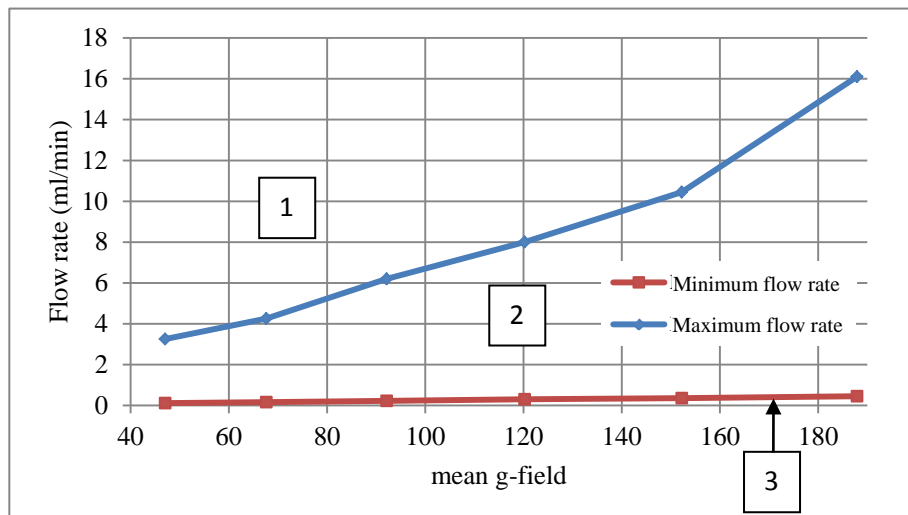


Table 3.2.2 and Figure 3.2.9 show that with increasing rotational speed, both the maximum flow rate and the minimum flow rate increased. From 500 RPM to 1000 RPM, maximum flow rate increased 5 times and minimum flow rate increased 8 times. Area 1 in Figure 3.3.9 is the initial condition area in which the CCC centrifuge cannot hold any sheep RBCs in coil. Area 2 is the initial condition area in which the CCC centrifuge can hold some of the sheep RBCs in coil. Area 3 is the initial condition area in which the CCC centrifuge can hold all intact sheep RBCs in the coil.

The minimum and maximum flow rates for RBCs from 8 other species were also at ranges of rotational speed from 500 to 1000RPM was also determined by this method. Results are shown in Table 3.2.2. As seen in Fig 3.2.9 both the minimum and maximum flow rates increased with increasing rotational speed. Importantly difference between the values of these for RBCs from the different species can also be seen. For example Figure 3.2.10 compares the minimum and maximum flow rates for the RBCs of sheep, guinea pig and hen.

Table 3.2.2. Minimum flow rate and maximum flow rate for different RBCs in species in Milli-CCC®. Column A: 8.2 ml; 1 mm ID.

Rotation (RPM)		hen	guinea pig	horse	rat	rabbit	dog	mouse	sheep
500	min FR	0.22	0.14	0.13	0.13	0.13	0.12	0.11	0.11
	max FR	3.05	2.24	2.98	2.87	2.13	2.62	1.92	3.25
600	min FR	0.32	0.21	0.18	0.18	0.17	0.17	0.17	0.16
	max FR	4.10	3.42	3.98	3.91	2.95	3.69	2.67	4.25
700	min FR	0.45	0.31	0.24	0.23	0.24	0.23	0.23	0.22
	max FR	5.80	4.80	5.78	5.67	4.22	5.38	3.77	6.20
800	min FR	0.58	0.42	0.37	0.35	0.33	0.33	0.33	0.30
	max FR	7.70	6.52	7.72	7.68	5.75	7.26	5.12	8.00
900	min FR	0.75	0.51	0.45	0.43	0.41	0.38	0.36	0.36
	max FR	9.50	8.03	9.54	9.51	6.98	8.72	6.27	10.45
1000	min FR	0.93	0.65	0.53	0.52	0.53	0.53	0.48	0.45
	max FR	11.95	10.77	11.92	11.85	9.33	11.76	8.26	16.10

* unit of minimum flow rate and maximum flow rate is ml/min.

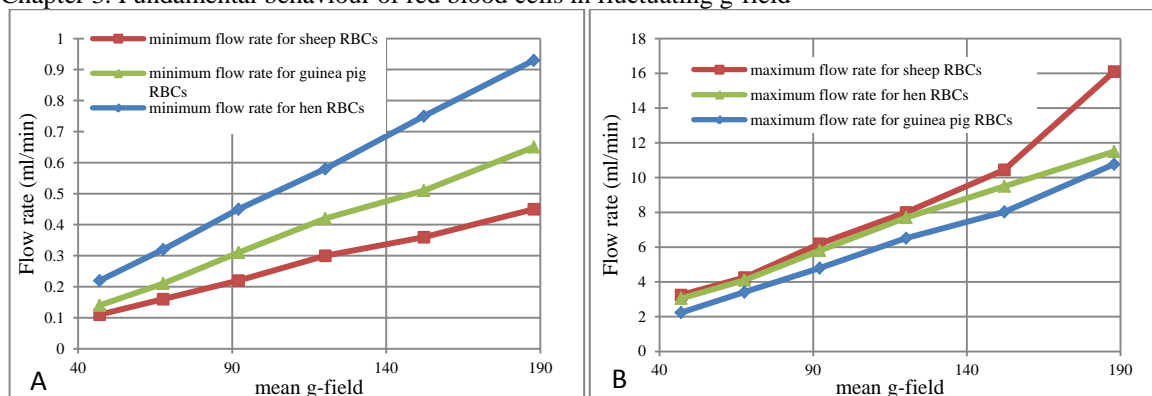


Figure 3.2.10. Minimum / maximum flow rate comparison between sheep, hen and guinea pig RBCs at different rotational speed in Milli-CCC (Column A: 8.2 ml; 1 mm ID). A) Minimum flow rate; B) Maximum flow rate.

Figure 3.2.10 shows guinea pig RBCs requires a higher minimum flow rate than sheep RBCs which means it was easier to sediment guinea pig RBCs in the column than sheep RBCs. It is noted that the minimum flow rate for guinea pig RBCs cannot sediment some of sheep RBCs. Hen RBCs were the easiest RBCs to sediment. Figure 3.2.10 also shows guinea pig RBCs require lower maximum flow rate than sheep RBCs which means guinea pig RBCs were easier to be eluted than sheep RBCs as this maximum flow rate cannot push out all sheep RBCs. But maximum flow rates for hen RBCs were in the middle of guinea pig and sheep RBCs, which indicates hen RBCs were easier to be pushed out than sheep RBCs but harder than guinea pig RBCs. Therefore, generally, for sediment, from easy to difficult, the order was hen RBCs, guinea pig RBCs and then sheep RBCs, whereas for maximum flow rate at which cannot sediment RBCs at all the order was guinea pig RBCs, hen RBCs and then sheep RBCs.

These studies showed that different RBCs required different operating conditions to retain them in the coil and to elute them. This indicated the potential to develop a separation methodology based on varying the operating conditions.

3.2.9. Behaviour of sheep RBCs in Milli-CCC®: Studies on the integrity of cells retained and then eluted from the column (PEAK B)

3.2.9.1. Introduction

As results above have shown, PEAK B comprises RBCs retained in the coil under the initial flow conditions and subsequently eluted by increasing flow rate and or increasing the rotations speed (g-field). Centrifugation of the fractions making up PEAK B showed that all the absorbance measured at 405 nm was sedimentable indicating it did not include

Chapter 3. Fundamental behaviour of red blood cells in fluctuating g-field
any free Hb. By contrast PEAK A could contain cells that had not been retained and any free haemoglobin remaining after preparation of the cells for loading. To check on the integrity of the sheep RBCs recovered in PEAK B they were re-run under the same conditions to see if any haemoglobin was released, which would appear in a new PEAK A.

3.2.9.2. Method

Instrument set up: Instrument set up: Milli-CCC[®] (described in 2.2.1.1) with column A (described in 2.2.1.2) rotating in clockwise direction; pumping from tail to head direction; 0.32 ml sample loop; column temperature as 15 °C.

1. Set rotational speed as 1200 RPM.
2. Sheep blood sample was pumped into column via injection port by 0.5 ml/min as initial flow rate.
3. Change flow rate to 5 ml/min, rotational speed as 500 RPM after isotonic buffer was pumped 2 × column volumes.
4. Collect data by UV detector and sample fractions (1 ml/fraction) then import to Origin8 to calculate peak area for PEAK A (as described in 2.5.2). Then plot graph by volume as horizontal axis and voltage as vertical axis.
5. Choose one fraction which has the highest concentration as inject sample.
6. Set rotational speed as 1200 RPM, selected fraction in step 5 was pumped into column via injection port by 0.5 ml/min as initial flow rate.
7. Change flow rate to 5 ml/min, rotational speed as 500 RPM after isotonic buffer was pumped 2 × column volumes.
8. Collect data by UV detector and sample fractions (1 ml/fraction) then import to Origin8 to calculate peak area for PEAK A (as described in 2.5.2). Then plot graph by volume as horizontal axis and voltage as vertical axis.
9. Compare peak area difference of PEAK A for first experiment (original sheep blood) and second experiment (PEAK B fraction as sample) and make a table.

Results are shown in section 3.2.6.3.

3.2.9.3. Results

Figure 3.2.11a shows the preparation of PEAK B by retaining the cells in the coil at 0.5 ml/min at 1200 RPM and then eluting PEAK B by reducing the rotational speed to 500 RPM and increasing the flow to 5 ml/min. Figure 3.2.11b show the re-run of the fraction with highest absorbance under the same conditions.

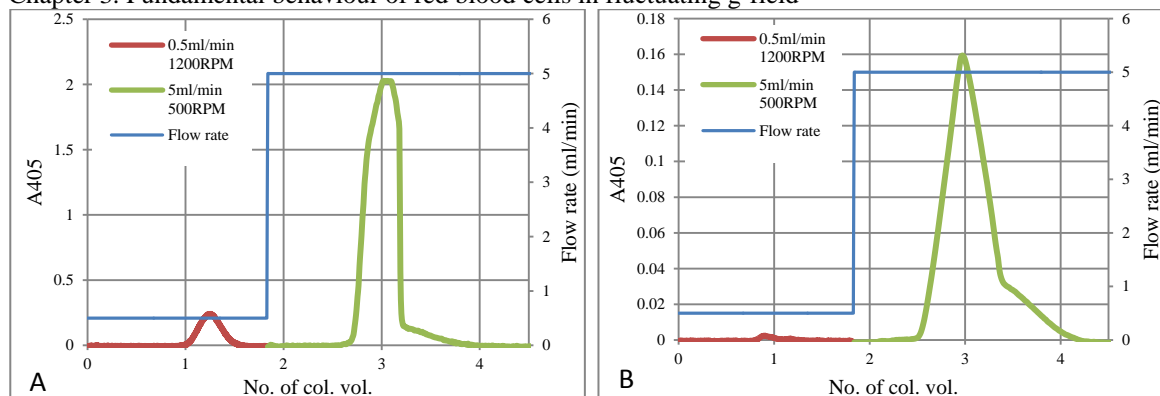


Figure 3.2.11. Results comparison between sheep blood as sample and fraction from PEAK B as sample. 0.32 ml of A) Sheep blood sample and B) Fractionated sample from PEAK B of 3.3.20.a was injected to CCC coil (Column A: 8.2 ml; 1 mm ID) from tail to head at 1200 RPM at 0.5 ml/min as initial flow rate. Eluent monitored at 405 nm. Operation condition changed to 5 ml/min, 500 RPM to eluted retained sheep RBCs after $2 \times$ column volumes.

A comparison of for the original sample of sheep blood the re-run of PEAK B under the same CCC condition is shown in Table 3.2.3.

Table 3.2.3. Comparison peak area of PEAK A between sheep blood as sample and PEAKB as sample.

Sample	Peak area A (mVMin)	Peak area B (mVMin)	Ratio % (A/B)	Area % (PEAK A)	Area % (PEAK B)
Sheep blood	0.71947	6.40255	11.23%	10.10%	89.89%
PEAK B	0.00495	0.72758	0.68%	0.67%	99.32%

Table 3.2.3 shows after CCC process, peak area percentage of PEAK B increased from 89.89% to 99.32%. Although the rerunning experiment still has a tiny PEAK A, it has decreased to only 0.67%.

Importantly, this result also shows that the separation process does not cause the RBCs to lyse as when RBCs in PEAK B, which are free of Hb are reprocessed there is no appearance of Hb in PEAK A. This is an important control to show that the process for RBCs is not damaging.

3.2.10. Comparison between behaviour of RBCs ghost cell and intact RBCs

3.2.10.1. Introduction

Free Hb is not sedimentable at the g-fields generated in the CCC and is thus eluted at the first column volume (in PEAK A) whereas sheep RBCs are affected by the g-field and us can be sedimented at the minimum flow rate condition. RBC ghosts, which are the RBCs

Chapter 3. Fundamental behaviour of red blood cells in fluctuating g-field membrane that remains intact after haemolysis, has an intermediate size between Hb and intact RBCs, and are less sedimentable. The target of 3.2.10 was to examine the behaviour of RBCs ghost in a minimum flow rate condition and establish where they eluted. Since blood samples loaded might also include lysed RBCs, the other target of 3.2.10 was to check whether these can be removed together with free Hb in the PEAK A regions, and thus to retain intact sheep RBCs only in the column (as shown in section 3.2.11.3).

3.2.10.2. Method

Instrument set up: Instrument set up: Milli-CCC[®] (described in 2.2.1.1) with column A (described in 2.2.1.2) rotating in clockwise direction; pumping from tail to head direction; 0.32 ml sample loop; column temperature as 15 °C.

1. Set rotational speed as 1000 RPM, sheep blood sample was pumped into column via injection port by 0.5 ml/min as initial flow rate.
2. Change flow rate to 5 ml/min, rotational speed as 500 RPM after isotonic buffer was pumped $2 \times$ column volumes.
3. Collect data by UV detector to plot graph by volume as horizontal axis and voltage as vertical axis.

3.2.10.3. Results

The results for behaviour of ghost cells sample are shown in Figure 3.2.12.

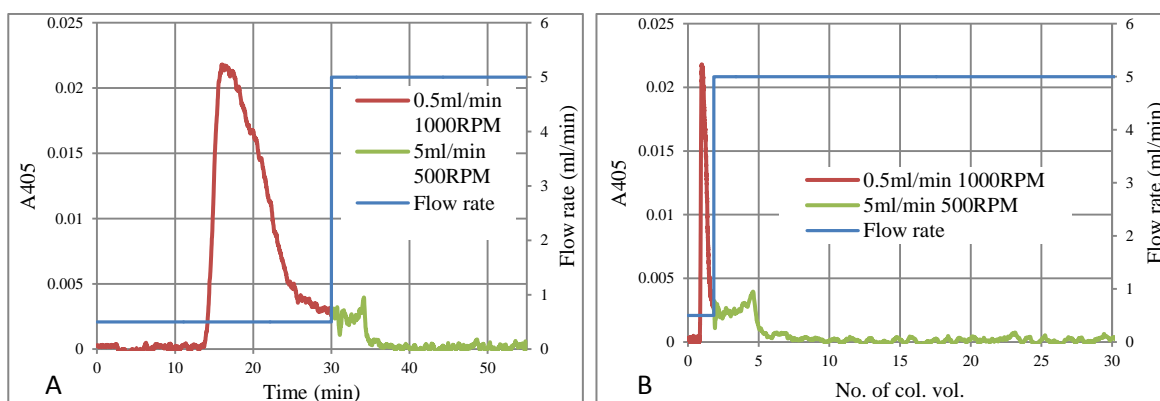


Figure 3.2.12. Behaviour of RBCs ghost cells at minimum condition for intact RBCs. A) Results plot against time; B) Results plot against column volume. 0.32 ml of sheep RBCs ghost cell suspended in isotonic buffer was injected to CCC coil (Column A: 8.2 ml; 1 mm ID) from tail to head at 1000 RPM at 0.5 ml/min as initial flow rate. Eluent monitored at 405 nm. Operation condition changed to 5 ml/min, 500 RPM to eluted retained sheep RBCs after $2 \times$ column volumes.

Figure 3.2.12 shows, sheep RBCs ghost cells were eluted around the 2nd column volume under the initial flow conditions. This is in contrast to free Hb and intact sheep RBCs

Chapter 3. Fundamental behaviour of red blood cells in fluctuating g-field
which elute close to 1 column volume. Another difference was that the ghosts showed more of a tail than free Hb (i.e. the elution of sheep RBCs ghost cells was not finished within $2 \times$ column volumes). Since intact sheep RBCs are not eluted at this operation condition, but are retained, this minimum flow rate condition can also be applied to remove free Hb, sheep RBCs ghost cells and RBCs fragments and separating them from the retained intact sheep RBCs in the column.

3.3. Discussion

3.3.1. Pumping direction and Rotational direction

Section 3.2.1 shows that the sheep RBCs in the “cantilever system” moved to tail direction whether the rotational direction was clockwise or counter-clockwise whereas section 3.2.2 shows for the CCC coil to retain sheep RBCs in the column, a pumping from tail to head was always required whether the column is rotated in clockwise direction or counter-clockwise direction.

Figure 3.2.3 shows that to retain sheep RBCs, a tail to head injection was always required. Since sheep RBCs naturally move to the tail, pumping isotonic buffer from head to tail actually helps sheep RBCs to move out of the column. On the contrary, while pumping isotonic buffer from tail to head, the pumping flow was against the movement of sheep RBCs and then this helps to retain the sheep RBCs.

Furthermore, if considering the spiral direction of column, the movement of sheep RBCs always follows the direction of rotation. Therefore, in conclusion:

1. To retain sheep RBCs in the column, the pumping direction should against the rotational direction.
2. To elute sheep RBCs out of the column, the pumping direction should follow the rotational direction.

3.3.2. Minimum and Maximum operational conditions: influence of flow rate and rotational speed

3.3.2.1. Minimum and maximum operational conditions

From the results in section 3.2.4, by changing the initial operational condition, several features were observed, listed below,

1. With increasing initial flow rate / decreasing initial rotational speed, peak area of PEAK A (haemoglobin and non-retained RBCs) increases and the peak area of PEAK B (retained RBCs) decreases.
2. Provided the initial flow rate reached a high enough value at any particular rotational speed, PEAK B disappeared, meaning that all components come out in PEAK A and no cells would be retained in the coil of CCC centrifuge. This condition is called maximum operational condition (maximum flow rate + minimum rotational speed).

3. Provided the initial flow rate reached a low enough value at any particular rotational speed, PEAK A contained Hb only and all the intact cells can be retained in coil. This condition is called minimum operational condition (minimum flow rate + maximum rotational speed).
4. Some of the cells can be eluted (pushed out) together with Hb in PEAK A when the flow rate was in the range of minimum and maximum operational condition.

3.3.2.2. Minimum and maximum flow rates for different species of RBC: influence of, cell diameter and cell density

Table 3.2.2 and Figure 3.2.10 together with all the results for sheep RBCs showed that RBCs from different species differed in their minimum and maximum flow rates. Attention is now given to what properties of these cells might give rise to these differences. This might also give insight into the physical basis for the different behaviours and for the separation process that is developed in Chapter 7 based on this.

The relationship between minimum / maximum flow rate and cell diameter for a series of different species of RBCs is shown in Figure 3.3.1.

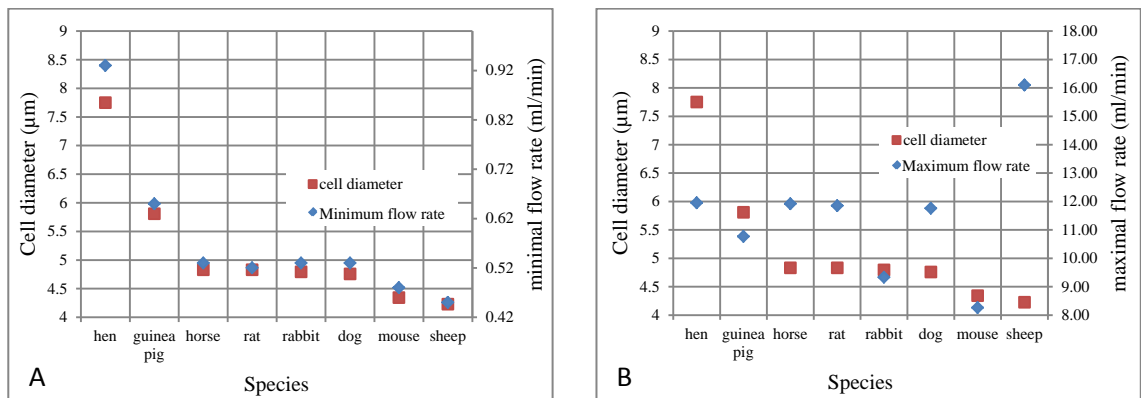


Figure 3.3.1. Relationship between minimum / maximum flow rate of RBCs from different species in Milli-CCC (Column A: 8.2 ml; 1 mm ID) and cell diameter. A) Minimum flow rate; B) Maximum flow rate.

Figure 3.3.1 shows a good relationship between minimum flow rate and RBCs diameter measured in Figure 2.5.3. It is seen that a greater diameter requires a higher minimum flow rate. However, the maximum flow rates shows no such relationship to RBCs diameter as shown in Figure 3.3.2 which indicates the elution behaviour is not dependent on single cell size only.

A comparison between minimum flow rate and cell volume / cell density is shown in Figure 3.3.2.

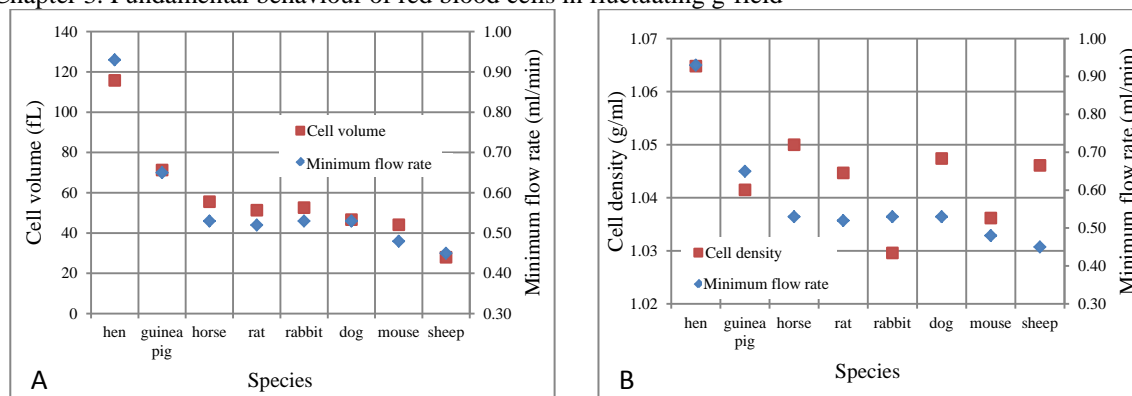


Figure 3.3.2. Relationship between minimum flow rate (1000 RPM) for different species on RBCs in Milli-CCC (Column A: 8.2 ml; 1 mm ID) and cell volume / cell density. A) Cell volume; B) Cell density. Data was taken from Figure 2.5.4 and Table 3.2.3.

Figure 3.3.2.a shows, similar to Figure 3.3.1.a, that the minimum flow rates also show a good relationship with cell volumes. For example a higher cell volume requires a higher minimum flow rate. By contrast Figure 3.3.2.b shows the different densities of the RBCs has no correlation with minimum flow rate.

The above analysis shows that RBCs with a greater diameter / cell volume require a higher minimum flow rate which indicates the greater diameter / cell volume RBCs are easier to sediment in this environment. A particular example of this is the hen RBC, which is the largest RBC used in this study. Although hen RBCs are the densest of the RBCs studied the density order shown in Table 2.3.7, suggests that the density difference did not strongly influence the minimum flow rate. For example sheep RBCs are much denser than most of other RBCs but were the most difficult to sediment and be retained. However, one would expect the density of RBCs to be a factor in sedimentation rate as predicted by the Stokes' equation. The reason this appears not to be the case might be because the density differences between the RBCs studied were too small to change the sedimentation behaviour in this CCC mode of operation. Therefore, the size of RBCs is the major factor to influence the minimum flow rate.

3.3.2.3. Elution of ghost cells in minimum operational condition

Figure 3.2.12 shows the elution of RBCs ghost cells at a minimum operational condition. This elution is different from both that of free Hb in PEAK A as the ghost cells were eluted in a peak with a long tail. This may reflect the heterogeneity of the ghost preparation compared with intact cells. From a separation viewpoint it suggests that in the fluctuating g-field, RBCs ghost cells were retained somewhat by the effect of g but still could be

Chapter 3. Fundamental behaviour of red blood cells in fluctuating g-field eluted while intact RBCs were retained in the coil. Therefore, one application of the use of the minimum operational condition is to separate different components of the blood sample by sedimenting RBCs in column while eluting protein and cell membrane fragments. A similar result has been reported in the elution of rat liver cells in a nonsynchronous flow through coil planet centrifuge (Fig 1.3.14; Ito et al 1983). Here cell debris was eluted before elution of all intact liver cells.

3.3.3. Theoretical analysis of Flow behaviour of cells in rotating coils

3.3.3.1. Comparison of experimentally determined of min Flow data with theoretical equation developed by Fedotov et al

An equation has been developed by Fedotov et al (2005) to describe the flow rate (V_f) which retains particles in the carrier liquid flow in a rotating coiled column. This flow rate is equivalent to the minimum flow rate described in this thesis in previous chapters observed as the minimum flow rate at which cells are just retained in the CCC coil.

$$V_f \approx \frac{R^2 \omega^3 r_p^4 \Delta \rho^2}{r \eta^2} \quad \text{[Equation 3.3.3.1a]}$$

Where, V_f : the flow rate that retained particles in the flow; R : revolution radii; ω : the angular speed of column rotation; r_p : particle radius; $\Delta \rho$: the difference between the densities of the particle and the carrier liquid; r : rotation radii; η : viscosity of the carrier liquid.

For the Milli-CCC[®] column used in this thesis these values are as follows:

$r = 0.039 \text{ m}$; $R = 0.05 \text{ m}$;

Viscosity of buffer was considered as viscosity of water $\eta = 0.001 \text{ kg/(s}\cdot\text{m)}$;

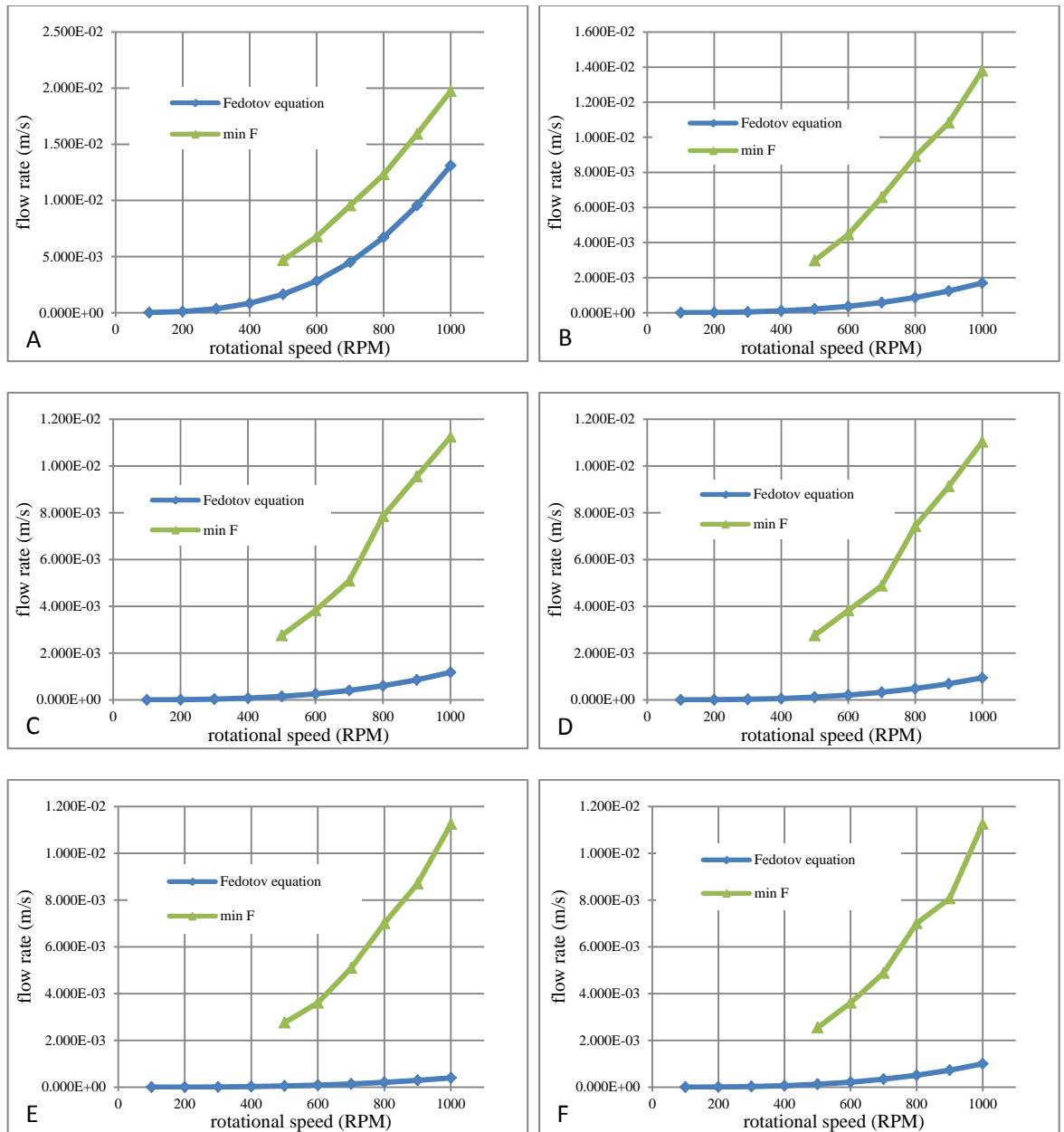
density of water = 1 g/ml.

Diameter and densities of RBCs in species were taken from section 2.5.3 and section 2.5.4.

V_f was calculated for the RBCs of the 8 species studied, at all the operational rotational speeds used. To be able to compare the calculated values with those presented previously in this thesis, RPM has been used rather than ω to aid comparison with figures in previous chapters which have been plotted against RPM. From an operational standpoint, one appreciates RPM conditions rather than ω .

Chapter 3. Fundamental behaviour of red blood cells in fluctuating g-field

In Figure 3.3.3 8 the minimum flow rates determined in this thesis for the RBCs of the 8 species studied are plotted against the rotational speed. In addition the values of V_f calculated from the "Fedotov Equation"., It is clear that these predicted values of V_f show much lower at all rotational speeds that the minimum Flow rate determined experimentally (Figure 3.3.3).



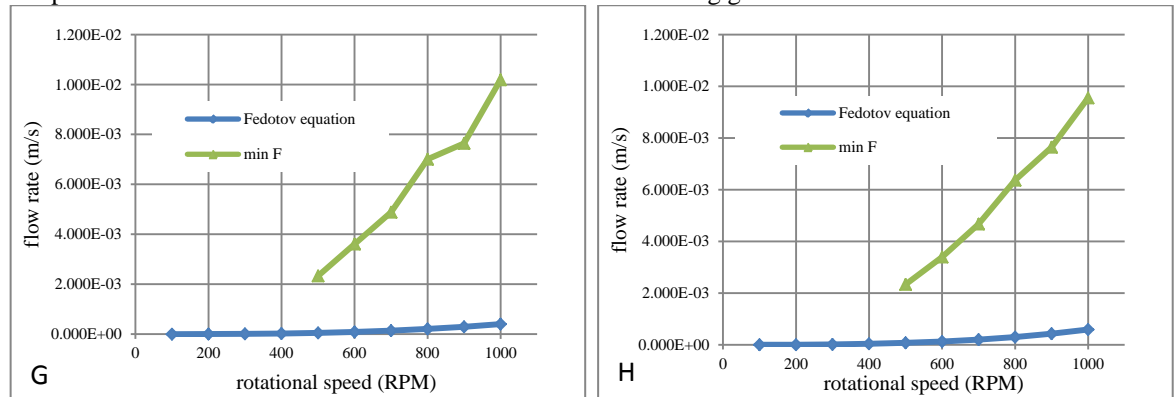


Figure 3.3.3. Comparisons between V_f and Minimum flow rate shows Minimum flow rates do not fit the calculated V_f . A) Hen; B) Guinea pig; C) Horse; D) Rat; E) Rabbit; F) Dog; G) Mouse; H) Sheep. V_f and Minimum flow rates plotted against rotational speed.

Figure 3.3.3 shows V_f and Min flow rate have different absolute values although their general dependence on rotational speed show similarly shaped curves. In Equation 3.3.3.1a, R and r are fixed parameters of the machine, η is viscosity of the carrier liquid, and ω is based on different rotational speeds. Only the radius of cells and density of cells vary. Therefore attention was given to examining if the values of r and density used, derived from experimental measurements, might be the reason that V_f does not match the experimentally determined minimum flow rate. As Fedotov et al. (2005) have commented, due to the dependence of V_f on the fourth power of the radius and the square of the density difference, there will be great sensitivity in the effects of these two parameters on the value of V_f .

3.3.3.2. Source of deviation from “Fedotov Equation”: Impact of values of cell radius and density used to calculate V_f

Attention has therefore been given to the impact on the values of cell radius and density on the calculated values. Can these be altered to values that bring the calculated values of V_f agree with the experimental vales of minimum flow rate.

i. Impact of cell radius only

If density was considered to be “correct” and all difference were contributed to arise from the radius contribution. The values of radius that are required for the calculated value of V_f to match the experimentally determined value of minimum Flow were be calculated and are shown in Table 3.3.1.

Chapter 3. Fundamental behaviour of red blood cells in fluctuating g-field

Table 3.3.1. Comparisons of each species of RBCs of measured cell radius with radius calculated to be required for calculated values of V_f to match experimentally determined min flow at different rotational speeds.

	r (measurement) (E-06 m)	r (theoretical) (E-06 m)						r (theoretical) / r (measurement) for 1000 RPM (ratio)	ratio ⁴
		500 RPM	600 RPM	700 RPM	800 RPM	900 RPM	1000 RPM		
Hen	3.88	5.03	4.82	4.68	4.51	4.40	4.29	1.11	1.51
Guinea pig	2.90	5.62	5.42	5.33	5.20	5.00	4.90	1.69	8.13
Horse	2.42	5.02	4.75	4.55	4.59	4.41	4.25	1.76	9.55
Rat	2.42	5.31	5.03	4.76	4.79	4.61	4.47	1.85	11.7
Rabbit	2.40	6.53	6.09	5.91	5.79	5.60	5.52	2.30	28.1
Dog	2.38	5.06	4.81	4.62	4.58	4.34	4.36	1.83	11.3
Mouse	2.17	5.66	5.51	5.29	5.24	4.90	4.87	2.24	25.3
Sheep	2.11	5.02	4.81	4.64	4.53	4.34	4.24	2.01	16.3

* Take 1000 RPM as example as it is a common operational rotational speed.

Table 3.3.1 shows the calculated radius required for V_f to match experimentally determined minimum flow was always higher than the measured values of cell radius. At 500 RPM, this was generally twice as high as the measured radius, and with increasing rotational speed the calculated radius decreased. This greater value of radius may suggest aggregation of cells so that the effective radius of the species moving in the coil is larger than that of single cells.

From 500 RPM to 1000 RPM, the theoretical r decreased with increasing of rotational speed. This may suggest a flattening effect of g-field on the cell aggregations and may be also a less aggregation effect.

At all rotational speeds the theoretical radius was greater than the experimental value. Column 9 of Table 3.3.1 shows the ratio of theoretical to experimental radius calculated for values at 1000 RPM. Importantly it is clear that this ratio varies with the different erythrocytes which suggest there are additional parameters causing this difference that are cell specific. This aspect will be discussed further below. The last column of Table 3.3.1 shows the value of this ratio to the power 4 and its significance will also be discussed later.

An additional complicating factor that needs to be considered is that the size of the RBCs will not be homogeneous. There will be a range of sizes as the results of the Coulter sizing measurements described in section 2.5.3 show (Figure 2.5.3 – Figure 2.5.5). The min flow will be determined by the smallest cells as these will be retained less readily than the larger cells. This is an even lower measured value of r needs to be used, rather than the average value shown in Table 3.3.1.

ii. Impact of cell density only

Secondly the density can also be considered as completely contributing to the difference, so that the experimental determine radius is used. Table 3.3.2 shows the values of densities for the RBCs that are required for the calculated value of V_f to agree with the experimentally determined value of min Flow.

Table 3.3.2. The comparisons of each RBCs in species for theoretical and measured density at different rotational speeds.

	density (measurement) (g/ml)	density (theoretical) (g/ml)						density (theoretical) / density (measurement) for 1000 RPM (ratio)	ratio ²
		500 RPM	600 RPM	700 RPM	800 RPM	900 RPM	1000 RPM		
Hen	1.06	1.11	1.10	1.09	1.09	1.08	1.08	1.11	1.51
Guinea pig	1.04	1.16	1.14	1.14	1.13	1.12	1.12	1.69	8.13
Horse	1.05	1.22	1.19	1.18	1.18	1.17	1.15	1.76	9.55
Rat	1.04	1.22	1.19	1.17	1.18	1.16	1.15	1.85	11.7
Rabbit	1.03	1.22	1.19	1.18	1.17	1.16	1.16	2.30	28.1
Dog	1.05	1.21	1.19	1.18	1.18	1.16	1.16	1.83	11.3
Mouse	1.04	1.25	1.23	1.22	1.21	1.18	1.18	2.24	25.3
Sheep	1.05	1.26	1.24	1.22	1.21	1.19	1.19	2.01	16.3

* Take 1000 RPM as example as it is common operational rotational speed.

Table 3.3.2 shows with increasing rotational speed, the theoretical density decreased slightly. Importantly it can be seen that the values required to simulate the experimentally determined min Flow are not very different from the measured values. This suggests that errors in the values of density are not as important as the effect of the cell radius noted above. In addition the density terms appears to the power 2 in equation 3.3.3.1a, (shown in Column 10 in Table 3.3.2) in contrast to the radius appearing to the power 4 (Column 10 in Table 3.3.2). The similar theoretical densities and measured density of hen RBCs is understandable as hen RBCs is the only RBCs that gave similar V_f and minimum flow rate.

iii. Impact of cell radius and density jointly

Even though the impact of density appears much less than radius, one can consider that the difference between V_f and minimum flow rate may be contributed from both radius and density, therefore $r^4\Delta\rho^2$ should be considered and calculated as an unit as cell property parameter (Table 3.3.3).

Table 3.3.3. The comparisons of each RBCs in species for theoretical and measurement $r^4\Delta\rho^2$ at different rotational speeds.

	$r^4\Delta\rho^2$ (measurement) (E-20)	$r^4\Delta\rho^2$ (practical) (E-20)						$r^4\Delta\rho^2$ (practical) / $r^4\Delta\rho^2$ (measurement) for 1000 RPM (ratio)	ratio
		500 RPM	600 RPM	700 RPM	800 RPM	900 RPM	1000 RPM		
Hen	94.7	270	227	201	174	158	143	1.51	1.51
Guinea pig	12.3	172	149	139	126	107	99.6	8.13	8.13
Horse	8.51	159	128	107	111	94.6	81.2	9.55	9.55
Rat	6.80	159	128	103	105	90.4	79.7	11.7	11.7
Rabbit	2.89	159	121	107	98.8	86.2	81.2	28.1	28.1
Dog	7.20	147	121	103	98.8	79.9	81.2	11.3	11.3
Mouse	2.91	135	121	103	98.8	75.7	73.6	25.3	25.3
Sheep	4.24	135	114	98.3	89.8	75.7	69.0	16.3	16.3

* Take 1000 RPM as example as it is common operational rotational speed.

3.3.3.3. Introduction of factor α into “Fedotov Equation” to correct theoretical values to experimental values of minimum flow

It is clear from the results in Tables 3.3.1, 3.3.2 and 3.3.3 that although the calculated value of V_f is different from the observed minimum flow rate, there is a relationship between them at each rotational speed. This can be expressed by introducing a term α :

$$V_f \times \alpha = \text{minimum flow rate} \quad \text{[Equation 3.3.3.1b]}$$

Table 3.3.4 shows the values of V_f and min flow and hence α at the different rotational speeds for each of the species of RBCs.

Table 3.3.4 Comparison between V_f and Minimum flow rate for each RBCs at different rotational speed. Calculation of Term α as $\alpha = \text{minimum flow rate}/V_f$

	Rotational speed (RPM)	500	600	700	800	900	1000
hen	V_f (m/s) =	1.64E-03	2.83E-03	4.50E-03	6.71E-03	9.56E-03	1.31E-02
	Min Flow (m/s) =	4.67E-03	6.79E-03	9.55E-03	1.23E-02	1.59E-02	1.97E-02
	$\alpha = \text{Min F}/V_f =$	2.85	2.40	2.12	1.83	1.67	1.51
	α/α_{1000} (Min F/ V_f)/(Min F 1000RPM/ V_f 1000RPM)	1.89	1.59	1.41	1.22	1.11	1.00
guinea pig	V_f (m/s) =	2.12E-04	3.66E-04	5.82E-04	8.69E-04	1.24E-03	1.70E-03
	Min Flow (m/s) =	2.97E-03	4.46E-03	6.58E-03	8.91E-03	1.08E-02	1.38E-02
	$\alpha = \text{Min F}/V_f =$	14.0	12.2	11.3	10.3	8.75	8.13
	α/α_{1000} (Min F/ V_f)/(Min F 1000RPM/ V_f 1000RPM)	1.72	1.50	1.39	1.26	1.08	1.00

Chapter 3. Fundamental behaviour of red blood cells in fluctuating g-field

horse	vf (m/s) =	1.47E-04	2.54E-04	4.04E-04	6.03E-04	8.59E-04	1.18E-03
	Min Flow (m/s) =	2.76E-03	3.82E-03	5.09E-03	7.85E-03	9.55E-03	1.12E-02
	$\alpha = \text{Min F} / V_f =$	18.7	15.0	12.6	13.0	11.1	9.55
	$\frac{\alpha/\alpha_{1000}}{(\text{Min F} / V_f)/(\text{Min F}_{1000\text{RPM}} / V_{f1000\text{RPM}})}$	1.96	1.57	1.32	1.36	1.16	1.00
rat	vf (m/s) =	1.18E-04	2.03E-04	3.23E-04	4.82E-04	6.86E-04	9.42E-04
	Min Flow (m/s) =	2.76E-03	3.82E-03	4.88E-03	7.43E-03	9.12E-03	1.10E-02
	$\alpha = \text{Min F} / V_f =$	23.4	18.8	15.1	15.4	13.3	11.7
	$\frac{\alpha/\alpha_{1000}}{(\text{Min F} / V_f)/(\text{Min F}_{1000\text{RPM}} / V_{f1000\text{RPM}})}$	2.00	1.60	1.29	1.31	1.13	1.00
rabbit	vf (m/s) =	5.01E-05	8.65E-05	1.37E-04	2.05E-04	2.92E-04	4.01E-04
	Min Flow (m/s) =	2.76E-03	3.61E-03	5.09E-03	7.00E-03	8.70E-03	1.12E-02
	$\alpha = \text{Min F} / V_f =$	55.1	41.7	37.1	34.1	29.8	28.1
	$\frac{\alpha/\alpha_{1000}}{(\text{Min F} / V_f)/(\text{Min F}_{1000\text{RPM}} / V_{f1000\text{RPM}})}$	1.96	1.48	1.32	1.22	1.06	1.00
dog	vf (m/s) =	1.25E-04	2.15E-04	3.42E-04	5.10E-04	7.26E-04	9.96E-04
	Min Flow (m/s) =	2.55E-03	3.61E-03	4.88E-03	7.00E-03	8.06E-03	1.12E-02
	$\alpha = \text{Min F} / V_f =$	20.4	16.8	14.3	13.7	11.1	11.3
	$\frac{\alpha/\alpha_{1000}}{(\text{Min F} / V_f)/(\text{Min F}_{1000\text{RPM}} / V_{f1000\text{RPM}})}$	1.81	1.48	1.27	1.22	0.98	1.00
mouse	vf (m/s) =	5.04E-05	8.71E-05	1.38E-04	2.06E-04	2.94E-04	4.03E-04
	Min Flow (m/s) =	2.33E-03	3.61E-03	4.88E-03	7.00E-03	7.64E-03	1.02E-02
	$\alpha = \text{Min F} / V_f =$	46.3	41.4	35.3	33.9	26.0	25.3
	$\frac{\alpha/\alpha_{1000}}{(\text{Min F} / V_f)/(\text{Min F}_{1000\text{RPM}} / V_{f1000\text{RPM}})}$	1.83	1.64	1.40	1.34	1.03	1.00
sheep	vf (m/s) =	7.34E-05	1.27E-04	2.02E-04	3.01E-04	4.28E-04	5.87E-04
	Min Flow (m/s) =	2.33E-03	3.40E-03	4.67E-03	6.37E-03	7.64E-03	9.55E-03
	$\alpha = \text{Min F} / V_f =$	31.8	26.8	23.2	21.2	17.8	16.3
	$\frac{\alpha/\alpha_{1000}}{(\text{Min F} / V_f)/(\text{Min F}_{1000\text{RPM}} / V_{f1000\text{RPM}})}$	1.96	1.65	1.43	1.30	1.10	1.00

Table 3.3.4 shows that the values of α decrease with increasing rotational speed and the ratio of α to α at 1000 RPM decreases from about 2 for 500 RPM to 1 for 1000 RPM, of course determined by the definition of this ratio .

Therefore, the ratio value: $\frac{1000}{\text{RPM}}$, corrects for the influence of g-field on V_f .

Because this changing ratio is based on α , therefore, the equation is improved as:

$$V_{fc} \approx \frac{R^2 \omega^3 r_p^4 \Delta \rho^2}{r \eta^2} \cdot \frac{1000}{\text{RPM}} \cdot \alpha \quad [\text{Equation 3.3.3.1c}]$$

Where V_{fc} is now the improved calculated value for V_f for each cell.

The new values calculated by improved equation 3.3.3.1d are shown in Figure 3.3.4.

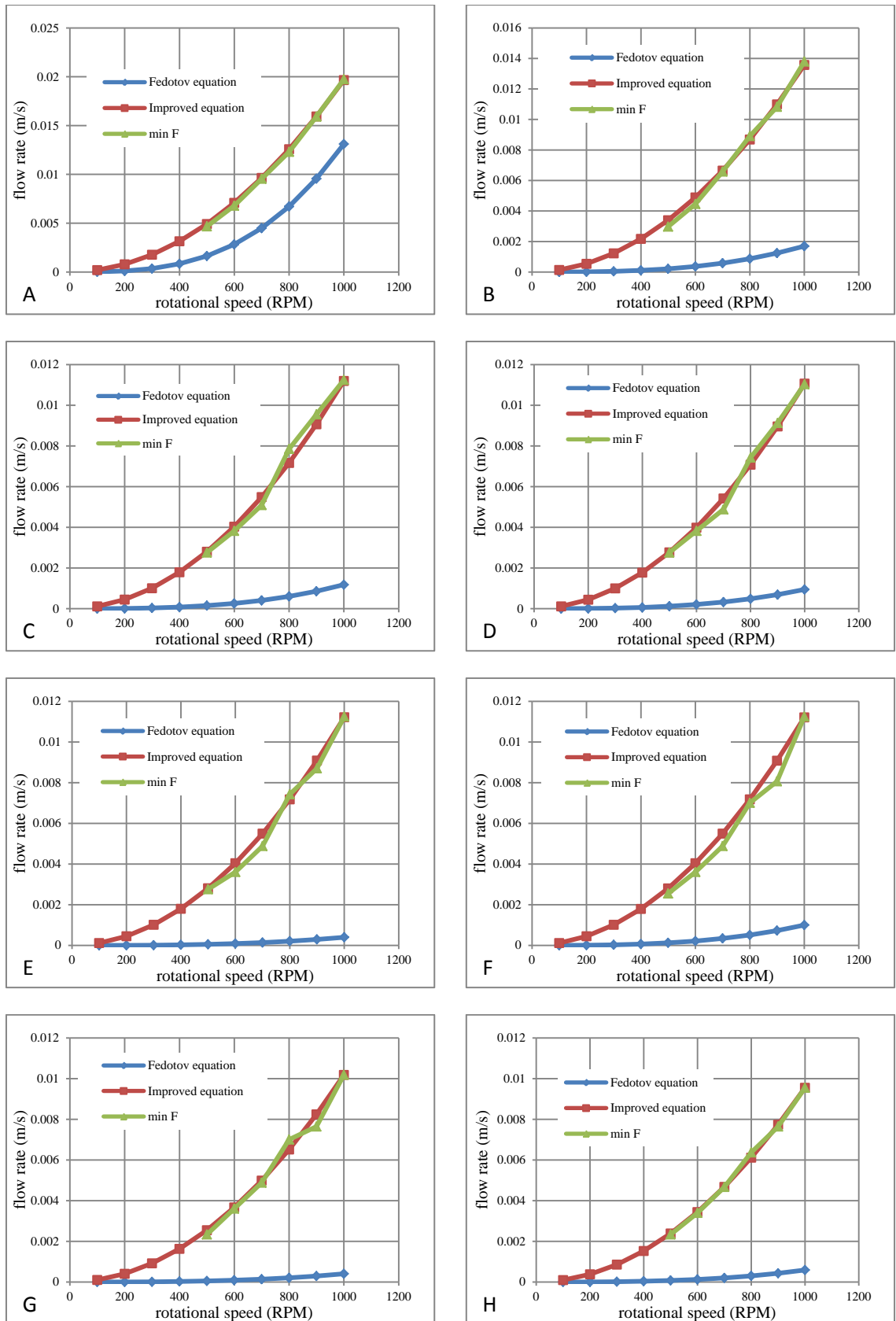


Figure 3.3.4. Comparison between Fedotov equation, improved equation and min F. A) Hen; B) Guinea pig; C) Horse; D) Rat; E) Rabbit; F) Dog; G) Mouse; H) Sheep. V_f plotted against rotational speed.

The improved equation provides a very close fit with the experimentally determined values for minimum flow rate. Although There will have been errors in the values of radius and density measurements which make the value α not exactly precise, the values of α for each species of RBCs are listed below (Table 3.3.5).

Table 3.3.5. Suggested coefficient α for each RBCs.

Species	Hen	Guinea pig	Horse	Rat	Rabbit	Dog	Mouse	Sheep
α	1.5	8.1	9.5	11.7	28.1	11.3	25.3	16.3

As discussed, although the size of the RBCs will not be homogeneous, the value α was calculated based on average value but not the smallest value. Therefore, the suggested coefficient α will be different if calculation is based on the smallest diameter value. But this change will only influence the value of α but not the equation 3.3.3.1c.

3.3.3.4. Possible explanations for cell specific properties that give rise to the cell specific differences between experimental Min flow and calculated V_f from “Fedotov Equation”: correlations with α

Table 3.3.5 shows that α varies with the species of RBC. Thus there are cell specific differences over and above differences in radius and density between the behaviour of the cells observed (min Flow) and that calculated by the model which considers the flow properties of particles in terms of radius and density only. Consideration is given below to what these cell specific properties might be.

One general property of cells is that their surfaces have a negative charge arising from exposure of surface located sialic acids at the termini of carbohydrate chains on glycoproteins and glycolipids. The former are more dominant in generating the surface charge as they are exposed further way from the membrane lipid bilayer than the former. A measure of this surface charge is given by the electrophoretic mobility of cells. For the RBCs in this study, these values taken from the literature are shown in Table 3.3.6 and compared with the values of α obtained in this thesis. It is of course important to appreciate that the values of mobilities were not obtained from the cells in this study and these literature values may be expected to show some variation from the actual values of the cells in this study, but the literature values do provide a start to test the hypothesis that surface charge might be a contributing factor to the values of α .

Table 3.3.6. Electrophoretic mobilities and coefficient α of RBCs in species. From Seaman, 1975.

Alpha and electrophoretic mobility from Seaman chapter		
	alpha	mobility in saline ($\mu\text{msec}^{-1}\text{V}^{-1}\text{cm}$)
hen	1.5	0.83
dog	11.25	1.28
horse	9.5	1.16
mouse	25.25	1.1
rabbit	28	0.48
sheep	16.25	1.14
rat	11.5	1.28

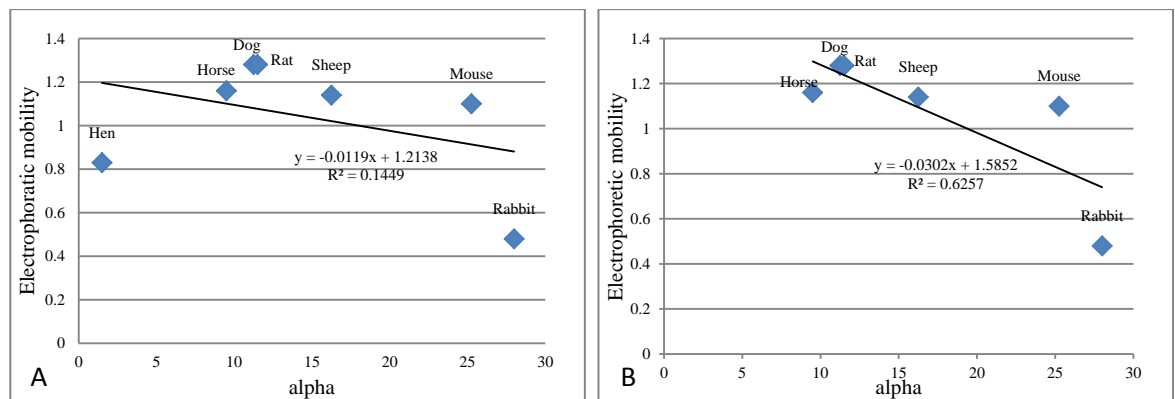


Figure 3.3.5. Comparison between electrophoretic mobility and alpha in species. A) with hen data; B) without hen data.

Figure 3.3.5.a shows the values of α plotted against electrophoretic mobility. There does not appear to be a trend. However, the hen RBC is very different from the mammalian RBCs: it is nucleated and oval in shape. If the hen RBC is removed from the analysis, and comparison made for the mammalian RBCs only that are all non-nucleated and similar in shape the results shown in Figure 8.2.6.b are obtained.

There appears to be a correlation between α and the electrophoretic mobilities: α is bigger the lower is the mobility that is with lower surface charge. This is linear with an r value of 0.791 which for 6 data points (4 degrees of freedom) has a P value of <0.065 (Pearson's r , in statistical significance testing). This suggests, for mammals RBCs, there is a suggestive correlation (not significant) between these two values indicating the behaviour of the RBCs is influenced by surface properties also and not just size and density. Possibly the reason α increases, - i.e. there is great departure from the theoretical value, with decreasing surface charge could be that the lower charge is associated with great tendency to aggregation. Aggregated cells would be expected to behave differently from single cells, on which the theoretical calculated values are based.

3.4. Conclusion

In this chapter the behaviour of cells flowing in a single phase of isotonic buffer in a rotating coil in a Milli-CCC has been established, principally using sheep RBCs. Depending on the flow rate and rotational speed, cells can be completely retained in the column and subsequently eluted by altering the flow and speed. Low flow rate and high rotation lead to retention. If higher flow rates and /or lower rotational speeds are used cells are not retained and elute at the column volume along with any free haemoglobin

The retention of the RBCs was influenced by the rotational direction and pumping flow direction. Since movement of RBCs followed the direction of rotation to the tail end of column while rotation, the operational condition to retain RBCs in the column required the pumping direction to be against the rotational direction (from tail to head). To elute the RBCs, the pumping direction should follow the rotational direction (from head to tail).

The sedimentation requirements for intact RBCs that lead to their being retained were defined as minimum operational conditions. By contrast, the conditions that did not sediment any RBCs were defined as maximum operation conditions. A CCC process at minimum flow rate eluted RBCs ghost cells as well as free Hb after the 1st column volume of isotonic buffer pumping. Therefore, minimum operational condition separates intact RBCs, from the blood sample as the retained RBCs can be eluted after the operational conditions are changed

Studies with RBCs from 8 different species showed differences in their ability to be retained in the coil, which will form the basis of a cell separation methodology in following chapters. It was established that size is the major factor in sedimentation but not in the elution of cells. When the flow rate was low, the smaller RBCs were to be easier to sediment; when the flow rate was high, to elute cells size is not a determining factor. Density did not show influence on sedimentation or elution.

The conditions to retain RBCs in the coil can be modelled by a theoretical equation developed by Fedotov et al (2005) provided a correction factor α is introduced to correct for cells specific departure from the predicted value. There are indications that α may be related to cell surface charge, which of course differ between the cells studies.

In the next chapter other surface properties – deformability and aggregation are investigated as having a role in the behaviour of cells in rotating coils.

Chapter 4. Influence of cell membrane deformability on RBCs in fluctuating g-field

4.1. Summary

The effects of operational conditions on behaviours of different RBCs populations were described in Chapter 3. The experimentally determined flow rate at which RBCs were retained in the column (initial flow) was found to be predicted by a theoretical equation developed by Fedotov et al (2003) which included cell properties (radius and density), medium properties (viscosity and density) and the rotational speed that generated the fluctuating g-field provided a correction factor α value was introduced. This factor was different for the 8 different RBCs studied indicating that the “Fedotov Equation” required a cell specific parameter to be included. In Chapter 3 some indication that this might relate to cell surface charge was presented. In this chapter attention is given to the possibility that membrane deformability might also be a contributing factor the flexibility (deformability) of sheep and hen RBCs was reduced by fixation of their membranes by glutaraldehyde. The behaviour of fixed and unfixed RBCs in sedimentation and elution were studied in the Milli-CCC[®] using the same coil (Column A: 8.2 ml; 1 mm ID) as was used for all of the experiments. It was found that fixation reduced the ability of the cells to be retained in the coil and increased their ease of elution. Evidence is presented that fixation, which decreases cell deformability, decreased the departure from the Fedotov equation, indicating that the correction factor α , described in Chapter 3, probably contains a deformability parameter.

4.2. Experimental

4.2.1. Retention of fixed RBCs

4.2.1.1. Introduction

As discussed in Chapter 3, PEAK A consists of the components which can be eluted by initial operational condition. At minimum operational conditions, only free Hb can be eluted in PEAK A. Therefore, the behaviour of fixed RBCs was investigated to see if fixation of RBCs altered the same minimum operational condition. A detailed procedure to examine the elution of fixed RBCs in PEAK A, which reflects decreased retention in the column, is listed as below:

4.2.1.2. Method

Chapter 4. Influence of cell membrane deformability on RBCs in fluctuating g-field
Instrument set up: Instrument set up: Milli-CCC[®] (described in 2.2.1.1) with column A (described in 2.2.1.2) rotating in clockwise direction; pumping from tail to head direction; 0.32 ml sample loop; column temperature as 15 °C.

1. Set rotational speed as 500 RPM.
2. Fixed sheep RBCs were re-suspended in isotonic buffer and pumped into column via injection port using an initial flow rate of 0.15 ml/min.
3. Isotonic buffer was pumped for 2 × column volumes through the coil and the eluting components were collected in fractions as 2 ml/tube.
4. From No.1 to No.7 fractions were analysed in a plate reader at 405 nm before and after centrifugation (as described in 2.5.1).

This experiment was repeated with washed unfixed sheep RBCs to act as the unfixed control sample also performed with fixed hen RBCs re-suspended in isotonic buffer and washed unfixed hen RBCs by injection at 0.75 ml/min at 500 RPM. Results are shown in section 4.2.1.3.

The minimum flow rate of fixed sheep RBCs over the range of 500 – 1000 RPM was determined as described in Section 3.2.5 for unfixed sheep RBCs. Results are tabulated in Table 4.2.1.

4.2.1.3. Results

The comparisons between fixed and unfixed sheep RBCs are shown in Figure 4.2.1.

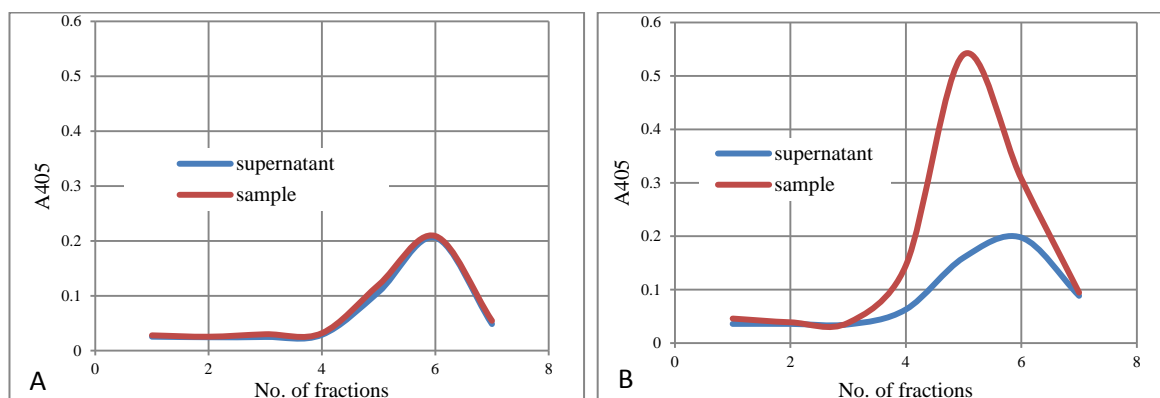


Figure 4.2.1. Comparisons of elution of PEAK A (non-retained material) between fixed and unfixed sheep RBCs. A) For unfixed sheep RBCs. B) For fixed sheep RBCs. 0.32 ml of unfixed sheep blood sample or glutaraldehyde fixed sheep RBCs suspension in isotonic buffer was injected to CCC coil (Column A: 8.2 ml; 1 mm ID) from tail to head at 0.15 ml/min at 500 RPM. Fractions were collected 2 ml/tube. Fractionated samples were analysed by plate reader before (sample value) and after (supernatant value) centrifugation (3000 RPM; 10 mins) (as described in 2.5.1).

Figure 4.2.1.a shows that the absorbance of PEAK A is not decreased on centrifugation confirming the PEAK A contains no cells, only Hb, and thus that all unfixed sheep RBCs have been retained. By contrast Figure 4.2.1.b, shows that the absorbance of PEAK A is decreased markedly on centrifugation indicating that PEAK A contains eluted RBCs as well as Hb. Thus fixation decreased the retention of sheep RBCs in the coil and hence the minimum operating condition is reduced on fixation.

The result of comparison of PEAK A between fixed and unfixed hen RBCs is shown in Figure 4.2.2.

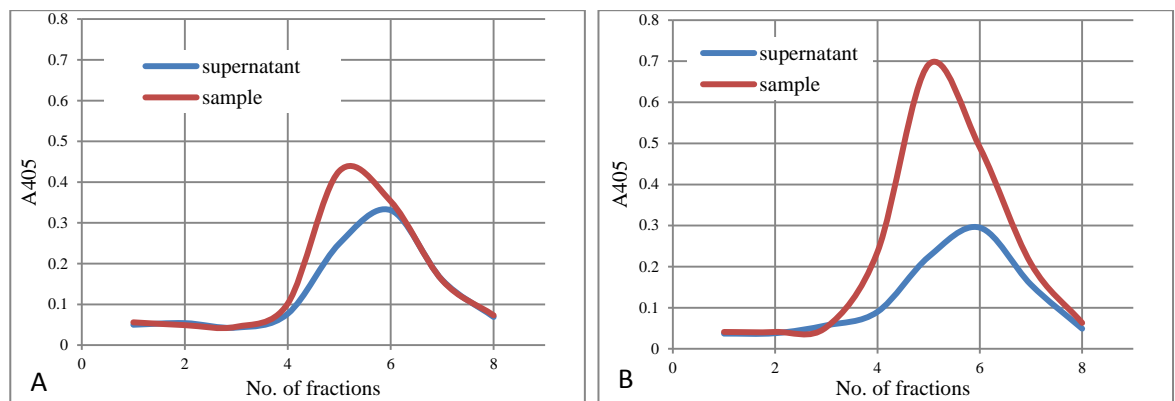


Figure 4.2.2. Comparisons of elution of PEAK A (non-retained material) between fixed and unfixed hen RBCs. A) For unfixed hen RBCs. B) For fixed hen RBCs. 0.32 ml of unfixed hen blood sample or glutaraldehyde fixed hen RBCs suspension in isotonic buffer was injected to CCC coil (Column A: 8.2 ml; 1 mm ID) from tail to head at 0.75 ml/min at 500 RPM. Fractions were collected 2 ml/tube. Fractionated samples were analysed by plate reader before (sample value) and after (supernatant value) centrifugation (3000 RPM; 10 mins) (as described in 2.5.1).

Figure 4.2.2.a shows that some hen RBCs were eluted in PEAK A as the absorbance of PEAK A decreased on centrifugation of the samples. However although Figure 4.2.2b also showed a decrease in PEAK A absorbance after centrifugation, also indicating cells being eluted, this decrease is much larger. There fixation of hen RBCs also reduced the retention of cells in the coil, and thus reduced the minimum operating condition.

The minimum flow rate of fixed sheep RBCs in each rotational speed is shown in Table 4.2.1.

Table 4.2.1. The minimum flow rate comparison for fixed sheep RBCs and unfixed sheep RBCs at different rotational speeds.

Rotational speed (RPM)	Maximum g (m/s ²)	Mean g (m/s ²)	Minimum g (m/s ²)	fixed sheep RBCs (ml/min)	unfixed sheep RBCs (ml/min)
500	60.9	47	33	0.07	0.11
600	87.8	67.6	47.5	0.11	0.16
700	119.4	92.1	64.7	0.15	0.22
800	156	120.2	84.4	0.2	0.3
900	197.5	152.2	106.9	0.25	0.36
1000	243.8	187.9	131.9	0.32	0.45

* the data of unfixed sheep RBCs is taken from Table 3.2.1.

Table 4.2.1 shows a decrease of minimum flow rate after cell fixation, which suggests it is harder to sediment fixed RBCs than unfixed RBCs.

4.2.2. Elution behaviour of fixed RBCs

Section 4.2.1 shows RBCs were eluted easier after they were fixed during the sedimentation process (minimum operating condition) Therefore, it was necessary to investigate whether fixed RBCs were also easier to be pushed out of column during elution operations.

4.2.2.1. Fixed RBCs elution in step flow at relatively high g-field (1000 RPM)

4.2.2.1a. Introduction

A step flow method was used to investigate the elution differences between fixed and unfixed RBCs. The detailed method applied to analyse elution behaviours of fixed hen and sheep RBCs with step increased flow rate in high g-field is listed below:

4.2.2.1b. Method

Instrument set up: Instrument set up: Milli-CCC[®] (described in 2.2.1.1) with column A (described in 2.2.1.2) rotating in clockwise direction; pumping from tail to head direction; 0.32 ml sample loop; column temperature as 15 °C.

1. The initial rotational speed was set at 1000 RPM.
2. Blood sample was pumped in to column via injection port by initial flow rate as 0.5 ml/min.
3. The flow rate of pumping isotonic buffer was changed as the table below:

Flow rate	Period of flow (column volumes)
<i>Sedimentation mode at 1000 RPM</i>	
0.5 ml/min	2 column volumes

<i>Elution mode at 1000 RPM</i>	
2 ml/min	4 column volumes
4 ml/min	4 column volumes
6 ml/min	10 column volumes
8 ml/min	10 column volumes
10 ml/min	10 column volumes
<i>Elution mode of retained RBCs at 0 RPM</i>	
5 ml/min	-

4. Collect data by UV detector to plot graph by time or no. of column volume as horizontal axis and voltage as vertical axis, respectively.

This experiment was performed for unfixed sheep blood sample and fixed sheep RBCs re-suspended in isotonic buffer; unfixed hen blood sample and fixed hen RBCs re-suspended in isotonic buffer. Results are shown in section 4.2.2.1c.

4.2.2.1c. Results

i. Sheep RBCs in step flow mode elution at 1000 RPM

The elution of unfixed sheep RBCs and glutaraldehyde fixed sheep RBCs using a step increased flow rate at 1000 RPM are shown in Figure 4.2.3 and Figure 4.2.4.

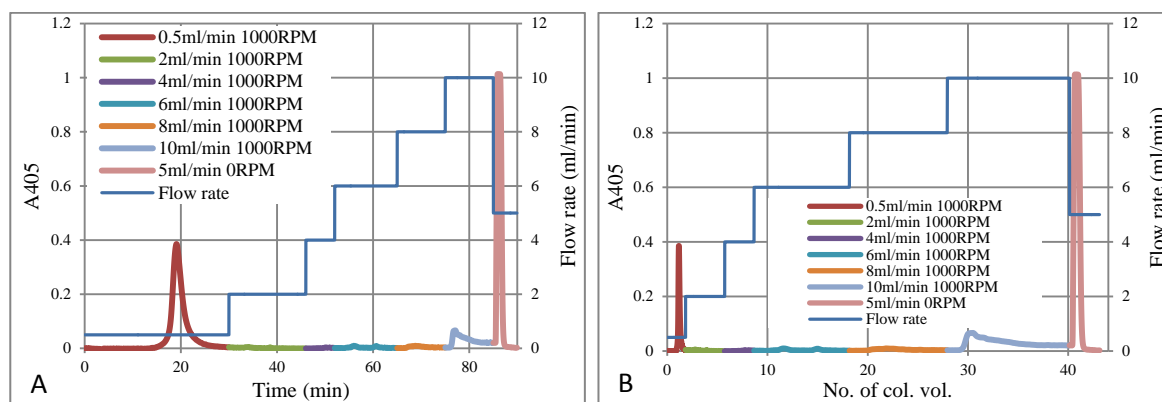


Figure 4.2.3. Elution of unfixed sheep RBCs by step flow at 1000 RPM. A) Elution profile plotted against time. B) Elution profile against column volume. 0.32 ml of sheep blood sample was injected into CCC coil (Column A: 8.2 ml; 1 mm ID) at 1000 RPM at 0.5 ml/min. Eluent monitored at 405 nm. Flow rate was increased to 2 ml/min and then in steps of 4, 6, 8 and 10 ml/min. Retained RBCs were eluted at 5 ml/min at 0 RPM.

Chapter 4. Influence of cell membrane deformability on RBCs in fluctuating g-field

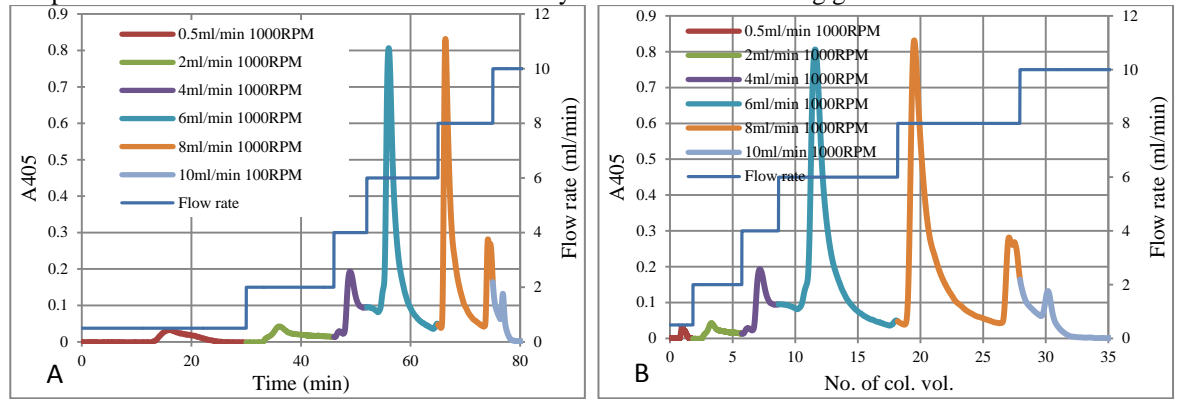


Figure 4.2.4. Elution of glutaraldehyde fixed sheep RBCs by step flow at 1000 RPM. A) Elution profile plotted against time. B) Elution profile against column volume. 0.32 ml of glutaraldehyde fixed sheep RBC suspension in isotonic buffer was injected into CCC coil (Column A: 8.2 ml; 1 mm ID) at 1000 RPM at 0.5 ml/min. Eluent monitored at 405 nm. Flow rate was increased to 2 ml/min and then in steps of 4, 6, 8 and 10 ml/min.

The elution of unfixed and glutaraldehyde fixed sheep RBCs were different. Figure 4.2.3 shows that fixed sheep RBCs were much easier to be eluted than the unfixed sheep RBCs as they were eluted at relatively low flow rate (6 ml/min & 8 ml/min) while unfixed sheep RBCs could not be eluted at these flow rate and were retained in the column until a relatively high flow rate (10 ml/min) was applied.

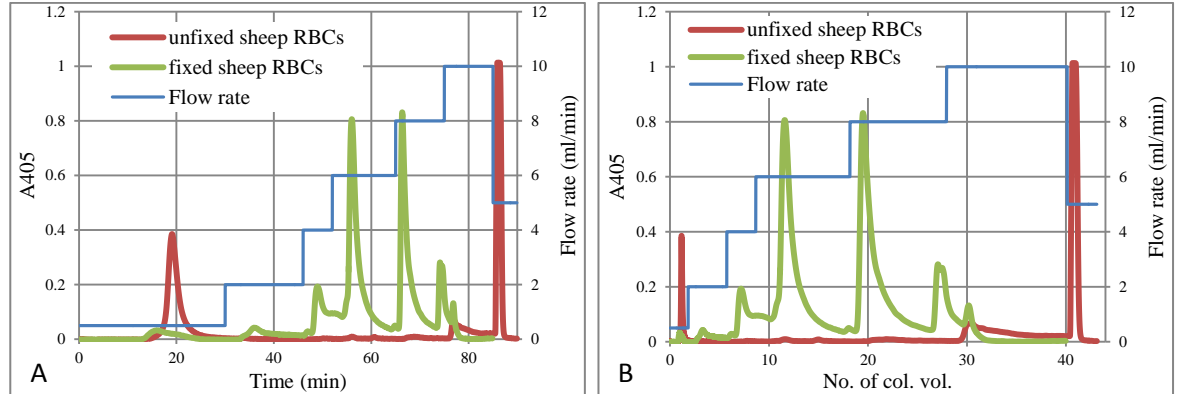


Figure 4.2.5. Comparison between the elution behaviour of unfixed and glutaraldehyde fixed sheep RBCs in step flow gradient flow modes at 1000 RPM. Shows the fixed sheep RBCs were eluted earlier than unfixed sheep RBCs. Data taken from Figure 5.2.7 and Figure 5.2.8.

ii. Hen RBCs in step flow mode elution at 1000 RPM

The result of eluting unfixed and glutaraldehyde fixed hen RBCs in step flow mode at 1000 RPM are shown in Figure 4.2.6 and Figure 4.2.7.

Chapter 4. Influence of cell membrane deformability on RBCs in fluctuating g-field

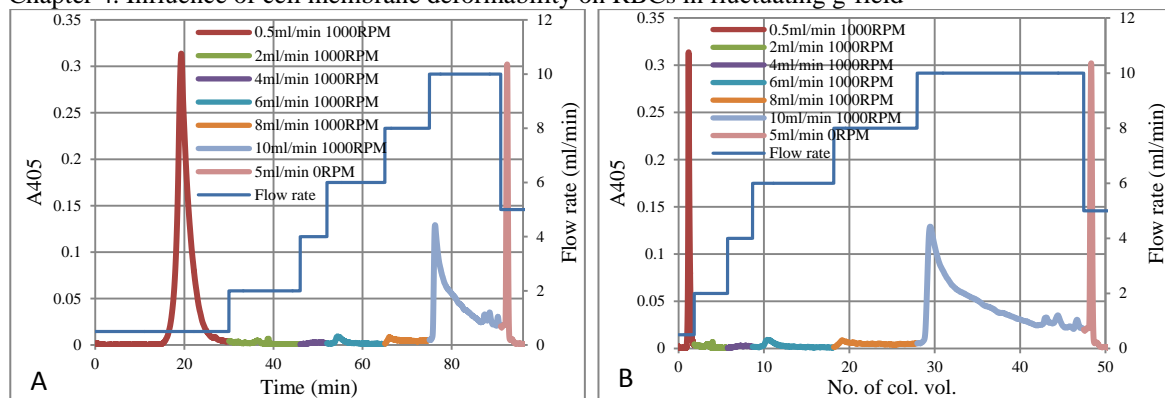


Figure 4.2.6. Elution of unfixed hen RBCs by step flow at 1000 RPM. A) Elution profile plotted against time. B) Elution profile against column volume. 0.32 ml of hen blood sample was injected into CCC coil (Column A: 8.2 ml; 1 mm ID) at 1000 RPM at 0.5 ml/min. Eluent monitored at 405 nm. Flow rate was increased to 2 ml/min and then in steps of 4, 6, 8 and 10 ml/min. Retained RBCs were eluted at 5 ml/min at 0 RPM.

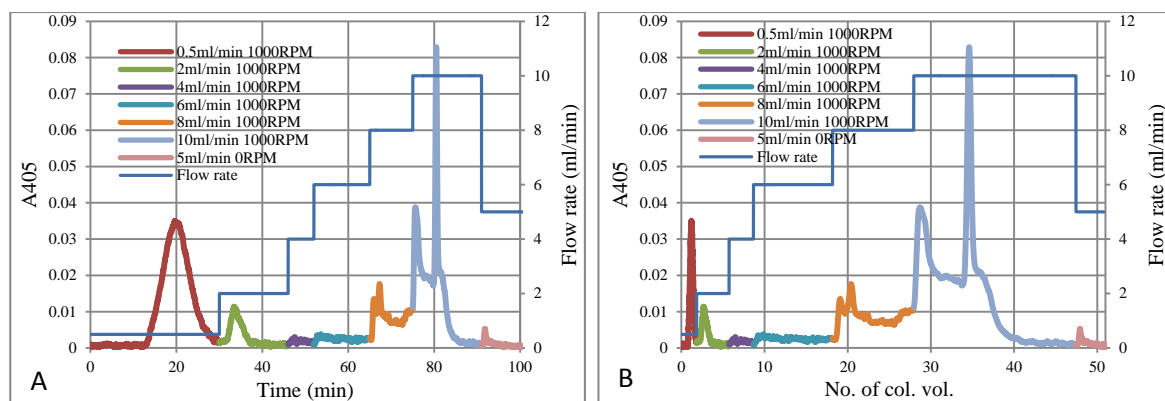


Figure 4.2.7. Elution of glutaraldehyde fixed hen RBCs by step flow at 1000 RPM. A) Elution profile plotted against time. B) Elution profile against column volume. 0.32 ml of glutaraldehyde fixed hen RBC suspension in isotonic buffer was injected into CCC coil (Column A: 8.2 ml; 1 mm ID) at 1000 RPM at 0.5 ml/min. Eluent monitored at 405 nm. Flow rate was increased to 2 ml/min and then in steps of 4, 6, 8 and 10 ml/min. Retained RBCs were eluted at 5 ml/min at 0 RPM.

Figure 4.2.6 shows the unfixed hen RBCs were retained in column until 10 ml/min when some eluted, but some were still retained in the column and were only eluted in the pump out condition of 0 RPM and 5 ml/min. Compared with this, the fixed hen RBCs started to elute at 8 ml/min and then were almost fully eluted all at 10 ml/min and very few were seen in the pump out. Thus fixed hen RBCs were easier to elute than hen RBCs (see also Figure 4.2.8).

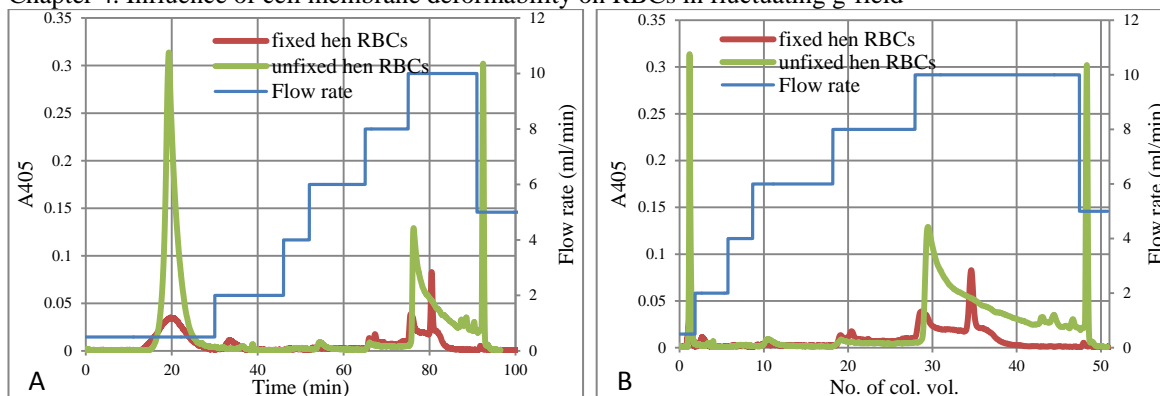


Figure 4.2.8. Comparison between the elution behaviour of unfixed and glutaraldehyde fixed hen RBCs in step flow gradient flow modes at 1000 RPM. A) Elution profile plotted against time. B) Elution profile against column volume. Similar elution behaviours are seen with fixed hen RBCs eluting a little earlier than unfixed one. Data taken from Figure 5.2.10 and Figure 5.2.11.

However, the recovery of glutaraldehyde fixed hen RBCs elution was low and sedimented RBCs retained in the coil were also difficult to remove. This is discussed later in section 4.3.2.

4.2.2.2. Fixed RBCs elution in step flow at relatively low g-field (500 RPM)

4.2.2.2a. Introduction

During the step flow elution of fixed hen RBCs in 1000 RPM, an extremely low recovery was observed. In order to decide whether high g-field is the reason for the strong sedimentation of fixed hen RBCs, the rotational speed was decreased to 500 RPM in this section.

4.2.2.2b. Method

Instrument set up: Milli-CCC[®] (described in 2.2.1.1) with column A (described in 2.2.1.2) rotating in clockwise direction; pumping from tail to head direction; 0.32 ml sample loop; column temperature as 15 °C.

1. The initial rotational speed was set at 500 RPM.
2. Blood sample was pumped in to column via injection port by initial flow rate as 0.5 ml/min.
3. The flow rate of pumping isotonic buffer was changed as the table below:

Flow rate	Period of flow (time)
<i>Sedimentation mode at 500 RPM</i>	
0.5 ml/min	30 mins

<i>Elution mode at 500 RPM</i>	
1 ml/min	15mins
1.5 ml/min	15mins
2 ml/min	15mins
2.5 ml/min	15mins
3 ml/min	15mins

4. Collect data by UV detector to plot graph by time or no. of column volume as horizontal axis and voltage as vertical axis, respectively.

This experiment was performed using unfixed and fixed sheep RBCs and also unfixed and fixed hen RBCs. all re-suspended in isotonic buffer. Results are shown in section 4.2.2.c.

4.2.2.c. Results

i. Sheep RBCs in step flow mode elution at 500 RPM

The results of eluting unfixed and glutaraldehyde fixed sheep RBCs in step flow mode at 500 RPM are shown in in Figure 4.2.9 and 4.2.10.

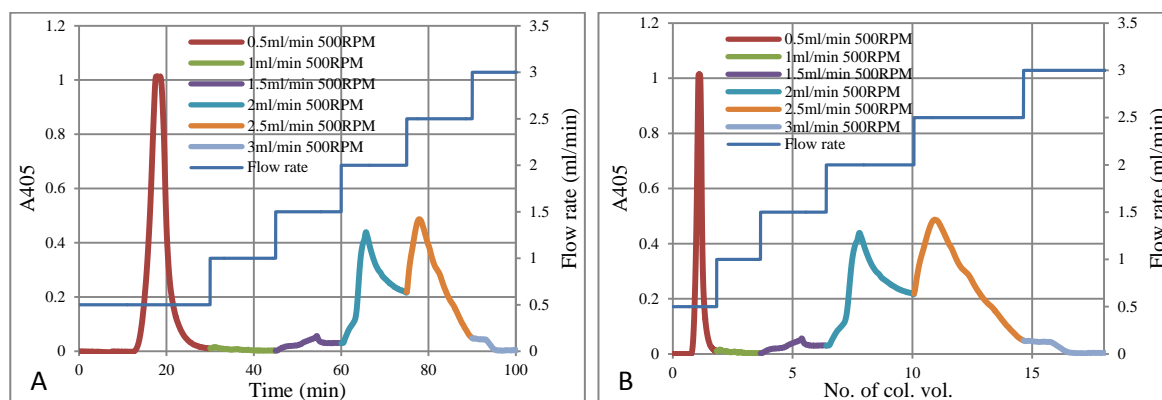
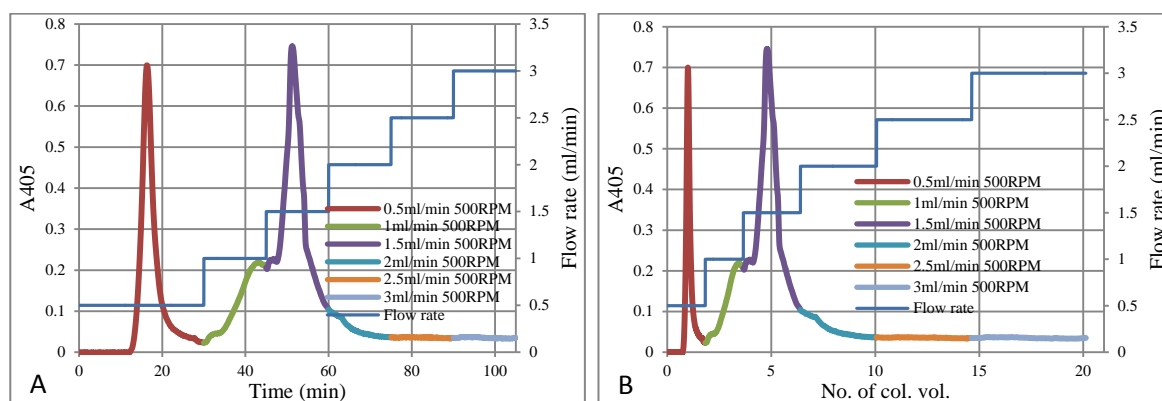


Figure 4.2.9. Elution of unfixed sheep RBCs by step flow at 500 RPM. A) Elution profile plotted against time. B) Elution profile against column volume. 0.32 ml of sheep blood sample was injected into CCC coil (Column A: 8.2 ml; 1 mm ID) at 500 RPM at 0.5 ml/min. Eluent monitored at 405 nm. Flow rate was increased to 1 ml/min and then in steps of 1.5, 2, 2.5 and 3 ml/min at 500 RPM.



Chapter 4. Influence of cell membrane deformability on RBCs in fluctuating g-field

Figure 4.2.10. Elution of glutaraldehyde fixed sheep RBCs by step flow at 500 RPM. A) Elution profile plotted against time. B) Elution profile against column volume. 0.32 ml of glutaraldehyde fixed sheep RBC suspension in isotonic buffer was injected into CCC coil (Column A: 8.2 ml; 1 mm ID) at 500 RPM and 0.5 ml/min. Eluent monitored at 405 nm. Flow rate was increased to 1 ml/min and then in steps of to 1.5, 2, 2.5 and 3 ml/min all at 500 RPM.

The performance of unfixed / fixed sheep RBCs under these conditions of lower g-field again showed that fixed sheep RBCs were easier to elute than unfixed sheep RBC: unfixed sheep RBCs were eluted at 2 ml/min and 2.5 ml/min while the fixed sheep RBCs were be eluted mainly at 1.5 ml/min and all were eluted before 2.5 ml/min. The two sets of elution profiles are compared directly in Figure 4.2.11.

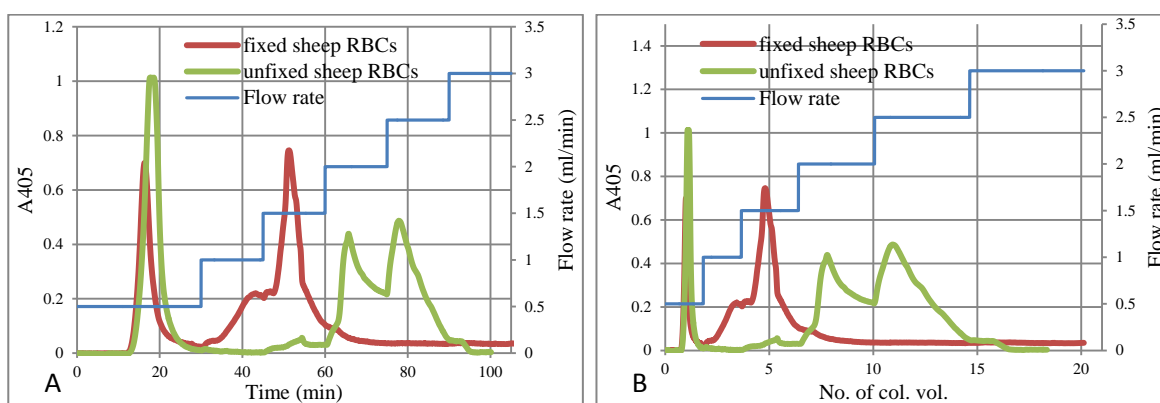


Figure 4.2.11. Comparison between the elution of unfixed and glutaraldehyde fixed sheep RBCs in step flow at 500 RPM. A) Elution profile plotted against time. B) Elution profile against column volume. Data taken from Figure 4.2.9 and Figure 4.2.10.

ii. Hen RBCs in step flow mode elution at 500 RPM

The results of eluting unfixed and glutaraldehyde fixed hen RBCs in step flow under the lower g-field conditions of 500 RPM are shown in Figure 4.2.12 and Figure 4.2.13.

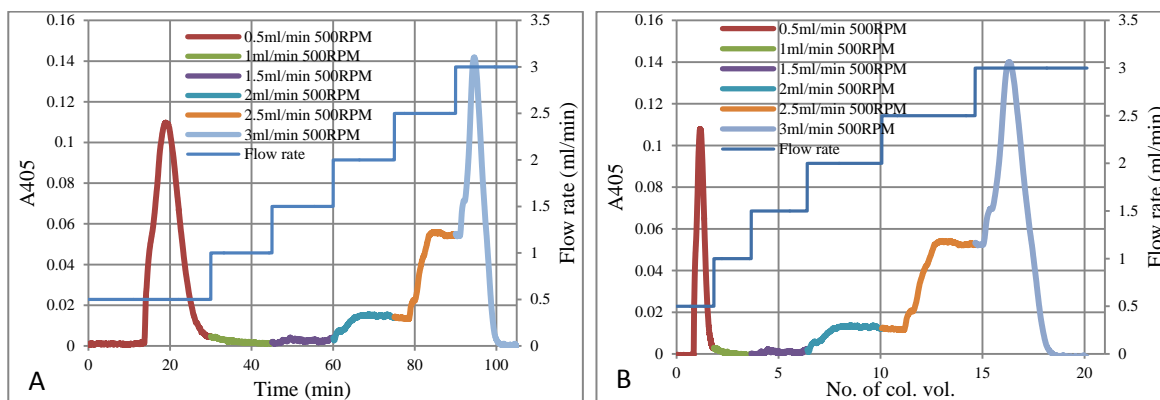


Figure 4.2.12. Elution of unfixed hen RBCs by step flow at 500 RPM. A) Elution profile plotted against time. B) Elution profile against column volume. 0.32 ml of hen blood sample was injected into CCC coil (Column

A: 8.2 ml; 1 mm ID) at 500 RPM at 0.5 ml/min. Eluent monitored at 405 nm. Flow rate was increased to 1 ml/min and then in steps of 1.5, 2, 2.5 and 3 ml/min at 500 RPM.

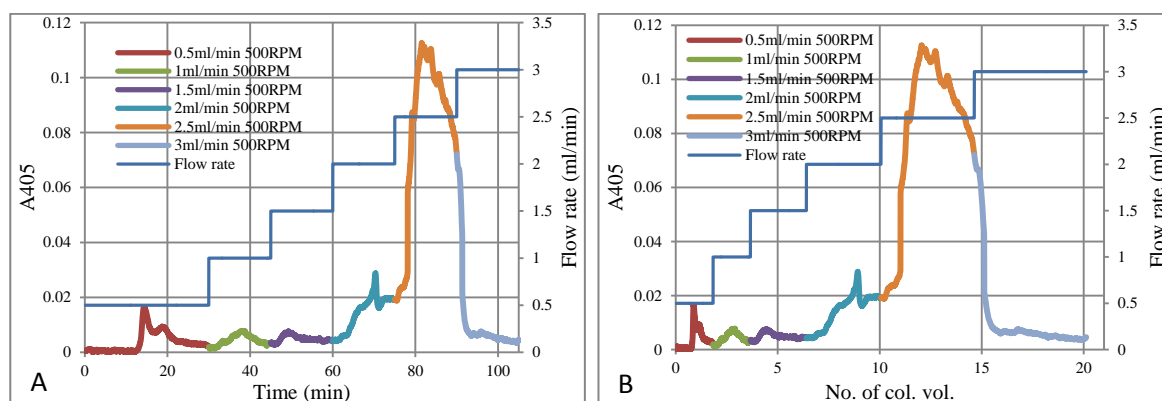


Figure 4.2.13. Elution of glutaraldehyde fixed hen RBCs by step flow at 500 RPM. A) Elution profile plotted against time. B) Elution profile against column volume. 0.32 ml of glutaraldehyde fixed hen RBC suspension in isotonic buffer were injected into CCC coil (Column A: 8.2 ml; 1 mm ID) at 500 RPM and 0.5 ml/min. Eluent monitored at 405 nm. Flow rate was increased to 1 ml/min and then in steps of to 1.5, 2, 2.5 and 3 ml/min all at 500 RPM.

In marked contrast to the low recovery of fixed hen RBCs when step flow elution was made at 1000 RPM, good recovery was obtained when elution was performed at 500 RPM and there was no difficulty in eluting the cells that had been retained (sedimented) in the column.

Comparison of Figure 4.2.12 and Figure 4.2.13, shows that fixed hen RBCs are easier to be eluted than the unfixed hen RBCs as unfixed hen RBCs were eluted mainly at 3 ml/min whereas fixed hen RBCs were eluted at 2.5 ml/min.

Figure 4.2.14 provided a direct comparison of the elution profiles of unfixed and glutaraldehyde fixed hen RBCs under the lower g field conditions of 500 RPM. Fixed hen RBCs eluted a little earlier than unfixed RBCs. However, it is important to compare this result with Figure 4.2.11, which shows the effect of fixation on the elution of sheep RBCs under the same condition. Clearly the elution of hen RBCs is less affected by fixation than is the elution of sheep RBCs.

Chapter 4. Influence of cell membrane deformability on RBCs in fluctuating g-field

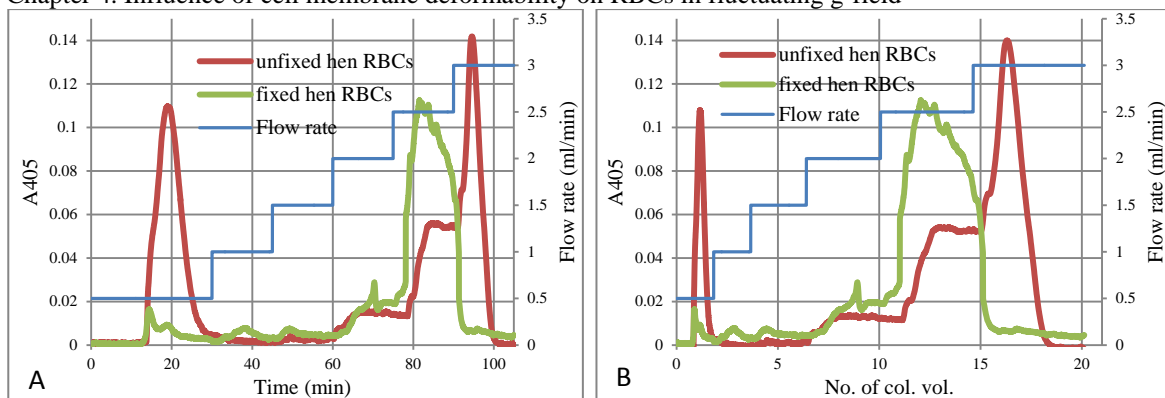


Figure 4.2.14. Comparison between the elution of unfixed and glutaraldehyde fixed hen RBCs in step flow at 500 RPM. A) Elution profile plotted against time. B) Elution profile against column volume. Fixed hen RBCs are eluted a little earlier than unfixed hen RBCs. Data taken from Figure 4.2.12 and Figure 4.2.13.

4.3. Discussion

4.3.1. Discussion of sedimentation and elution behaviours of unfixed and glutaraldehyde fixed RBCs

4.3.1.1. Fixed cells are less retained than unfixed cells

Section 4.2 has shown that both hen and sheep RBCs when fixed are less readily retained during flow in a fluid filled column rotated to generate fluctuating g conditions. This is observed under minimum flow rate condition and step flow elution.

These results indicate that the flexibility of RBCs influences their behaviour in the column. Drawing on analogies with flow of RBCs in vivo, in capillaries, possible reasons for this marked difference in behaviour include the following.

- i) One contributing factor might be related to local viscosity effects as the cells retained in the column will be located at the wall, therefore generating a higher local viscosity area than elsewhere in the column. The viscosity of fixed RBCs will be higher than unfixed RBCs (Bishop et al., 2001) since flexible unfixed RBCs will be easier to deform and squeeze between gaps between cell-cell while the fixed RBCs will not. Unfixed RBCs can deform to their minimum cross-section in the flow stream near the wall of the column (Alizadehrad et al., 2012), thereby reducing the viscosity and effective size.
- ii) In addition the cells possibly deform to move through the column in tank-treading motion or steady-state cell shape in Poiseuille flow (Hosseini & Feng, 2009). By contrast, fixed RBCs have lost this capacity and so are exposed to the flow stream at their original size. Thus the effective cell size that the flow force works on fixed cells is larger and generates a higher force on fixed RBCs pushing them more strongly so that fixed RBCs are retained less readily.
- iii) The results of fixed RBCs at minimum flow rate also show they are easier to be eluted than unfixed RBCs, which demonstrates that the differences in behaviour in the column between fixed and unfixed RBCs are seen not only in the eluting process but also in cell sedimentation in the column initially.
- iv) The traditional sedimentation rate equation (Stokes equation) is (Equation 4.3.1a):

$$v = \frac{d^2(\rho_p - \rho_L) \times g}{18\eta} \quad \text{[Equation 4.3.1a]}$$

Where v = sedimentation rate or velocity of the sphere; d = diameter of the sphere; ρ_p = particle density; ρ_L = liquid density; η = viscosity of liquid medium; g = gravitational force.

Because fixed RBCs will generate an area of higher local viscosity than unfixed RBCs (Bishop et al., 2001) at low shear rate, the sedimentation rate of fixed RBCs will be smaller than unfixed RBCs. Hence the fixed RBCs should be harder to sediment and easier to elute. At low shear rate, the dominant factor is aggregation rather than deformation (Liu & Liu, 2005). Therefore, the low flow rate will not deform the RBCs too much. The effect of diameter is small while the main change of the increased viscosity is a dominant factor. The experimental results are in thus qualitative agreement with the Stokes equation.

v) Table 4.2.1 compares the dependence of initial flow on rotational speed for both unfixed and fixed sheep RBCs. Figure 4.3.1 shows that, after fixation, sheep RBCs required lower minimum flow rates.

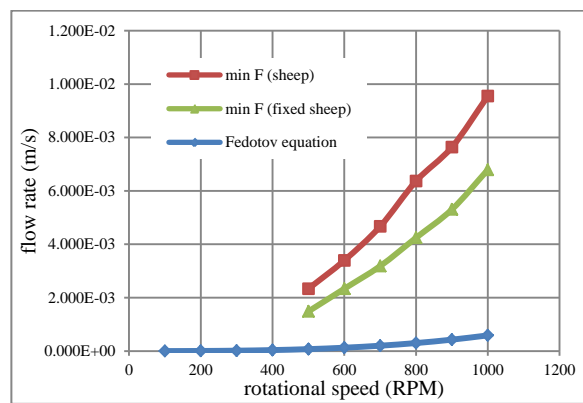
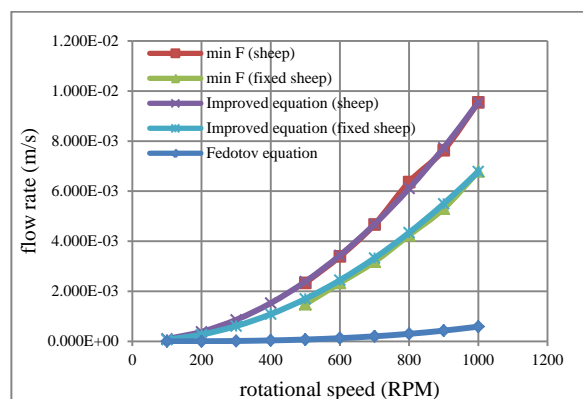


Figure 4.3.1. Dependence of initial flow rate on rotational speed for fixed and unfixed sheep RBCs.

Figure 4.3.1 also show the dependence predicted by the Fedotov equation based on assuming no change in cell radius and density on fixation. Experimentally determined values are markedly different from those predicted by the theoretical equation.

It was possible to correct the calculated value for fixed sheep RBCs to agree very closely with the experimental values by introducing a value of 11.55 for the correction factor α . This is smaller than the value of α of 16.25 required for unfixed sheep RBCs (Figure 4.3.2).



Chapter 4. Influence of cell membrane deformability on RBCs in fluctuating g-field
Figure 4.3.2. Comparison between Fedotov equation, improved equation and min F. A) Hen; B) Sheep. V_f plotted against rotational speed (Column A: 8.2 ml; 1 mm ID).

This indicates that increasing the flexibility of the sheep RBCs (by fixation) decreases the deviation of the behaviour of the cells from those predicted by the Fedotov equation. Since this equation has not parameter for flexibility, it is possible that the cell specific deviations observed for unfixed RBCs may result to some extent arising from differences in flexibility,

4.3.1.2. Fixation affects the performance of sheep RBCs more than hen RBCs

Fixation affects the performance of sheep RBCs more than hen RBCs as the ratio of peak shift for fixed sheep RBCs compared to unfixed ones is much greater than that of for hen RBCs (Figure 4.2.11 and Figure 4.2.14). As the deformability is different for different species (Bishop et al., 2001), one explanation for this difference in elution behaviour is that the initial deformability for hen RBCs is lower than that of for sheep RBCs. Therefore, the less deformability for hen cells makes them appear “hard” before fixation and the fixation makes less of a change to their deformability with nucleus. Compared to this, the sheep RBCs are “soft” with higher deformability and the fixation makes significant deformation difference from unfixed sheep RBCs to fixed ones.

The elution order in Field Flow Fractionation is determined by the distance of particles from the main flow (Reschiglian et al., 2005). Therefore, compared to unfixed RBCs, due to their lower deformability, fixed RBCs must be closer to the higher flow velocity when they sediment which leads to the quicker elution.

Another factor might be axial migration. The gradient shear rate introduced axial migration has been described in both rotational viscometers (Bishop et al., 2001) and steric field-flow fractionation and other techniques (Tong & Caldwell, 1995; Geislinger & Franke, 2014). The hydrodynamic lift force tends to move cells towards the channel centre (Tong & Caldwell, 1995). No direct observation of axial migration phenomena has been made for CCC centrifuges, but an asymmetry of forces is generated provided the flow rate is different between two sides of RBCs, as exist in a shear rate gradient.

4.3.2. Discussion of on the difficulty to remove cells formed by sedimentation of fixed hen RBCs in high g-field

The recovery of fixed hen RBCs at 1000 RPM was low. The fixed hen RBCs that were retained in the column were extremely hard to elute even when the rotational speed was

Chapter 4. Influence of cell membrane deformability on RBCs in fluctuating g-field reduced to 0 RPM. They appeared to be sticking on the wall. However these “stuck” fixed hen RBCs still can be eluted after they were soaked in buffer for some time. Pictures of those “sticky” fixed hen RBCs after they were eluted are shown in Figure 4.3.3.

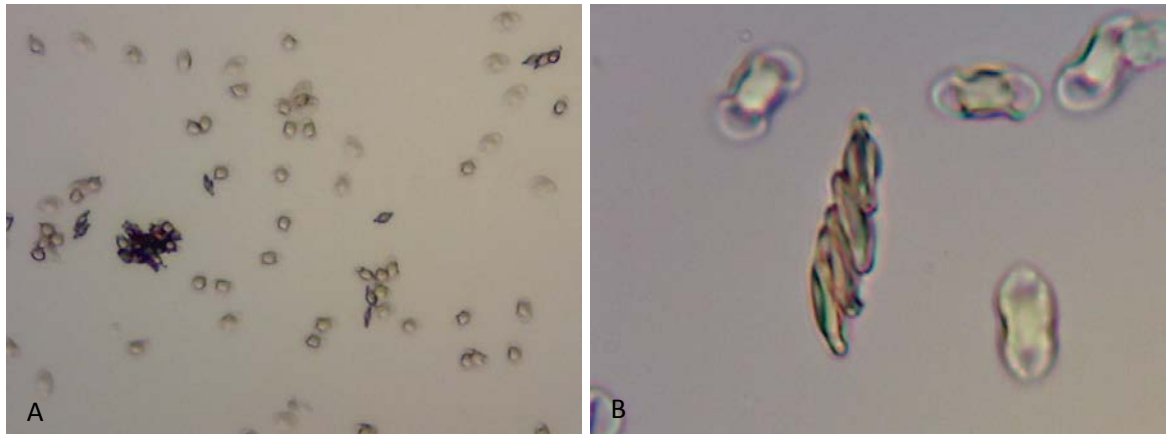


Figure 4.3.3. The eluted “sticky” fixed hen RBCs. A) General view of eluted components (100X). B) An aggregation from the difficult removed cell sedimentation (400X).

In Figure 4.3.3, those special “sticky” fixed hen RBCs were not significantly different from the unfixed hen RBCs. Haematocrit is one factor of RBCs aggregation which will markedly increase the viscosity of whole blood from low haematocrit to high haematocrit (Chien et al., 1970). Due to the influence of g-field, RBCs accumulated at the wall of column which follows the direction of g-field, which makes a highly concentrated RBCs area. Therefore, the local haematocrit is high which would create and lead to situations of high RBCs aggregation. In addition, the fixation of RBCs also increases viscosity (Bishop et al., 2001), therefore, these two important factors work to cause fixed hen RBCs to have increased aggregation under the influence of the g force. Those fixed hen RBCs not involved in this aggregation clump will be eluted as seen in Figure 4.2.7. To confirm this hypothesis a lower g-force was generated at 500 RPM. The gMin generated by 500 RPM is 24 and gMin generated by 1000 RPM is 96.2 (van den Heuvel & Konig, 2011), therefore, compared to 1000 RPM condition, only 25% g force was applied on cells at 500 RPM . The lower g-level may not “press” RBCs to the wall so hard and make a relatively lower haematocrit area to reduce the scale of RBCs aggregation. As Figure 4.2.13 shows, no such aggregation happened at 500 RPM. This indicates the importance of the g-field generating unfavourable conditions for cell separations such as aggregation.

Some unusual fixed hen RBCs were eluted at 1000 RPM (Figure 4.3.3.b), as these look s like rouleaux aggregation (Wagner et al., 2013). If so, this suggests that the shear rate during the sedimentation is small enough to allow such rouleaux to generate (Liu & Liu, 2005). Interestingly, these aggregates cannot be eluted or extruded from the column during

Chapter 4. Influence of cell membrane deformability on RBCs in fluctuating g-field
the experiment. Only after prolonged soaking in the column of these fixed hen RBCs aggregates could cells be eluted. So, the clump aggregation is not permanent but required the existence of the g-field.

4.4. Conclusion

An influence of RBCs deformation on the behaviour of both sheep and hen RBCs in Milli-CCC[®] centrifuge has been demonstrated. Both glutaraldehyde fixed sheep and hen RBCs were eluted easier than unfixed sheep and hen RBCs under the same operation condition. This difference between fixed and unfixed cells was observed both in the initial sedimentation process (minimum operating condition) and elution process.

The results from this chapter confirmed the performance of RBCs in CCC centrifuge is influenced by factors in addition to size and operational conditions and indicates that membrane flexibility needs to be considered as a contributing factor. This is supported by the finding that fixation of sheep RBCs decreased the correction factor α required to be applied to the theoretical “Fedotov equation” for it to fit the experimental data.

How deformability might affect cell behaviour has been discussed and suggestions made that cell aggregation might be a factor increasing the size of the eluting species. In addition influence on the sedimentation rate, effective elution cell / aggregate size (minimum cross-section area) for pumping flow, local haematocrit and viscosity, the distance to the main flow within the column have also been considered as mechanisms by which altered deformability might influence cell retention and elution.

Having established operating conditions for retention of cells and their subsequent elution, and that these differ for different cells: RBCs from different species and also between fixed and unfixed cells, the next Chapter focuses on exploring this insight to develop separations of different cells.

Chapter 5. Behaviour of RBCs elution and flow cell separation

5.1. Summary

The influence of the initial operational conditions on the behaviour of RBCs and the sedimentation requirements of RBCs in fluctuating g-field was described in chapter 3 and chapter 4 discussed the influence of cell deformability. This chapter applies the results of these earlier studies to developing cell separation procedures.

In this chapter, a flow gradient operation is first described as it is a simple way to elute intact RBCs. Sheep and hen RBCs showed different elution behaviours which were maintained when a mixture of sheep and hen RBCs was injected, so that the flow gradient was able to separate the mixture.

Because a long operation time was required for the flow gradient elution method, a step flow method of elution was developed and was also successful in separation the mixture of sheep and hen RBCs.

However, some sheep RBCs eluted in early fractions well separated from their major position of elution. This problem was overcome by an understanding of elution behaviour of RBCs, and an improved step flow elution operation developed which improved the elution behaviour of RBCs and good cell separation results were obtained.

With this improved step flow elution operation, loading studies showed stable cell separation results even when the volume of injected blood sample was 50% of the column volume.

A mixture of Fixed and unfixed sheep RBCs was separated based on their different elution orders. This was facilitated by the addition of a surfactant (Tween[®] 20) to the buffer to hinder the aggregation encountered with this cell mixture.

5.2. Experimental

5.2.1. Behaviour of RBCs elution

Elution studies in Section 3.2.3.3 showed that the sedimented RBCs can be eluted either by increasing the flow rate or decreasing the rotational speed. However, the changes described were quite large and did not exploit the possibilities of subtler changes in flow. This chapter explores in details modes of elution to optimise the elution conditions. Initially a flow gradient with very small increments in flow was developed (Section 5.2.1.1). Although this was successful, and identified finely the elution conditions required for

Chapter 5. Behaviour of RBCs elution and flow cell separation
different cells, it was very slow and therefore a faster elution method was developed to separate a mixture of sheep and hen RBCs using stepped flow (Section 5.2.1.2) In this method the flow was increased in a large step to the point when hen RBCs eluted, after which again the flow was increased to the critical flow needed to elute the sheep RBCs, a method designed to reduce process time.

5.2.1.1. RBCs elution in flow gradient

5.2.1.1a. Introduction

A flow gradient method was developed to analyse the behaviour of sheep and hen RBCs after they had been retained in the column by sedimentation. Therefore, in the beginning, the minimum operational condition was set as initial condition to sediment all intact cells and then, with the increases in the flow rate, the sediment RBCs were gradually eluted out of the column.

The detailed method for flow gradient applied to analyse elution behaviour of hen and sheep RBCs is listed below:

5.2.1.1b. Method

Instrument set up: Milli-CCC[®] (described in 2.2.1.1) with column A (described in 2.2.1.2) rotating in clockwise direction; pumping from tail to head direction; 0.32 ml sample loop; column temperature as 15 °C.

1. The initial rotational speed was set at 900 RPM.
2. Blood sample was pumped into column via injection port by initial flow rate as 0.5 ml/min.
3. After isotonic buffer was pumped 2 column volumes, the flow rate was increased at a rate of 0.2 ml/min per 2 mins until all RBCs were eluted out of column.
4. Collect data by UV detector to plot graph by time as horizontal axis and voltage as vertical axis.

This experiment was performed with hen blood sample, sheep blood sample, and a mixed blood sample (by mixing hen blood : sheep blood (v/v) = 2:1; sample contained: 1.42E+08 hen RBCs and 2.1E+08 sheep RBCs).

For the mixed blood sample, the fractionated samples were collected and examined by light microscope as table below:

Fraction No.	Flow rate (ml/min)	Time (hrs)
1	8.1 - 8.3	1.76 - 1.8
2	8.5 - 8.7	1.83 - 1.9
3	8.9	1.9 - 1.93
4	9.1	1.93 - 1.97
5	9.3	1.97 - 2
6	9.5 - 9.7	2 - 2.07
7	9.9 - 10.3	2.07 - 2.1

Results are shown in section 5.2.1.1c.

5.2.1.1c. Results

The result of eluting hen and sheep blood samples in a flow gradient are shown in Figure 5.2.1.

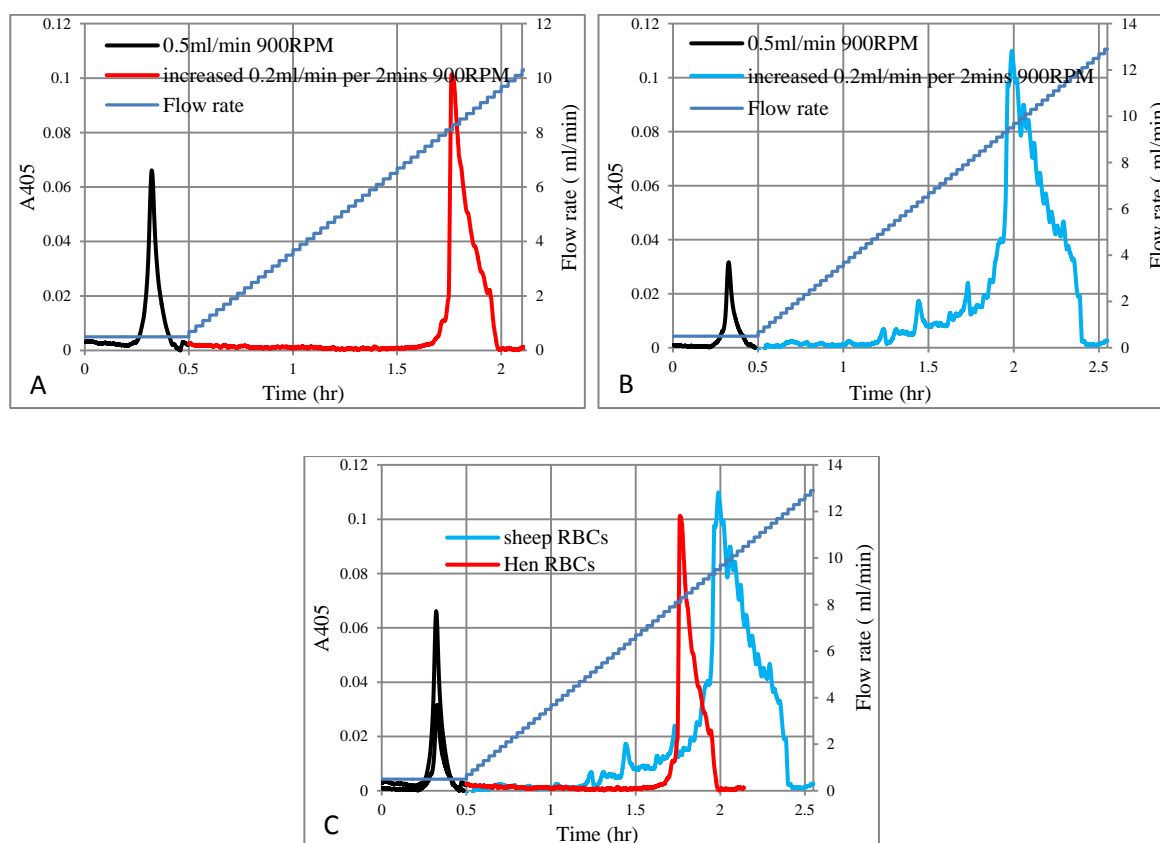


Figure 5.2.1. Elution of sheep blood sample in flow gradient. A) Hen blood sample. B) Sheep blood sample. C) Comparison between hen RBCs and sheep RBCs elution behaviours. 0.32 ml of hen / sheep blood sample was injected into CCC coil (Column A: 8.2 ml; 1 mm ID) at 900 RPM at 0.5 ml/min. Eluent monitored at 405 nm. Gradient increased by steps of 0.2 ml/min every 2 mins after isotonic buffer had been pumped for 2 column volumes to elute Hb (Peak A).

All hen RBCs were eluted before 2 hours by the flow gradient (elution starts from 1.6 hours) with the highest point of peak at 1.75 hours (Figure 5.2.1.a.). Compared to this, sheep RBCs required a higher flow rate, being eluted before 2.4 hours by the flow gradient

(elution starts from 1.2 hours) with the highest point of peak shown at 2 hours (Figure 5.2.1.b.). Therefore, as a cell population, hen RBCs were easier to be eluted by the flow gradient than sheep RBCs. However, the elution peak of sheep RBCs is much broader than hen RBCs, with the consequence that part of the sheep RBCs was easier to be eluted than hen RBC, although a large proportion of sheep RBCs were retained longer than hen RBCs. Thus there is a degree of overlap between the two samples with the elution peak of hen RBCs is in the middle of the broader elution peak of sheep RBCs and with the finish of the hen RBC elution peak earlier than the sheep RBC elution peak. When these two elution profiles are compared (Fig 5.2.1.c) this elution difference suggests a potential rough separation (Figure 5.2.1.c.) if hen and sheep RBCs keep the same chromatographic performance while they are mixed.

The result of eluting a mixed hen/sheep blood sample in this flow gradient is shown in Figure 5.2.2.

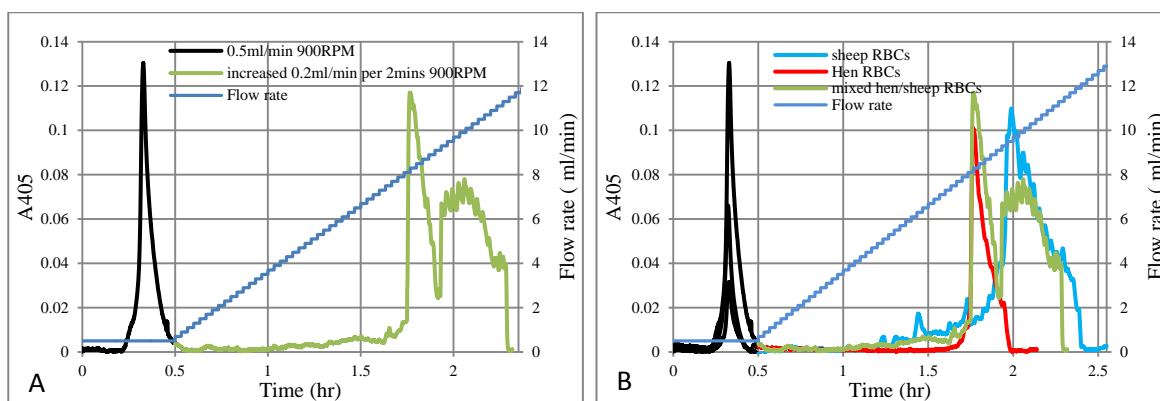


Figure 5.2.2. Elution of mixed hen/sheep RBCs sample in flow gradient. A) Elution of mixed blood sample. B) Comparison between elution of hen RBCs, sheep RBCs and mixed RBCs. 0.32 ml of mixed hen/sheep blood sample (1.42×10^8 hen RBCs and 2.1×10^8 sheep RBCs) was injected into CCC coil (Column A: 8.2 ml; 1 mm ID) at 900 RPM at 0.5 ml/min. Eluent monitored at 405 nm. Gradient increased by steps of 0.2 ml/min every 2min after isotonic buffer had been pumped for 2 column volumes.

The shape of elution peak of the mixture of hen/sheep RBCs (Figure 5.2.2) kept the features of the combined elution peak (Figure 5.2.1.c): the broad elution signal was split into two peaks with an obvious drop after the first peak. The locations of the two peaks covered the locations of hen and sheep RBCs elution peaks while they chromatographed separately. A cell number analysis by haemocytometer is shown in Figure 5.2.3.

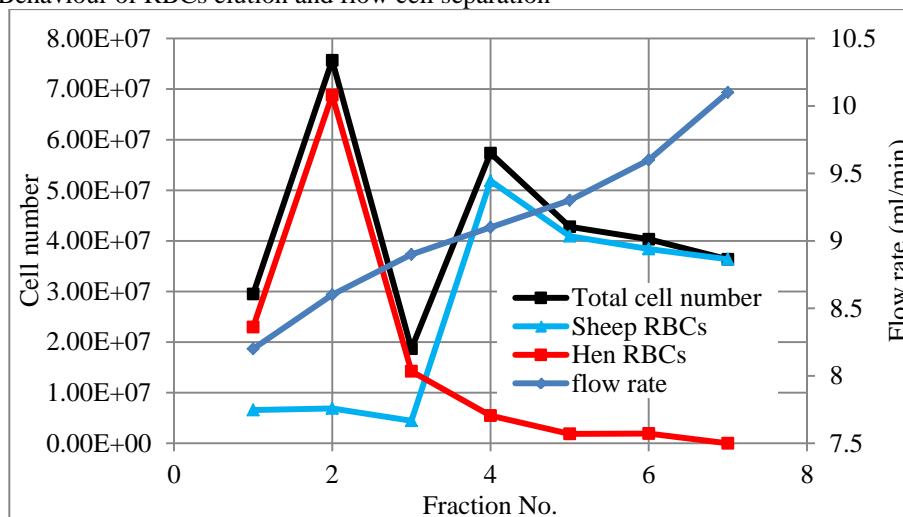


Figure 5.2.3. Cell number analysis for each fraction from the mixed hen / sheep blood sample elution in flow gradient which shows the number of hen RBCs in the first 3 fractions were majority cell and the number of sheep RBCs increased in fraction No.4. (Fraction No.1: 8.1 ml/min - 8.3 ml/min (1.76 hr - 1.83 hr); Fraction No.2: 8.5 ml/min - 8.7 ml/min (1.83 hr - 1.9 hr); Fraction No.3: 8.9 ml/min (1.9 hr - 1.93 hr); Fraction No.4: 9.1 ml/min (1.93 hr - 1.97 hr); Fraction No.5: 9.3 ml/min (1.97 hr - 2 hr); Fraction No.6: 9.5 ml/min - 9.7 ml/min (2 hr - 2.07 hr); Fraction No.7: 9.9 ml/min - 10.3 ml/min (2.07 hr - 2.1 hr))

The microscope examination shows the detailed elution order as hen RBCs were eluted with some sheep RBCs in the beginning and then the number of sheep RBCs was obviously increased with a decreasing number of hen RBCs. As designed (Figure 5.2.1.a), the first finished elution is hen RBCs while the sheep RBCs are retained in the column longer than the hen RBCs. However, there is a great overlap between the hen and sheep elution peaks.

5.2.1.2. RBCs elution in step flow

5.2.1.2a. Introduction

As the separation described in 5.2.1.1 required a long operation time, one of the ideas to shorten the time was to retain all the cells in the column by sedimentation and then increase flow rate to a flow rate to elute one type of cell population and then increase to a higher flow rate to elute the other cell population. As the elution flow rate for hen RBCs determined in 5.2.1.1 was around 9.2 ml/min, therefore, the first elution flow rate was designed as 9.2 ml/min to elute hen RBCs. A higher flow rate 17 ml/min was chosen to elute sheep RBCs.

5.2.1.2b. Method

Instrument set up: Milli-CCC[®] (described in 2.2.1.1) with column A (described in 2.2.1.2) rotating in clockwise direction; pumping from tail to head direction; 0.32 ml sample loop; column temperature as 15 °C.

1. The initial rotational speed was set at 1000 RPM.
2. Blood sample was pumped into column via injection port by initial flow rate as 0.5 ml/min.
3. The flow rate of pumping isotonic buffer was changed as the table below:

Flow rate	Period of flow (time)
<i>Sedimentation mode at 1000 RPM</i>	
0.5 ml/min	30 min
<i>Elution mode at 1000 RPM</i>	
2 ml/min	30 s
4 ml/min	30 s
6 ml/min	30 s
8 ml/min	30 s
9.2 ml/min	43 min
<i>Elution mode of retained RBCs at 1000RPM</i>	
17 ml/min	-

4. Collect data by UV detector to plot graph by time or no. of column volume as horizontal axis and voltage as vertical axis, respectively.

This experiment was performed with hen blood sample, sheep blood sample, and a mixed blood sample (by mixing hen blood : sheep blood (v/v) = 4:1; sample included: 1.40E+08 hen RBCs and 1.63E+08 sheep RBCs).

For the mixed blood sample, the fractionated samples were collected and examined by light microscope as table below:

Fraction No.	Flow rate (ml/min)	Volume (ml)	Time (min)
1	9.2	50 ml	32 - 37.43
2	9.2	50 ml	37.43 - 42.86
3	9.2	50 ml	42.86 - 48.29
4	9.2	50 ml	48.29 - 53.72
5	9.2	50 ml	53.72 - 59.15
6	9.2	50 ml	59.15 - 64.58
7	9.2	50 ml	64.58 - 70
8	9.2	≈ 50 ml	70 - 75
9	17	-	-

Results are shown in section 5.2.1.2c.

5.2.1.2c. Results

The result of eluting hen RBCs in step flow is shown in Figure 5.2.4 which shows that the hen RBCs started to elute at 9.2 ml/min as a broad peak. Raising the flow to 17ml/min gave no additional elution, confirming that all cells were eluted at 9.2ml/min. This was a similar behaviour to that observed for hen RBCs eluted by a gradient flow mode.

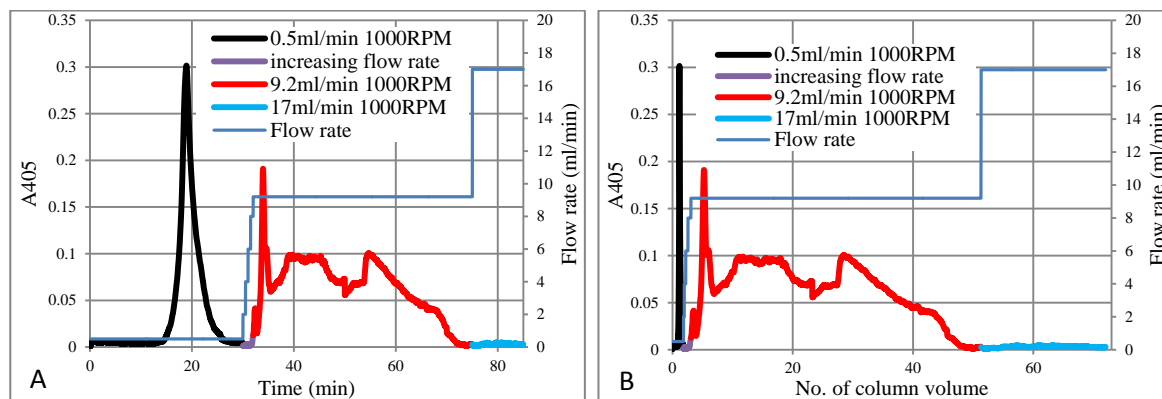


Figure 5.2.4. Elution of hen blood sample by a step increase in flow. A) Elution profile plotted against time. B) Elution profile against column volume. 0.32 ml of hen blood sample was injected into CCC coil (Column A: 8.2 ml; 1 mm ID) at 1000 RPM at 0.5 ml/min. Eluent monitored at 405 nm. After 2 column volumes, flow rate was increased to 2 ml/min and then in steps of 4, 6, 8 ml/min per 30s (total 2 mins) and 9.2 ml/min for 50 column volumes. Retained RBCs were eluted at 17 ml/min at 1000 RPM.

The result of eluting of sheep RBCs in step flow is shown in Figure 5.2.5.

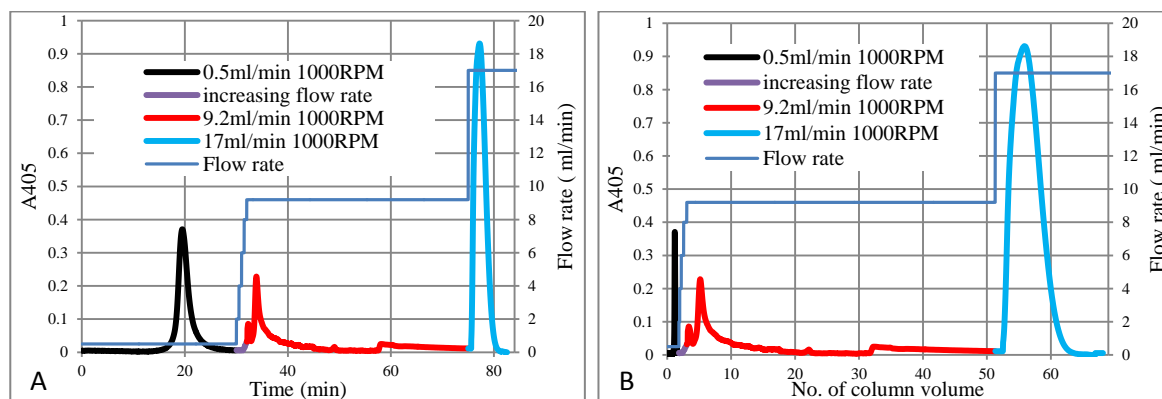


Figure 5.2.5. Elution of sheep blood sample by a step increase in flow. A) Elution profile plotted against time. B) Elution profile against column volume. 0.32 ml of sheep blood sample was injected into CCC coil (Column A: 8.2 ml; 1 mm ID) at 1000 RPM at 0.5 ml/min. Eluent monitored at 405 nm. Flow rate was increased to 2 ml/min and then in steps of 4, 6, 8 ml/min per 30s (total 2 mins) and 9.2 ml/min for 50 times of column volume. Retained RBCs were eluted at 17 ml/min at 1000 RPM.

Figure 5.2.5 shows the majority of sheep RBCs were retained in the column after the eluting flow was raised to 9.2 ml/min with a minority of the sheep RBCs being eluted in the beginning part of the 9.2 ml/min flow.

Figure 5.2.6 makes a direct comparison of these two elutions. Apart from a small peak of sheep RBCs at the onset of the step change it can be seen that all the hen RBCs were less retained in the column should be well separated from the sheep RBCs which required to be eluted after the second step change, provided behaviour with a mixed load of hen and sheep RBCs behaved similarly to that of the hen and sheep RBCs run separately.

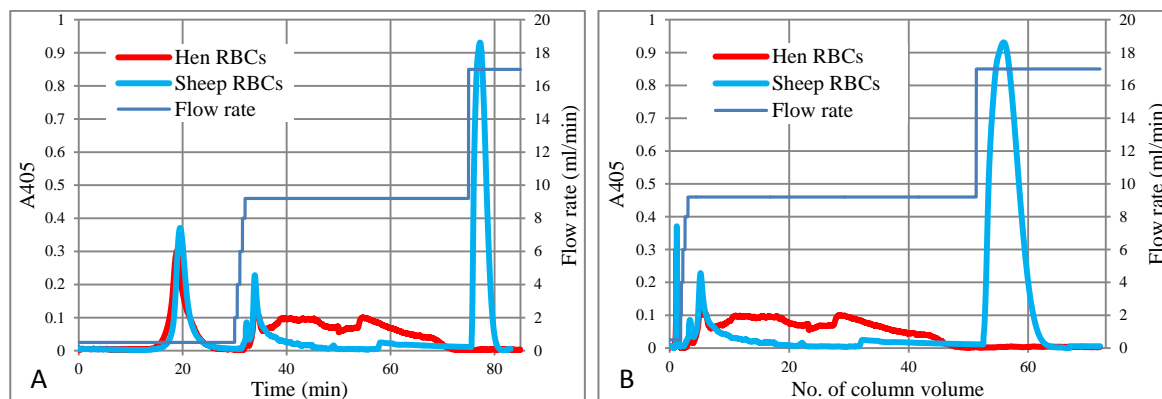


Figure 5.2.6. Comparison between the elution behaviour of hen and sheep RBCs in step flow gradient flow modes. A) Elution profile plotted against time. B) Elution profile against column volume. Similar elution behaviours are seen with hen RBCs eluting a little earlier than sheep RBCs with part of sheep RBCs eluted at location of the beginning of hen RBCs elution. Data taken from Figure 5.2.4 and 5.2.5.a mixture of hen and sheep RBCs was run (Figure 5.2.7).

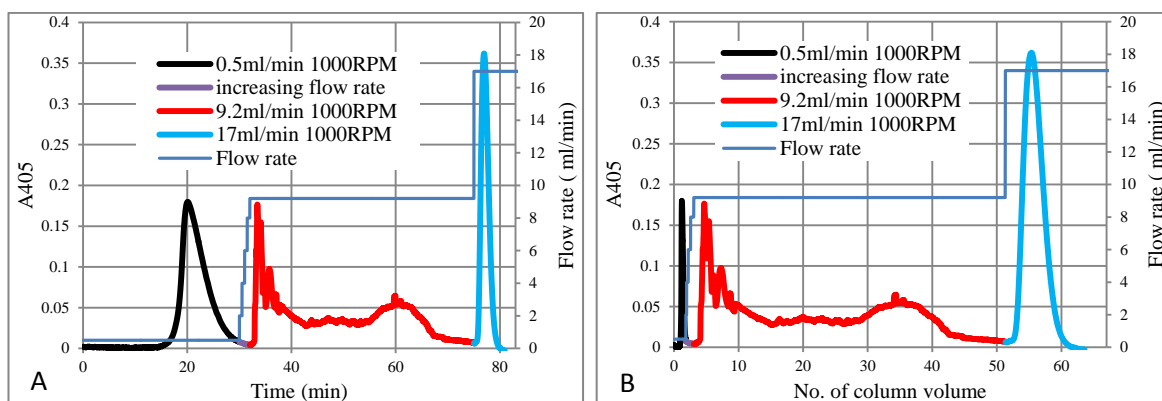


Figure 5.2.7. Elution of mixed hen/sheep blood sample by a step increase in flow. A) Elution profile plotted against time. B) Elution profile against column volume. 0.32 ml of mixed hen/sheep blood sample (sample included: 1.40×10^8 hen RBCs and 1.63×10^8 sheep RBCs) was injected into CCC coil (Column A: 8.2 ml; 1 mm ID) at 1000 RPM at 0.5 ml/min. Eluent monitored at 405 nm. After 2 column volumes Flow rate was increased to 2 ml/min and then in steps of 4, 6, 8 ml/min per 30s (total 2 mins) and 9.2 ml/min for 50 times of column volume. Retained RBCs were eluted at 17 ml/min at 1000 RPM.

A cell number analysis by haemocytometer was also performed (Figure 5.2.8).

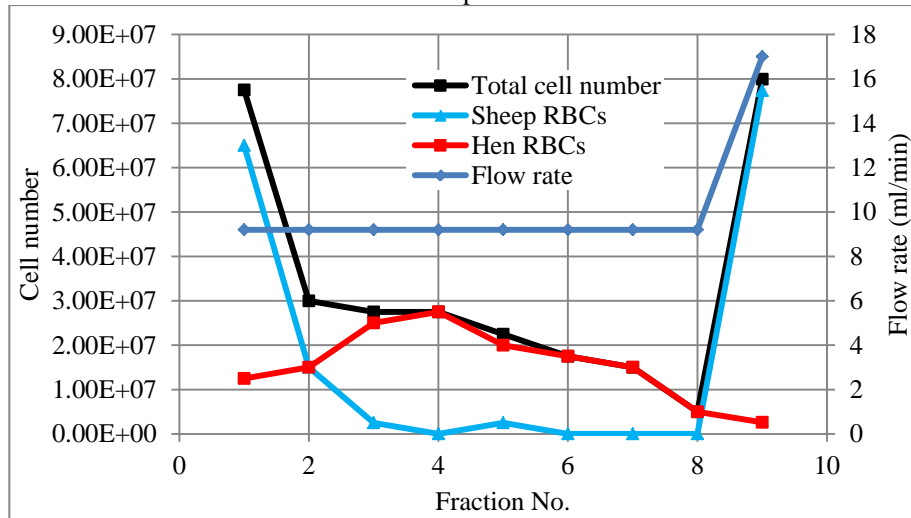


Figure 5.2.8. Cell number analysis for each fraction in step flow. It shows most of cells were sheep RBCs in the first 2 fraction, but its number was decreased from fraction No.2 and then stopped eluting soon in next fractions until fraction no.9 which was the 17 ml/min fraction. Most of hen RBCs were eluted in the 9.2 ml/min which has a cell number increasing and decreasing process as designed (Figure 4.2.8). (Fraction No.1: 32 min - 37.43 min (9.2 ml/min); Fraction No.2: 37.43 min - 42.86 min (9.2 ml/min); Fraction No.3: 42.86 min - 48.29 min (9.2 ml/min); Fraction No.4: 48.29 min - 53.72 min (9.2 ml/min); Fraction No.5: 53.72 min - 59.15 min (9.2 ml/min); Fraction No.6: 59.15 min - 64.58 min (9.2 ml/min); Fraction No.7: 64.58 min - 70 min (9.2 ml/min); Fraction No.8: 70 min - 75 min (9.2 ml/min); Fraction No.9: 17 ml/min)

Figure 5.2.7 shows there was a sharp peak eluted immediately after the first step change to 9.2 ml/min which the cell counting analysis showed was predominantly sheep RBCs with a smaller content of hen RBCs. This was followed by a broad peak of hen RBCs which were completely eluted. This peak contained no sheep RBCs. On changing the flow to 17 ml/min sheep RBCs, uncontaminated by hen RBCs were rapidly eluted. Overall the elution was as predicted by Figure 5.2.7, although the proportion of sheep RBCs in the early eluting peak was higher. The problem of this early elution of a proportion of the sheep RBCs is addressed in the following section. Flow cell separation in fluctuating g-field

5.2.1.3. Flow cell separation in improved step flow

5.2.1.3a. Introduction

A surprising observation made in the previous section was that while hen RBCs could be retained and then eluted completely by an increase in flow, by contrast a proportion of sheep RBCs were readily eluted by the first increase in flow, whilst the remained require a much great flow to elute them. In this section operational conditions were modified to reduce this early eluting peak. These improvements include:

1. Started to increase the flow rate after isotonic buffer had been pumped for 1 column volume instead of 2 column volumes to save operation time.
2. Short incremental increased in flow instead of a single large step.
3. Use a lower flow rate to elute hen RBCs to reduce elution of sheep RBC, by making it easier for them to sediments.
4. Elute retained sheep RBCs at 2 ml/min at 0 RPM instead of eluting at a high flow rate at high rotational speed to avoid diluting the sheep RBC fraction

5.2.1.3b. Method

Instrument set up: Milli-CCC[®] (described in 2.2.1.1) with column A (described in 2.2.1.2) rotating in clockwise direction; pumping from tail to head direction; 0.32 ml sample loop; column temperature as 15 °C.

1. The initial rotational speed was set to 1000 RPM.
2. Blood sample was pumped into column via injection port by initial flow rate as 0.5 ml/min.
3. The flow rate of pumping isotonic buffer was changed as the table below:

Flow rate	Period of flow (column volumes)
<i>Sedimentation mode at 1000 RPM</i>	
0.5 ml/min	1 column volume
<i>Elution mode at 1000 RPM</i>	
2 ml/min	1 column volume
4 ml/min	1.5 column volumes
6 ml/min	1.5 column volumes
8 ml/min	50 column volumes
<i>Elution mode of retained RBCs at 0 RPM</i>	
2 ml/min	-

4. Collect data by UV detector to plot graph by time or no. of column volume as horizontal axis and voltage as vertical axis, respectively.

This experiment was performed with hen blood sample, sheep blood sample, and the mixed blood sample (by mixing hen blood : sheep blood (v/v) = 4:1; sample included: around 1.5E+08 hen RBCs and 1.78E+08 sheep RBCs).

For mixed blood sample, the fractionated samples were collected and examined by light microscope as described below:

Fraction No.	Flow rate (ml/min)	Volume (ml)	Time (min)
1	8	50	25 - 31.25
2	8	50	31.25 - 37.5
3	8	50	37.5 - 43.75
4	8	50	43.75 - 50
5	8	50	50 - 56.25
6	8	50	56.25 - 62.5
7	8	50	62.5 - 68.75
8	8	50	68.75 - 75
9	2	-	-

Results are shown in section 5.2.2.1c.

5.2.1.3c. Results

The result of eluting of hen RBCs with this improved step flow is shown in Figure 5.2.9 and the result for sheep RBCs is shown I Figure 5.2.10.

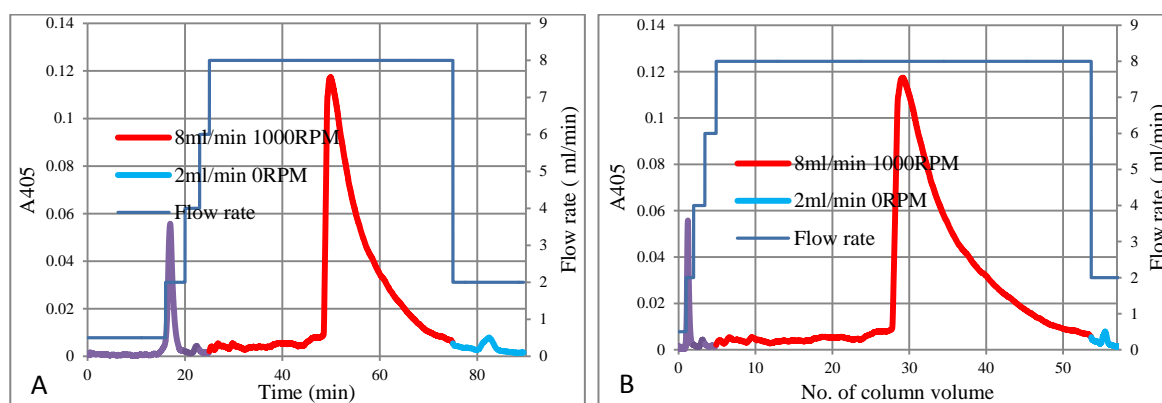


Figure 5.2.9. Elution of hen blood sample by an improved step increase in flow. A) Elution profile plotted against time. B) Elution profile plotted against column volume. 0.32 ml of hen blood was injected into CCC coil (Column A: 8.2 ml; 1 mm ID) at 1000 RPM at 0.5 ml/min for $1 \times$ column volume. Eluent monitored at 405 nm. Flow rate was increased to 2 ml/min ($1 \times$ column volume) and then in steps of 4 ($1.5 \times$ column volumes), 6 ($1.5 \times$ column volumes), and 8 ml/min for $50 \times$ column volumes. Retained RBCs were eluted at 2 ml/min at 0 RPM.

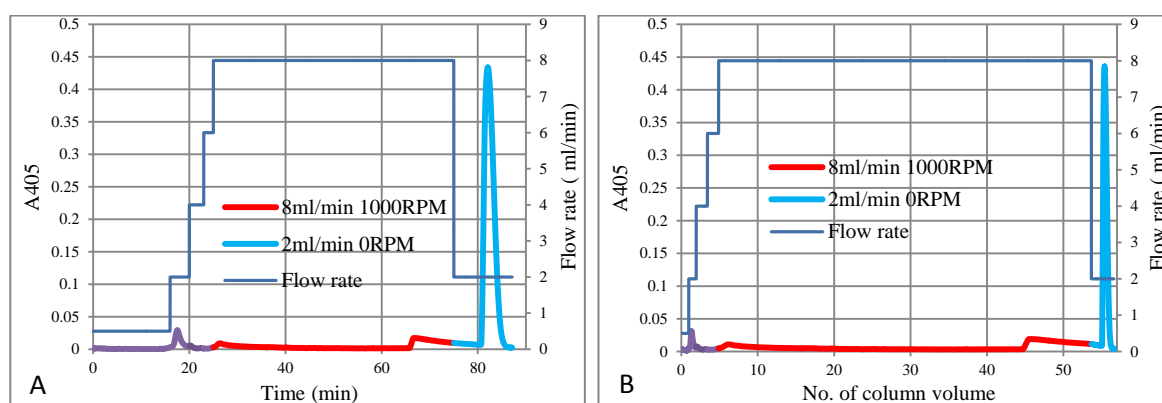


Figure 5.2.10. Elution of sheep blood sample by an improved step increase in flow. A) Elution profile plotted against time. B) Elution profile plotted against column volume. 0.32 ml of sheep blood was injected into CCC coil (Column A: 8.2 ml; 1 mm ID) at 1000 RPM at 0.5 ml/min for 1 × column volume. Eluent monitored at 405 nm. Flow rate was increased to 2 ml/min (1 × column volume) and then in steps of 4 (1.5 × column volumes), 6 (1.5 × column volumes), and 8 ml/min for 50 × column volumes. Retained RBCs were eluted at 2 ml/min at 0 RPM.

Figure 5.2.9 shows hen RBCs were eluted with a flow rate of 8 ml/min with no cells being eluted with the earlier steps in the flow of 2, 4 and 6 ml/min. Hen RBCs were eluted out of the column at 48 mins and the whole elution finished within 50 × column volumes. Figure 5.2.10 shows that a small proportion of sheep RBCs were eluted at the beginning of the 8 ml/min flow step, but soon, the signal returned to 0 and all remaining cells were retained in the column until the late stage of 8 ml/min elution when again there was a small blip. However the majority of sheep RBCs were still retained in the column and required 2 ml/min at 0RPM to be eluted. Compared with the elution conditions used in section 5.2.1.2, these improved conditions have markedly reduced the appearance of sheep RBCs in early elution before hen RBCs and well before the bulk of the sheep RBCs. Super imposing Figures 5.2.9 (hen RBCs) and Figure 5.2.10 (sheep RBCs) in Figure 5.2.11 clearly indicates that these improved conditions should be able to separate a mixtures of the types of RBCs.

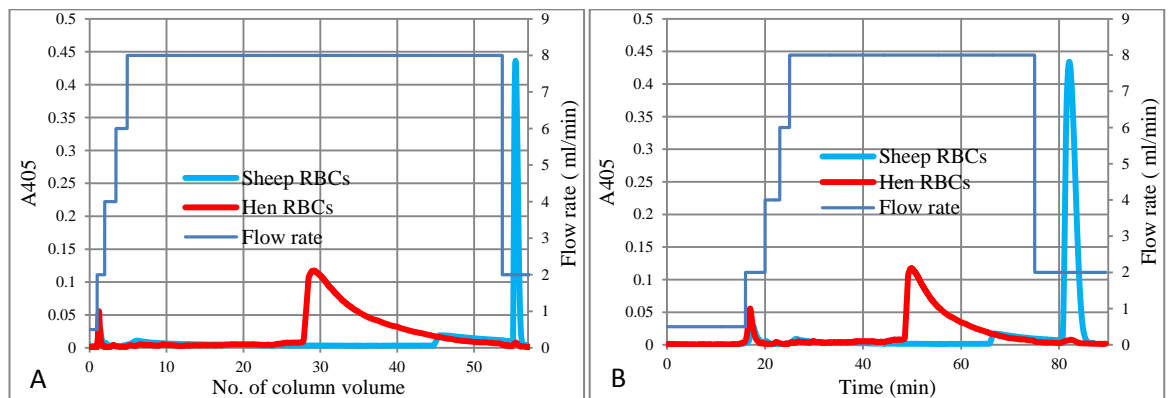


Figure 5.2.11. Comparison between the elution behaviour of hen and sheep RBCs in improved step flow gradient flow modes. A) Elution profile plotted against time. B) Elution profile plotted against column volume. Similar elution behaviours are seen with hen RBCs retaining first and then eluting earlier than sheep RBCs with part of sheep RBCs eluted at location where hen RBCs were retained in column. Data taken from Figure 5.2.9 and 5.2.10.

The result of eluting of a mixture of hen and sheep RBCs using the improved step flow method is shown in Figure 5.2.12, together with the result of cell number analysis by haemocytometer in Figure 5.2.13.

Chapter 5. Behaviour of RBCs elution and flow cell separation

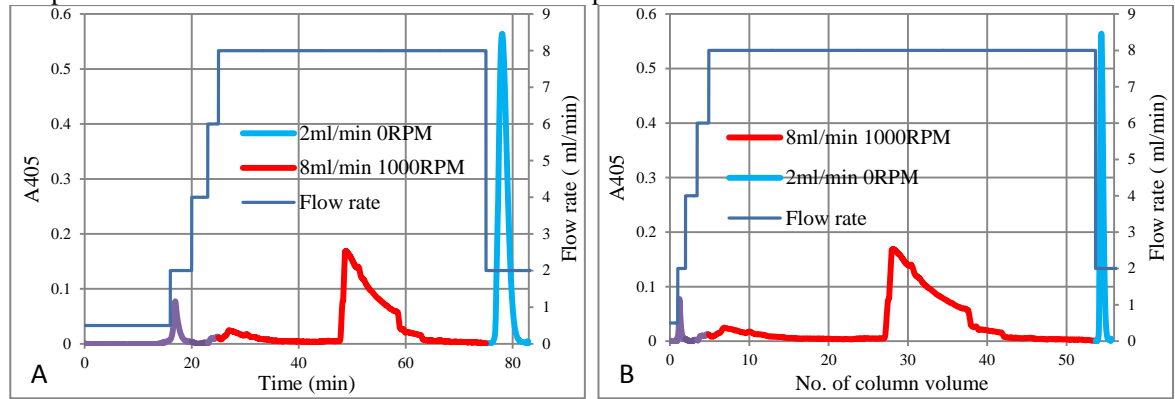


Figure 5.2.12. Elution of mixed hen and sheep blood sample by an improved step increase in flow. A) Elution profile plotted against time. B) Elution profile plotted against column volume. 0.32 ml of mixed hen/sheep blood (sample includes: 1.5×10^8 hen RBCs and 1.78×10^8 sheep RBCs) was injected into CCC coil (Column A: 8.2 ml; 1 mm ID) at 1000 RPM at 0.5 ml/min for $1 \times$ column volume. Eluent monitored at 405 nm. Flow rate was increased to 2 ml/min ($1 \times$ column volume) and then in steps of 4 ($1.5 \times$ column volumes), 6 ($1.5 \times$ column volumes), and 8 ml/min for $50 \times$ column volumes. Retained RBCs were eluted at 2 ml/min at 0 RPM.

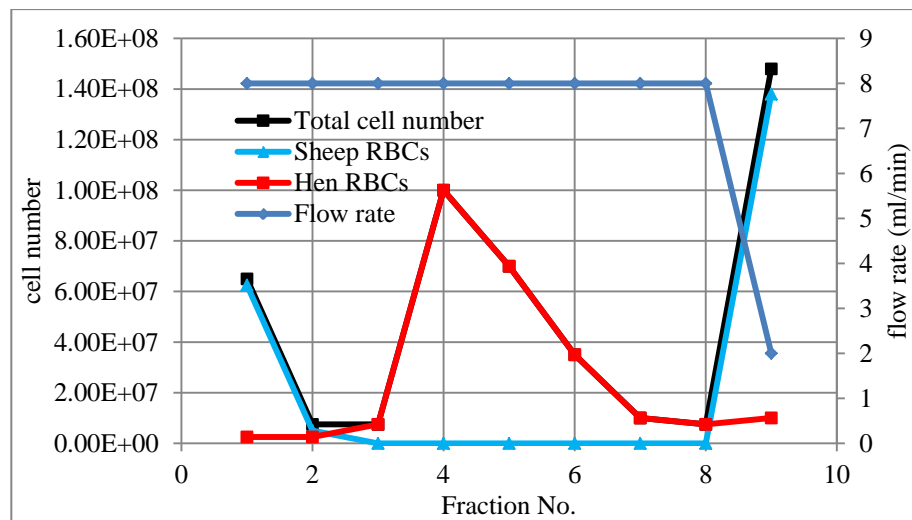


Figure 5.2.13. Cell number analysis for each fraction in improved step flow which shows part of the sheep RBCs were at the beginning of 8 ml/min and the hen RBCs were eluted in the middle of 8 ml/min. Left sheep RBCs in the column until 2 ml/min as designed (Figure 18). (Fraction No.1: 25 min - 31.25 min (8 ml/min); Fraction No.2: 31.25 min - 37.5 min (8 ml/min); Fraction No.3: 37.5 min - 43.75 min (8 ml/min); Fraction No.4: 43.75 min - 50 min (8 ml/min); Fraction No.5: 50 min - 56.25 min (8 ml/min); Fraction No.6: 56.25 min - 62.5 min (8 ml/min); Fraction No.7: 62.5 min - 68.75 min (8 ml/min); Fraction No.8: 68.75 min - 75 min (8 ml/min); Fraction No.9: 2 ml/min).

The mixed hen/sheep RBCs repeated the behaviour of eluting hen and sheep RBCs separately as the elution order is part of the sheep RBCs, eluting early, then hen RBCs and finally the rest of the sheep RBCs. The fraction no.1 and no.2 show the quicker eluted sheep RBCs. Hen RBCs elution starts from fraction no.3 to fraction no.8 with process of

Chapter 5. Behaviour of RBCs elution and flow cell separation number increased and decreased. Fraction no.9 shows the majority of cell were sheep RBCs. However, the microscopic analysis of the fractions shows that this “anomalous” early eluting peak of sheep RBC was still significant at ca 29%. Subsequently it was found that by using “rectangular” tubing, rather than the “circular” tubing of Column A, described above, this “anomalous” early peak with sheep RBCs could be removed. This is discussed in Chapter 6.

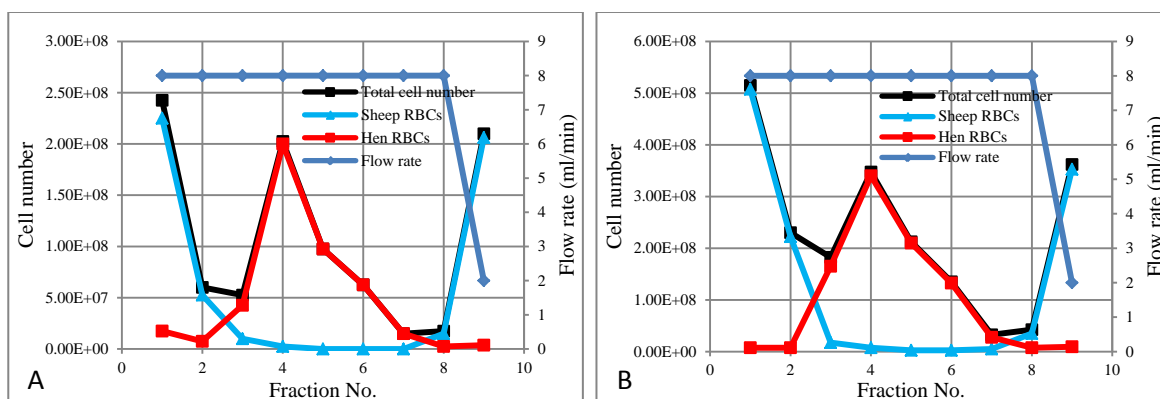
5.2.2. Loading test of flow cell separation

5.2.2.1. Introduction & Method

The flow cell separation described in 5.2.1.3 showed a good separation result, except for the early “anomalous” peak obtained with sheep RBCs. These results had all been obtained using an injection volume that was 3.9% of the column volume. In this section the effect of s increasing the number of cells loaded on the separations and also on the appearance of the early eluting peak of sheep RBCs is examined. Samples were chromatographed using loops of increasing volume: sample loop B, C and D (9%, 19% and 50% of column volume respectively).

5.2.2.2. Results

A cell number analysis by haemocytometer for different sample loop is shown in Figure 5.2.14.



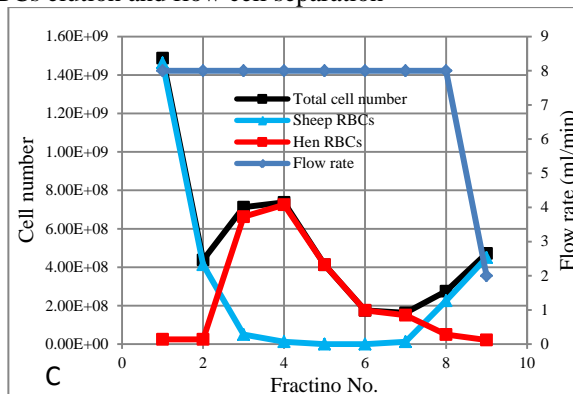


Figure 5.2.14. Cell number analysis for each fraction in improved step flow by different sample loops.

A) 0.73 ml sample loop. 0.73 ml (9% of column volume) of mixed hen/sheep blood (sample includes: $4.85\text{E}+08$ hen RBCs and $4.75\text{E}+08$ sheep RBCs) was injected into CCC coil (Column A: 8.2 ml; 1 mm ID) at 1000 RPM at 0.5 ml/min for $1 \times$ column volume. Eluent monitored at 405 nm. Flow rate was increased to 2 ml/min ($1 \times$ column volume) and then in steps of 4 ($1.5 \times$ column volumes), 6 ($1.5 \times$ column volumes), and 8 ml/min for $50 \times$ column volumes. Retained RBCs were eluted at 2 ml/min at 0 RPM.

B) 1.52 ml (19% of column volume) of mixed hen/sheep blood (sample includes: $1.06\text{E}+09$ hen RBCs and $1.04\text{E}+09$ sheep RBCs) was injected into CCC coil (Column A: 8.2 ml; 1 mm ID) at 1000 RPM at 0.5 ml/min for $1 \times$ column volume. Eluent monitored at 405 nm. Flow rate was increased to 2 ml/min ($1 \times$ column volume) and then in steps of 4 ($1.5 \times$ column volumes), 6 ($1.5 \times$ column volumes), and 8 ml/min for $50 \times$ column volumes. Retained RBCs were eluted at 2 ml/min at 0 RPM.

C) 4.05 ml (50% of column volume) of mixed hen/sheep blood (sample includes: $2.21\text{E}+09$ hen RBCs and $2.56\text{E}+09$ sheep RBCs) was injected into CCC coil (Column A: 8.2 ml; 1 mm ID) at 1000 RPM at 0.5 ml/min for $1 \times$ column volume. Eluent monitored at 405 nm. Flow rate was increased to 2 ml/min ($1 \times$ column volume) and then in steps of 4 ($1.5 \times$ column volumes), 6 ($1.5 \times$ column volumes), and 8 ml/min for $50 \times$ column volumes. Retained RBCs were eluted at 2 ml/min at 0 RPM.

Although the elution order and results are similar to Figure 5.2.13, it is clear that as the number of cell loaded was increased, a greater proportion of sheep RBCs eluted in the first peak, before the hen RBC, than were retained and subsequently eluted with the pump out step of 2 ml/min at 0 RPM.

5.2.3. Separation of fixed and unfixed sheep RBCs in step flow

5.2.3.1. Introduction

In Chapter 4 both Sheep and hen RBCs showed different elution behaviour in the Milli-CCC after they had been fixed with glutaraldehyde (Figure 4.2.5); fixed RBCs were eluted more readily than unfixed cells. This provided some support for a possible contribution of membrane deformability to determining the flow behaviour of cells in fluctuating g field. In this section the flow separation of fixed and unfixed RBCs is described, giving an example of a cell separation based on difference in deformability. As fixed RBCs cannot

be lysed by water it was possible to distinguish between unfixed and fixed RBCs in fractions by spinning down the cells and re-suspending them in water, and spinning down again. If absorbance at 405nm of the supernatant increases after the re-suspension in H₂O, then it means the fractionated sample contains intact unfixed sheep RBCs, which had been lysed when re-suspended in water.

5.2.3.2. Method

Instrument set up: Milli-CCC[®] (described in 2.2.1.1) with column A (described in 2.2.1.2) rotating in clockwise direction; pumping from tail to head direction; 0.73 ml sample loop; column temperature as 15 °C.

1. The initial rotational speed was set at 1000 RPM.
2. Blood sample was pumped in to column via injection port by initial flow rate as 0.5 ml/min.
3. The flow rate of pumping isotonic buffer was changed as the table below:

Flow rate	Period of flow (column volumes)
<i>Sedimentation mode at 1000 RPM</i>	
0.5 ml/min	2 column volumes
<i>Elution mode at 1000 RPM</i>	
2 ml/min	4 column volumes
4 ml/min	4 column volumes
6 ml/min	10 column volumes
8 ml/min	10 column volumes
10 ml/min	12 column volumes
<i>Elution mode of retained RBCs at 0RPM</i>	
5 ml/min	-

4. Collect data by UV detector to plot graph by time or no. of column volume as horizontal axis and voltage as vertical axis, respectively.
5. The fractionated samples were collected from 2 ml/min elution per 5min. The elution condition for each fractions is listed below:

Fraction No.	Elution condition	Fraction No.	Elution condition
1	2 ml/min; 1000 RPM	7	8 ml/min; 1000 RPM
2	2 ml/min; 1000 RPM	8	8 ml/min; 1000 RPM
3	4 ml/min; 1000 RPM	9	10 ml/min; 1000 RPM
4	6 ml/min; 1000 RPM	10	10 ml/min; 1000 RPM
5	6 ml/min; 1000 RPM	11	5 ml/min; 0 RPM
6	6 ml/min; 1000 RPM	12	5 ml/min; 0 RPM

6. Fractionated samples were analysed by read A405 for both sample and supernatant (described in 2.5.1); and then fractionated samples were also

analysed by read A405 for both sample and supernatant again by re-suspending in H₂O. Then plot graph by fraction no. as horizontal axis and absorption value as vertical axis.

Results are shown in section 5.2.3.3.

5.2.3.3. Results

The results of the separation of unfixed and glutaraldehyde fixed sheep RBCs using step flow at 1000 RPM are shown in Figure 5.2.15.

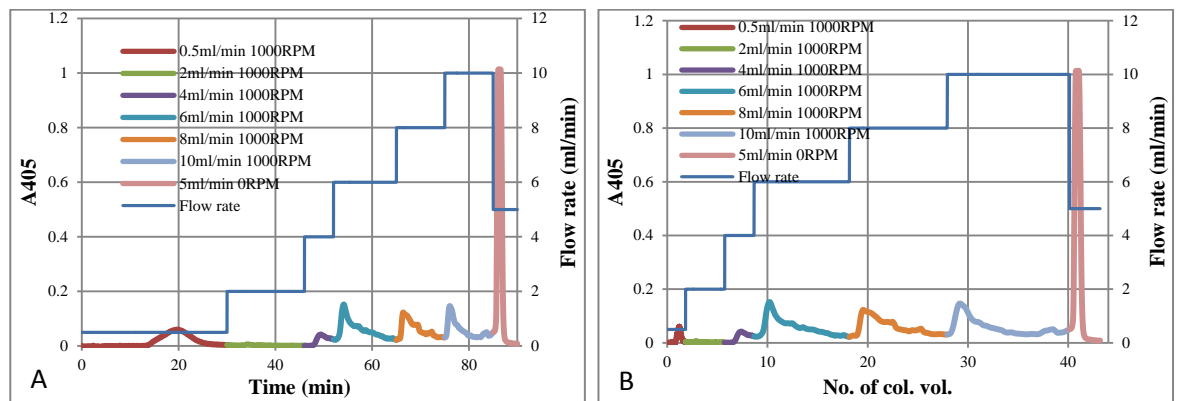


Figure 5.2.15. Elution of a mixture of unfixed and glutaraldehyde fixed sheep RBCs. A) Elution profile plotted against time. B) Elution profile against column volume. 0.73ml of a mixed RBC (mixing by 0.4 ml sheep blood sample and 0.4 ml glutaraldehyde fixed sheep RBC suspension in isotonic buffer) suspension in isotonic buffer were injected into CCC coil (Column A: 8.2 ml; 1 mm ID) at 1000 RPM and 0.5 ml/min. Eluent monitored at 405 nm. Flow rate was increased to 2 ml/min and then in steps of 2 ml/min to 10 ml/min all at 1000 RPM. The fractionated samples were collected from 2 ml/min elution per 5 mins as described in section 5.2.2.4.

The A405 results of fixed and unfixed sheep RBCs separation are shown in Figure 5.2.16.

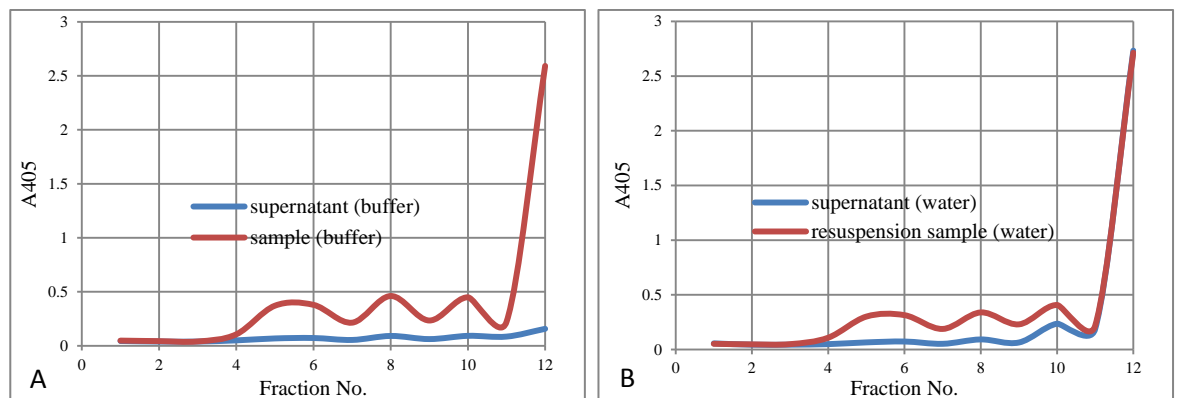


Figure 5.2.16. Comparison of A405 for original fractionated sample. A) Original fractionated samples in buffer. B) Fractionated samples of re-suspension in water. For results of original fractionated samples: the supernatant line shows no free Hb in fractions which makes no contribution to the A405 of the sample. For results of samples of re-suspension in water: the fraction 10, 11, 12 show increase compare to Figure 39.

Especially for fraction 11 and 12, which the supernatant value equals the sample value which means free Hb contributed to all the A405 value of the sample.

Figure 5.2.16 shows that the peaks eluted around fractions 5, 8, 10 and 12 gave absorbances that were reduced after centrifugation, indicating that cells were present. After re-suspending the cells in water and then sedimenting the cells, the supernatant (Figure 5.2.16.b) showed little absorbance for peaks at 5, and 8, indicating that these peaks glutaraldehyde fixed cell only. The absorbance of the supernatant of fraction no. 10 increased after centrifugation indicating a mixture of fixed and unfixed cells. The peak at fraction no.12 had a signal for the supernatant that equalled that of the eluted cells indicating that this contained unfixed cells only.

5.2.4. Fixed sheep and hen RBCs separation in step flow; problems of cell aggregation, reduced by Tween[®] 20

5.2.4.1. Introduction

Although fixation decreased the ability of both sheep and hen RBCs to be retained in the column, these fixed cells still showed different elution behaviours: fixed sheep RBCs eluted at 500 RPM at 1.5 ml/min whereas hen RBCs eluted at 2.5 ml/min (Figure 4.2.10 and Figure 4.2.13). A mixture of sheep and hen fixed RBCs gave another model system to examine cell separability in the Milli-CCC.

5.2.4.2. Method

Instrument set up: Milli-CCC[®] (described in 2.2.1.1) with column A (described in 2.2.1.2) rotating in clockwise direction; pumping from tail to head direction; 0.73 ml sample loop; column temperature as 15 °C.

1. The initial rotational speed was set at 500 RPM.
2. A mixture of glutaraldehyde fixed sheep and fixed hen RBCs sample (by mixing 0.4 ml fixed sheep RBCs and 0.4 ml hen RBCs prepared suspension in isotonic buffer. Sample contains 5.5E+08 fixed sheep RBCs and 3.5E+08 fixed hen RBCs) was pumped in to column via injection port by initial flow rate as 0.5 ml/min.
3. The flow rate of pumping isotonic buffer was changed as the table below:

Flow rate	Period of flow (time)
<i>Sedimentation mode at 500 RPM</i>	
0.5ml/min	30mins
<i>Elution mode at 500 RPM</i>	

1ml/min	15mins
1.5ml/min	15mins
2ml/min	15mins
2.5ml/min	15mins
3ml/min	15mins
<i>Elution mode at 0 RPM</i>	
5ml/min	15mins

4. Collect data by UV detector to plot graph by time or no. of column volume as horizontal axis and voltage as vertical axis, respectively.

Fractions were collected from 15th min by different flow rates for 15min per tube, therefore 7 fractions were collected.

The elution procedure repeated the procedure in 6.2.2.2.i with preparing and eluting a mixture of glutaraldehyde fixed sheep and hen RBCs suspension by isotonic buffer with 0.5% Tween[®] 20.

Results are shown in section 5.2.4.3.

5.2.4.3. Results

i. Elution of a mixture of glutaraldehyde fixed sheep and glutaraldehyde fixed hen RBCs in isotonic buffer using step flow.

The results of elution of a mixture of glutaraldehyde fixed sheep and glutaraldehyde fixed hen RBCs re-suspended in isotonic buffer using step flow are shown in Figure 5.2.17.

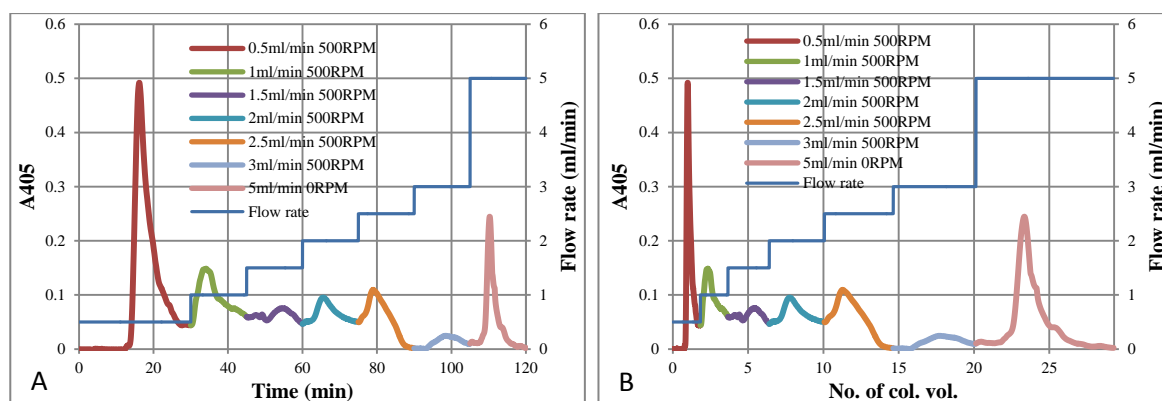


Figure 5.2.17. Elution of mixed glutaraldehyde fixed sheep and glutaraldehyde fixed hen. A) Elution profile plotted against time. B) Elution profile against column volume. 0.73 ml of a mixture of glutaraldehyde fixed sheep and hen RBC suspension (Sample contains 5.5×10^8 fixed sheep RBCs and 3.5×10^8 fixed hen RBCs) in isotonic buffer was injected into CCC coil (Column A: 8.2 ml; 1 mm ID) at 500 RPM and 0.5 ml/min. Eluent monitored at 405 nm. Flow rate was increased to 1 ml/min and then in steps of to 1.5, 2, 2.5 and 3 ml/min all at 500 RPM and 5 ml/min at 0 RPM.

A cell number analysis for fraction No.1 to No.6 by haemocytometer is shown in Figure 5.2.18.

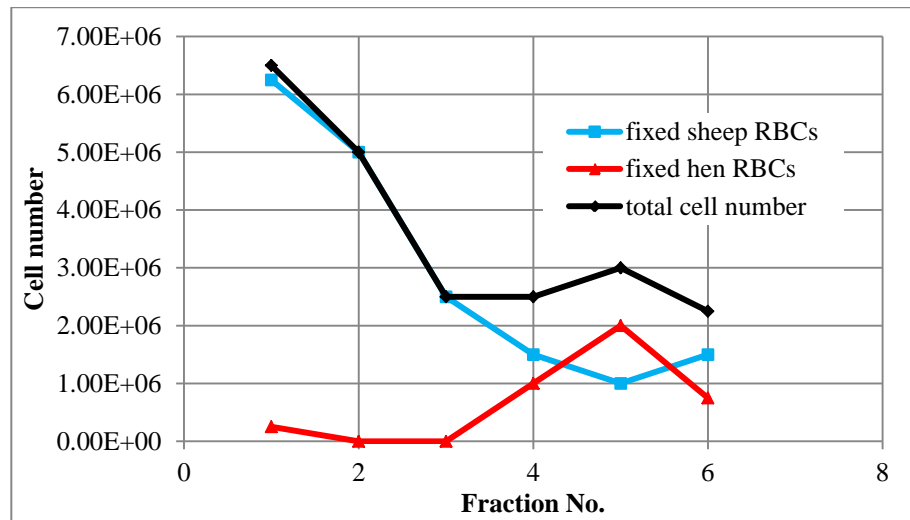


Figure 5.2.18. Cell number analysis for each fraction of eluting a mixture of glutaraldehyde fixed sheep and glutaraldehyde fixed hen RBCs in isotonic buffer. It shows a different eluting order as the fixed sheep RBCs eluted first, and then the fixed hen RBCs were eluted. However, the fixed sheep and hen RBCs aggregated together and these aggregations were eluted in Fraction No.7 which was not counted in this analysis. Fractions were collected from 15th min of the eluting for 15min per tube.

Figure 5.2.17 shows cells were eluted out of the column at each increased flow step up to ml/min and also that some cells, which had been retained in the column were eluted with the pump out condition of 5 ml/min at 0 RPM. However, the recovery from the step flow elution of both the fixed sheep and hen RBCs was low (around 50% for fixed sheep RBCs and around 20% for fixed hen RBCs) which suggests that a substantial number of were still retained in the column.

Examination of the fractions eluted, showed that the fixed sheep RBCs and fixed hen RBCs appeared to aggregated and not present as free cell. This is shown for fraction 7 (Figure 5.2.19) eluted in the pump out mode which contained both hen and sheep RBCs. The fixed hen RBCs were eluted as large aggregates with fixed sheep RBCs “stuck” to fixed hen RBCs or “trapped” in the fixed hen RBCs aggregates. The presence of both hen and sheep RBCs in this fraction, taken together with the profile shown in Figure 5.2.19 shows that:

- i) fixed sheep RBCs eluted in two places – early and in the pump out;
- ii) fixed hen RBCs eluted as a main peak, but containing sheep RBCs;
- iii) both cell types appeared in the pump out;
- iv) cell aggregation was extensive.

These flow conditions clearly did not separate the fixed cells and gave rise to concerns about aggregation and recovery.

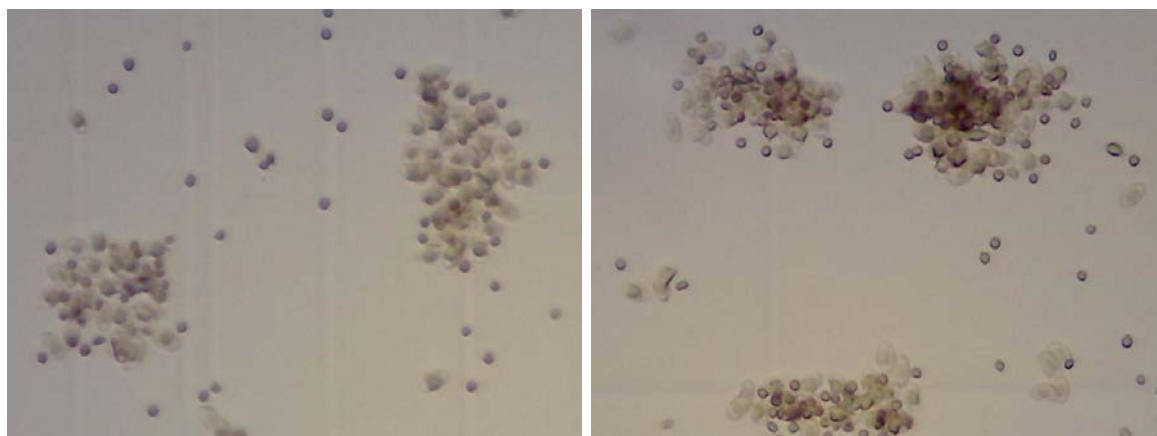


Figure 5.2.19. Light microscopy examine for fraction no.7 of elution a mixture of glutaraldehyde fixed hen and fixed sheep RBCs in step flow by isotonic buffer. (400X)

ii. Use of surfactant Tween[®] 20 to reduce aggregation and improve elution and separation of mixture of a mixture of glutaraldehyde fixed sheep hen RBCs with in step flow in isotonic buffer

Minimise the aggregation problem described in section 5.2.4.3.i Tween[®] 20 was added to the buffer. Other work in BIB at the time had found that Tween[®] 20 overcame aggregation of certain nanoparticle in CCC flow separations (Hagedoorn, 2013). The effect of adding Tween[®] 20 on the elution the fixed cell mixture is shown in Figure 5.2.20.

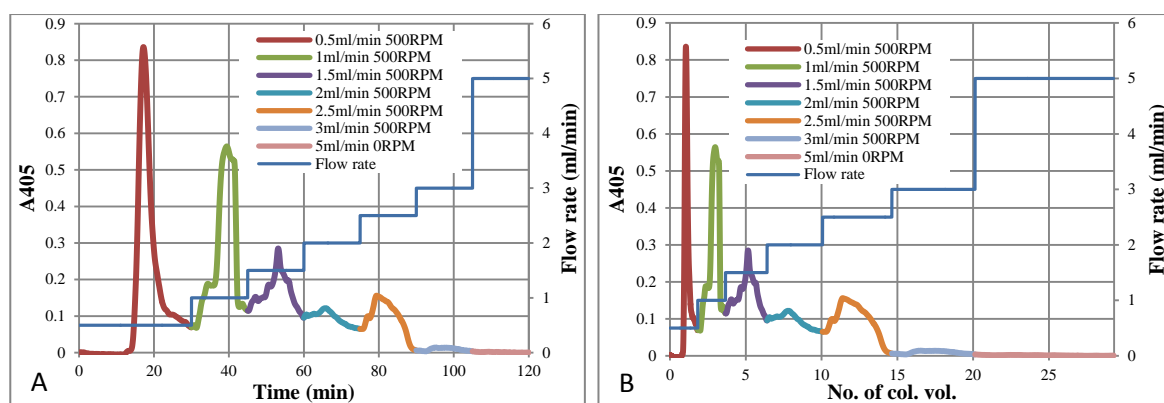


Figure 5.2.20. Elution of a mixture of glutaraldehyde fixed sheep and glutaraldehyde fixed hen RBCs by a step increased flow in isotonic buffer with 0.5% Tween[®] 20 with rotational speed at 500 RPM. A) Elution profile plotted against time. B) Elution profile against column volume. 0.73 ml of a mixture of glutaraldehyde fixed sheep and glutaraldehyde fixed hen RBC suspension (Sample contains 5.5E+08 fixed sheep RBCs and 3.5E+08 fixed hen RBCs) in isotonic buffer with 0.5% Tween[®] 20 was injected into CCC coil (Column A: 8.2 ml; 1 mm ID) at 500 RPM and 0.5 ml/min. Eluent monitored at 405 nm. Flow rate was increased to 1 ml/min and then in steps of to 1.5, 2, 2.5 and 3 ml/min all at 500 RPM and 5 ml/min at 0 RPM.

A cell number analysis for fractions No.1 to No.6 by haemocytometer is shown in Figure 5.2.21.

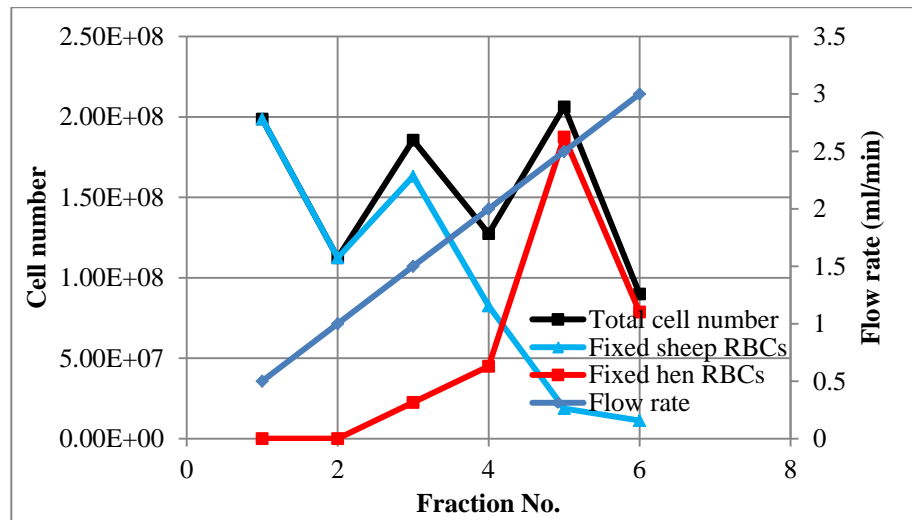


Figure 5.2.21. Cell number analysis for each fraction of eluting a mixture of glutaraldehyde fixed hen and glutaraldehyde fixed sheep RBCs in step flow by isotonic buffer with 0.5% Tween[®] 20 as the fixed sheep RBCs eluted first, and then the fixed hen RBCs were eluted later with a mixed period during 2 ml/min.

Figure 5.2.20 shows that all RBCs were eluted during the step flow since the “pump out” mode of 5 ml/min at 0 RPM showed no elution of cells. In addition it appears that the fixed sheep RBCs are easily eluted and fraction 1 and 2 were quite free of hen RBCs. Fixed hen RBCs eluted as a peak in Fraction 5. This order of elution fixed sheep RBCs before fixed hen RBCs: Although there is some overlap between the two peaks, there is a degree of separation elution order was similar to that obtained when the cells were run separately (Figure 4.2.10 and 4.2.13).

What is very clear is that the aggregation problems encountered with this cell mixture were strikingly overcome by the addition of Tween[®] 20.

5.3. Discussion

5.3.1. Rotation with flow gradient

As 0.5 ml/min (tail – head), 900 RPM (clockwise) is around the minimum flow rate for both sheep RBCs and hen RBCs, therefore the free Hb was always eluted in first peak and intact cells were retained in the column. Figure 5.2.1.a and Figure 5.2.1.b show the hen RBCs were eluted from 1.6 hr to 2 hr and sheep RBCs were eluted from 1.3 hr to 2.4 hr with a main elution peak at 2 hr. Therefore, the elution time for sheep RBCs was longer than hen RBCs but elution of hen RBCs was finished earlier than sheep RBCs. The main elution time of the hen RBCs was significantly different as hen RBCs was eluted quicker than most of the sheep RBCs. This gives an opportunity to separate mixed RBCs if hen RBCs and sheep RBCs can retain this behaviour in mixed hen/sheep RBCs sample as is suggested by Figure 5.2.1.c.

Although the elution of mixed hen/sheep RBCs sample kept the main features of hen and sheep RBCs elution separately- Figure 5.2.2 shows a UV signal with two partially resolved peaks around 1.9 hrs, the main problem with these conditions for separation were also still kept: the elution time of hen RBCs is actually in the middle of the elution time of sheep RBCs. This broad peak of sheep RBCs elution gives rise to some mixed fractions being recovered during the separation of the mixed hen/sheep RBCs sample. Since the location of the main peaks for hen and sheep RBCs elution were maintained in the mixed hen/sheep RBCs elution, it was considered that to method use a higher rotational speed, as a higher rotational speed makes a greater difference in eluting flow rate/eluting time between hen RBCs and sheep RBCs, thereby increasing the distance between hen and sheep elution peaks. However, the higher rotational speed results in a highly diluted fraction because it requires a higher elution flow rate. A higher rotational speed also requires an even longer time to increase the flow rate, again contributing to the final fractionated samples being highly diluted. Therefore, 900 RPM was chosen as a compromise choice of conditions between a relatively great difference of eluting flow rate/eluting time of hen/sheep RBCs, shorter operation time and higher fractionated samples concentration. Although flow gradient separation in 900 RPM only showed a partly separation, it successfully showed the fundamental different behaviour between those 2 populations of RBCs especially the different elution times under the general influence of factors (size, density, flexibility, etc.) and helped to design the cell separation between hen and sheep RBCs.

5.3.2. Rotation with step flow

The logical question after the flow gradient experiment was could one use one flow rate to and elute one cell population, and then another flow rate to elute the other cell population (since this operation will use a shorter time than using a flow gradient. Therefore step flow experiments were designed to find the appropriate flow rates to separate these cells: a lower flow rate to elute hen RBCs only, a flow rate increase elute sheep RBCs.

However the results show that the elution behaviour does not exactly follow this design. Although Figure 5.2.4 show hen RBCs were eluted within $50 \times$ column volumes under 9.2 ml/min, the same flow rate also eluted a few sheep RBCs but retained most of them in the column until after $50 \times$ column volumes a relatively higher flow rate of 17 ml/min was used to elute them as shown in Figure 5.2.5. Therefore, one important issue turns on the impact of the lower flow rate stage: not only one population of cell (hen RBCs) were eluted but part of the other population of cell (sheep RBCs). However, when we review the results of flow gradient, this problem does not only show in step flow but also in the flow gradient. As the elution peak of sheep RBCs is much broader than hen RBCs this also suggests that part of the sheep RBCs were easier to be eluted than hen RBCs. Thus, we should not to be surprised for the quicker eluted sheep RBCs as it is not a new problem but was also seen from flow gradient experiments. It also suggests the eluting behaviour of sheep RBCs is stable, repeatable and predictable, even when the operation condition has been changed.

Figure 5.2.7 shows the absorbance detection analysis result for the mixed blood sample eluted at 9.2 ml/min initially and then 17 ml/min, which is confirmed by the cell number analysis in Figure 5.2.8 showing that the eluting features of hen and sheep RBCs are retained in the mixture. Not surprisingly, the first 2 fractions were a mixture of hen and sheep RBCs at the lower flow rate, and then the remaining sheep RBCs were eluted after the flow rate condition was changed.

Microscopic examination of the retained sheep RBCs and the quicker eluted sheep RBCs confirmed that there was not difference in size. In order to answer the question of why were sheep RBCs were both easier to be eluted and be retained than hen RBCs, attention has been given to the related technique of field flow fractionation (FFF). In FFF there are 2 main types of elution orders: normal mode and steric/hyperlayer mode. The normal mode elutes macromolecules and submicrometer particles, and the feature of it is the lower the molar mass or size of the sample component, the shorter is the time required by the component to exit the channel because of the greater component cloud elevation and the deeper cloud penetration into the faster streamline. The steric/hyperlayer mode is for

micron-sized particles, the larger particles are eluted faster than smaller particles (Reschiglian et al., 2005). As a factor, the size of hen RBCs and sheep RBCs influences the elution order. Therefore, if the elution of sheep RBCs is similar to the normal mode of FFF, then the sheep RBCs should be eluted quicker than hen RBCs, but if the elution of sheep RBCs is similar to the steric/hyperlayer mode of FFF, the hen RBCs should be eluted quicker than sheep RBCs. The results obtained in the Milli[®] CCC column shows that the mixed fractions behave neither as the pure normal mode nor the steric/hyperlayer mode but rather show a mixed mode behaviour as the elution order was part of sheep is as fast as or even faster than whole hen RBCs which is faster than the retained sheep RBCs. As there was no obviously difference between the quicker eluted sheep RBCs and retained sheep RBCs.

Since in FFF, size influences the mode of elution, one possibility is the size of sheep RBCs is in the middle of normal and steric modes, and makes the behaviour split into both easier to eluted and retained. If we examine the facts more, we will find size does influence the elution order but not the eventual determinant of the elution order, such as flexibility and aggregation which is discussed in chapter 4.

The other issue in Figure 5.2.6 is the signal of hen RBCs is much lower than sheep RBCs. This is due to the cell number of hen RBCs being lower than the cell number of sheep RBCs in the same volume. Since in the separated experiment, the sample loop was 0.32 ml and the blood sample was collected from original blood, therefore, the naturally lower cell number makes lower signal. In mixed hen/sheep RBCs, to makes sure the cell number of hen and sheep RBCs were equivalent, the volume was not the same when the two types of blood were mixed.

However, although the step flow operation was still not successful completely separated hen/sheep RBCs, the step flow result still gave a better separation ratio of hen RBCs in sheep RBCs than the flow gradient approach. Some fractions are still mixed since hen RBCs were eluted with some sheep RBCs in the beginning of 9.2 ml/min. But the operation time was decreased to 1.25 hours which half the time required for the flow gradient method.

Additionally step flow leads to a discussion of how do cells / particles move in the column? Due to the elution mode as 2 steps, it might suggest 2 cell movement possibilities. I call the first possibility “buffet mode”, and the other “competition mode”. In buffet mode, due to all cells sedimenting in the column in the beginning of the elution, once a flow rate was set

up, it elutes what it can elute but leave the rest where they are, just as in buffet, people pick up what they like and move on. The evidence for this possibility comes from the behaviour of sheep RBCs, as not all of sheep RBCs were eluted in the beginning but some sheep RBCs were retained in the column at lower flow rate (first person to pick up) until a high flow rate was set (the other person to pick up). Before the flow rate changes, it looks like nothing happens to the retained sheep RBCs, as the lower flow rate only elutes what it can elute but leaves others still retained. In the competition mode, cells/particles do not stop moving. The forces balance is the key to elution in my hypothesis, therefore, as long as the force is not balanced. Because the eluting force is greater than the retaining force, cells are moving to the outlet and they will be eluted out of the column sooner or later. This is just like runners in a competition, even though they are slow, they will in time reach the end point.

To test which possibility is the correct one, the elution flow rate was decreased to 8 ml/min. At this flow rate, although hen RBCs cannot be eluted immediately, based on the hypothesis, there is one point hen RBCs will start to be eluted no matter how long it takes. Also, due to the part of sheep RBCs being eluted before hen RBCs, if the decreased flow rate retains hen RBCs a little and then elutes them, there is a chance to elute those quicker sheep RBCs before the elution of hen RBCs. This would avoid any mixture of cells in the fractions

5.3.3. Cell separation in improved step flow

As the elution mode appears to be neither normal mode nor steric/hyperlayer mode, but rather a mixed mode, as some sheep RBCs were easier to be eluted, the operation was improved as described in 5.2.2.1 based on the hypothesis. This approach was not to improve the separation but also to provide support for the hypothesis.

Figure 5.2.9 shows that although the first half of the elution is actually eluting nothing, the hen RBCs starts its elution in the middle and is completed within the remaining elution time. So what happened in the column is not like what is observed at outlet: the outlet shows “buffet” behaviour whereas behaviour shows “competition” behaviour. Both hen RBCs and sheep RBCs start to move when eluting force and retaining force are not balanced. During the movement, the different speeds of movement (behaviour) shows up as the hen RBCs move faster than most of sheep RBCs in the “competition” behaviour. Therefore, 8 ml/min was chosen as the elution flow rate to elute hen RBCs, even though compared to 9.2 ml/min (the flow rate which is can elute hen RBCs “immediately”), 8

ml/min elution is “wasting” time. Based on the hypothesis, hen RBCs are on their way to the outlet during the first half of elution time. As the result shows, hen RBCs and sheep RBCs moved to the outlet after 8 ml/min. But generally, hen RBCs moved faster than sheep RBCs while some sheep RBCs moved even faster than hen RBCs. These faster sheep RBCs (maybe more aggregated) were eluted in the beginning of 8 ml/min when the hen RBCs were still creeping in the column. After 23 times of column volume elution, they were arrived at the outlet and were elute.

Compared to later eluted hen RBCs, the quicker eluted sheep RBCs keep their behaviour as they are still be eluted at the beginning of the 8 ml/min elution (with a decreased cell number if compare between Figure 5.2.7 and Figure 5.2.10). Therefore, the improved operation did retain hen RBCs and left sufficient time for the quicker sheep RBCs to be eluted in order to avoid mixed elutions.

Microscopic analysis of the eluted fractions showed 4 peaks (Figure 5.2.12). The first peak includes free Hb only but as this peak is being eluted both hen and sheep RBCs are retained in the column and start to move to outlet. The second peak is the peak of those quickly eluted sheep RBCs - since they are faster than all other cells, they are eluted in the beginning of 8 ml/min while hen RBCs was still moving to the outlet. The third peak is the hen RBCs - as they finally finished the long journey and are eluted out of column while the remaining sheep RBCs are retained. The fourth peak was the retained sheep RBCs peak - as they did not finish the competition to reach the outlet within the operational time, and were pumped out.

The other improved operation explored was an initial condition of 0.5 ml/min at 1000 RPM only applied for 1 time of column volume rather than 2 columns volumes as used before, then increased to 2 ml/min. It is because 0.5 ml/min is slow that one column volume can be used as after the first column volume, the cell sedimentation has been achieved and cells are ready for the competition generated by increasing flow rate. But a longer time was taken to increase the flow rate increasing as this helps to reduce the number of quicker sheep RBCs elution under lower elution flow.

All in all, the result shows the elution order of mixed hen/sheep RBCs was:

quicker eluted sheep RBCs < hen RBCs < remaining sheep RBCs.

Therefore, the problem of sheep RBCs being both easier to be eluted and be retained was fully used to slow the elution time of hen RBCs to improve the separation. The

disadvantage of mixed elution was turned into advantage, making the more controlled and giving all cells enough time to be eluted with around 1 hour with good separated ratio of hen and sheep RBCs in the fractions.

5.3.4. Loading capacity test

The loading capacity of this separation method was examined after the successful separation mode was established. The separation behaviour of improved step flow operation found to be repeatable up 50% of the column volume of blood (the highest load examined) with a load of over $4.8E+09$ cells injected into the column. Interestingly, the FFF method discussed in developing the hypothesis described above, works only with very low loads of cells.

One interesting thing is that the more sheep cells that were injected, the more sheep cells were easier to be eluted before hen RBCs. A suggestion for this phenomenon is that with the more sheep cells loaded, it is the easier for them to aggregate and to form “cell cloud” as in FFF. “Cell cloud” is closer to the main flow and also provides a much greater effective elution size than any individual hen RBCs. So, logically, the sheep RBCs in “cloud” should be eluted faster than hen RBCs. Therefore, again, it suggests this separation method is not based on size of cells or density of cells only (for example, loading cell number here). In fact, the final behaviour of one type of cell is a consequence of the influences of number of factors, so that not only one of them can determine the elution order.

5.3.5. Discussion of separation of unfixed and fixed sheep RBCs

From Figure 4.2.5, in Milli-CCC[®], fixed sheep RBCs have markedly different performance compared to unfixed sheep RBCs: the fixed RBCs can be totally eluted while retaining most of unfixed sheep RBCs in the column. Therefore, a mixed fixed/unfixed sheep RBCs sample was injected at the same operation conditions to test whether the fixed sheep RBCs can be separated from the unfixed sheep RBCs. To be able to distinguish between fixed and unfixed cells, advantage was taken of the fact that fixed RBCs can be re-suspended in water with no haemolysis whereas unfixed RBCs will lyse and release free Hb.

The optical density analysis at 405 nm also showed an interesting result. When the supernatant value matches the sample value, it means the sample has free Hb only, and no cells. Figure 5.2.16.a, shows clearly that the supernatant value kept around 0, which means these fraction include intact cells only, however, the Figure 5.2.16.b showed after the

fractions No.10, 11 and 12 showed an increased supernatant value, which means these samples included intact unfixed sheep RBCs. Therefore, Figure 5.2.16 confirmed that the fixed and unfixed sheep RBCs can be separated by this method, and also shows the fixed and unfixed sheep RBCs also keep the same behaviour when they were mixed as they did when run separately

5.3.6. Discussion of separation of fixed sheep RBCs and fixed hen RBCs

Tween[®] 20 is a polysorbate surfactant, and this had been used in latex particle separation to avoid aggregation by Milli-CCC[®] in Brunel Institute for Bioengineering (Hagedoorn, 2013).

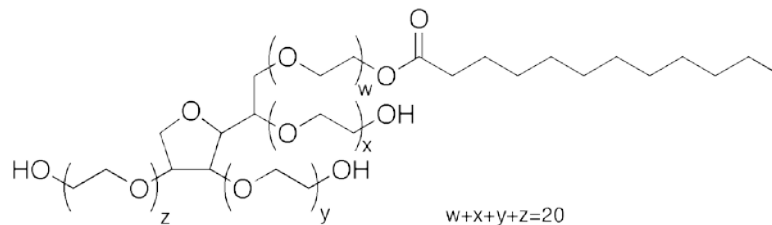


Figure 5.3.1. Structure of Tween[®] 20.

Tween[®] 20 associate hydrophobically with the cell by the long hydrophobic “tails” inserting into the lipid bilayer. Therefore, the distance between cells was increased, and a more hydrophilic surface on the RBCs developed. When a mixture of fixed sheep RBCs and fixed hen RBCs were examined (Figure 5.2.18) the aggregation of both fixed hen RBCs and fixed sheep RBCs formed during elution. The phenomenon of aggregation of fixed hen RBCs also occurred when eluting them at 1000 RPM in Chapter 4. In Chapter 4, fixed hen RBCs aggregation disappeared when the rotational speed was decreased to 500 RPM. However, even when this lower rotational speed was used with the mixture of fixed RBCs aggregation still occurred, which suggests that the fixed sheep RBCs help the aggregation. But not all of the fixed sheep RBCs were in the aggregates. Fraction No.1 to fraction No.6 in Figure 5.2.18, show some fixed sheep RBCs kept eluting out of column.

It is hard to tell whether the fixed sheep took part in the aggregation or were trapped in the aggregation that occurred by fixed hen RBCs. But because such aggregation was not observed when fixed hen RBCs were run on their own, the role of fixed sheep RBCs in this aggregation must be important. If we consider the relative sizes of fixed hen RBCs and fixed sheep RBCs, the aggregation might happen due to the fixed sheep RBCs filling the gap between each fixed hen RBCs so as to “glue” the fixed hen RBCs together. However,

in the case of unfixed cells both sheep RBCs and hen RBCs have flexibility and the gap between cell to cell may not so easily to glue as they may deform to disperse or hinder the potential aggregation.

On the other hand the fixed sheep RBCs showed in all fractions, which also suggests they were trapped in the aggregates. Therefore, maybe the “glue” pattern and “trap” pattern occurred in the same time as not so many fixed sheep RBCs were required to form the aggregates but after the aggregation occurred, some of the spare fixed sheep RBCs were then trapped in them. The trapped fixed sheep RBCs might be the reason why, except for those fixed sheep RBCs “glued” with fixed hen RBCs, not all the remaining fixed sheep RBCs behave as when they were eluted separately.

These complications caused by aggregation were, however, not difficult to remove. By adding Tween[®] 20 to the medium aggregation was hindered the recovery was normal. The change in the cell surface polarity provided by the Tween[®] 20 improved the separation of fixed sheep RBCs and fixed hen RBCs Using a detergent might not be appropriate with unfixed cells, if there was a need to overcome an aggregation problem, as the detergent might cause lysis. However, these model studies on the aggregation problems encountered with fixed cells do give insight into the need to select operating conditions that minimise aggregation.

5.4. Conclusion

In this chapter, the effects of operational condition on the elution behaviour of RBCs were investigated to design conditions to separate a model mixture of sheep and hen RBCs. One would expect that that hen RBCs with their greater size would be eluted quicker than the smaller sized sheep RBCs. However an unexpected result was obtained: some of sheep RBCs were eluted faster than hen RBCs, and the remainder were eluted later. Therefore, the mixture was only partially separated.

By understanding the features of how sheep RBCs were both easier to be eluted and to be retained, a more controlled operation was established to separate mixed hen RBCs and sheep RBCs. However, this problem of early eluting sheep RBCs still persisted. It should be noted that this was overcome when columns of altered geometry were used (Chapter 6).

Loading capacity test confirmed the established method provided a good stability on separation results when mixed blood injection volume was increased from 4% of the column volume 50% of the column volume.

Fixed sheep RBCs and unfixed sheep RBCs were separated based on their different behaviour. Although problems of cell aggregation were encountered that hindered efficient separations, these were overcome by adding a surfactant to the medium hinder aggregation.

Chapter 6. Behaviour of RBCs elution in different tube shape

6.1. Summary

The effects of operational condition and cell properties on the behaviour of RBCs in fluctuating g-field have been described from Chapter 3 to Chapter 5. During these studies beneficial effects for the fractionation of latex particles (1 - 3 μm) using different tube geometries in Brunel CCCs were found in our research group (Hagedoorn, 2013) based on an earlier report by Degenhardt et al (2001). This prompted the study described in this chapter, in which the influence of the geometry of the CCC column, the tube shape, on the behaviour of RBCs in both the sedimentation process and the elution process is describe This study include the use of rectangular coils which have had little attention compared with circular coils.

The behaviour of RBCs was compared between circular columns with different inner diameters (columns A and B), and rectangular columns (C and D) with the same cross sectional area, and with different orientations of the tube geometry. To study the sedimentation behaviour, the relationship between different ID circular column and minimum flow rate and the relationship between circular and rectangular columns and minimum flow rate were investigated. The influences of the directions of pumping and coil rotation on the behaviours of RBCs in circular and rectangular column are also described.

RBCs of different species showed different elution times when subjected to a flow gradient, but these did not depend on cell density or size. This different behaviour of RBCs in rectangular columns led to successful flow cell separations of a mixture of sheep and hen RBCs was obtained without any of the difficulties of the early eluting sheep RBCs encountered with the circular coil, discussed in Chapter 5. In addition a mixture of rabbit and hen RBCs was readily separated in the rectangular coil. The benefits of the selections of rectangular coils for cell separations are discussed.

6.2. Experimental

The columns used in this chapter are described in section 2.2.1.2. Table 2.2.1 is presented here again for ease of comparison. The rectangular coils C and D differed in the orientation of the rectangle as shown in Figure 2.2.1b and c: the rectangle in coil C lay “flat” whereas the rectangle in coil D was “upright”. These terms will be used to distinguish coils C and D.

Table 7.2.1. Parameters of the CCC columns compared in this chapter (same as Table 2.2.1).

Column	Shape	Size (mm)	Total volume of column (ml)	Length of column (m)	R (mm)	r (mm)	Beta
A	circular	1.0	8.2	11.05	50	34.25-39	0.685-0.78
B	circular	1.6	20.4	10.16	50	28.1-37.7	0.56-0.75
C	Rectangular "flat"	2.5 × 0.8	25.8	12.91	50	25.0-37.0	0.5-0.74
D	Rectangular "upright"	0.8 × 2.5	29.2	14.61	50	25.2-37.2	0.5-0.74

6.2.1. Sedimentation behaviour of RBCs in different CCC columns

6.2.1.1. Sedimentation behaviour of RBCs in 1.6 mm ID circular column B

6.2.1.1a. Introduction

The minimum flow rates required by sheep RBCs in the 1.6 mm ID circular column B at different flow rates was determined to provide a comparison with column A (ID 1.0mm) previously described, using the method described in section 3.2.7.

6.2.1.1b. Method

Instrument set up: Milli-CCC[®] (described in 2.2.1.1) with column B (described in 2.2.1.2) rotating in clockwise direction; pumping from tail to head direction; 0.32 ml sample loop; column temperature as 15 °C. Results are shown in section 7.2.1.1b.

6.2.1.1c. Results

As defined in Chapter 3, the minimum operational condition is the initial condition under which only free Hb elutes in Peak A, while all intact RBCs are sedimented in the column. The results for column B are shown in Table 6.2.1, compared with the values obtained in Chapter 3 for column A.

Table 6.2.1. A comparison of minimum flow rate for sheep RBCs at different rotational speed using column A (ID 1.0mm) and column B (ID 1.6mm)

rotational speed (RPM)	500	600	700	800	900	1000
max g-level*	60.9	87.8	119.4	156	197.5	243.8
mean g-level*	47	67.6	92.1	120.2	152.2	187.9
min g-level*	33	47.5	64.7	84.4	106.9	131.9
minimum flow (column A) (ml/min) [#]	0.11	0.16	0.22	0.3	0.36	0.45
minimum flow (column B) (ml/min)	0.29	0.43	0.56	0.75	0.96	1.12
Linear flow (column A) (cm/s) [#]	0.23	0.34	0.47	0.64	0.76	0.95
Linear flow (column B) (cm/s)	0.24	0.36	0.46	0.62	0.80	0.93

* Calculated as described by van den Heuvel and König (2011)

[#] Data: the minimum flow rate of sheep RBCs for column A (1 mm ID circular column) was taken from Table 3.2.2.

As shown in table 6.2.1, minimum flow rate for sheep RBCs in column B was greater than that in column A, which suggests sheep RBCs were easier to sediment in the greater ID circular column. Although the minimum flow rates were different, when these are converted into linear minimum flow rate, these were the same for the two columns. This indicates that it is the linear flow rate that is the important parameter determining the sedimentation of cells in the coil.

6.2.1.2. Influence of flow direction and coil rotation on the sedimentation behaviour of RBCs in circular column B and rectangular columns (C and D)

6.2.1.2a. Introduction

The relationship of pumping direction and rotational direction in circular column A has been described in section 3.2.2. RBCs were retained in the column when the pumping direction was against the rotational direction; RBCs were eluted when the pumping direction followed the rotational direction. In extending the study from circular to rectangular columns it was first necessary to establish if the pumping direction had a similar or different effect for rectangular coils compared to circular coils. The experiment described in section 3.2.2 was repeated using greater ID circular column (B) and the rectangular columns (C and D).

6.2.1.2b. Method

Instrument set up: Milli-CCC[®] (described in 2.2.1.1) with column B, C and D (described in 2.2.1.2); 0.32 ml sample loop; column temperature as 15 °C.

1. Column of CCC instrument was filled with isotonic buffer.
2. The column in the CCC instrument rotated in either clockwise direction or counter-clockwise direction at an initial rotational speed as 1000 RPM.
3. Sheep blood was injected through the sample injection port into the coil under an initial flow rate as 1 ml/min in either the tail to head direction or head to tail direction.
4. Isotonic buffer was pumped for $2 \times$ column volumes through the coil and the eluting components were collected in fractions as 2 ml/tube.
5. Eluted Peak A fractions were analysed in a plate reader at 405 nm before and after centrifugation (as described in 2.5.1).

This experiment was repeated using column B, C and D (described in 2.2.1.2), pumping from either tail to head (rotated in clockwise direction) or head to tail (rotated in counter-clockwise direction). Results are shown in section 6.1.1.2c.

6.2.1.2c. Results

i. Sedimentation behaviour of sheep RBCs in circular column B (ID 1.6mm)

Figure 6.2.1 shows that absorbance readings for fraction obtained for sheep RBCs in Peak A before and after centrifugation. Circular column B with ID 1.6mm was used with a flow rate of 1 ml/min (tail to head) at 1000 RPM rotating the coil clockwise.

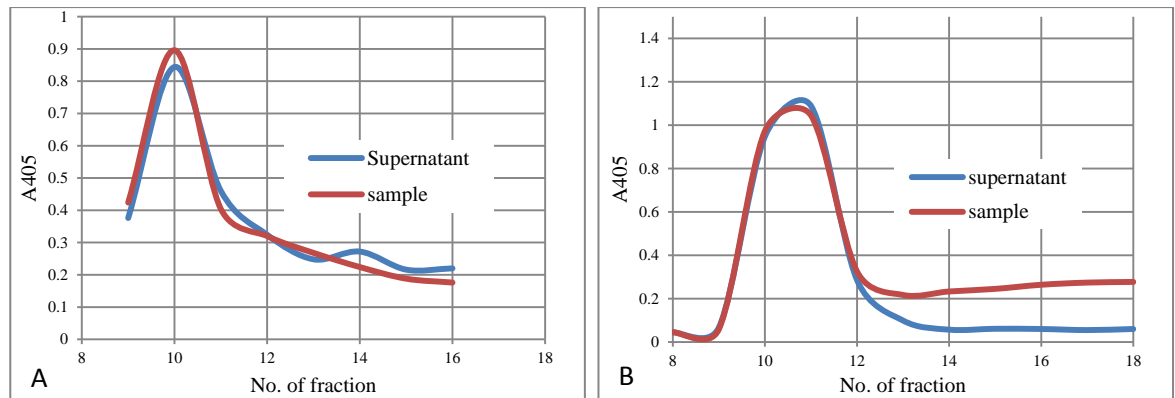


Figure 6.2.1. Absorbance (A₄₀₅) of fractions PEAK A eluting sheep blood sample in 1.6 mm ID circular column B. A) At 1ml/min (tail to head), 1000 RPM (clockwise); B) At 1ml/min (head to tail), 1000 RPM (counter-clockwise). In condition A all cells can be retained in the column while pumping from tail to head as the A₄₀₅ of supernatant equalled A₄₀₅ of sample after the free Hb elution (such as fraction No.15). In condition B cells kept eluting in the column as the A₄₀₅ of supernatant was lower after free Hb elution (fractions No.13-18).

Compared to Figure 3.2.3, (Column A: 1 mm ID circular column) the sedimentation behaviour of sheep RBCs in column B (1.6 mm ID circular column) as shown in Figure 6.2.1 is similar showing that pumping from tail to head retained RBCs in the column and pumping from head to tail eluted RBCs. Therefore, the change of inner diameter did not affect the influence of operational conditions on the sedimentation behaviour of sheep RBCs.

ii. Sedimentation behaviour of sheep RBCs in rectangular columns C and D

The result of A₄₀₅ for eluting sheep blood sample in the rectangular column (column C) at 1 ml/min (tail to head), 1000 RPM (clockwise) is shown in Figure 6.2.2.

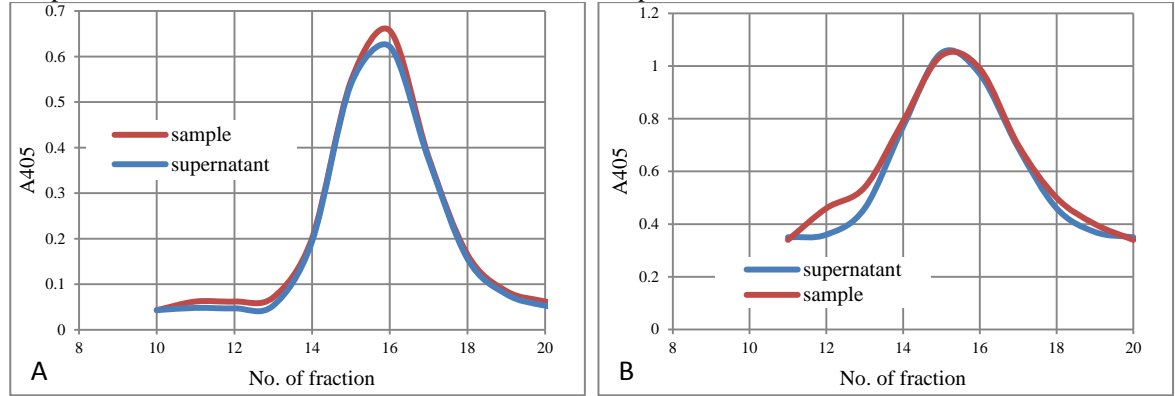


Figure 6.2.2. A405 of Peak A for eluting sheep blood sample by rectangular column C (2.5 mm × 0.8 mm). A) At 1 ml/min (tail to head), 1000 RPM (clockwise); B) 1 ml/min (head to tail), 1000 RPM (counter-clockwise) which shows both 2 pumping directions can retain sheep RBCs in the column as the A405 of supernatant = A405 of sample (such as fraction No.20) after the free Hb elution.

The result of A405 for eluting sheep blood sample in the rectangular column (column D) at 1 ml/min (tail to head), 1000 RPM (clockwise) is shown in Figure 6.2.3.

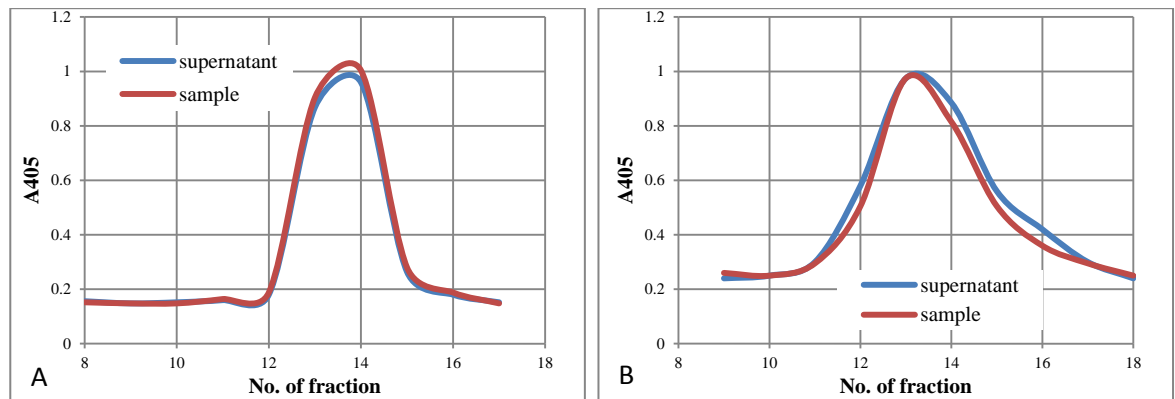


Figure 6.2.3. A405 of Peak A for eluting sheep blood sample by rectangular column D (0.8 mm × 2.5 mm). A) At 1 ml/min (tail to head), 1000 RPM (clockwise); B) 1 ml/min (head to tail), 1000 RPM (counter-clockwise) which shows both 2 pumping directions can retain sheep RBCs in the column as the A405 of supernatant = A405 of sample (such as fraction No.17) after the free Hb elution.

By comparing Figure 6.2.1 to Figure 6.2.3, Figure 6.2.1 shows the 1.6 mm ID circular column generates same behaviour of cells as 1 mm ID circular column which the cells are retained in the column while the pumping direction is against the rotational direction (cells should be injected from tail to head). However, from Figure 6.2.2 and Figure 6.2.3, the results show rectangular columns do not follow this behaviour: cells were retained for both pumping directions, both against and following the rotational direction. Therefore, obviously the circular columns retain cells less easily as rectangular columns do. This shows an important advantage of rectangular columns.

6.2.2. Elution behaviour of RBCs in 1.6 mm ID circular column

Flow cell separation in column A (1 mm ID) was described in section 5.2.2. In this section cell separation was examined in column B with 1.6 mm ID to determine if there was any influence on the separation of changing the ID.

6.2.2.1. Introduction

In order to investigate whether the relationship between elution conditions and different ID circular columns was related to the sectional area difference, the linear flow rate was kept the same: eluting in column B at 2.56 times the flow rates used with column A as the cross sectional area for column B was 2.56 times of cross sectional area for column A. The procedure used is detailed below:

6.2.2.2. Method

Instrument set up: Milli-CCC[®] (described in 2.2.1.1) with column B (described in 2.2.1.2) rotating in clockwise direction; pumping from tail to head direction; 0.32 ml sample loop; column temperature as 15 °C.

1. The initial rotational speed was set to 1000 RPM.
2. Mixed blood sample (sample included: around 7.5E+08 hen RBCs and 8.5E+08 sheep RBCs) was pumped in to column via injection port by initial flow rate as 1.3 ml/min.
3. The flow rate of pumping isotonic buffer was changed as the table below:

Flow rate	Period of flow (column volumes)
<i>Sedimentation mode at 1000 RPM</i>	
1.3 ml/min	1 column volume
<i>Elution mode at 1000 RPM</i>	
5.1 ml/min	1 column volume
10.2 ml/min	1.5 column volume
15.4 ml/min	1.5 column volume
20.5 ml/min	50 column volume
<i>Elution mode of retained RBCs at 0 RPM</i>	
5 ml/min	-

4. Collect data by UV detector to plot graph by time or no. of column volume as horizontal axis and voltage as vertical axis, respectively.
5. The eluted cells in 5 ml/min at 0 RPM was collected and examined by biological microscope.

6.2.2.3. Results

In section 4.2.2, a cell separation of sheep and hen RBCs using step flow in column A. Section 6.2.1.1 showed that the minimum flow conditions for columns A and B were the same when calculated as linear flow rates. Therefore, the objective of this section is to investigate how the elution flow rate in column B is related to the elution flow rate in column A: are they the same when corrected to linear flow rate?

The result of elution behaviour of mixed sheep and RBCs in step flow in column B with the same linear flow rate as the separation condition used in section 5.2.2 is shown in Figure 6.2.4.

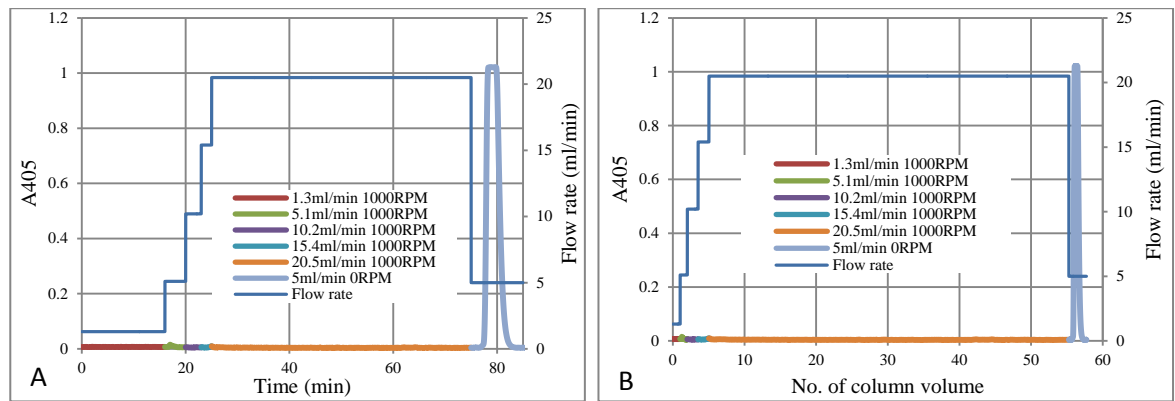


Figure 6.2.4. Elution of mixed hen/sheep blood sample by a linear increased step flow. A) Elution profile plotted against time. B) Elution profile plotted against column volume. 0.73 ml of mixed hen/sheep blood sample (sample included: $7.5E+08$ hen RBCs and $8.5E+08$ sheep RBCs) was injected into CCC coil (Column B: 20.4 ml; 1.6 mm ID) at 1000 RPM at 1.3 ml/min. Eluent monitored at 405 nm. Flow rate was increased to 5.1 ml/min (for 1 column volume) and then in steps of 10.2 (for 1.5 column volumes), 15.4 (for 1.5 column volumes), and 20.5 ml/min for 50 times column volume. Retained RBCs were eluted at 5 ml/min at 0 RPM.

Figure 6.2.4 shows no cells were eluted during the step elution process. The fraction eluted at 0 RPM and 5 ml/min is shown in Figure 6.2.5, which shows the RBCs were still mixed. However, since the linear flow rate used for column B was the same as the linear flow rate that eluted cells in column A with cell separation (section 4.2.2) it is clear that, Figure 6.2.4 indicates that the relationship between the effects of different column inner diameter and elution conditions is not the same as for the minimum flow rate for the sedimentation process. The same linear flows in columns A and B did not produce the same elution effects.

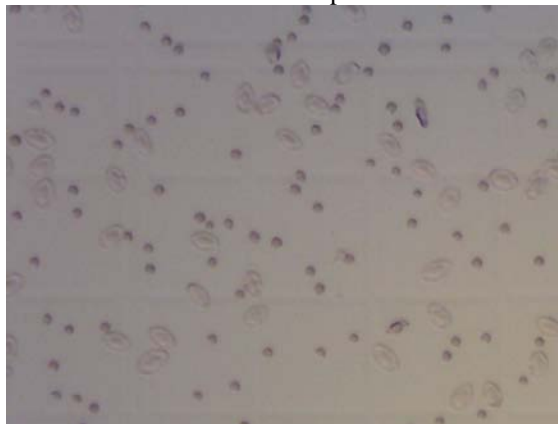


Figure 6.2.5. The fraction eluted from column B in Figure 6.2.4 using 5 ml/min at 0 RPM shows that the hen and sheep RBCs were still mixed. (100X).

6.2.3. Elution behaviour of RBCs in rectangular columns (Columns C and D)

After the investigation of flow cell separation in column B, the elution behaviour of RBCs in the 2 rectangular columns: column C and D with different rectangular directions (“flat” and “upright” respectively) were investigated. Because RBCs showed good retention behaviour in these rectangular column even when pumping from head to tail, cell separation under both pumping directions was examined.

6.2.3.1. Elution behaviour of RBCs by pumping from tail to head in rectangular columns C and D

6.2.3.1a. Introduction

The elution times for sheep and hen RBCs in rectangular columns C and D were determined using a flow gradient.

6.2.3.1b. Method

Instrument set up: Milli-CCC[®] (described in 2.2.1.1) with column C or D (described in 2.2.1.2) rotating in clockwise direction; pumping from tail to head direction; 0.32 ml sample loop; column temperature as 15 °C.

1. The initial rotational speed was set to 500 RPM
2. Blood sample was pumped in to column via injection port by initial flow rate as 0.5 ml/min.

3. After isotonic buffer had been pumped for 1.5 column volumes, the flow rate was increased in steps of 0.5 ml/min every 5 mins until all RBCs were eluted out of column.
4. Collect data by UV detector to plot graph by time or no. of column volume as horizontal axis and voltage as vertical axis, respectively.

Results are shown in section 6.2.3.1c.

6.2.3.1c. Results

i. Results of elution behaviour of RBCs in column, using a flow gradient pumped from tail to head are shown in Figure 6.2.6.

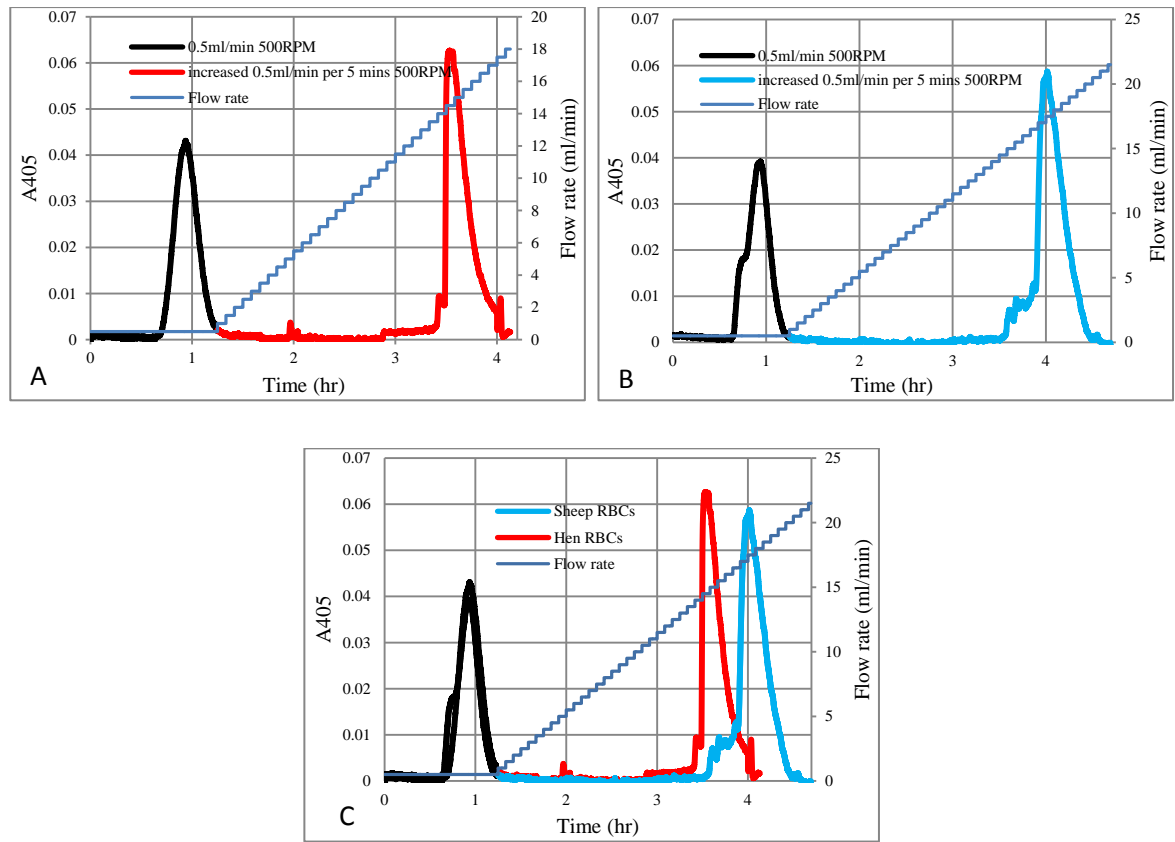


Figure 6.2.6. Elution of blood sample in column C using a flow gradient. A) Hen blood sample. B) Sheep blood sample. C) Comparison of hen and sheep RBCs behaviours. 0.32 ml of hen/sheep blood sample was injected into CCC coil (Column C: 25.8 ml; 2.5 mm × 0.8 mm) at 500 RPM at 0.5 ml/min, pumping from tail to head. Eluent monitored at 405 nm. After isotonic buffer had been pumped for 1.5 column volumes the flow rate was increased in steps of 0.5 ml/min every 5 mins.

All hen RBCs were eluted before 4 hours when the flow gradient had reached 14.5 ml/min with completion by 17.5 ml/min) with the highest point of peak shown at 15 ml/min (Figure 7.2.15.a). Compared to it, all sheep RBCs were eluted later, with a peak at 4hr the flow rate had reached 15 ml/min, being completed by 20.5 ml/min) with the elution at 18

Chapter 6. Behaviour of RBCs elution in different tube shape ml/min (Figure 6.2.6.b). Therefore, hen RBCs were more easily eluted by the flow gradient than sheep RBCs in this column. This elution time difference suggests a possible separation (Figure 6.2.6.c) if hen and sheep RBCs keep the same performance when they are mixed.

ii. Results of elution behaviour of RBCs in flow gradient by column D when pumping from tail to head

The results are shown in Figure 6.2.7.

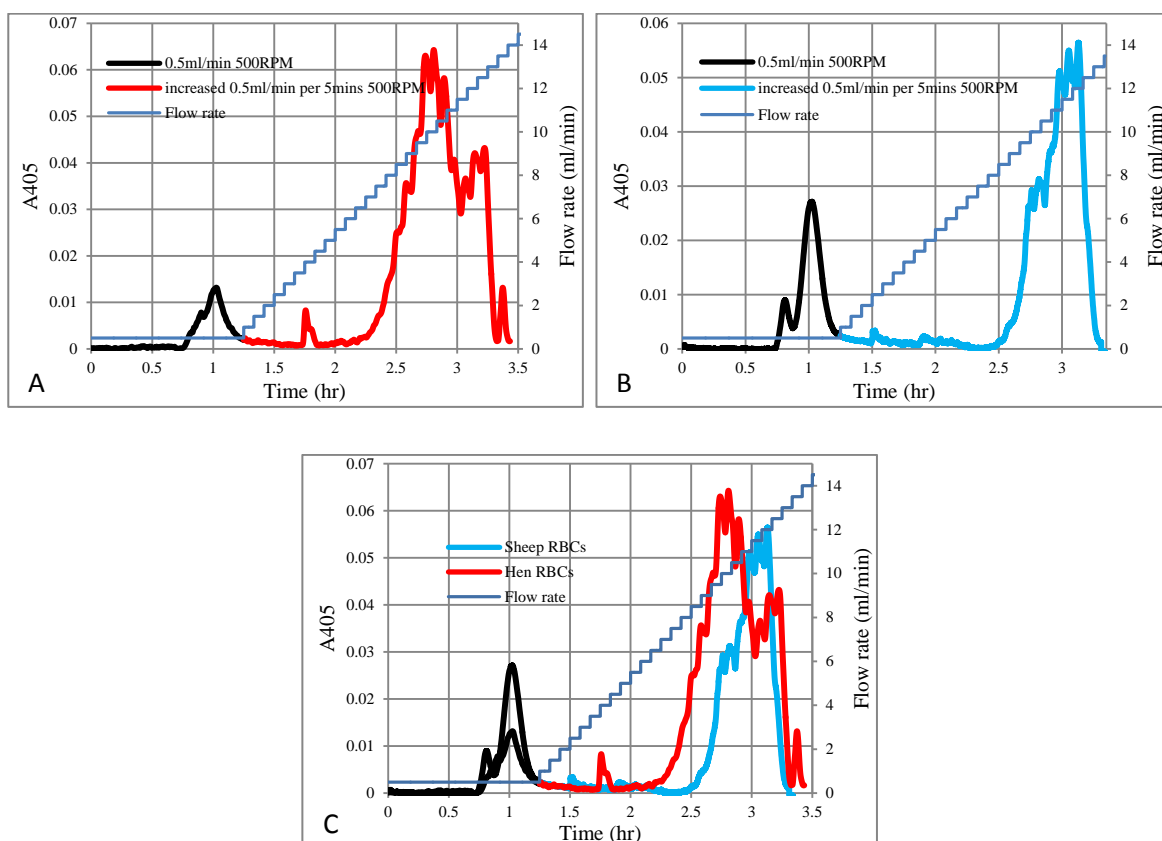


Figure 6.2.7. Elution of blood sample in flow gradient by column D. A) Hen blood sample. B) Sheep blood sample. C) Comparison between hen RBCs and sheep RBCs elution behaviours. 0.32 ml of hen/sheep blood sample was injected into CCC coil (Column D: 29.2 ml; 0.8 mm × 2.5 mm) at 500 RPM at 0.5 ml/min, pumping from tail to head. Eluent monitored at 405 nm. After isotonic buffer had been pumped for 1.5 column volumes the flow rate was increased in steps of 0.5 ml/min every 5mins..

Both hen and sheep RBCs were eluted around 3 hours by the flow with the sheep RBCs eluting as a broader peak. The hen RBCs eluted a little earlier, but a comparison of peaks shown in Figure 6.2.7 C shows that in contrast to column C, using column D in the same flow mode of tail to head would not give a separation of a mixture. This results shows that the orientation of the column has a marked effect on its efficiency for cell separations. By comparing Figure 6.2.6.c and Figure 6.2.7.c, it shows column C requires higher flow rate

Chapter 6. Behaviour of RBCs elution in different tube shape
 to elute both hen and sheep RBCs than column D, although column C and column D were built with the same β value and generates the same g-field with the rectangular shape direction being the only difference between them. Again, this shows that the orientation of the coil can be a critical factor in influencing the behaviour of cells flowing in a fluctuating g field. The “flat” orientation gives greater retention of cells and better cells separations than the “upright” orientation.

6.2.3.2. Flow cell separation of sheep and hen RBCs in rectangular column

6.2.3.2a. Introduction

The results of 6.2.3.2 showed that sheep and hen RBCs were eluted at different flow rates column providing the possibility to separate a mixture of sheep and hen RBCs. In addition it appeared that elution occurred over a narrow range of flow rates, so that rather than gradually increase the flow rate, using a slow gradient, a faster but still efficient separation could be obtained by selection of larger changes in flow (steps). These possibilities are tested in this section.

6.2.3.2b. Method

Instrument set up: Milli-CCC[®] (described in 2.2.1.1) with column C (described in 2.2.1.2) rotating in clockwise direction; pumping from tail to head direction; 0.73 ml sample loop; column temperature as 15 °C.

1. The initial rotational speed was set to 1000 RPM
2. The mixed blood sample (sample included: around 7.5E+08 hen RBCs and 8.5E+08 sheep RBCs) was pumped in to column via injection port at an initial flow rate of 1 ml/min.
3. The flow rate of pumping isotonic buffer was changed as the table below:

Flow rate	Period of flow (column volumes)
<i>Sedimentation mode at 1000 RPM</i>	
1 ml/min	2 column volumes
<i>Elution mode at 500 RPM</i>	
6 ml/min	1 column volume
12 ml/min	41 column volume
<i>Elution mode of retained RBCs at 0 RPM</i>	
5 ml/min	-

4. Collect data by UV detector to plot graph by time or no. of column volume as horizontal axis and voltage as vertical axis, respectively.
5. The fractionated samples were collected 50 ml per tube from the elution of 12 ml/min (20 fractions were collected from 12 ml/min and 1 fraction was collected under 5 ml/min) and examined by biological microscope.

Results are shown in section 6.2.3.2c.

6.2.3.2c. Results

Results of this separation are shown in Figure 6.2.8.

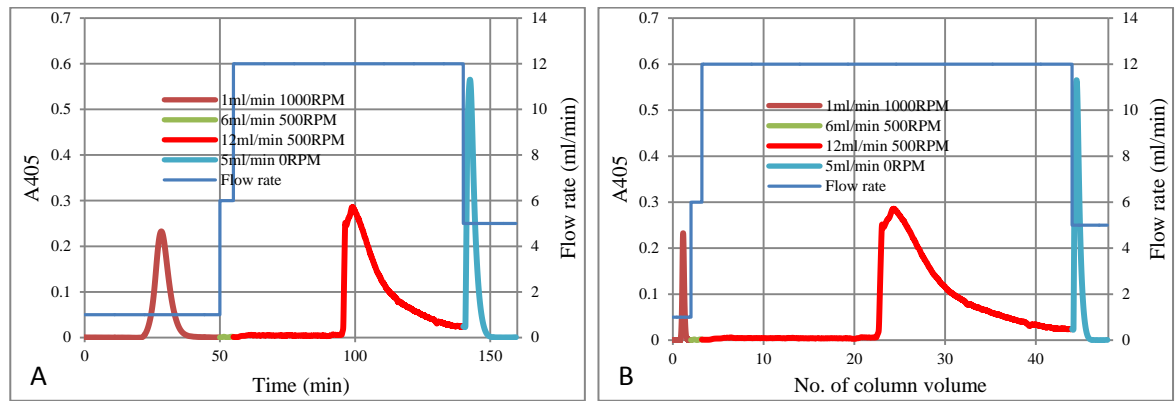


Figure 6.2.8. Elution of mixed hen/sheep blood sample by a step increase in flow. A) Elution profile plotted against time. B) Elution profile plotted against column volume. 0.73 ml of mixed hen/sheep blood sample (sample included: $7.5E+08$ hen RBCs and $8.5E+08$ sheep RBCs) was injected into CCC coil (Column C: 25.8 ml; 2.5 mm \times 0.8 mm) at 1000 RPM at 1 ml/min. Eluent monitored at 405 nm. Rotational speed was reduced to 500rpm and flow rate was increased to 6 ml/min for 1 column volume) and then speed decreased to 500 RPM then in steps 12 ml/min for 41 times of column volume. Retained RBCs were eluted at 5 ml/min at 0 RPM.

A cell number analysis by haemocytometer is shown in Figure 6.2.9.

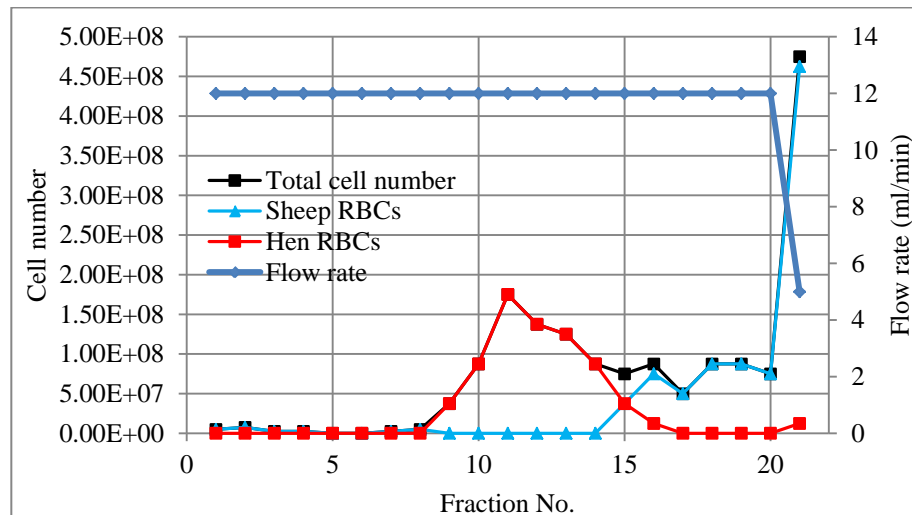


Figure 6.2.9. Cell number analysis for each fraction from Figure 6.2.8 obtained by step flow using 2.5mm × 0.5mm rectangular column (column C). 50 ml fractions were collected from the elution of 12 ml/min (20 fractions were collected from 12 ml/min and the last fraction was collected at 5 ml/min and 0 RPM). This Hen RBCs were eluted easier than sheep RBCs with a small overlap in 15th and 16th fractions only.

Figure 6.2.9 shows the elution order in the step flow. Very few sheep RBCs were eluted in the first 4 fractions, and after these the eluted number of sheep RBCs decreased to 0. Hen RBCs started to elute in the 9th fraction and all fractions up to 15th contained only hen RBCs. Except for a small proportion of sheep RBCs that were eluted in the beginning of 12 ml/min, all the t sheep RBCs were retained in the column after the elution of hen RBCs and were then eluted using pump out conditions of 5 ml/min at 0 RPM. This fraction contained a few hen RBCs. As a conclusion, the mixture of sheep RBCs and hen RBCs was successfully separated in step flow using the rectangular column C.

6.2.3.3. Elution behaviour of RBCs in species by flow gradient in rectangular column (column C)

6.2.3.3a. Introduction & method

Different RBCs in species showed different maximum flow rate in chapter 3 which indicates different elution behaviours. In order to examine the elution time of different RBCs in species in rectangular column C, a flow gradient was used. The detailed procedure of eluting RBCs in species in flow gradient in rectangular columns was the same as the procedure in section 6.2.3.1. The rectangular column C was used as this has proved more successful for cell separations than the rectangular column D, as discussed above.

This experiment was performed using RBCs of rabbit, guinea pig, horse, rat, mouse and dog. Results are shown in section 6.2.3.3b.

6.2.3.3b. Results

The result of eluting blood sample in species using a flow gradient in 2.5 mm × 0.8 mm rectangular column (column C - “flat” orientation) is shown in Figure 6.2.10.

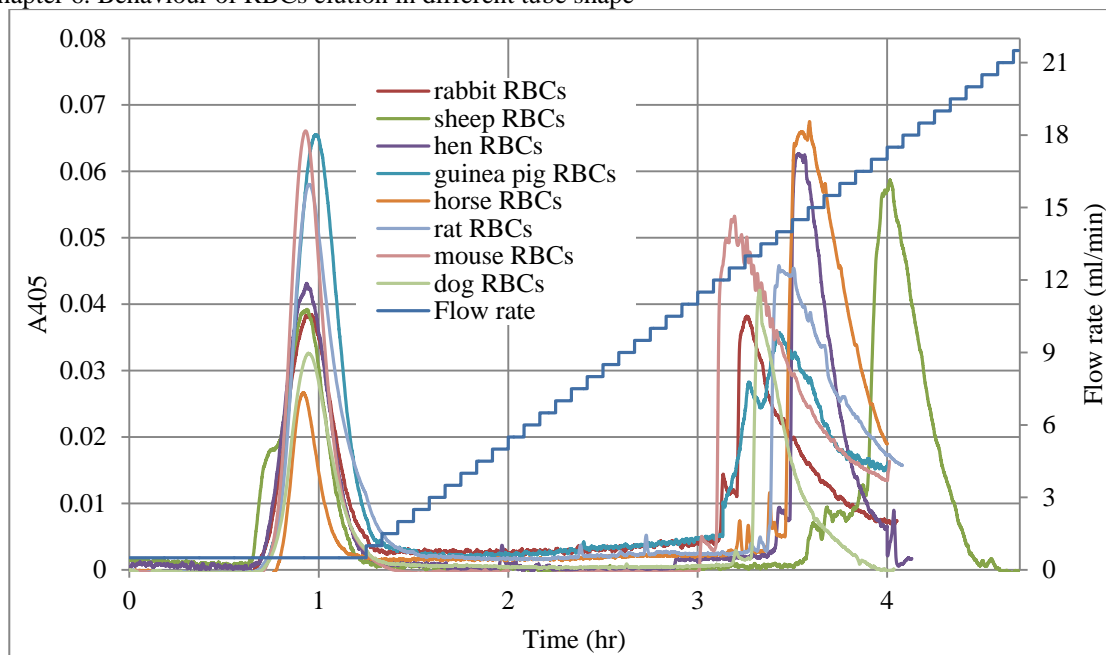
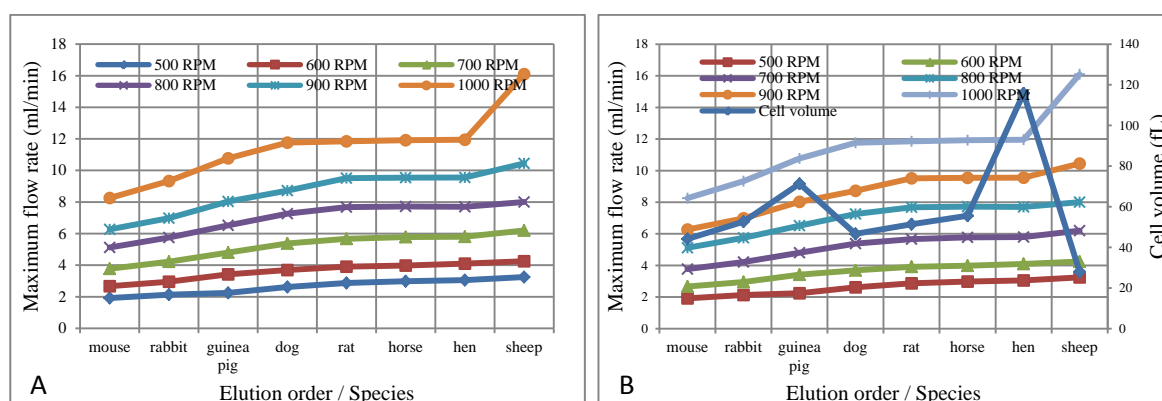


Figure 6.2.10. Comparison between elution of blood sample in species using a flow gradient in rectangular (“flat”) column C. 0.73 ml of blood sample in species (rabbit; sheep; hen; guinea pig; horse; rat; mouse; dog) was injected into CCC coil (Column C: 25.8 ml; 2.5 mm × 0.8 mm) at 500 RPM at 0.5 ml/min, pumping from tail to head. Eluent monitored at 405 nm. Gradient increased by steps of 0.5 ml/min every 5mins after isotonic buffer was pumped 1.5 × column volumes. Data of hen RBCs and sheep RBCs were taken from Figure 7.2.15.

Figure 6.2.10 shows different blood sample in species gave different elution times. Interestingly, the elution order is the same as the order of maximum flow rate as shown in Figure 6.2.11, which was mouse RBCs (eluted at 11.5 ml/min), rabbit (eluted at 12.5 ml/min), guinea pig (eluted at 12.5ml/min), dog (eluted at 13 ml/min), rat (eluted at 13.5 ml/min), horse (eluted at 14.5 ml/min), hen (eluted at 14.5 ml/min) and sheep (eluted at 15 ml/min, mainly in 17 ml/min). Therefore, the elution order follows the order of maximum flow rate. Figure 6.2.11 also shows the cell diameters and densities for these RBCs and it is important to note that the elution order does not follow the order of cell diameter as was the case for minimum flow rate, nor is it significantly related to cell density.



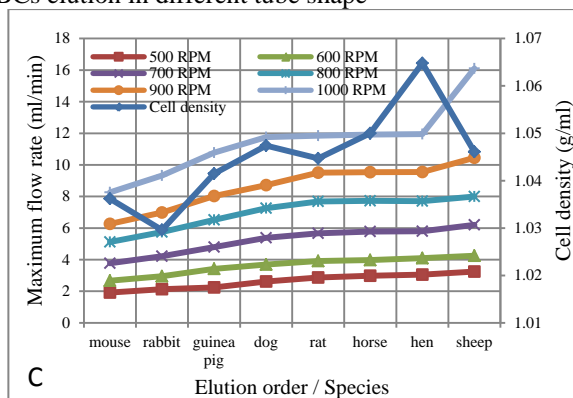


Figure 6.2.11. Relationship between maximum flow rate, cell volumes, cell density and elution order. A). Comparison between maximum flow rate and elution order in rectangular column C. Data was taken from Table 3.2.3 and Figure 7.2.20. B) Comparison between maximum flow rates, cell volumes and elution order in rectangular column C. Data was taken from Table 3.2.3, Figure 2.5.4 and Figure 7.2.20. C) Comparison between maximum flow rates, cell density and elution order in rectangular column. Data was taken from Table 3.2.3, Table 2.5.3 and Figure 6.2.10.

6.2.3.4. Flow cell separation of rabbit and hen RBCs in rectangular column C

6.2.3.4a. Introduction

As different species of RBCs were eluted at different time / flow rate as shown in 6.2.3.3, a separation of rabbit and hen RBCs by step flow was examined as an additional example of cell separation. Rabbit RBCs were selected as they can be eluted earlier than hen RBCs, whereas sheep RBCs, examined in earlier sections, eluted later than hen RBCs.

6.2.3.4b. Method

Instrument set up: Milli-CCC[®] (described in 2.2.1.1) with column C (described in 2.2.1.2) rotating in clockwise direction; pumping from tail to head direction; 0.73 ml sample loop; column temperature as 15 °C.

1. The initial rotational speed was set to 1000 RPM
2. The mixed blood sample (sample included: around 2.9E+08 rabbit RBCs and 2.8E+08 hen RBCs) was pumped in to column via injection port by initial flow rate as 1.5 ml/min.
3. The flow rate of pumping isotonic buffer was changed as the table below:

Flow rate	Period of flow (column volumes)
<i>Sedimentation mode at 1000 RPM</i>	
1.5 ml/min	2 column volumes

<i>Elution mode at 500 RPM</i>	
7 ml/min	1 column volume
14 ml/min	10 column volume
<i>Elution mode of retained RBCs at 0 RPM</i>	
5 ml/min	-

4. Collect data by UV detector to plot graph by time or no. of column volume as horizontal axis and voltage as vertical axis, respectively.
5. The fractionated samples were collected 25 ml from the elution of 7 ml/min and 50 ml per tube from the elution of 14 ml/min (4 fractions were collected from 14 ml/min and 1 fraction was collected under 5 ml/min) and examined by biological microscope.

Results are shown in section 6.2.3.4c.

6.2.3.4c. Results

The result of eluting mixed rabbit / hen blood sample using step flow in 2.5 mm × 0.8 mm rectangular column (column C) is shown in Figure 6.2.12.

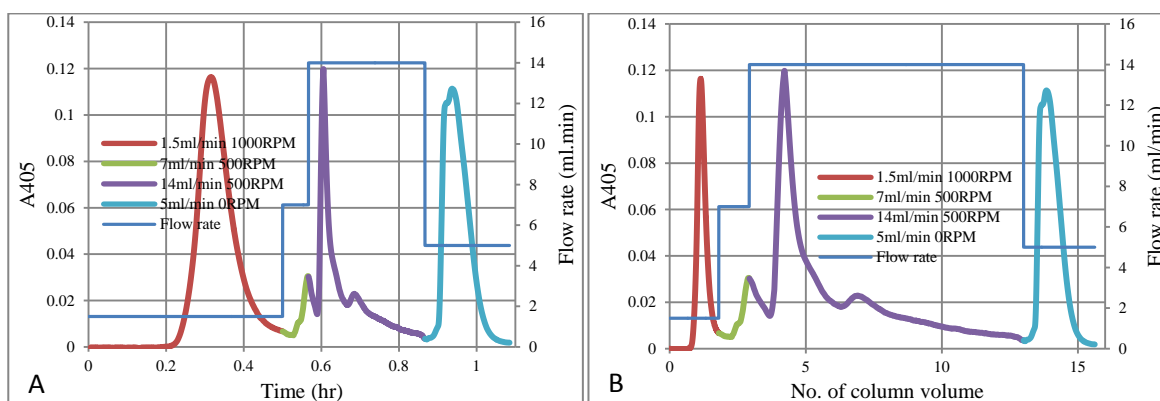


Figure 6.2.12. Elution of mixed rabbit/hen blood sample by a step increase in flow. A) Elution profile plotted against time. B) Elution profile plotted against column volume. 0.73 ml of mixed rabbit/hen blood sample (sample included: 2.9E+08 rabbit RBCs and 2.8E+08 hen RBCs) was injected into CCC coil (Column C: 25.8 ml; 2.5 mm × 0.8 mm) at 1000 RPM at 1.5 ml/min. Eluent monitored at 405 nm. Flow rate was increased to 7 ml/min (1 column volume) and rotational speed decreased to 500 RPM then in steps 14 ml/min for 10 times of column volume. Retained RBCs were eluted at 5 ml/min at 0 RPM.

A cell number analysis by haemocytometer is shown in Figure 6.2.13.

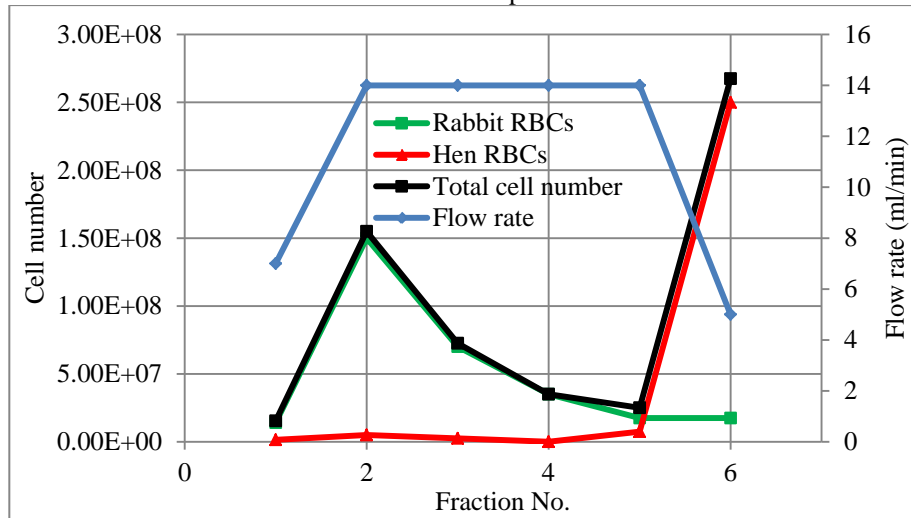


Figure 6.2.13. Cell number analysis for each fraction obtained as described in Figure 6.2.12 using step flow in 2.5mm × 0.5mm rectangular column (column C). The fractionated samples were collected 25 ml from the elution of 7 ml/min and 50 ml per tube from the elution of 14 ml/min (4 fractions were collected from 14 ml/min and the last fraction was collected under 5 ml/min, 0 RPM). Rabbit RBCs were eluted easier than hen RBCs with a small overlap in 5th fractions only. Almost all hen RBCs were eluted after elution of rabbit RBCs.

Figure 6.2.13 shows the expected elution order in the step flow as rabbit RBCs were eluted quicker than hen RBCs. Rabbit RBCs were eluted between 7 ml/min and 14 ml/min. Hen RBCs were not eluted until fraction No.5 with the majority of hen RBCs being retained in the column until they were eluted using the pump out conditions of 5 ml/min at 0 RPM. This fraction of hen RBCs contained very few rabbit RBCs. As a conclusion, the mixture of rabbit RBCs and hen RBCs was successfully separated in step flow using rectangular column C.

6.3. Discussion

6.3.1. Minimum flow rate for sheep RBCs in column A and column B

The interesting comparison between minimum linear flow rate in column A and column B was shown in table 6.2.1. It showed the change of inner diameter from 1 mm to 1.6mm ID did not influence the minimum linear flow rate for one cell population. Although inner diameter change influenced the sedimentation behaviour of RBCs in circular column, the key of sedimentation condition to retain all RBCs was the same linear flow rate.

6.3.2. The sediment behaviour of RBCs in rectangular column

These studies showed a marked difference in behaviour between circular and rectangular columns, Figures 6.2.1, 6.2.2 and 6.2.3 show that compared with the circular columns used (A and B), RBCs can be retained in the rectangular columns (C and D) no matter which pumping direction was used (either against or following the rotational direction). By contrast, RBCs can only be retained in circular column while pumping from tail to head. This difference probably comes from the different secondary flows in those 2 tube shapes. In the circular column, the large secondary flow is generated in the whole column but the secondary flow only occurs in the corners of rectangular columns. Therefore, some of the RBCs in the circular coils may be trapped by the secondary flow and then eluted when pumping from head to tail. But in rectangular columns, as no strong secondary flow exists in the tube, the sedimentation was easier for RBCs even when pumping from head to tail which follows the movement direction of RBCs.

6.3.3. Elution of mixed RBCs in rectangular columns C and D

By comparing elution results between column A (Figure 5.2.13) and column C (Figure 6.2.9), column C gave a clear separation of a mixture of sheep and hen RBCs as only a few sheep RBCs were eluted ahead of hen RBCs. Due to the bigger cross sectional area of column C than column A, a greater elution flow rate was also required for column C which led to diluted fractions and a large consumption of buffer. For column C, the separation results can be even better by using a greater rotational speed to enlarge the elution difference between hen RBCs and sheep RBCs, but again, it also requires a higher elution flow rate. Therefore, a high rotational speed has the disadvantage of large amount of isotonic buffer consumption and diluted fractions being obtained, although column C provided better separation results.

A direct comparison can be made between column B, C and D as they provide the same cross sectional area. Figure 6.2.7 showed the elution time of hen RBCs was the same as elution time of sheep RBCs in column D and Figure 7.2.15 showed a much greater elution difference in column C. Therefore, by comparing column B, C and D, it can be decided that column D should not be used to separate cells; a partial cell separation was obtained by column B; and a the best cell separation result was obtained by column C which showed a clear elution order difference between hen and sheep RBCs.

Considering the geometry of the 3 columns, the direction of the g field is important. Column D provided the smallest area to sediment cells, followed by the circular column B; the largest sediment area was provided by column C. Therefore, assuming the same number of RBCs was injected into each column, the height of cell sedimentation in column D was the highest and then column B and the last was column C. Therefore, it suggests the RBCs in column C were the closest to the main flow which has the highest flow rate. This higher flow rate layer leads to quicker elution with no time for sheep and hen RBCs to elute differently. In fact, the elution flow rates in the 3 columns supported this, as the elution flow rate for column D was the smallest and then the column B, and for column C. Therefore, by comparing column B, C and D, it indicates the geometry of tube with flat orientation (column C) provides best for cells to sediment in the direction of g and to help the different cell population to behave differently.

6.3.4. Elution order and flow cell separation in column rectangular column C

The differences of maximum flow rate shown in Table 3.2.3 suggest different elution orders. In Figure 6.2.10, this elution order was confirmed. The elution order was rabbit, hen and the last was sheep RBCs. This needs to be compared to their relative sizes which increase in the order, sheep, rabbit and hen. For mouse and sheep RBCs which had similar size, they showed completely different elution behaviours (mouse RBCs can be eluted much easier than sheep RBCs). Therefore, Figure 6.2.10 also showed the elution behaviour was not only based on single size factor, but also cell properties. These might include flexibility and aggregation.

Rabbit, hen and sheep RBCs were taken as examples to achieve the flow cell separation as the nucleated hen RBCs can be distinguished from the rabbit and sheep RBC, and rabbit RBCs was eluted quicker than hen while sheep RBCs was retained more than hen RBCs as shows in Figure 6.2.13. During these 2 flow cell separations, the combination of flow

Chapter 6. Behaviour of RBCs elution in different tube shape
gradient and step flow showed the high efficiency of analysis and separation RBCs. After the elution flow rate was obtained by flow gradient, the step flow separated mixed RBCs easily, demonstrating the possibility of this flow method for cell separations.

6.4. Conclusion

In this chapter, the influence of constructive structure of tube shape on behaviour of RBCs was investigated. Firstly, the minimum flow conditions in circular columns of different diameter (A and B) columns were the same when the flow rate was expressed as the minimum linear flow, correcting the flow rate for the varying cross sectional area. However the elution conditions between the circular columns with different inner diameters differed even when expressed as linear flow rate and the greater ID column B required much higher flow rates to elute RBCs than column A with the smaller ID.

Secondly, circular columns required cells to be pumped against the rotational direct, tail to head for cells to be retained. By contrast, rectangular columns can retain RBCs when the pumping direction was against or following the rotational direction. This indicates better retention and more difficult RBCs elution in the rectangular column.

Thirdly, elution order was hen RBCs followed by sheep RBCs and this was the same whether eluted tail to head or head to tail. But the difference is insufficient to give cell separation. A possible reason for the similar elution order is that pumping from head to tail, and the flow direction in rectangular column (column C and D) can be ignored as the movement of RBCs to the tail end may be dominant.

But the tube shape did change the behaviour of RBCs greatly during pumping from tail to head and an influence of the area of sedimentation appears important. The column C, with its “flat” orientation of the rectangular tubing, provided the largest area for cells to sediment this gave the best cell separation results; whereas a partial separation was obtained with circular column B column which provided a smaller area to sediment; and the column D, with the smallest area, showed no elution difference between sheep and hen RBCs in this column.

Using the “flat” rectangular column C, rabbit / hen RBCs and sheep / hen RBCs were successfully separated by step flow based on their elution order..

Therefore, from chapter 3 to chapter 6, the influences of operational condition, cell properties and constructive structure on the elution and sedimentation behaviour of RBCs in fluctuating g-field were all investigated.

Chapter 7. General discussion and conclusion

The behaviour of RBCs in fluctuating g-field was described in this thesis with attention given to operational conditions, RBCs properties and tube geometry shape. The instrument used in this thesis was the Milli-CCC[®] which is commercially available worldwide with standard column design and temperature control. The retention of cell / particle in the column was described as a problem for a number of different cells / particles separation in section 1.1, therefore research in this thesis has focused on 2 aspects of cell behaviour in the Milli-CCC[®]: sedimentation and elution. These studies have revealed that the behaviour of RBCs described in this thesis has similarities with other cell/particle separations but also has its unique features.

7.1. Discussion of sedimentation behaviour of RBCs

The problem of cells sedimenting in the column, and therefore being retained, has been reported during the cell / particles separation articles, such as separation of human and sheep erythrocytes (Ito et al., 1980) and retention of a solid sample (Fedotov et al., 2003). In the case of non-synchronous CCC, such problems have been overcome by using a slow rotation of the coil such as .6 RPM (Ito et al 1979). Shinomiya et al (2005) retained cells when the coil rotation was 0 RPM, and then were able to elute cells by increasing it. Thus retention was avoided by optimizing operational conditions (Sutherland, personal communication). For these reason it was important to understand the sedimentation behaviour of the RBCs.

7.1.1. Movement of RBCs in rotating coiled columns

The movement behaviour of RBCs in rotating coiled columns was described in section 3.2.1 using sheep RBCs in CCCE cantilever column. In addition, although not observed directly, movement of sheep RBCs was also discussed in section 6.3 as this the movement also occurred in rectangular columns.

The conclusion of these studies was that no matter which types of column were used, the RBCs always moved to the tail end of the column, whereas any air bubble present moved to the other end of column, the head (Ito, 2005). This raises an interesting question. The rotation motion creates an Archimedean screw force, which causes all objects of different density to move toward one end called the head end. However this is opposite to what was observed in the CCCE cantilever column. As shown in Figure 1.1.16, the head end was the

movement direction for both bubble and bead (particle). But, can this model be used to describe the situation in the columns used in this study with RBCs?

Some differences must be considered. First, the rotation pattern shown in the model in Figure 1.1.16 and planetary rotation in CCC are different. The rotation in Figure 1.1.16 shows only 1 rotation around 1 axis whereas planetary rotation has both rotation and a revolution. Therefore the g-field generated in this helical or spiral coil model (Figure 1.1.16) is constant whereas in CCC is fluctuating. The second difference is the rotational speed as both in Figure 1.1.16 or the helical model, the rotational speed is slow, which may not generate high enough g-field to retain beads/particles in the column.

However, it still leaves the question that even if RBCs can be retained in the column, then what is the reason for RBCs moving to the tail? This problem is more interesting if another fact is considered. The basic function of CCC centrifuge at a high rotational speed is a pump, which can pump liquid out of head end when the other end is connected into liquid. Liquid can also be pumped out from head end at a lower rotational speed when air is pumped in the middle of column, which is the method generally used to determine the head end after a column has been set up. Therefore due to the liquid being pumped to the head end, even if there is movement of RBCs, the direction of this should also be the head, i.e. in the same direction as the liquid. However, what was observed was that of the RBCs moved to the tail end, and the isotonic buffer did not pump out from the head. This may have been because the rotational speed used in this thesis was not sufficiently high to overcome the effect of the low i.d. of 1 mm, due to the tension effect being strong enough to hold the buffer in the coil.

The movement of RBCs to the tail may also be understood by analogy with the behaviour of 2-phase systems in rotating coils. In 2-phase system, only one phase occupies the head end and the other occupies the tail (Grudzień, 2011). This is explained by considering that both of them are trying to occupy the head end, as both of them move toward head, but only one can win this competition. Interestingly it is the lighter phase that occupied the head and the denser phase that occupies the tail, which shows that there is a density distribution from head to tail for liquid-liquid systems. If we extend this to the air-liquid-solid system as shown in Figure 3.2.1 and Figure 3.2.2, the phenomenon can be understood as a density distribution process in which not all objects move to the head during the rotation. Therefore the tail movement of RBCs is reasonable as the air moves to head and the RBCs moved to tail. This tail movement of RBCs was observed CCCE cantilever column, 1 mm i.d. circular column and also in rectangular columns, therefore, it is a

constant finding. So, compared to the traditional views, this tail movement of RBCs may indicate a limitation of the definition of column ends.

Although with pumping flow, a similar mathematical simulation was described by Fedotov et al. (2005) as at a certain flow rate, “the larger particles move against the carrier flow and smaller particles move in the direction of flow”. Therefore, with decreasing flow rates more particles will move against the carrier flow, i.e. to the tail. Thus at zero flow rate all particles will move to the tail, as has been observed in this thesis.

7.1.2. Pumping direction and rotational direction

To continue the above discussion, the conclusion of section 3.2.2 in Milli-CCC[®] (1.0 mm i.d.) and section 6.2.1.2, in Milli-CCC[®] (1.6 mm i.d.), the pumping direction is against the rotational direction to retain RBCs and the pumping direction follows the rotational direction to elute RBCs. Therefore, the operation conditions adopted were to pump the isotonic buffer from tail to head.

Interestingly, the influence of rotation direction and flow direction was researched in nonsynchronous CCC (Ito et al., 1983) as shown in Figure 1.3.13 in which their Method I has rotation and flow opposite, and Method II has them in the same direction. After the pumping direction was switched in method II, a broader elution peak was obtained and peak shapes switched. However, because both of these operational conditions used (method I & II) did not retain RBCs in the column, a direct comparison with the results in this thesis cannot be made. However, the longer elution time and broader peak obtained with method II, in which rotation and flow had same direction, retained RBCs more. This is opposite to the conclusion of the relationship between operational direction and rotational direction in this thesis. However, as the g-field generated by non-synchronous CCC is quite different from that generated by J-type, the comparison between these 2 conclusions may not be valid. However, cell separations results described in this thesis for the synchronous CCC showed differences from those obtained with the synchronous CCC.

As discussed in section 6.3, rectangular column did not follow the rule of pumping direction and rotational direction shown for circular column. Since the pumping direction did not change the sedimentation results, it showed an easier retention of RBCs.

7.1.3. Discussion of minimum and maximum operational condition

Minimum and maximum initial operational condition are an important concept in this thesis: the minimum operational condition means retaining all intact RBCs and maximum operational condition means eluting all intact RBCs.

A similar description was reported in Figure 1.3.23 which was to investigate the influence of different β value on the retention of solid particles (Fedotov et al., 2003). Obviously, as long as a β value is greater than 0.25 for J-type CCC, which gives the direction of g-field pointed to outside constantly, a smaller β value indicates a smaller g-field. Therefore, to understand Figure 1.3.23 in terms of minimum and maximum operational condition is straight forward. When the β value was increased from 0.38 to 0.86, the g-field was increased, but the initial flow rate was not increased. Therefore, when the g-field was low, due to a low rotational speed and/or small β value, the initial flow rate can elute more solid sample out of coil since the minimum flow rate for this rotational speed was low. But the same initial flow rate cannot elute RBCs when the β value increased as the minimum flow rate was also increased. Therefore, in Figure 1.3.23, 3 regions were also labelled as region I (the condition to retain all particles), region II (the condition to elute some of the particles) part of solid and region III (the condition to elute all particles). This is a similar description to Figure 3.2.9 based on the behaviour of RBCs in this thesis.

Therefore, the 3 β values and different rotational speeds in Figure 1.3.23 can be calculated and converted into g-field as Figure 3.2.9. Then, a g-field suggests a minimum or maximum flow rate for one solid / cell / particles to sediment or eluted.

Fedotov has also described one kind of particle behaviour in the simulation where particles are retained in the flow (Fedotov et al., 2005). This simulation indicates “the retention of particles in the carrier liquid flow can be attained only for a very narrow range of particle size even under strictly specified experimental conditions”. The minimum operational conditions are those specified experimental conditions. Therefore, for some conditions such as a lower initial flow rate than minimum flow rate, although the fractionated samples analysis shows no difference to samples fractionated under minimum operational condition, when cells are sedimented and retained, in fact, the RBCs have moved back towards the tail inside of the column.

7.2. Discussion of elution behaviour of RBCs

As mentioned, the sedimentation of RBCs in the column can be a problem for cell separation methods in CCC. Although all previous cell separations were achieved by non-synchronous CCC, this problem of sedimentation was treated with various strategies. Some

of them optimized the operational condition to avoid the sedimentation then elute cells in different elution order with no retained cells in the column. In other strategies some cells were eluted and others retained, to be eluted later. However, in contrast to all of these strategies, the separation method described in this thesis required complete cell sedimentation before they were separated.

7.2.1. Comparison of cell separation by non-synchronous CCC and J-type CCC

The fundamental elution and separation behaviour of RBCs was described in chapter 5. The separation in the same isotonic buffer as used in this thesis of sheep RBCs and human RBCs was reported in Figure 1.3.10 and Figure 1.3.12 using non-synchronous CCC. There are several obvious differences between the RBCs separation in non-synchronous CCC and J-type CCC.

From the instrument constructive aspects, first, the column was different. RBCs separation in 1979 used eccentric columns and the column used in this thesis was a multilayer column.

Second, the g -field was different. The direction of g -field in non-synchronous changed from perpendicular towards the wall to perpendicular away from the wall. But the direction of g -field with the β value of the column used in the J-type CCC was always towards the wall. Therefore, in addition to the influence of column construction on flow pattern, the involvement of the g -field was also different. For non-synchronous CCC separation, although not mentioned by Sutherland et al. (1979) in their paper, the principle of separation should be based on a balance between the sedimentation rate and the size dependent effect of flow. Because of the direction of the g -field is switching from one side to other side, an optimized rotational condition was selected to avoid RBCs sedimentation. Since RBCs are moving from one side of column to the other side continuously at different rates for different cell populations, the pumping flow acts as an extra force to push RBCs to the outlet gradually. Therefore, this is why all such separations required a slow flow rate as a quick flow rate would not give enough time to enlarge and exploit the small sedimentation rate difference between different cell populations. Therefore, the key point for this avoiding sedimentation strategy is the choice of the correct rotational speed combined with correct revolution speed. Even so, as described, the largest human RBCs were still retained in the column after the separation of the majority of cells (Ito et al., 1979).

Compared to the nonsynchronous separations described above, the method in this thesis requires sedimentation before separation because it was based on different elution behaviours between cell populations but not different sedimentation rates. This resulted in separations based on different cell properties: for non-synchronous CCC separation, the smaller size cell - sheep RBCs were eluted first, then the bigger size cell - human RBCs. But for the method in this thesis, generally, bigger size cell - hen RBCs were eluted first then the smaller size cell - sheep RBCs. However, because the separation order was not based on simply on size but could be complicated by cell aggregation, some sheep RBCs were eluted quicker even before hen RBCs because they were aggregated. This phenomenon increased with increased RBCs number injected into column.

The elution time was also different because non-synchronous CCC separation avoided the sedimentation of RBCs, therefore, the first eluted RBCs were eluted after the first column volume while other RBCs were slowly eluted with different retained behaviours. Compared to this, the components eluted in the peak after first column volume in J-type CCC was free Hb and RBCs ghost cells. The RBCs were eluted only when the flow rate was high enough to push them out. Generally, due to these principle differences, non-synchronous CCC requires low flow rate with smaller cell eluted first whereas J-type CCC requires high flow rate with bigger effective sizes (few cells or aggregates) being eluted first. Both of these separation methods required finely controlled operational conditions.

In another cell separation strategy used for non-synchronous CCC, such as Figure 1.3.14, some cells were retained in the coil, and then eluted. However, the separation order of this method is the same as the first strategy, therefore, because smaller cells were eluted first, and the bigger or even aggregated cells were retained. But this mode is similar to that used in this thesis in that some cells were retained and then eluted.

7.2.2. Comparison with nonsynchronous CCC separation of blood cell components

Figure 1.3.18 shows that, RBCs were separated from other cell components by changing rotational speed in the nonsynchronous CCC. The same result can be achieved by any minimum operational conditions in Milli-CCC[®] operation. Comparing these 2 CCC methods for blood cell components separations, RBCs were retained in the column in both of them whilst eluting other cell components out of column. The elution process of RBCs for both these methods required operational condition change as this rotational speed was increased from 0 RPM – 10 RPM as RBCs were eluted around 10 RPM in the non-

synchronous CCC separation. For the method in this thesis, either the flow rate or rotational speed must change into an elution condition to release the retained RBCs.

Comparing the 2 methods, the changing operational condition process of the method in this thesis can also be used to separate cells directly by correct controlled conditions. But for nonsynchronous CCC, as shown in Figure 1.3.18, the only parameter that can be adjusted is rotational speed. However, changing this also changes the direction of g-field which cannot maintain the retention environment anymore and RBCs will be eluted directly. Therefore, if the flow rate was high enough, then the elution time for different cell populations will be close which as shown in Figure 1.3.18 and Figure 1.3.19, the elution time of sheep RBCs and human RBCs were the same. Or else, a small flow rate is required to be applied after the elution of other cell components, and the rotational speed adjusted to elute retained cell populations.

7.2.3. Comparison with particle separations by Fedotov et al.

Different particles separation by Fedotov and colleagues were reviewed in Chapter 1 (Section 1.3.4; Figure 1.3.23 to Figure 1.3.28). The feature of his separation is the application of step flow. Different sizes of particles were retained in the column first then eluted: one size of particles by one increased flow rate step. Therefore, the results always show a clearly relationship between the eluted particle size and the elution flow rate. Interestingly, as the Figure 5.2.9 showed for results in this thesis, hen RBCs were not eluted immediately the flow rate has been increased but required some further time to elute. This phenomenon suggested the elution pattern in the column was not the “buffet” elution but “competition” as discussed in section 5.3.2. Therefore if consider Fedotov’s results, such as Figure 1.3.26, where each flow rate eluted one particle size, then possibly one flow rate step (such as step 5) might also elute the particles in next flow rate step (such as step 6) if a longer elution time was allowed.

Is the “buffet” the pattern of particles separation and the “competition” the pattern of cell separation? Because particles are obviously retained, particle separation is based on the retention ability of particles; therefore, it leads to the greater size of particles being retained longer in the column. But for cell separation, the eluting force might be more important as the effective elution size changed the elution time and the elution order did not follow the change of cell size. Without similar particle experiment as elution hen RBCs, the answer is difficult to tell.

Will particles behave like RBCs is an interesting question since it relates the principles of 2 separations? As all results of Fedotov's separation, from 100 nm to 10 μm , the smaller particles were always eluted before the larger particles and the relationship between size and their eluted flow rate is strong. But for the cell separation in this thesis, sheep RBCs and hen RBCs behaved like a "sandwich" in which part of sheep RBCs were eluted before hen RBCs while some sheep RBCs were retained in the column. This is quite different from the separation of particles described by Fedotov et al. (2003) and shown in Figure 1.3.26, where 10 μm particles were eluted after 5 μm precisely. This demonstrated that the size is definitely not the only factor which influences separation in cell separations. The particle separation might not be compared to cell separation, as there are distinct differences between the particles and cells. That is why the cell properties analysis in this thesis is important and necessary.

7.2.4. Comparison with latex particles in BIB

Circular column and rectangular column were also applied in 1.1 μm and 3 μm latex particles elution in Brunel Institute for Bioengineering (Hagedoorn, 2013). During eluting latex particles in circular column, both 1.1 μm and 3 μm particles cannot be retained and eluted after the first of column volume; but in rectangular column, the 3 μm latex particles were retained significantly. Interestingly when considering the difference between circular and rectangular column during eluting RBCs, the rectangular column leads an easier retention of cells. As discussed in section 6.3, probably the smaller secondary flow is the reason of this influence of column geometry.

But the latex particle separation described by Fedotov et al. (2000) (Figure 1.3.24) showed a retention for 1.6 μm latex particle and elution of 0.6 μm particles. Due to the different experimental conditions between those 2 latex elutions, the comparison between them is difficult. However the only reason that 1.1 μm latex particles were retained was a too high flow rate combined with a too low g-field were used. Therefore, whether retention / sedimentation is required depends on the particle and needs to be part of the separation strategy. Cell / particles can be separated by eluting with no sedimentation at the first column volume, while retaining some populations if one can choose to sediment all of them in the column with no elution at all and then elute the sediment by step flow. So, which strategy should be chosen depends on the behaviour cell / particles. If they are easier to sediment, then sediment them by controlling the conditions; if they are easier to elute, then elute them in designed condition. Therefore it is not necessary to avoid cell sedimentation or to purposely sediment cells.

The particle elution simulation was calculated by Fedotov et al. (2005). However, by comparing the cell separation in this thesis and particle separation by Fedotov and colleagues, the elution of cells were more complicated than particles. Some of behaviours can be compared with his simulation as discussed above, but some of behaviours such as the quicker eluted sheep RBCs cannot be explained.

As long as β value is greater than 0.5, the direction of tangential velocity is constant (as shown in Figure 1.1.25) but the value changes with the smallest value being when column rotates 180° . By contrast, the direction of the g-field, as shown in Figure 1.1.26, fluctuates but also reaches the smallest value when column rotates 180° . The critical condition when cells move along the column is interesting. Obviously, cells are less retained in the smaller g-field, so, their chance to move will be when column rotates 180° . But at this rotation, the smallest tangential velocity also occurs. Also when the cells are exposed to the highest tangential velocity (at 0° and 360°), they will also be exposed to the highest g-field, which will favour sedimentation rather than elution. Therefore, there is a balance between the sedimentation and elution conditions.

7.2.5. Comparison with field flow fractionation and elutriation

The cell separation methods described in this thesis is different to the cell separation methods by non-synchronous CCC but more similar to field flow fractionation (FFF) and elutriation, as FFF provides vertical external force to retain cells and the elutriation applied a centrifugal force in the opposite direction to the flow to retain cells.

As discussed in section 5.3.2, the cell separation is considered as 3 modes in FFF which are normal mode (elution from small to large cell), steric and hyperlayer mode (elution from large to small cell). Normally the smaller cells were eluted in normal mode, and the large cells were eluted in the others mode as although the size of cells are small, they move as a “cloud” and the elution speed depends on how deeper the “cloud” penetrates into the main flow (Reschiglian et al., 2005). It is so similar to the behaviour of part of sheep RBCs that aggregated into “cloud” and thus penetrated deeper into the main flow and were eluted quicker than less aggregated sheep RBCs.

Elutriation uses a special centrifuge chamber to achieve cell separation. This is broader from inlet to outlet. Obviously this design makes a smaller and smaller linear flow rate through this chamber, then the cells distribute in this chamber on the basis of size. In the cell separations studies in this thesis the linear minimum flow has been shown to be the determining factor for the sedimentation and retention of cells in the coil. In the cell

separation studies in this thesis linear minimum flow has been shown to be a determining factor for the sedimentation and retention of cells in the coil. In addition, the linear minimum flow rate is the key to convert minimum flow rate between different ID of columns.

Cell separations both using Milli-CCC[®] in this thesis and FFF require high flow rate to elute retained cell and also give separations that are not completely dependent of the size of cells but on the behaviour of cells in the selected operational conditions.

The situation is actually more complicated than described above for a number of reasons:

- The direction of g-field must be considered in more detail. The direction of g-field points to outside of column (when β value is greater than 0.25) is not specific since this direction is swinging with the column rotating actually. Therefore, except when the g-field is vertical to sediment cells, the tangential g-field also works on cells. But the direction of the tangential g-field towards either left or right is based on the rotation degree. As a result, cells are eluted by the combination of pumping flow force and the swinging tangential centrifugal force.
- The pumping direction has been shown very important to the behaviour of RBCs therefore, the force which causes cells to move to the tail cannot be ignored.
- In addition to the forces discussed above, the friction between cells and cells to the wall should also be considered.
- The flow pattern also needs to be considered. How does the g-field influence the flow pattern? Will the fluctuating g-field change the flow profile? This is important as the distance of the sedimented cell layer from the main flow is the key to elution order. When the RBCs were injected in the fluctuating g-field, they were not all positioned in the same flow profile: some of them were further from the wall to which sedimentation occurred than others. The sedimentation process for them was different as they needed to cross the main flow area before they sedimented. RBCs show different shapes and orientation at the different shear rates that are generated by the flow profile, as shown, for example, in Figure 1.4.8. So different positions in the coil lead to different effects of sedimentation and flow. Thus some cells can appear in the rapidly eluting peak A, because they are trapped in the main flow whereas others are retained because they were not positioned in the main flow. These of course are eluted later in peak B. There is no difference between these two groups of cells, they just elute different because of their different initial positions when injected into the coil.

- Also, the flow may affect the sedimentation because RBCs can deform under the different shear rates. And local viscosity is changed by the cell sedimentation and will affect behaviour of RBCs during the elution.
- Another factor is the constructive structure of the coil. The change of tube shape has been demonstrated to alter cell behaviour as a result of flow pattern change. Then the influence of different column orientations (Figure 1.1.8) is also worth to investigate.
- Cell properties also have a role and the thesis has given evidence for surface charge and membrane flexibility. But how these properties influence cell behaviour requires further investigation to provide a general model for the behaviour of cells in rotating coils. That is the reason and importance of cell properties and tube shape investigation in this thesis.

This discussion shows the complexity of elution cell in fluctuating g-field. Computational fluid dynamics simulation might help to understand the flow pattern in the fluctuating g-field, and then as many rheology simulations have achieved previously the RBCs can be introduced into the simulation model to describe their flow separation behaviour.

7.3. Conclusion

The behaviour of RBCs in fluctuating g-field was investigated in this thesis. The research considered the behaviour of RBCs into sedimentation behaviour and elution behaviour based on different processes. The behaviour of RBCs was investigated mainly from 3 aspects which were operational conditions, cell properties and constructive structure (tube shape).

During the sedimentation process, the initial operational condition is important as it influence the amount of sediment RBCs in the column. An operational condition can retain all intact RBCs was called minimum operational condition. The value of linear minimum flow rate against g-field is a constant and characteristic value which differed for a range of RBCs from different species. With increased initial flow rate or decreasing of initial rotational speed, more and more RBCs were eluted. The maximum operational condition was obtained when all intact RBCs were eluted. Because the minimum operational condition retained intact RBCs whilst eluting free Hb and cell fragments, the minimum operational condition can be applied to separation of blood components.

Because different RBCs population behave differently during the elution process, it was possible to separate, sheep RBCs and hen RBCs using a step flow. Rectangular columns in

optimum orientations were found to be superior to separate cells as they provided greater space for cell sedimentation.

The separation of sheep RBCs and hen RBCs showed an unexpected feature in that part of the sheep RBCs eluted with the hen RBCs while the remainder were left in the coil. The more sheep RBCs injected, the more sheep RBCs were eluted with the hen RBCs. In order to avoid this complication, the elution flow rate for the hen RBCs was selected to cause the hen RBCs not to be eluted quickly, permitting some sheep RBCs to elute before the hen peak, which was relatively cleaner. However, the remaining sheep RBCs were retained more than the hen and were eluted later. Changing the coil from circular to rectangular reduced but did not completely eliminate this early eluting sheep RBC peak. A suggested explanation for this behaviour is that some sheep RBCs aggregate and it is these that are eluted early. This shows that aggregation in the coil can be a complicating factor. Cell deformability of RBCs was also found to be an important factor. After cell fixation by glutaraldehyde, RBCs were easier eluted in both sedimentation process and elution process. The difference of elution behaviour between unfixed and fixed sheep RBCs was so significant that the unfixed and fixed sheep RBCs were separated in step flow. But the aggregation occurred during elution of a mixture of fixed hen RBCs and fixed sheep RBCs. By adding Tween[®] 20 to avoid the aggregation, the fixed RBCs mixture was separated.

In this thesis a number of operating factors and cell properties have been shown to be important in determining how these cells behave in rotating coils. An understanding of the relative contribution of these has led to conditions which permit cell separations. Some of these features were expected such as the sedimentation behaviour of the cells being related to cells size and density, but a new finding was that cell deformability as also a determining factor. In addition there appeared to be contributions from surface properties cells which have not previously been reported for flow separations of this type.

An additional important finding in this study was that this method worked well for large numbers of cells, and so the system has the potential for scaled up cell separations.

However, as demonstrated by the number of complicating factors revealed, more work is needed to refine the method and this might include the following:

- The role of surface charge revealed in this study requires direct confirmation such as studies on cells in which the sialic acid has been removed by neuraminidase to increase aggregation. A low ionic strength buffer should also be used to expand the thickness of layer on cell surface to decrease aggregation.

Chapter 7. General discussion and conclusion

- There is a need for computational fluid dynamics to reveal the flow patterns in the coils as these clearly effect how cells are sedimented and eluted. This would lead to improved coil design in terms of shape and size.
- There is also need to compare the cell behaviour in different coiled column designs. This may help to seek the best coiled column design for cell separation.
- Direct measurement of cell deformability is required to link this directly to cell flow behaviour.
- The aggregability of cells also requires a measure to see if this relates directly with cell flow behaviour
- Cells other than RBCs need to be examined to show the generality of the phenomena observed in this thesis.

Appendix

The following abstracts were written/submitted as a result of this research project.

- *Poster presented at IChemE Young Researcher's Meeting, Birmingham, United Kingdom, 2013.*

Stem cell therapy requires the separation of differentiated from undifferentiated stem cells. The aim of our research is to investigate and develop new cell separation methods based on use of Counter-Current Chromatography (CCC) centrifuges in field flow fractionation mode that could be applied to stem cell purification. To understand the behaviour of cells in CCC centrifuges we have started with a study of the effect of flow rate, rotational speed (fluctuating g force) and cell flexibility on the behaviour of a model system of sheep and hen red blood cells, which differ markedly in size & shape, flowing in a single phase of physiological saline.

- *Poster and flash presentation presented at the 8th international conference on Counter-current Chromatography, London, United Kingdom, 2014.*

Flow separation of red blood cells in fluctuating g-field

Tian Han*, Derek Fisher and Svetlana Ignatova

Brunel Institute for Bioengineering, Brunel University, Uxbridge, UB8 3PH, UK
tian.han@brunel.ac.uk Fax: +44 (0) 1895 274608

As part of the aim of Brunel Institute for Bioengineering's Advanced Bioprocessing Centre to develop innovative flow separation methodologies, we are examining the potential for new cell separation methods based on the use of flow fractionation in fluctuating g-fields generated in rotating coil columns. We are characterising the effects of operational conditions (flow rate and rotational speed); cell properties (cell flexibility and cell aggregation); and column shapes (different inner diameters and coil geometries) on the flow behaviour of a model system of red blood cells (RBCs) from different species, which differ markedly in size, shape & density, flowing in a single phase of buffered saline.

Operational Conditions: For a particular rotational speed, there was a minimum flow rate which caused all the cells to be retained in the column and a maximum flow rate at which all cells were eluted. Both the minimum and maximum flow rates were increased when a higher rotational speed was applied. Differences in the behaviour of sheep & hen RBCs have been used to develop a separation method using a quasi-linear flow gradient. The separation time could be reduced by using a step flow gradient. The effect of cell load and direction of rotation on the behaviour of RBCs in the column will also be reported.

Cell Properties: We have found that the minimum flow rate correlated with cell diameter/cell volume of the RBCs as expected for a sedimentation related process whereas the maximal flow rate showed no correlation with cell diameter/cell volume. Also cell deformability changes the flow separation behaviour of the cells. The flow behaviour of sheep RBCs before and after chemical cross-linking (fixation) of the cell membrane with glutaraldehyde will be reported. Fixation renders the normally deformable RBCs rigid, and

resulted in the fixed sheep RBCs eluting significantly earlier than unfixed cells. This difference was great enough that a mixture of deformable (unfixed) and non-deformable (fixed) sheep RBCs could be separated. Fixed cells tended to show cell aggregation, which could be reduced by the addition of surfactant.

Column Geometry: For columns with the same cross sectional area, a “horizontal” rectangular column provided better separation than a circular column and a “vertical” rectangular column gave the least efficient separation. A possible explanation for this behaviour will be given. We demonstrated that the developed separation method using the circular column can be applied to different column geometries and different species of RBCs as validated on a mixture of rabbit and hen RBCs.

Similarities and differences of this work with other reports on cell/particle separations by Flow Field Fractionation (FFF) in rotating coiled columns in single phases and also in aqueous two phase systems (ATPS) will be discussed [1-4].

References

- [1] Y. Ito et al., (1979). *Analytical Biochemistry*, 94, 249-252.
- [2] K. Shinomiya et al., (2005). *J. Liq. Chromatog. & Rel. Techn.*, 28, 835-846.
- [3] O.N. Katasonova et al., (2003). *J. Anal. Chem.*, 58, 5, 473-477.
- [4] P.S. Fedotov et al., (2005). *J. Anal. Chem.*, 60, 4, 310-316.

References

References

- Alizadehrad D., Imai Y., Nakaaki K., Ishikawa T. and Yamaguchi T. (2012). *Quantification of red blood cell deformation at high-hematocrit blood flow in microvessels*. *Journal of Biomechanics*, 45, 2684-2689.
- Bauer J. (1999). *Advances in cell separation: recent developments in counterflow centrifugal elutriation and continuous flow cell separation*. *J. Chrom. B.*, 722, 55-69.
- Berthod A. (2002). *Countercurrent chromatography the support-free liquid stationary phase*. *Comprehensive analytical chemistry*, edited by Barcelo D. Elsevier science B.V., Amsterdam, The Netherlands. ISBN 0-444-50737-X.
- Berthod A., Friesen J.B., Inui T. and Pauli G.F. (2007). *Elution-Extrusion Countercurrent Chromatography: Theory and Concepts in Metabolic Analysis*. *Anal. Chem.*, 79(9), 3371-3382.
- Bishop J.J., Popel A.S., Intaglietta M. & Johnson P.C. (2001). *Rheological effects of red blood cell aggregation in the venous network: A review of recent studies*. *Biorheology*, 38, 263-274.
- Blanchette V.S., Kuhne T, Hume H & Hellmann J. (1995). *Platelet transfusion therapy in newborn infants*. *Transfus Med Rev*, 9(3), 215-230.
- Bourton E.C. (2008). *Countercurrent chromatography of proteins using aqueous two – phase systems*. PhD Thesis, Brunel University, London, United Kingdom. http://library.brunel.ac.uk/uhtbin/cgiisirs/x/UXBRIDGE/0/57/5?user_id=WEBSERVER&searchdata1=418326+{ckey}
- Chien S., Usami S. & Bertles J.F. (1970). *Abnormal rheology of oxygenated blood in sickle cell anemia*. *J. Clinical Investigation*, 49, 623-634.
- Complete blood count and biochemistry reference values in rabbits. (n.d.). Retrieved March 17, 2014, from http://www.medirabbit.com/EN/Hematology/blood_chemistry.htm.
- Conway W.D. (1990). *Countercurrent chromatography: apparatus theory & applications*. VCH Publishers Inc., New York, USA. ISBN 0-89573-331-5.
- Craig L.C. & Post P. (1949). *Apparatus for Countercurrent distribution*. *Anal. Chem.*, 21, 500-504.

References

- Degenhardt A., Schwarz M., Winterhalter P. and Ito Y. (2001). *Evaluation of different tubing geometries for high-speed counter-current chromatography*. J. Chrom. B., 922, 355-358.
- Fedotov P.S. (2002). *Untraditional applications of Countercurrent chromatography*. J. Liq. Chrom. & Rel. Technol., 25, 13-15, 2065-2078.
- Fedotov P.S., Ermolin M.S., Savonina E.Yu., Kronrod V.A. & Spivakov B.Ya. (2010). *Fraction of nano- and microparticles in a rotating conoidal coiled column*. J. Anal. Chem., 65, 12, 1209-1214.
- Fedotov P.S., Kronrod V.A. & Kasatonova O.N. (2005). *Simulation of the motion of solid particles in the carries liquid flow in a rotating coiled column*. J. Anal. Chem., 60, 4, 310-316.
- Fedotov P.S., Spivakov B.Ya. & Shkinev V.M. (2000). *Possibility of field-flow fractionation of macromolecules and particles in a rotating coiled tube*. Anal. Sci., 16, 535-536.
- Fedotov P.S., Sutherland I.A., Wood P. & Spivakov B.Ya. (2003). *Retention of solids in rotating coiled columns: the effect of β value and tubing material*. J. Liq. Chrom. & Rel. Technol., 26, 9&10, 1649-1657.
- Fernando S. (2011). *Monoclonal antibody (mAb) purification by Counter Current Chromatography*. PhD Thesis, Brunel University, London, United Kingdom. <http://bura.brunel.ac.uk/handle/2438/6522>
- Fisher D., Francis G.E. & Rickwood D eds. (1998). *Cell Separation. A Practical Approach*. Oxford Uni. Press. ISBN 0-19-963580-3.
- Garrard I.J., Fisher D. & Sutherland I.A. (2008) *Dynamic Extraction: A high speed, high capacity purification process that is rapidly saleable*. LC-GC North America, 26(5), 424-438.
- Geislinger T.M. & Franke T. (2014). *Hydrodynamic lift of vesicles and red blood cells in flow – from Fåhræus & lindqvist to microfluidic cell sorting*. Adv. Colloid & IntSci. doi: 10.1016/j.cis.2014.03.002.

References

- Grasa P., Perez-Pe R., Abecia A., Forcada F., Muino-Blanco T. & Cebrian-Perez J.A. (2005). *Sperm survival and heterogeneity are correlated with fertility after intrauterine insemination in superovulated ewes*. *Theriogenology*, 63, 748-762.
- Grudzień L.A. (2011). *Enantioseparation using a counter-current bioreactor*. PhD Thesis, Brunel University, London, United Kingdom. <http://bura.brunel.ac.uk/handle/2438/6496>
- Hagedoorn T. (2013). *Fractionation of Latex Particles in a Coil Planet Centrifuge*. Internship Project. *Brunel Institute of Bioengineering*.
- Harris J.M., Case M., Snyder R.S. & Chenault A.A. (1984). *Cell separation on the Countercurrent chromatograph*. *J. Liq. Chrom.*, 7(2), 419-431.
- Heywood-waddington D., Peters T.J. & Sutherland I.A. (1986). *The dynamics of phase partition A study of parameters affecting rate liver organelle partitioning in aqueous two-polymer phase systems*. *Biochem. J.*, 235, 245-249.
- Hosseini S.M. & Feng J.J. (2009). *A particle-based model for the transport of erythrocytes in capillaries*. *Chem. Eng. Sci.* 64, 4488-4497.
- Isabel A., Perrez G., Sancho P. & Pinilla M. (1998). *Surface and metabolic properties of microcytic and macrocytic human anaemic red blood cells detected in polymer aqueous two-phase systems*. *J. Chrom. B*, 711, 301-307.
- Ito Y. & Bowman R.L. (1970). *Countercurrent chromatography: liquid-liquid partition chromatography without solid support*. *Science*, 167, 281-283.
- Ito Y. & Shinomiya K. (2001). *A new continuous flow cell separation method based on cell density: principle, apparatus, and preliminary application to separation of human buffy coat*. *J. Clinical Apheresis*, 16, 186-191.
- Ito Y. (1979). *The toroidal coil planet centrifuge without rotating seals applied to Countercurrent chromatography*. *Anal. Biochem.* 102, 150-152.
- Ito Y. (1980). *Toroidal coil planet centrifuge for Countercurrent chromatography*. *J. Chrom*, 192, 75-87.
- Ito Y. (1981). *Minireview Countercurrent chromatography*. *J. Biochem. Biophys Methods*, 5, 105-129.

References

- Ito Y. (1981). *New continuous extraction method with a coil planet centrifuge*. J. Chrom. A, 207, 2, 161-169.
- Ito Y. (1986). *A new angle rotor coil planet centrifuge for Countercurrent chromatography. Part I, Analysis of acceleration*. J. Chrom., 358, 313-323.
- Ito Y. (1991). *Recent advances in counter-current chromatography*. J. Chrom., 528, 3-25.
- Ito Y. (1991). *Review Recent advances in countercurrent chromatography*. J. Chrom., 538, 3-25.
- Ito Y. (1996). *Principle, apparatus, and methodology of high-speed Countercurrent chromatography*. High-speed Countercurrent chromatography, Ito Y. and Conway W.D. Eds. Chemical Analysis Series, Vol.132.
- Ito Y. (2005). *Origin and evolution of the coil planet centrifuge: a personal reflection of my 40 years of CCC research and development*. Separation & Purification Reviews, 34, 131-154.
- Ito Y. (2007). *Origin and evolution of the coil planet centrifuge: a personal reflection of my 40 years of CCC research and development*. Separation & Purification Reviews, 34, 131-154.
- Ito Y., Bramblett G.T., Bharnagar R., Huberman M., Leive L.L. et al. (1983). *Improved nonsynchronous flow-through coil planet centrifuge without rotating seals: principle and application*. Sep. Sci. Technol. 18, 1, 33-48.
- Ito Y., Bramblett G.T., Bhatnagar R. (1983). *Improved nonsynchronous flow through coil planet centrifuge without rotating seals: principle and application*. Sep. Sc. Technol., 18, 1, 33-48.
- Ito Y., Carmeci P. & Steele R. (1977). *Continuous flow method for determination of erythrocyte osmotic fragility*. American Journal of Hematology, 2, 403-412.
- Ito Y., Carmeci P. & Sutherland I.A. (1979). *Nonsynchronous flow through coil planet centrifuge applied to cell separation with physiological solution*. Anal. Biochem, 94, 249-252.
- Ito Y., Carmeci P., Bhatnagar R. (1980). *The nonsynchronous flow through coil planet centrifuge without rotating seals applied to cell separation*. Separation Science and Technology, 15, 9, 1589-1598.

References

- Ito Y., Suaudeau J. & Bowman R.L. (1975) *New flow through centrifuge without rotating seals applied to plasmapheresis*. Science, 189, 999-1000.
- Ito Y., Weinstein M.A., Aoki I., Harada R. Kimura E. & Nunogaki K. (1966). *The coil planet centrifuge*. Nature, 212, 5066, 985-987.
- Ito Y., Sandlin J. & Bowers W.G. (1982). *High-speed preparative counter-current chromatography with a coil planet centrifuge*. J. Chrom. A., 244, 2, 247-258.
- Katasonova O.N., Fedotov P.S., Spivakov B.Ya. & Filippov M.N. (2003). *Behavior of solid microparticles in their fractionation on a rotating coiled column*. J. Anal. Sci., 58, 5, 473-477.
- Kazufusa S., Koji K., Hisashi O., et al. (2007). *Protein and cell separations using nonsynchronous coil planet centrifuge*. J. Liq. Chrom. & Rel. Technol., 30, 2681-2698.
- Klein G.C., Addison B.V., Boone J.S. & Moody M.A. (1968). *Effect of type of red blood cells on antistreptolysin O titer*. American Society for Microbiology, 16, 11, 1761-1763.
- Lee J., David H. et al. (2003). *A new small coil-volume CCC instrument for direct interfacing with MS*. J. Liq. Chrom. & Rel. Technol., 26, 9&10, 1345-1354.
- Leive L., Cullinane L.M., Ito Y. & Bramblett G.T. (1984). *Countercurrent chromatographic separation of bacteria with known differences in surface lipopolysaccharide*. J. Liq. Chrom., 7, 2, 403-418.
- Liu Y. & Liu W.K. (2005). *Rheology of red blood cell aggregation by computer simulation*. Journal of Computational Physics. 220, 139-154.
- Martin A.J.P. & Synge R.L.M. (1941). *A new form of chromatogram employing two phases*. Biochem. J., 35, 1358-1368.
- Menet J.M. & Thiebaut D. (1999). *Countercurrent chromatography. Chromatographic science series, Vol 82*. Marcel Dekker, Inc., New York, NY. ISBN 0-8247-9992-5.
- Menet J.M. (2001). *Aqueous two-phase solvent systems for Countercurrent chromatography*. Encyclopedia of chromatography, New York, 61-63.
- Nowaczewski S. & Kontecka H. (2012). *Haematological indices, size of erythrocytes and haemoglobin saturation in broiler chickens kept in commercial conditions*. Animal Science Papers and Reports, 30, 2, 181-190.

References

- Okada T., Metcalfe D.D. & Ito Y. (1996). *Purification of mast cells with an improved nonsynchronous flow through coil planet centrifuge*. International Archives of Allergy & Immunology, 109, 376-382.
- Ollero M., Pascual M.L., MuinoBlanco T., Cebrian-Perez J.A. & Lopez-Perez M.J. (1994). *Revealing surface changes associated with maturation of ram spermatozoa by centrifugal Countercurrent distribution in an aqueous two-phase system*. J. Chrom. A., 668, 173-178.
- Pascual M.L., Muino-Blanco T., Cebrian-Perez J.A. & Lopez-Perez M.J. (1994). *Acquisition of viable-like surface properties of sperm cells by adsorption of seminal plasma proteins revealed by centrifugal Countercurrent distribution*. Biology of the Cell, 82, 75-78.
- Percoll-methodology and applications. (n.d.). Retrieved March 17, 2014, from <http://202.38.193.234/spfx1/admin/picture/200752919841517.pdf>
- Perez-pe R., Muino-Blanco T. & Cebrian-Perez J.A. (2001). *Sperm washing method alters the ability of seminal plasma proteins to revert the cold shock damage on ram seperm membrane*. International Journal of Andrology, 24, 352-359.
- Petrov Yu.P. & Pinaev G.P. (2002). *A new approach based on monitoring of phase formation kinetics for examination of biological particles and cells, using aqueous two phase polymer systems*. Biochim. BBiophy. Acta, 1573, 39-47.
- RBC indices. (n.d.). Retrieved March 17, 2014, from <http://www.nlm.nih.gov/medlineplus/ency/article/003648.htm>.
- Reference values for laboratory animals. (n.d.). Retrieved March 17, 2014, from <http://www.ahc.umn.edu/rar/refvalues.html>.
- Reschiglian P., Zattoni A., Roda B., Michelini E & Roda A. (2005). *Field-flow fractionation and biotechnology*. Trends in Biotechnology. 23, 9. 475-483.
- Sancho P., Delgado M.D., Garcia-perez A.L. & Luque J. (1986). *Fractionation of bone marrow cells by Countercurrent distribution in aqueous polymer two-phase systems*. J. Chrom, 380, 2, 339-345.
- Seaman G.V.F. (1975). *The Red Blood Cell*. Vol. 2, End Edn. Academic Press. New York.
- Shape P.T. (1988). *Methods of Cell Separation*, Amsterdam, Elsevier science publishers B.V. ISBN 0-444-80927-9.

References

- Sharpe P.T. (1984). *Cell surface "chromatography"*. Trends in Biomedical Sciences, Sept., 374-377.
- Shibusawa et al. (1992). *Type-XLL cross-axis synchronous flow through coil planet centrifuge for separation of biopolymers*. United States Patent, patent no. 5114589.
- Shibusawa Y. & Ito Y. (1998). *Purification of proteins with aqueous two-phase solvent systems by Countercurrent chromatography*. Prep. Biochem. & Biotechnol., 28, 2, 99-136.
- Shibusawa Y. (1997). *Lipoproteins: comparison of different separation strategies*. J. Chrom. B, 699, 1997, 419-437.
- Shibusawa Y., Chiba T., Matsumoto U. & Ito Y. (1995). *Countercurrent chromatographic isolation of high- and low-density lipoprotein fractions from human serum*. ACS Symposiumseries, 593, 121-128.
- Shibusawa Y. & Ito Y. (2001). *Cross-axis coil planet centrifuge for the separation of proteins*. Encyclopedia of chromatography, 212-214.
- Shinomiya K., Kabasawa Y., Yanagidaira K. & Sasaki H. (2003). *Protein separation by nonsynchronous coil planet centrifuge with aqueous-aqueous polymer phase systems*. J. Chrom. A, 1005, 103-112.
- Shinomiya K., Kobayashi K., Oshima H., Okada T., Yanagidaira K. & Ito Y. (2007). *Protein and cell separations using nonsynchronous coil planet centrifuge*. J. Liq. Chrom. & Rel. Technol., 30, 2681-2698.
- Shinomiya K., Okada T. & Ito Y. (2005). *Elutriation of blood cell components and mast cells by nonsynchronous coil planet centrifuge*. J. Liq. Chrom. & Rel. Technol., 28, 835-846.
- Shiono H., Chen H.M., Okada T. & Ito Y. (2007). *Colony forming cell assay for human hematopoietic progenitor cells harvested by a novel continuous flow cell separation method*. J. Chrom. A, 1151, 153-157.
- Shiono H., Okada T. & Ito Y. (2005). *Application of a novel continuous flow cell separation method for separation of cultured human mast cells*. J. Liq. Chrom. & Rel. Technol., 28, 2071-2083.

References

- Skuse D.R. & Jones R.N. (1992). *Hydroxypropyl cellulose/poly(ethylene glycol)-co-poly(propylene glycol) aqueous two-phase systems: system characterization and partition of cells and proteins*. *Enzyme Microb. Technol.*, *14*, 785-790.
- Snyder G.K. & Sheafor B.A. (1999). *Red blood cell: centerpiece in the evolution of the vertebrate circulatory system*. *Integrative and Comparative Biology*, *39*, 189.
- Spivakov B.Ya., Maryutina T.A., Fedotov P.S., Ignatova S.N., Katasonova O.N., Dahmen J. & Wennrich R. (2002). *Separation of substances in rotating coiled columns: from trace elements to microparticles*. *J. Anal. Chem.*, *57*, 10, 928-934.
- Stendahl O., Magnusson K.E., Tagesson C., Cunningham R. & Edebo L. (1973). *Characterization of mutants of Salmonella typhimurium by Countercurrent distribution in an aqueous two-polymer phase system*. *Infection and immunity, Apr.*, 573-577.
- Sutherland I.A. & Heywood-Waddington D. (1987). *Countercurrent chromatography as a tool in subcellular studies*. *Methodological surveys in biochemistry and analysis: cells, membranes and disease, including Renal*. Reid E., Cooke G.M.W. & Luzio J.P. Eds. 153-159. Plenum Press, New York. ISBN 978-1-4684-1283-3.
- Sutherland I.A. & Ito Y. (1978). *A note on counter-current chromatography for separating cells and organelles by distribution in two phase polymer systems*. *Cell populations: methodological surveys (B) biochemistry*, Reid E. Eds. Vol. 9, 217-219. Ellis Horwood, Chichester.
- Sutherland I.A. & Ito Y. (1978). *Toroidal coil chromatography – a new high speed, high resolution method of separating cells and cell organelles on their distribution in two-phase polymer systems*. *High Resolution Chromatography & Chromatography Communications, (September)*, 171-172.
- Sutherland I.A. & Ito Y. (1980). *Cell separation using two-phase polymer systems in a nonsynchronous flow through coil planet centrifuge*. *Anal. Biochem.*, *108*, 367-373.
- Sutherland I.A. (1985) *Countercurrent chromatography – application to separations of viable biological material based on partition in aqueous two-phase polymer systems*. *Chromatography international*, *7*, 11-15.
- Sutherland I.A., Heywood-Waddington D. & Ito Y. (1987). *Counter-Current Chromatography: Applications to the separation of biopolymers, organelles and cells using either aqueous-organic or aqueous-aqueous phase systems*. *J. Chrom.*, *384*, 197-207.

References

- Tong X.M. & Caldwell Karin D. (1995). *Separation and characterization of red blood cells with different membrane deformability using steric field-flow fractionation*. J. Chrom. B, 674, 39-47.
- Van Alstine J.M., Synder R.S., Karr L.J. & Harris J.M. (1985). *Cell separation with Countercurrent chromatography and thin-layer Countercurrent distribution in aqueous two-phase system*. J. Liq. Chrom., 8, 12, 2293-2313.
- van den Heuvel R. N.A.M. & Konig C.S. (2011). *Improved g-level calculations for coil planet centrifuges*. J. Chrom. A, 1218, 6038-6043.
- van den Heuvel R. N.A.M. & Sutherland I.A. (2007). *Observations of established dual flow in a spiral dual-flow counter-current chromatography coil*. J. Chrom. A, 1151, 99-102.
- Wagner C., Steffen P. & Svetina S. (2013). *Aggregation of red blood cells: from rouleaux to clot formation*. Comptes Rendus Physique. 14, 459-469.
- Walter H., Brookes D.E. & Fisher D. eds (1985). *Partitioning in Aqueous Two-Phase Systems*. Academic press, London. ISBN 0-12-733860-8.
- Wilkes J.M., Leake D.S., Morris W.B., Sutherland I.A. & Peters T.J. (1982). *Isolation and fractionation of plasma lipoprotein classes by two-phase Countercurrent partition in poly(ethylene glycol)/dextran solutions*. Biochem, Soc. Trans. 10, 246-247.
- Wood P.L. (2010). *Critical β -value of all coil planet centrifuges*. J. Chrom. A, 1217, 1283-1292.
- Yoichi S. & Ito. Y. (1998). *Purification of proteins with aqueous two-phase solvent systems by countercurrent chromatography*. Prep. Biochem. & Biotech., 28, 2, 99-136.